1st AXEMA-EurAgEng Conference

2017 February 25

Les rendez-vous Techniques AXEMA

EurAgEng

Intensive and environmentally friendly agriculture: an opportunity for innovation in machinery and systems

APS Axema Promotion & Services

SITMAFGR Le Réseau Scientifique et Technique de l'Agroéquipement

SIMA

1st AXEMA-EurAgEng Conference

2017 February 25

Intensive and environmentally friendly agriculture: an opportunity for innovation in machinery and systems

An update of academic and industrial research and developments

at Parc des Expositions de Villepinte, Paris, France

An introduction to SIMA 2017.

Title

"1st AXEMA-EurAgEng Conference; Intensive and environmentally friendly agriculture: an opportunity for innovation in machinery and systems"

The proceedings are published, electronically only, on-line via the AXEMA and EurAgEng websites.

Contact Details:

The European Society of Agricultural Engineers, Bullock Building, Cranfield, Beds., MK43 0GH, UK

AXEMA – Union des Industriels de l'Agroéquipement, 19 rue Jacques Bingen, 75017 PARIS, FRANCE

ISBN: 978-0-9930236-1-3 (Publisher EurAgEng, Cranfield, UK).

ISSN is not available as this publication is not a periodical.

Table of Contents *Click on title to go directly to the paper*

Does technology always make a farmer's life easier? Perceived usability of a technologically developed tractor cab: a comparison between novice and expert users.
Federica Caffaro, Maurizio Cutini, Carlo Bisaglia, Eugenio Cavallo

The benefits of electrification: application on a rotary rake
Nicolas Gauer, Jean-Michel Lebars, Mathieu Schott

The AEF – Powering Precision Farming with ISOBUS
Andrew Olliver

Aerial multispectral imagery for site specific weed management
Marine Louargant, Corentin Cheron, Nathalie Vigneau, Gawain Jones, Sylvain Villette, Christelle Gée

Autonomous navigation of a platform with UVc-light to prevent crop infestation by powdery mildew
Andreas De Preter, Jan Anthonis , Peter Melis, Jan Swevers, Goele Pipeleers

Multi-sensor fusion method for crop row tracking and traversability operations
Bernard Benet, Roland Lenain

Low cost active devices to estimate and prevent off-road vehicle from rollover
Dieumet Denis, Benoit Thuilot, Roland Lenain, Michel Berducat

Narrow tractor development: emissions, mother regulation, comfort and precision farming - All in the same space
Massimo Ribaldonea, Stefano Dominoni

Tools and methods to develop and validate soil-wheel interaction model and knowledge.
P. Heritier, D. Miclet, E. Piron, M. Chanet, R. Lenain

Innovative Field Test Methods for Tillage Tools
Christian Rechberger, Peter Riegler-Nurscher, Johann Prankl, Franz Handler

Experimental justification of the conveying parameters for the air-seeders
Andrii Yatskul, Jean-Pierre Lemière

Centrifugal fertilizer spreader : control of working width and fertilization quality
Tien-Thinh Le, Emmanuel Piron, Denis Miclet, Alaa Chateauneuf, Michel Berducat, Phillipe Heritier

A virtual spreader to overcome experimental limits: Example of use to deepen the meaning of the transverse coefficient of variation
Sylvain Villette, Emmanuel Piron, Denis Miclet

Centrifugal spreader eco-evaluation method: Sulky Econov example
E. Pirona, D. Micleta, N. De-Freitasa, L. Leveilléb, T. Juhelb, Y. Guyomarch

Reliability approach for fatigue design on mechanical structure in agricultural domain
F. Lefebvre, I. Huther, P. Letort

Biolubricants for mobile equipment
J. Dromby, L. Vanden Eckhoudt, M. Lesterlou

Empirical fuel consumption model of tractor road travels
Didier Debroize, Frédéric Gauthier

Hydrostatic transmission designed to energy efficiency and productivity
Jean Heren, Mathilde Demoulin

Environmental impact assessment of field mechanisation for a sustainable agriculture
Jacopo Bacenetti, Daniela Lovarelli, Marco Fiala

Disseminating and Promoting Smart Farming Technologies – The Smart AKIS Network.
David Tinker, Maria Kernecker, Andrea Knierim, Angelika Wurbs, Sandra Wolters, Frits van Evert, Natalia Bellostas, Samy Aït-Amar , Thanos Balafoutis, Spyros Fountas

A typology of the uses of precision farming in an arable crops oriented region in Northern France
Alicia Ayerdi Gotora, Elisa Marraccini, Christine Leclercq, Olivier Scheurer

Spray deposition in a wind tunnel: perspectives of spray drift simulation based on a kinetic approach of wind speed effects.
Majid Alheidary, Jean-Paul Douzals, Herve Foubert

Does technology always make a farmer's life easier? Perceived usability of a technologically developed tractor cab: a comparison between novice and expert users.

Federica Caffaro [a,*], Maurizio Cutini [b], Carlo Bisaglia [b], Eugenio Cavallo [a]

[a] Institute for Agricultural and Earthmoving Machines (IMAMOTER), National Research Council of Italy (CNR), Torino, Italy

[b] Consiglio per la Ricerca in Agricoltura e l'Analisi dell'Economia Agraria – Unità di Ricerca per l'Ingegneria Agraria; Laboratorio di Treviglio (CREA-ING), Treviglio (Bergamo), Italy

* Corresponding author. Email: e.cavallo@imamoter.cnr.it

Abstract

Since tractors have been introduced in agriculture, many important technological improvements have been adopted, marking important steps in the development of these machines. However, technology may raise some issues about its usability, especially for those people who are not used to it. The present study investigated the perceived usability of the tractor cab interface in a group of novices and experts approaching a tractor equipped with a Continuously Variable Transmission (CVT). Electronics plays a major role in controlling the performance of this type of transmission and the tractor cab has been designed to hold and integrate this technology. Eight novice and eight expert tractor drivers participated in the study. During the first contact with the machine and after having performed different tasks representative of some fieldwork with the tractor, participants filled in a questionnaire about the perceived usability of the controls and of the touch-screen display and the general perception of safety, comfort, learnability and solidity of the machine. The same tasks were performed and the same measures taken also for a tractor equipped with a mechanical transmission, to have a benchmark against which to compare data about the CVT vehicle. The results of the study showed that novices found the vehicle to be equipped with controls and devices that made it difficult to learn how they had to be triggered. Experts did not report similar difficulties. Implications for the redesign of the layout of a technologically developed tractor cab and for targeted training interventions are discussed.

Keywords: Agricultural machinery, Ergonomics, Questionnaire, User satisfaction, User trial.

1. Introduction

User acceptance, satisfaction, and perceived usability of innovative technologies represent a key factor in promoting the diffusion of these technologies (Venkatesh, 2000). The concept of usability has been in used since the 1980s (Chen and Germain, 2009). It is rooted in usability engineering, where Human-Computer Interaction (HCI) examines how users interact with computer technology to make this interaction effective. ISO 9241-11(1998) defines usability as '*the extent to which a product can be used by specified users to achieve specified goals with effectiveness, efficiency and satisfaction in a specified context of use"*. Perceived usability - defined as*"…the degree to which a person believes that using a particular system would be free of effort*" (Davis, 1989, p. 82)- arises in particular as a critical variable in predicting and explaining the use of a technological system (Davis, 1989; Henderson and Divett, 2003). Davis (1989) found 6 different components of this construct, referring to the clearness, flexibility, controllability, ease of learn, ease of becoming skillful, and ease of use.

HCI research seeks to understand and utilize the determinants of user technology acceptance to influence the technology design and implementation processes and minimize user' resistance. The emphasis is placed on understanding users' usage behaviors when interacting with the human-machine interface (HMI) of a technological system, through usability testing and evaluation methods, which are targeted to ensure that users can operate a technology efficiently, effectively, and satisfactorily (Preece and Rodgers, 2002). The HMI of a technological system is the part of an electronic machine or device which serves for the information exchange between the operator/user and the machine/device. It provides the operator with a large amount of information and functionality which may however exceed user's cognitive resources, making it difficult for the user to retrieve and interpret information (Besnard and Cacitti, 2005). Previous studies showed that technologically advanced HMIs are more likely to give rise to operating errors, being a major cause of increased mental strain and user frustration, and resulting in occupational diseases as stress (Nachreiner et al., 2006). Such consequences bring economical costs due to the unexploited working time, and other disadvantages which cannot be measured in figures or assessed in economic terms, such as poorer corporate image (EU-OSHA, 2009). It becomes therefore important to adopt an ergonomic approach to the study of HCI, based no thedirect involvement of the users in the evaluation process of a system (Karwowski, 2006). With regard to this, the literature shows that the consultation of experts can be useful to obtain a more complete list of problems, whereas novice users are helpful in identifying the most severe issues (Sauer et al., 2010). According to Spires and Donley (1998) the contrast between experts and novices lies in the different organization of their conceptual structures. Experts have a mental representation (i.e., a hierarchical structure) of the concepts in the domain, whereas a novice's structure is more chaotic and disorganized.

1.1. Usability issues related to agricultural machinery

The massive introduction of technology in agriculture led to a revolution in farming, in terms of a huge increase in productivity, energy savings, lower environmental impact, and improvement of drivers' working conditions (Day et al., 2009). Technological innovations particularly apply to agricultural tractors, which are the most important and widespread machines in the sector (Iftikhar and Pedersen, 2011). One of the technological innovations that have marked a discontinuity in the development of tractors is the introduction of the Continuously Variable Transmission (CVT). The CVTs can change steplessly through an infinite number of effective gear ratios between minimum and maximum speeds and marked a great advance in tractors productivity improvement, work precision, energy efficiency, environment protection and driver's comfort (Cavallo et al. 2014).

The introduction of CVTs has deeply affected the layout of the controls in the tractor cabs. According to ISO 6682 (1986) standard, controls can be classified in primary controls, that are frequently and/or continuously used by the operator, and secondary controls, such as lights, windscreen wiper, starter, heating and air-conditioning system, ecc., less frequently used. Primary controls are those to control the vehicle such as the gearbox, the brakes, the steering wheel, the throttle, etc., and those to control the implements, such as the blade or the bucket in earth-moving machines, or the Power Take-Off (PTO) or the rear 3-point hitch lift in agricultural tractors. Hand-acted levers in mechanical transmissions have been replaced in CVT by on/off buttons and potentiometers for pre-setting or regulation acting on electro-hydraulic actuators, and monitors. Both primary and secondary controls had therefore been re-designed to accommodate and integrate the new technologies, with many advancements and changes as regards the Human Machine Interface (HMI) of the tractor working station (Yavad and Tewari, 1998). To the authors' knowledge, the design of the HMI of CVT tractors has not been investigated yet in terms of perceived usability and, thus, as a possible source of health and safety risks as, respectively, work-related stress and lack of attention.

Based on the previous considerations, the goal of the present contribution was to evaluate the HMI of a CVT tractor cab in terms of perceived usability in a group of novice and expert users. The investigation dealt, specifically, with the subjective responses about the ease of locating, interpreting and operating some controls and the accuracy of the information given by the displays, during both the first interaction with the machine and after performing a series of specific tasks with it. Understanding how real users interact with the machine helps in making recommendations for product improvement and for training actions development.

2. Materials and Methods

In order to reach the main aim of the research, a group of tractor drivers, including both experts and novices, has been involved in a field trial. Perceived usability was assessed by means of a questionnaire. Both experts and novices performed different tasks with the CVT tractor and also with a tractor equipped with a mechanical transmission. This choice was made to ensure that the 2 groups did not differ as regards the driving skills and thus results obtained with the CVT may be attributed specifically to the HMI of that technology.

2.1. Participants

Almost everyone in the usability field agrees that there are diminishing returns from having more users doing the same tasks: the more users you watch, the fewer new problems you see. According to Nielsen's studies (1995, 2000) the first three users are likely to encounter all of the most significant problems related to the tasks tested. Analyzing Nielsen's study, Kingman and colleagues (2005), based on the proportion of usability problems found by using different numbers of evaluators, built an equation to determine the optimal number of users for determining usability problems. They concluded that three to five experts would be the optimal for determining usability problems. In the present investigation, 16 male tractor drivers were involved in the trial. Eight out of the 16 participants had at least 5 years driving experience on CVT tractors and they were considered experts (as in Kumar et al., 2001). The remaining 8 participants did not have ever owned nor had operated a CVT tractor: they were considered novices. The experts had a mean age of 35.25 years (SD=11.65) and a mean driving experience of 20.00 years (SD=10.35). The novices had a mean age of 38.75 years (SD=13.91) and a mean driving experience of 26.13 years (SD=13.92).

2.2. The Tractors

The tractor with mechanical transmission used to check participants' tractor-driving skills (from now on, Tractor 1) had a transmission articulated in gears and ranges (i. e., High-Low; Rabbit-Snail) that presents controls mainly consisting of levers posed at the right side of the operator located, as usual in this tractor tipology, on the cab floor. They are directly onto the tractor frame. The remaining controls are placed on the right side console and are constituted of levers (Figure 1).

Figure 1. Controls' layout of the mechanical tractor used in the study.

As regards the CVT tractor (from now on, Tractor 2), the study has been anticipated by a survey to investigate the layout of the primary and secondary controls on 5 models of CVT tractors from different manufacturers currently available in Italy. The clutch, brake and throttle pedals and reverse lever close to the steering wheel have the same placing and function as in conventional mechanical transmission tractors. As shown in Figure 2 the remaining controls are placed on two main areas of the working station: the driver's seat armrest and the right side console.

Figure 2. Controls' layout of some CVT tractors currently available in Italy.

The controls layout reflects the hierarchy suggested by usage frequency (ISO 6682, 1986). The armrest controls are the most frequently used or those intended for precision work, requiring the constant attention of the operator, such as the hand throttle, the gearbox, the rear 3-point hitch lift, and the auxiliary hydraulics. The setting and adjustment controls, less frequently used, are located on the right side console. Some models include displays of different size located on the right side console or on the front right pillar of the cab. The model of CVT tractor used in the present study follows the scheme that introduces controls on the seat armrest and on the console on the right side of the tractor cab, and a display on the right side console.

2.3. Task Scenarios

Participants were asked to complete a series of tasks with both Tractor 1 and 2. The tasks were created by considering two main functions of the machine: driving on the road, and harrowing while maneuvering on farm road. The road driving task consisted in driving the tractor at a fixed forward speed of 20 kph on a 500 m track made of two 150 m stretch lines and two 100 m bends. The road driving task allowed the participants to achieve a baseline knowledge in operating the tractor before the more complex following task. During this trial, the participant was accompanied by an assistant, who sat in the trainer seat, in case support was needed.

The harrowing simulation task required the operator to drive the tractor and to operate the PTO, the rear 3-point hitch lift, and the auxiliary hydraulic couplings controls. The specific sub-tasks are reported in Table 1.

Table 1. List of sub-tasks participants had to perform with the 2 tractors.

Sub-tasks	Trad	cvt
Operate the auxiliary service coupling to open the harrow to be ready for working	Move a lever forward	Press a button on an handler
Operate the rear 3-point hitch lift to lower the harrow (without touching the test track)	Move a lever forward or backward	Rotate a small wheel or press a button
Switching the PTO on	Move a lever forward	Press a button
Forwarding the tractor at 10 km/h and following a fixed and bounded path	Look a table and choice the gear by levers and press the accelerator pedal	Press the accelerator pedal or move the handler till 10 km h^{-1}
Arrived near the bumps (simulating stones), operating the rear 3-point hitch lift to raise the harrow	Move a lever forward	Rotate a small wheel or press a button
Slow down till 7 km/h	Release the accelerator pedal	Release the accelerator pedal or move the handler till 7 km h^{-1}
Avoid to pass over the bumps	Moving the flywheel	Moving the flywheel
Operating the rear 3-point hitch lift to lower the harrow	Move a lever forward or backward	Rotate a small wheel or press a button
To bring again the forwarding speed at 10 km/h	Press the accelerator pedal	Press the accelerator pedal or move the handler till 10 km h^{-1}
Follow the path till the end	Moving the flywheel	Moving the flywheel
Stop the tractor	Press the clutch pedal and acting on the gear levers	Release the accelerator pedal or push a button
Operating the rear 3-point hitch lift to raise the harrow	Move a lever forward or backward	Rotate a small wheel or press a button
Switching the PTO off	Move a lever backward	Press a button
To operate the auxiliary service coupling to close the harrow as for road transfer	Move a lever backward	Press a button on an handler
Carry out a sharp turn as at the end of the field in a bounded space	Move the flywheel and operating with gear levers	Move the flywheel and the handler

The task required to drive on 100 m test track set with road bumps. Cones on the side of the track were used to indicate where the operator had to perform the different actions operating the appropriate controls. All the participants

performed the simulation harrowing task with each tractor 4 times, for a total time of about 10 minutes.

2.4. The Questionnaire

The perceived usability of the HMI of the tractor cab was assessed using a paper-and-pencil questionnaire developed by taking into account the instruments used in previous studies (Ferrari and Cavallo, 2013). The questionnaire has been pilot-tested before being used in the present study. The questionnaire was made of four parts. The first part gathered socio-demographic data about the participants, and their experience with agricultural machinery. In the second part the participants were asked to evaluate the usability of the HMI during the first contact with the cab, in terms of locating different controls (e.g. PTO, hydraulic system, lighting), using a six-point Likert scale (1932) without a central anchor (1 = I do not agree at all, 6= I strongly agree). In the third part of the questionnaire the participants were asked to evaluate the usability of the HMI of the cab after having performed the tasks, in terms of ease to operate the control devices, clearness and understandability of the levers/knobs, buttons, warning lights and accuracy of the information given by the display, using a six-point Likert scale without a central anchor (1 = I do not agree at all, 6= I strongly agree). The items of the second and third section of the questionnaire were designed considering the different components of the perceived usability of IT systems proposed by Davis (1989), and the critical elements regarding tractors' technological equipment and cab layout analyzed in previous studies (Ferrari and Cavallo, 2013). Participants were also asked to give a general evaluation of the learnability of the tractor, together with its safety, quality, and solidity (as in Ferrari and Cavallo, 2013). The forth part of the questionnaire contained open-ended questions aimed at pointing out any difficulty found in accomplishing the tasks and soliciting additional feedback on the arrangement and operation of the control devices in the cab, describing the reasons of the opinions expressed in the previous sections.

The first and second part of the questionnaire were filled in when the participant had just accessed the cabin and seated. The third and the fourth sections were completed after the tasks have been accomplished.

2.5 The Observation

While participants were driving the tractors, a trained research assistant reported whether the users achieved or failed each sub-task in an observational grid. The information was collected by one single observer, to avoid the inter-observer variability bias.

2.5 Data Analysis

Means and standard deviations were computed for data coming from close-ended questions. Then, a series of Student's t-tests was performed to compare novices' and experts' ratings for both tractors, and detect any significant difference between the 2 groups of participants. Significance level was set to $p<.05$. A content analysis (Weber, 1990) was performed on the answers given to the open-ended questions; the content of the answers was categorized by two independent judges to identify the more recurrent themes for each of the investigated topics.

3. Results and Discussion

As regards Tractor 1, the t-tests did not show any significant difference between novices and experts ($p>.05$ for all the comparisons), pointing out that all the participants interact in a similar way with the 'old-fashioned' machine. Moreover, the content analysis showed that participants did not report any particular difficulty in accomplishing the targeted tasks with Tractor 1, apart some discomfort for both experts and novices in activating the PTO control because of its placement behind the seat and the strength required to operate it.. For these reasons, in the next figures, data regarding Tractor 1 will be presented all together (not disentangling novices' and experts' ratings) and used as a benchmark for the assessment of Tractor 2.

As regards the first contact with the machine (Figure 3), the analysis showed that locating the PTO control and the lighting control was significantly more difficult for novices compared to experts ($t(14)= -1.93$, $p<.05$ and $t(14)=-2.53$, respectively). Open-ended questions revealed that these difficulties were mainly due to the fact that, according to the novices, these controls were placed in an unexpected area of the working station and, thus, more time was requested to make them out. A critical interaction with the PTO controls should be carefully considered, since most of the tractor operations are powered by the PTO and its misuse may lead to serious risks for operators' safety (PennState Extension, 2016). In Tractor 2, the PTO speed setting control was isolated from the PTO engaging/disengaging control: this can arise some considerations about the need of alternative design solutions and training interventions to make this control more outstanding, self-explanatory and immediately noticeable.

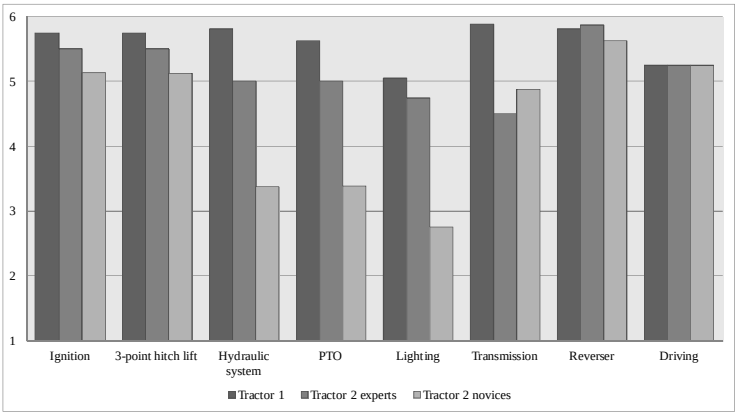

Figure 3. Perceived ease of locating controls in Tractor 1 and Tractor 2 (ratings mean value).

Observations about task completion showed that all the participants managed to accomplish the tasks, even though the open-ended question of the questionnaire revealed that three novices reported some difficulties in operating the PTO and the 3-point hitch lift controls when operating with the harrow in Tractor 2. This was due to the fact that there were too many functions and similar buttons among which to discriminate, instead of levers, each serving a different aim, commonly adopted in conventional mechanical transmission tractors. This evidence is consistent with the results of the t-tests, showing that novices found significantly more difficult to operate the 3-point hitch lift ($t(14)=-5.28$, $p<.01$), the hydraulic system ($t(14)=-3.46$, $p<.01$), the PTO ($t(14)=-2.54$, $p<.05$), the transmission ($t(14)=-3.04$, $p<.01$), and the driving ($t(14)=-3.13$, $p<.01$) controls. The difficulties in operating transmission controls could be easily interpreted by considering that the transmission of a CVT tractor is very different from that of a traditional mechanical machine: it requires to choose between a manual or an automatic management system of the driveline; it gives also the possibility to 1) set the maximum speed, 2) use a constant speed (cruise control), 3) work at constant PTO speed, 4) work in "Eco" or "power" mode, and 5) select the sensitivity of the throttle pedal. Because of this, the same control could assume different functions. In relation to the 3-point hitch lift, novices resulted accustomed to use hand levers and, as they weren't familiar with the practice of pre-setting the 3-point hitch lift, they found some difficulties in operating controls like small wheels and potentiometers. Similar considerations may be done about the ease of operating the hydraulic auxiliaries, requiring hydraulic valves to be set before the use. Moreover the same parameter could be set both on the display and on the dashboard at the right side of the operator's seat. This double source of information could have required a more complex cognitive processing (Wickens, 2008), hindering operators' actions.

When interacting with lever/knobs and buttons, the data discloses that, in general, novices perceived a lower level of usability, especially with regard to the ease of understanding what action each button controls and how to operate it (Figure 4). A significant difference between experts and novices as regards the ratings about the placement of the levers/knobs ($t(14)=-2.52$, $p<.05$), with novices founding levers/knobs to be in a quite odd place compared to what they expected, more than experts. As regards the usability of the buttons, the novices found significantly more critical to understand what the buttons represent ($t(14)=-2.59$, $p<.01$), also because of their colors, which were somewhat confusing ($t(14)=-2.77$, $p<.05$). The content analysis of the open-ended questions revealed some critical aspects also regarding the size of the buttons and their icons, since they were considered by all the participants to be too small to be immediately visible and recognizable. The icons referring to these controls were also considered unclear.

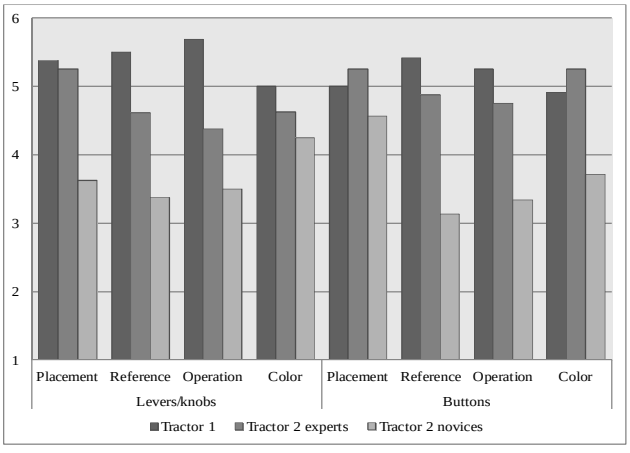

Figure 4. Perceived ease of use of levers/knobs and buttons in Tractor 1 and Tractor 2 (ratings mean value).

The critical aspects reported by the novices about the buttons may be interpreted by considering that in the CVT tractor used in the study the buttons were all placed very near to each other on the dashboard on the right side of the

operator's seat, with nothing apart from the color to distinguish between them. For instance, the button for setting the PTO speed was close to the controls of other functions, but aside from the button for the PTO engagement/disengagement. Moreover, as noticed earlier in this paper, the procedure of a preliminary setting of the PTO speed before switching it on was not immediate for the novices. This could contribute to enhance the cognitive workload (Wickens, 2008) when interacting with the buttons. The described difficulties in interpreting icons and signs is in line with some previous studies reporting low comprehension scores of safety pictograms affixed to agricultural machinery (Caffaro and Cavallo, 2015; Caffaro et al., 2017). This outcome should be examined more in depth since icons, signs and pictograms are supposed to be self explanatory and able to quickly communicate concepts and instructions, compared to written language (Edworthy and Adams, 1996). A critical aspect emerged also as regards the physical interaction with buttons: participants reported that buttons and icons or signals were not immediately seen due to their reduced size. This issue should be further investigated, especially with regard to particular groups of users like the elderly, whose rate is increasing in the agricultural population (Ilmarinen, 2006) and who are characterized by physical and cognitive impairments which may make it difficult to interact effectively with small devices.

Some differences emerged between novices and experts also with regard to the signal devices, the warning lights (Figure 5). It was significantly more difficult for the novices to understand what the lights referred to ($t(14)=-2.78$, $p<.05$) as they were not immediately visible ($t(14)=-2.26$, $p<.05$). As concerns displays (Figure 5), the analysis showed that the layout of the information on the screen was reported as significantly better ($t(14)=-2.57$, $p<.05$), and the priority given to essential information shown on the display was reported as significantly higher ($t(14)=-4.04$, $p<.01$) for experts than novices. Interestingly, the analysis of the open-ended questions pointed out that not only many novices but also one expert reported that there was too much information to be monitored on the screen, as a critical aspect.

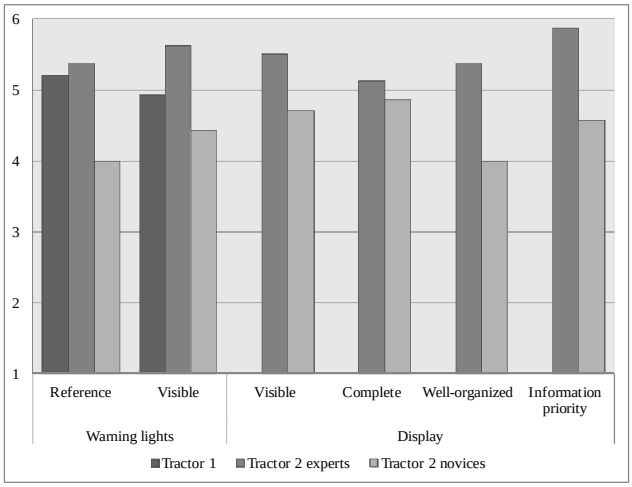

Figure 5. Understandability of the warning lights and perceived ease of use of the display in Tractor 1 and Tractor 2 (ratings mean value).

When asked to give a general evaluation of the machine, the novices gave lower ratings compared to experts for all the four aspects considered in Tractor 2 ($p<.05$ for all comparisons). Content analysis confirmed that the high level of technological development of the vehicle was perceived by most the participants as useful in reducing physical efforts and saving time in performing fieldwork. However, the tractor was not considered particularly safe nor solid, by the novices. A main issue was the poor sense of control on the activity and the vehicle when dealing with such a highly technological tractor, because too many tasks were delegated to the machine itself. Moreover, if a maintenance problem raises on the tractor, novice participants reported being worried about the fact that they would have not known exactly how to intervene on the vehicle.

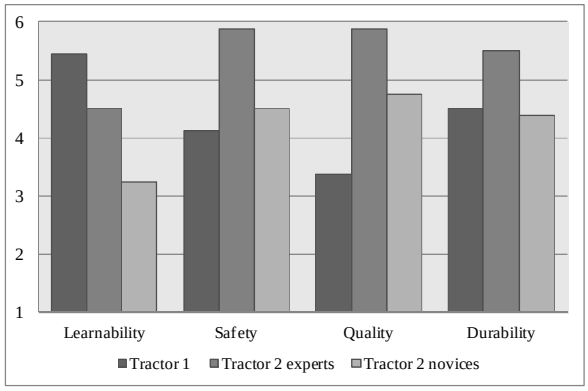

Figure 6. Overall assessment of the vehicle in Tractor 1 and Tractor 2 (ratings mean value).

Interestingly, Tractor 1 was rated higher with regard to its learnability but lower than Tractor 2 on all the other aspects. This is consistent with the fact that overall the participants found the technological machine to be useful in performing farm activities. They matched the 'innovative-owner' profile defined by Cavallo et al. (2015) as regards the adoption of technological innovations, however they seemed not to completely and correctly manage this technology, nor to take full advantage of all its benefits. This result may find an explanation in the construct of mental model, described by Norman (1988) as a user's internal representation of how he/she believes a system works, developed by interacting with the system. A mental model is a knowledge about the system, which allows the user to anticipate the behaviour of the system and to explain the system's responses. When a system is developed in a way which does not fit the users' mental model, ease of use and learnability become at stake, errors increase and performance decreases (Norman, 1988). This might be the case of the novice users interacting with Tractor 2: their mental models about how a HMI of a typical tractor should work, contrasted with the mental model of the designers of the HMI investigated in the study, making the system less intuitive and more difficult to use. It should be also considered that operators of agricultural tractors often find out the different functions of the controls in the tractor cab by a 'trials and errors' procedure: focused training sessions adopting behavioral modeling techniques -as hands-on demonstrations and behavioral simulations (Burke et al., 2006)- could be provided when buying a new machine, with some periodical refreshes in case of new technological releases. Particular attention should be also paid to how these training activities are organized, since perceived benefits are important incentives for the use of technology (Davis, 1989; Venkatesh et al., 2003): farmers should know how they can use new technologies equipping their tractors, in order to reduce the physical workload, increase economic benefits, and save time.

4. Conclusions

Technological innovation in agriculture should result in better working conditions. However, it can sometimes results in control systems that are more complicated to operate than mechanical ones, due to the great amount of information available for the users at the same time. The interaction between the HMI of a CVT tractor and the novice drivers involved in the present study pointed out that the interface may be not self-explanatory, making the provision of proper information and training by manufacturers an essential element for an effective improvement of the system.

Suggestions on how to improve the HMI to allow more accurate task completion and increase machine usability have been highlighted. Participants contributed with new ideas on how existing features could be improved and new features developed. Increased machine usability will play an important role for good market performances. To improve the quality of the HMIs and the human-machine interaction, it is therefore fundamental to consider the real users and their needs in the design process of technological systems (Nachreiner et al., 2006), adopting an ergonomic approach which takes account of both physical (such as perceptual processes) and psychological aspects (such as cognitive processes), to reinforce human factor potentials and reduce limitations (Nam et al., 2009).

References

Besnard, D., Cacitti, L., 2005. Interface changes causing accidents. An empirical study of negative transfer. Int. J. Hum-Comput. Stud. 62 (1), 105-125. http://dx.doi.org/10.1016/j.ijhcs.2004.08.002

Burke, M.J., Sarpy, S.A., Smith-Crowe, K., Chan-Serafin, S., Salvador, R.O., Islam, G., 2006. Relative effectiveness of worker safety and health training methods. American Journal of Public Health 96 (2), 315-324. http://dx.doi.org/10.2105/AJPH.2004.059840

Caffaro, F., Cavallo, E., 2015. Comprehension of safety pictograms affixed to agricultural machinery: a survey of users. Journal of Safety Research, 55, 151-158. http://dx.doi.org/10.1016/j.jsr.2015.08.008

Caffaro, F., Mirisola, A., Cavallo, E., 2017. Safety signs on agricultural machinery: Pictorials do not always successfully convey their messages to target users. Applied Ergonomics, 58, 156-166. http://dx.doi.org/10.1016/j.apergo.2016.06.003

Cavallo, E., Ferrari, E., Bollani, L., Coccia, M., 2014a. Strategic management implications for the adoption of technological innovations in agricultural tractor: the role of scale factors and environmental attitude. Technology Analysis & Strategic management 26 (7), 765-779. http://dx.doi.org/10.1080/09537325.2014.890706

Cavallo, E., Ferrari, E., Coccia, M., 2015. Likely technological trajectories in agricultural tractors by analysing innovative attitudes of farmers. International Journal of Technology, Policy and Management, 15 (2), 158-177. http://dx.doi.org/10.1504/IJTPM.2015.069203

Chen, Y. H., Germain, C. A., Rorissa, A. (2009). An analysis of formally published usability and Web usability definitions. In: *Proceedings of the American Society for Information Science and Technology*, 46 (1), 1-18.

Davis, F.D., 1989. Perceived usefulness, perceived ease of use, and user acceptance of information technology. MIS Quarterly 13 (3), 319-340.

Day, B., Field, L., Jarvis, A., 2009. The wrest park story 1924-2006. Chapter 3. Tractors and vehicles. 103 (Suppl.1), 36–47.

Edworthy, J., Adams, A.S., 1996. *Warnings: a research prospective*. London: Taylor and Francis.

European Agency for Safety and Health at Work (EU-OSHA), 2009. The human machine interface as an emerging risk. Office for Official Publications of the European Union, Luxembourg.

Ferrari, E., Cavallo, E., 2013. Operators' perception of comfort in two tractor cabs. Journal of Agricultural Safety And Health, 19 (1), 3-18. http://dx.doi.org/10.13031/2013.42539

Ilmarinen, J., 2006. *Towards a longer working life: aging and the quality of worklife in the European Union*. Helsinki, Finland: Finnish Institute of Occupational Health

ISO, 1986. Earth-moving machinery - Zones of comfort and reach for controls, ISO 6682. Geneva, Switzerland: International Organization for Standardization.

ISO. 9241-11 Ergonomic requirements for office work with visual display terminals (VDT)s - Part 11 Guidance on Usability, ISO 9241-11: 1998. Geneva, Switzerland: International Organization for Standardization.

Henderson, R., Divett, M.J., 2003. Perceived usefulness, ease of use and electronic supermarket use. International Journal of Human-Computer Studies 59 (3), 383-395. http://dx.doi.org/10.1016/S1071-5819(03)00079-X

Iftikhar, N., Pedersen, T.B., 2011. Flexible exchange of farming device data. Computers and Electronics in Agriculture,75, 52–63. http://dx.doi.org/10.1016/j.compag.2010.09.010

Karwowski, W., 2006. *International Encyclopedia of Ergonomics and Human Factors*, 2 ed.. Boca Raton, FL: CRC Press.

Kingman D. M., Yoder A. M., Hodge N. S., Ortega R., Field W. E., 2005. Utilizing Expert Panels in Agricultural Safety and Health Research, Journal of Agricultural Safety and Health 11, 61-74. http://dx.doi.org/10.13031/2013.17897

Kumar, A., Mahajan, P., Mohan, D., Varghese, M., 2001. IT—Information Technology and the Human Interface: Tractor vibration severity and driver health: a study from rural India. Journal of Agricultural Engineering Research 80 (4), 313-328. http://dx.doi.org/10.1006/jaer.2001.0755

Likert, R., 1932. A Technique for the Measurement of Attitudes, Archives of Psychology, 22 (140), 1-55.

Nachreiner, F., Nickel, P., Meyer, I., 2006. Human factors in process control systems: the design of human–machine interfaces. Safety Science 44 (1), 5-26. doi:10.1016/j.ssci.2005.09.003

Nam, C. S., Johnson, S., Li, Y., Seong, Y., 2009. Evaluation of human–agent user interfaces in multi-agent systems. International Journal of Industrial Ergonomics 39 (1), 192-201.

Nielsen, J., 1995. Scenarios in discount usability engineering. In: Caroll, J.M. (Ed.), *Scenario-based Design: Envisioning Work and Technology in System Development*. New York, NY: John Wiley and Sons.

Nielsen J., 2000. *Designing Web Usability*, Indianapolis, IN: New Riders Publishing.

Norman, D. A., 1988. *The psychology of everyday things*. New York, NY. Basic Books.

PennState Extension, 2016. Power Take-Off (PTO) Safety. Available at: <http://extension.psu.edu/business/ag-safety/vehicles-and-machinery/tractor-safety/e33> Accessed April 2016.

Preece, J., Rodgers, H. (2002). *Interaction design beyond human-computer interaction*. New York: John Wiley & Sons, Inc.

Sauer, J., Seibel, K., Rüttinger, B., 2010. The influence of user expertise and prototype fidelity in usability tests. Applied Ergonomics41 (1), 130-140. doi:10.1016/j.apergo.2009.06.003

Spires, H. A., Donley, J., 1998. Prior knowledge activation: Inducing engagement with informational texts. Journal of Educational Psychology 90 (2), 249–260.

Venkatesh, V. (2000). Determinants of perceived ease of use: Integrating control, and emotion into the Technology Acceptance Model. Information Systems Research, 11 (4), 343-365. http://dx.doi.org/10.1287/isre.11.4.342.11872

Venkatesh, V., Morris, M.G., Davis, G.B., Davis, F.D., 2003. User acceptance of information technology: Toward a unified view. MIS Quarterly 27 (3), 425-478.

Yadav, R., Tewari, V.K., 1998. Tractor operator workplace design-a review. Journal of Terramechanics 35, 41-53. http://dx.doi.org/10.1016/S0022-4898(98)00011-1

Weber, R.P., 1990. *Basic Content Analysis, 2* ed. Series: Sage University Papers. Quantitative Applications in the Social Sciences, vol. 49. London: Sage Publications Ltd.

Wickens, C.D., 2008. Multiple resources and mental workload. Human Factors 50 (3), 449-455.

The benefits of electrification: application on a rotary rake

GAUER Nicolas [a,*], LEBARS Jean-Michel [b], SCHOTT Mathieu [c]

[a] Electrical machine development, Kuhn, Saverne, France

[b] Deputy Head of electronics department, Kuhn, Saverne, France

[c] Mechanical engineer, Kuhn, Saverne, France

* Corresponding author. Email: nicolas.gauer@kuhn.com

Abstract

Several industries use since many decades electrical drive solutions for production. This improves productivity, quality of work, etc. And now the automotive industry uses more and more this technology for cars and trucks for mobility purpose. Why should it not be the same in agriculture? Thanks to work done in the AEF (Agricultural industry Electronics Foundation), the DC electrical interface between the tractor and the implement is standardized to 700V with a power supply up to 150kW. And this will open huge possibilities for the electrification of agricultural implements.

To evaluate how to integrate electrical power in implements and to show the benefits, Kuhn has decided to build a 4-rotors rotary rake demonstrator equipped with electric drive. For this demonstrator, it has been decided to replace the hydraulic drive of the current marketed machine with electrical motors driven by inverters. The paper shows first results during field tests through a comparison of the electrical driven machine with the current marketed KUHN 4-rotor rake GA13131. After some design challenges due to the integration of a new technology, the benefits of the electrification could be noted. By comparing the work done by both machines, we have observed a reduction of the power consumption with a better work quality and a reduced overall noise.

More generally, the advantages of electrification could be multiple and beneficial for both the machine manufacturer and the farmer. For the machine manufacturer, the main advantage is the ease to transmit power by solely cables. Another advantage is the ease to collect or control some physical parameters, like torque, current, speeds, voltages, etc. This will also allow to better design some mechanical parts and thus to reduce costs. For the farmer, the main advantages are better efficiency of the machine, reduction of the noise level and better work done by the machine due to the very fast reactivity of the electrical drive. Thanks to the reversibility of electrical motors, the rotor is also able to brake actively without adding mechanical parts. Moreover, there are no maintenance and no oil leak risks with electrical drive components.

Keywords: Electric drives, electrification, rotary rake, power system, high voltage, AEF

1. Introduction

The Kuhn product portfolio comprises a large number of agricultural machinery lines, in particular Hay and Forage equipment including rotary rakes. The Kuhn rotary rakes family is composed of 26 models from 1 to 4 rotors and from 3.2m up to 15m working width for the largest machine.

All single and twin Kuhn rotary rakes are mechanically driven using the PTO of the tractor. For these machines, the kinematic of the machine is simple enough to be able to transmit the power from the PTO of the tractor to the rotors with shafts and gear boxes. For the 4-rotors machines, the kinematic is much more complex and the driving of the rotors with shafts is much more difficult. This is why Kuhn has chosen to use hydraulic drive for these machines. They are equipped with a hydraulic generator and a hydraulic motor on each rotor. Furthermore, the hydraulic driving needs less maintenance and gives more smoothness to the drives of the machine regarding mechanical transmissions. These benefits are appreciated by intensive machine user like contractors.

In this paper, we will present another mean to transmit easily power to the rotors: electricity. Thanks to electrical drive, we expect to have new functionalities like individual speed settings and an improved raking process due to a better speed accuracy. Moreover, electrical drive has a very good efficiency.

The aim of this study was to design and build an electrified rotary rake in order to make measurements to confirm all these general assumptions. An input power measurement confirmed the efficiency gain by comparing the hydraulic machine to the electrical one.

2. Machine electrification

2.1. Presentation of the current marketed Kuhn 4 rotor rake

For this study, Kuhn decided to use his Gyro rake GA13131 with 12,5m working width. This ISOBUS machine is controlled through a terminal. Thanks to this terminal, the machine can be completely controlled (passing from road to field configuration and vice versa, adjustment of raking width…).

Figure 1. Kuhn GA13131 and control terminal

The transmission of power between the PTO of the tractor and the rotors is done through hydraulic power. Each rotor is equipped with a hydraulic motor which is supplied by an individual oil pump. Additionally, 2 other pumps (Figure 2; P2 and P5) are installed on this machine to provide 20% more speed for the front rotors in order to move the forage nearer to the middle of the rake. The oil flow of these pumps is controlled through the terminal.

In addition to the easy way to supply power to the rotors, the hydraulic system of this machine has some more advantages. To protect the mechanical parts, pressure bypass valves are installed and limit the drive torque of each rotor.

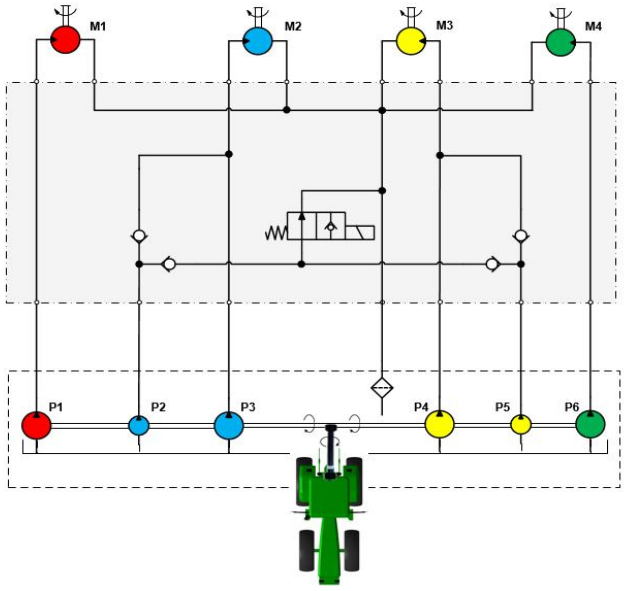

Figure 2. The Kuhn GA13131 hydraulic architecture

2.2. Motivations for the electrification of a 4-rotor rotary rake

Possible evolutions of the machine comprise the adaptation of some parameters like rotor speed, working height… as a result of some measured physical parameters like torque, working conditions… To achieve this we need to have a

precise control of the drive. Electrical power components allow a better control. In addition to the individual speed control loop and speed setting, the efficiency of the machine can be improved due on one hand to the overall better efficiency of electrical components, but also on the other hand to the elimination of the link between tractor engine speed and machine rotor speed. Other goals of the electrification of this machine were to improve the overall know-how about using electrical drives within agricultural machinery and to participate in the AEF working group dealing with this topic.

As we don't plan to produce this machine at this stage, we decided to build only a demonstrator and not a prototype. This had of course an impact on the choice of the components.

2.3. Electric drive architecture

Figure 3 shows the global electric architecture design. Each rotor of the machine is equipped with a 13kW electrical motor driven by an individual inverter. The aim of the inverter is to convert the DC voltage supplied by the generator into AC voltage whose frequency depends on the desired speed for the corresponding motor. The speed of each motor is individually controlled by a corresponding control loop.

The electricity for the machine is supplied directly from a tractor installed generator or from a front mounted generator. We chose to supply our machine with DC voltage in order to avoid any dependency on the tractor engine speed. The DC voltage has a level of 600 to 700V, to comply with the AEF High Voltage standard. Concerning the inverters, they communicate over a CAN bus (same bus as the machine ISOBUS) on J1939 protocol and are controlled with LabVIEW software for this demonstrator machine.

All other movements of the machine continue to be hydraulic controlled with the oil supplied from the tractor similar as on the current marketed machine and controlled by the ISOBUS ECU.

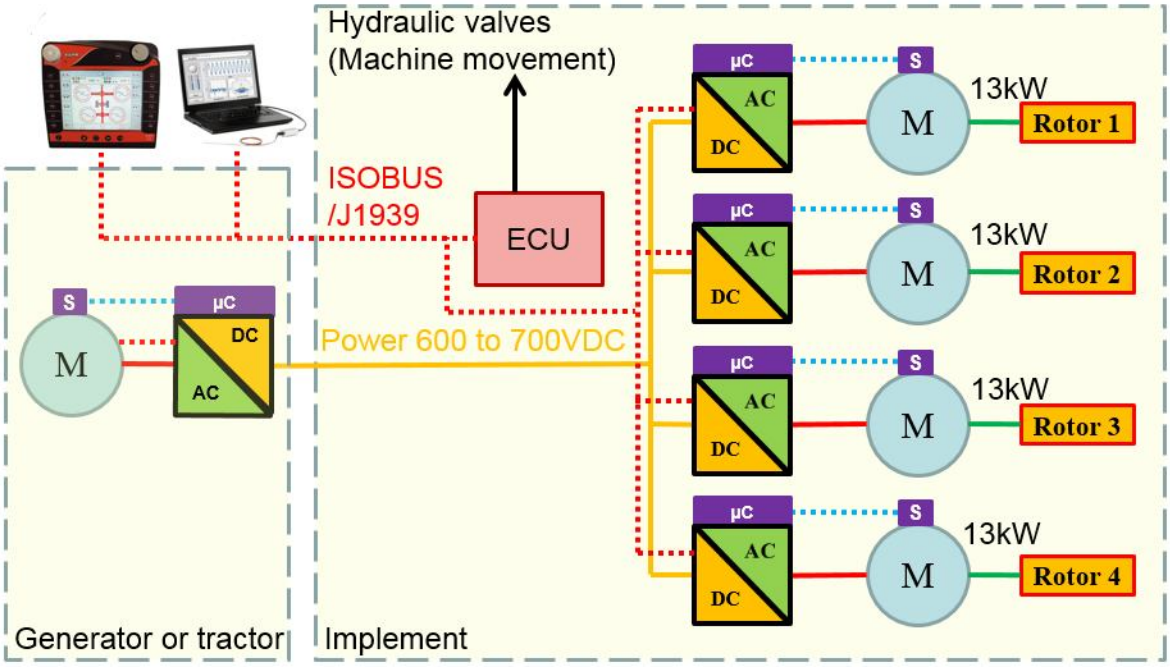

Figure 3. The electric drive architecture

2.4. Motor choice

As we decided to design and only build a demonstrator, the choice of the electric motor was mainly guided by available off-the-shelf products and the facility to integrate them in the machine. Moreover, as the motors are mounted at the end of arms supporting the rotors which are pivoted upwards for transport, the weight of the motors was also a critical point.

Table 1 and Table 2 show the main criteria for choosing the motor type and its cooling. For all these reasons, we decided to choose synchronous motors with a forced air convection cooling. We integrate them in the machine using a speed reducer and a belt drive (less complex).

Table 1. Motor type comparison

	DC	Induction	Synchronous
Dimensions/weight	High	Medium	Low
IP level	Low	Medium	High
Efficiency	Low	Medium	High
Inverter complexity	Low	Medium	High

Table 2. Motor Cooling comparison

	DC	Induction	Synchronous
Dimensions/weight	High	Medium	Low
Clogging risk	Low	High	Medium
Complexity	Low	Low	High

2.5. Other motor integration possibilities

Other manufacturers decided also to develop an electrical 4-rotor rotary rake like Agco/Fella, Claas and Pöttinger. Each manufacturer have chosen his own motor topology.

Agco/Fella uses a special developed motor which drives directly the rotor without gears (speed about 55 min-1). This solution is optimal in term of efficiency, noise, reliability and integration. The motor is cooled through natural convection, so that the risk of clogging of the motor's fan is avoided. This solution has the most advantages but leads to huge modifications of the rotor, to higher weight and to more costs due to the development of a special motor.

Claas uses a similar cooling technology for the same reasons, but they decided to use an off-the-shelf motor which turns at high speed. For this reason, a gear speed reducer is mounted between the motor and the rotor of the machine. The Claas solution seems to be bulky and heavy, but may be cheaper as the Agco/Fella solution.

Pöttinger and Kuhn use a light, very compact off-the-shelf motor, but with a forced air cooling system which may cause a clogging risk. Nevertheless, the consequences are limited because the motor is able to develop a reasonable power without always needing the fan, and most of the time this is sufficient.

2.6. Electric component integration

Figure 4 shows the integration of the electrical box and motor inverter. All these components are mounted within a housing at the oil tank position of the serial machine. The electrical box contains some fuses to protect the cables of the machine and relays to switch off the DC power supply in case of troubles.

The 4 inverters are water cooled and are connected to a pump and a heat exchanger. We decided to use water cooling in order to have only one heat exchanger which is easily cleanable. An automatic inversion of the fan rotation is implemented every couple of minutes to expel the dust particles.

The motor itself is equipped with a mechanical drive adaptation which was done with a minimum modification of the machine (using a belt drive). The motor is equipped with a 7:1 planetary gear reducer to adapt the high speed of the motor (approx. 3,800min^{-1}) to the speed of the rotor input (approx. 540 min^{-1}). A timing belt was used to ensure a maximal efficiency with a simple mechanical solution for coupling the motor reducer and the rotor.

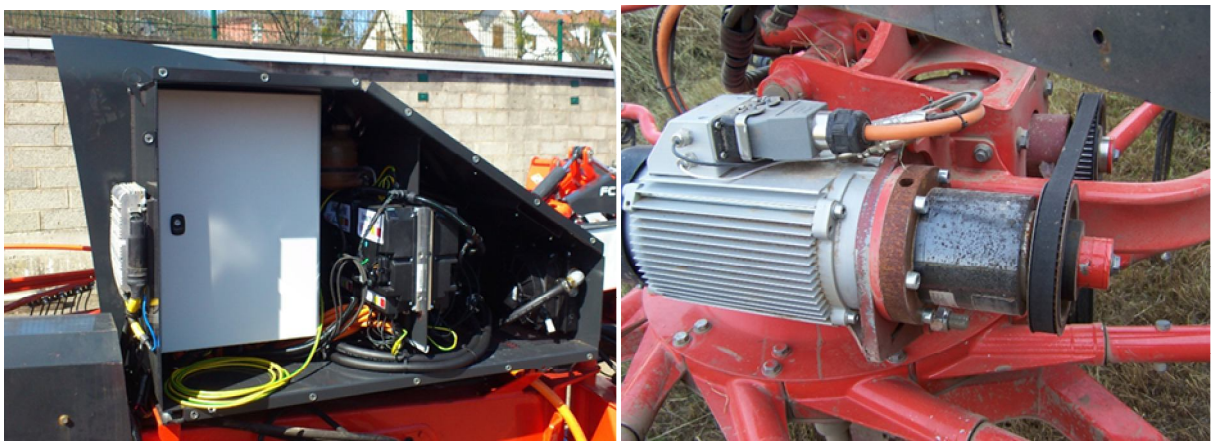

Figure 4. Electric component integration

3. Field tests

3.1. Description

During the field test in 2015 and 2016, we tested our demonstrator with 2 different generators: the Power Pack PP50 from Raussendorf and the generator of Fendt X Concept tractor. Our main tests with the Fendt tractor was to compare the efficiency of the electrified rotary rake with the current marketed machine in the same field conditions and the same settings. For the electrical driven machine, the input power was calculated by multiplying the input current and the input voltage. For the hydraulic driven machine, the power was obtained by measuring the rotation speed and the torque at the PTO. During all the tests, more than 100ha have been raked.

Figure 5 shows the instantaneous values of the input power of the electrical driven machine. On the graph we can identify the headlands and see that during work the power can vary significantly with some peaks up to 30kW.

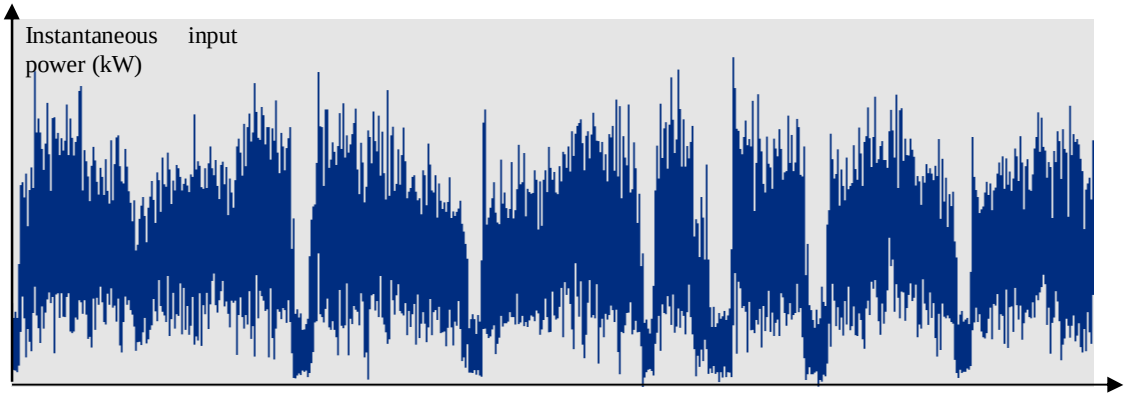

Figure 5. Electrical machine input power measurements

Additionally, we tested the work of the torque limitation of the motors which ensures sufficient lifetime for the belt and the mechanical parts of the rotors. We logged also some data coming from the inverters like motor speed, motor temperature, inverter temperature… to validate that they stay in their normal working limits.

3.2. Results

Figure 6 and Figure 7 show the comparison of the average power measurement for both machines: the hydraulic driven GA 13131 and the electrical driven eGA.

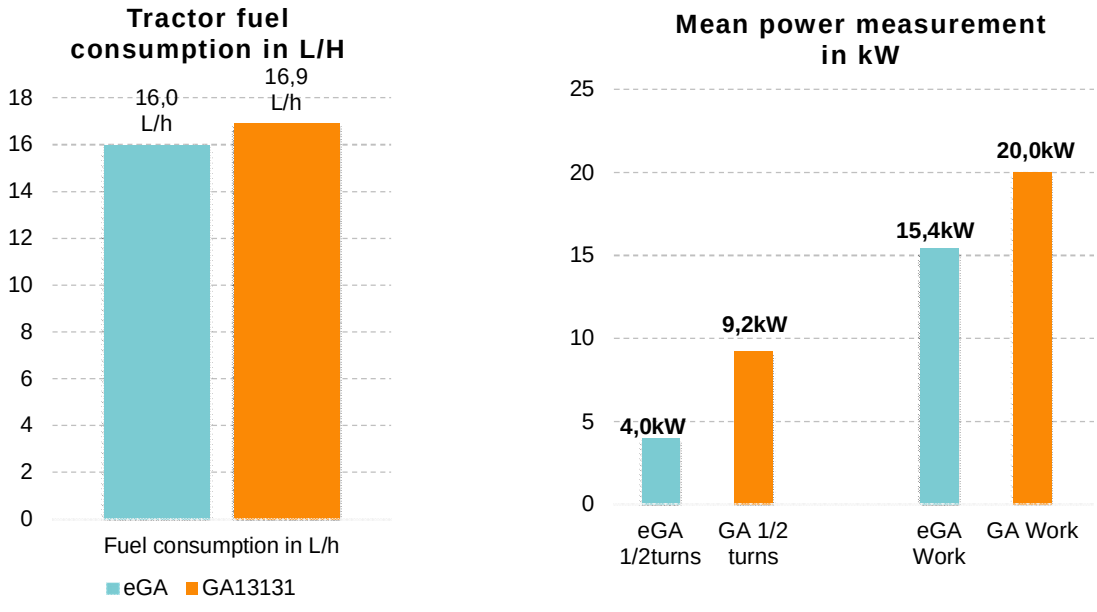

Figure 6. Tractor fuel consumption

Figure 7. Machine power needs

These tests results confirm our first expectations that the electrical driven machine will have a better efficiency than the hydraulic driven one. On the eGA, 23% of power is saved vs. the GA 13131. But this measured power doesn't include the efficiency of the electrical power generator. To consider the whole power chain, we measured also the fuel consumption of the tractor. By comparing these 2 values, we could determine that approximatively 1 liter of fuel per working hour could be saved with the electrical driven machine compared to the current marketed one. This represent a 5.3% fuel consumption reduction.

By comparing the power needed by the eGA and the fuel consumption of the tractor, we concluded that a large part (approx. 2/3) of the fuel is used by the tractor to pull the machine. As a consequence, the fuel savings resulting from the improvement of the efficiency remains small. This will for sure be an argument, but it will not be the main point today to justify the cost increase of the electrification of a rotary rake. The counter-part of the increased costs shall be found within the possibilities to improve the working process of the machine.

Thanks to the field tests, we also learned that there could be good benefits for the tractor driver to be able to survey some inverter values, i.e. the instant torque developed by the motors. In fact, this value reflects the reel working conditions of the machine. If these values are too high, this can result from a large amount of forage or from a wrong setting of the machine parameters, i.e. the working height of the rotors. This could also open the possibility to automate some settings of the machine, like the working height of the rotors which is key for a proper harvested hay.

Finally, we could also observe clogging of the motor fan in very dry conditions (hay). Even in this case, we have not seen any overheating of the motors, due to the fact that hay is very light and the power needed to rake hay is relatively low.

4. Conclusions

Thanks to our various tests and the experience we gained, we have shown that it is possible to use 700V DC electrical power to drive agricultural machines like a 4-rotor rotary rake. Moreover this study show the availability of commercial off-the-shelf electrical drive parts adapted to the agricultural machinery. The efficiency of both electrical driven and hydraulic driven machines were compared and the first results show the improved efficiency of the electrical driven machine together with the possibility to automate some functions or to collect and display real time data. Thanks to that data, the driver can adapt the machine settings to improve the raking process. Unfortunately, these arguments are today not sufficient to counter-balance the cost increase resulting from the expensive electrical parts which could reach up to 100% because of small volumes.

Some other benefits of the electrification could be more comfort due to the simplification of many operations for the driver, like speed changing, rotor working height adjustments … The connection between tractor and machine is also easier. Moreover, like hydraulic driving parts, electrical parts need no maintenance. There is also an environmental advantage because there is no oil leak risks. On the other hand, there could be some risks of being electrocuted, but this risk is reduced through an adequate protection system.

All these arguments could justify the electrification of an agricultural machine. Besides, the availability of electricity on the tractor or from a generator opens doors for powerful electrical actuators and for completely redesign the machines. This could enable significant improvements of agricultural processes.

The AEF – Powering Precision Farming with ISOBUS

Andrew Olliver
Team Lead Communication and Marketing, AEF
Email: andrew.olliver@cnhind.com

Abstract

This paper describes the work of the AEF – the Agricultural Industry Electronics Foundation – against the backdrop of the challenges that agriculture is facing today and in the future, and how cross-manufacturer compatibility of agricultural equipment relates to these issues. The organization is working on several topics relevant for improving compatibility and establishing transparency, which have been reviewed in this paper.

After that the AEF tools aimed at achieving these goals, i.e. the AEF ISOBUS Functionalities Concept, the AEF ISOBUS Conformance Test and the AEF ISOBUS Database, are examined

Keywords:
Agricultural equipment, compatibility, efficiency, electrification, farm management information systems, ISOBUS, ISO XML

1. Introduction

The increasing dynamics of agricultural markets poses a number of challenges for agriculture. Such as the scarcity of resources, climate change and the increasing demand for food and renewable materials. Consequently producers are facing the need for an increase of productivity. At the same time environmental sustainability has become one of the key issues in agriculture. Thus all technical and technological possibilities should be considered for a sustainable increase of efficiency and productivity (IVA, 2017).

Manufacturers of agricultural machinery play a crucial role in providing these technical solutions. Electronics are the key to making machinery more efficient, precise and economical, especially when combined with precision farming techniques. ISOBUS is one of the most important techniques for precision farming.

But although agricultural equipment manufacturers have been marketing a number of ISOBUS innovations, for years these have mostly been proprietary solutions. The lack of compatibility between machinery from different manufacturers resulting from this often led to frustration among customers; reliability of ISOBUS combinations in the field could only be achieved by purchasing all equipment from the same manufacturer. Apart from the fact that customers usually prefer to have a choice, only few manufacturers offer such a comprehensive range of products. Especially the European market is characterized by a number of equipment specialists.

Today compatibility across manufacturers or brands is increasingly considered as a competitive advantage. This renunciation of the idea that customers should buy all their machinery from one manufacturer fuels the desire for standards within the industry (AEF, 2012, p. 5 ff.).

1.1 Scope and limitations

This paper seeks to explore the AEF's work and its contribution to agriculture in its entirety. However, the complexity of topics involved does not allow covering everything in-depth. A more detailed exploration will be limited to farm management information systems (FMIS) and electrification of agricultural equipment.

1.2 Aim and Objectives

The aim of this paper is to explore the AEF's work and how it contributes to facing the challenges of agriculture.
This will be accomplished by fulfilling the following objectives:

1. Clarify issues related to the standardisation of agricultural equipment
2. Give an overview of the topics the AEF is working on. Special attention will be given to FMIS and the electrification of agricultural equipment.

2. Materials and Methods

The AEF's strategy to work against the above mentioned problems rests on two cornerstones – improving compatibility of agricultural machinery and establishing transparency towards customers.

The first part of the following section will review the issues relating to the standardisation of ISOBUS products.

The second part will give an overview of the topics the AEF is working on, with special attention to electrification of agricultural equipment and farm management information systems. Lastly this section will introduce the AEF Plugfests.

2.1 Compatibility – Issues

Customers tend to think that with machinery supporting ISOBUS anything is possible. But in practice it is not quite that easy. How well the components of an ISOBUS system work together depends on what they have in common, i.e. the functions supported by all of them. A lack of conceptual clarity regarding these functions has caused additional confusion, also among manufacturers.

A fully equipped ISOBUS system consists of various components, which all operate like small computers, such as the Terminal, Joystick, tractor and implement ECUs (Electronic Control Unit). The implement ECU is usually installed in the implement; which it controls, provides data and processes the user's command. The tractor ECU is the tractor's 'job calculator'; it provides information such as speed, power take-off RPM etc. on the Bus.

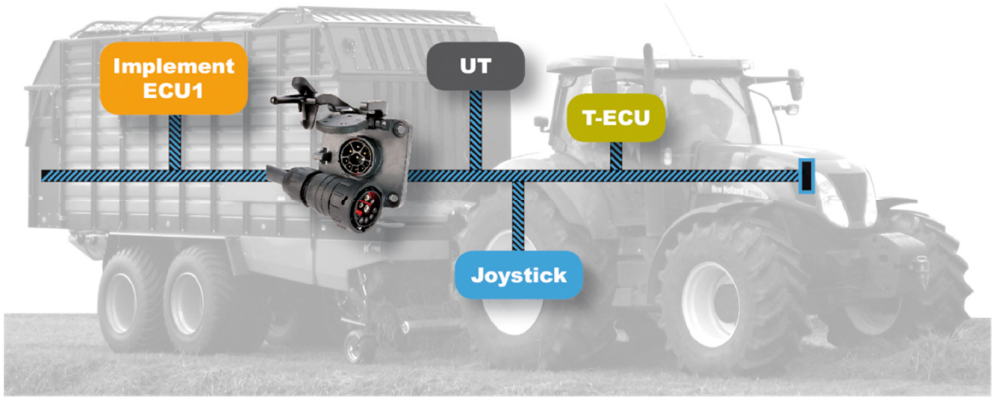

Figure 1: Components of an ISOBUS system (AEF, 2015).

The worldwide ISO 11783 (ISOBUS) standard defines the communication between agricultural machinery, mainly tractors and implements, and also the data transfer between these mobile machines and farm software applications. It incorporates parts of the previous standards LBS (DIN 9684) and the North American SAE J1939 and uses the same 29 bit CAN 2.0b protocol. But although ISO 11783 is of greater global significance and technically more comprehensive than the previous standards, it leaves room for interpretation.

2.2 The AEF Project Teams

The project teams form the basis of the AEF. Experts from member companies are working together in international teams to find solutions beneficial for the industry and, above all, for customers. Eleven teams exist to date, each assigned with a special topic. The scope of topics has extended from solving (compatibility) problems related to ISOBUS to other areas such as electric drives, high speed ISOBUS and farm management information systems, thus also addressing future demands.

The teams meet regularly and once a solution for a specific problem is found and agreed they draw up a guideline. These guidelines are detailed technical specifications created to complement the ISO standard to make it as clear and precise as possible, and to ensure new innovations are being incorporated. This aims at providing for improved cross-manufacturer compatibility of agricultural equipment. Together with the ISO 11783 standard, the AEF ISOBUS Guidelines should be used as the basis for manufacturers' to development ISOBUS products.

Final, released AEF Guidelines are sent to the ISO committee. With the next revision of the ISO 11783 a new AEF Guideline will typically be integrated into the standard. However, the creation of the international standard remains the task of the ISO – the International Organization for Standardization (AEF, 2012, p. 6 ff.).

Project Team 1: Conformance Testing

The primary objective of this team is to provide and maintain a state-of-the-art testing and certification process, which ensures that the ISOBUS components are fully compatible. The formal certification process is designed for execution by independent test institutes. The tools and protocols for these trials are also available to the agricultural industry as a whole in order to support the development of ISOBUS compliant components across the board.

Project Team 2: Functional Safety of Electronic Controls

The mission of this project team is to develop application guidelines for all manufacturers of agricultural equipment when safety related applications using the ISOBUS according to ISO 11783 are to be implemented. In this case all legal directives and standards such as ISO/DIS 25119, ISO 15077 have to be taken into consideration.

Project Team 3: Engineering and Implementation

The task here is to coordinate the market introduction of new ISOBUS features across the agriculture industry while continuing to monitor the ISOBUS engineering and implementation processes.

Project Team 4: Service and Diagnostics
The main task is to service combined ISOBUS systems from different OEMs. (The same high quality standards must be met between brands as for individual manufacturers). The result should become tangible with quick and efficient troubleshooting in order to achieve complete customer satisfaction. In addition the issue of technical documentation, exchange of information, FAQs and training are to be tackled here.

Project Team 5: ISOBUS Automation
This group is working on the definition of ISOBUS automation systems, referring to either tractor implement management systems or sequence control. Tractor implement management is where an implement can request control of certain tractor functions whereas sequence control is a headland management system, which blends tractor and implement functions into a single system that can be activated by the operator. Both scenarios rely on a robust security protocol and authentication procedure.

Project Team 6: Communication and Marketing
The marketing project team assumes marketing responsibility for ISOBUS technology both in the agriculture equipment industry and throughout the farming community. The focus is placed on promoting ISOBUS in the market and establishing the new ISOBUS Certified Label as the unique brand. To achieve this, the group coordinates various activities such as participation at industry conferences, shows and exhibitions along with corporate design and PR programs.

Project Team 7: High-voltage On-board Networks
Electric drives are becoming increasingly important in agricultural technology, as they have a number of significant advantages over hydraulic drives or PTOs. They are more precise, efficient and offer more possibilities for automation, and will thus pave the way for a new generation of agricultural equipment.
The basic idea behind the work of project team 7 is, that electric motors of marketable implements should be compatible with every tractor model, and that the output of the tractor should be the only limitation of power.
What has long been missing was a standardized interface for both direct and alternating current capable of providing enough power for large electric motors. The team was formed in 2010 and consists of four subgroups that have been working on mechanical and functional compatibility to ensure both safe and reliable operation. One of the most important milestones was reached in 2016 when the specification of the interface was finalised. The interface should be ready for launch this year.
Since the importance of ISOBUS technologies today and in the future is undisputed within the AEF, the decision that high-voltage on-board networks should be based on ISOBUS was a fundamental one, i.e. ISOBUS is necessary for the power supply of the implement.
The new interface delivers 700 V direct current, or three-phase 480 V alternating current with up to 150 kW power.

Project Team 8: Camera Systems
The first goal of this team was to find a solution for harmonizing the connectivity between cameras mounted on an implement and terminals mounted on the tractor. The solution focuses on today's needs for camera systems with analogue image transmission. Complex camera applications with digital image transmission were then added to the agenda (AEF, 2017a).

Project Team 9: Farm Management Information Systems (FMIS)
While the standardisation of the electronic interface between tractor and implement has been the initial focus of the AEF, the growing importance of data handling and exchange in agriculture has led to the creation of a team to deal with the standardisation of the ISO XML interface, i.e. the interface between the Task Controller and the FMIS (AEF, 2015a). A Task Controller is a control unit in the Terminal and serves as the link between farm computer, Terminal and implement ECU. It receives data coming from the farm computer, such as orders for field work, and transfers them via the CAN-Bus to the implement. The Task Controller is thus also responsible for the configuration and compression of data. Furthermore it manages the DGPS (Differential Global Positioning System) position and the corresponding nominal value from an application map and the actual value based on the current position. The Task Controller collects all this information and sends it back to the farm computer when the work is done. There are different ways of exchanging data between the Task Controller and Farm Management Systems, such as via USB, Bluetooth, WLAN or mobile communications (AEF, 2012, p. 24).

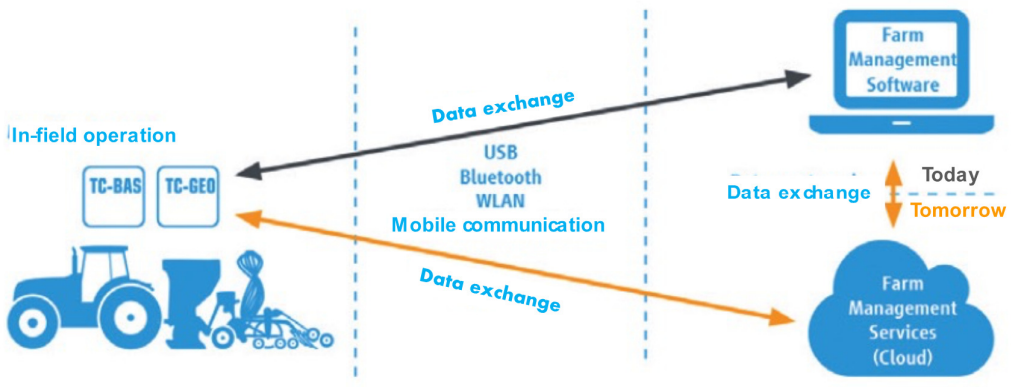

Figure 2: Data exchange between mobile machines and Farm Management Information Systems (AEF, 2015, p 2)

The ease of exchanging and handling data stands or falls with the industry defining a standard for interfaces which considers all necessary aspects of data exchange, and which can be implemented by manufacturers, i.e. tractor and implement manufacturers as well as farm software manufacturers, with a manageable effort. For customers, products which use these interfaces should be easy to handle and provide real added value (AEF, 2015b).

Project Team 10: High-speed ISOBUS
To meet the growing demand for data communication on ag equipment, this project team is exploring concepts for increasing bandwidth on the Bus.
The team's work will also pave the way for integration of new features and functions, such as the expansion of diagnostics, the support of electric drives, M2M communications, and connection of real-time video systems.

Project Team 11: Wireless In-field Communication
This team focuses on selecting suitable radio standards (such as WLAN) for machine-to-machine (M2M) communications. They will also examine communications encryption and functional reliability.
M2M communications allow machines to communicate directly while working together. A secure and standardized in-field radio communication system is required so that machines can control each other or simply exchange status information such as position, speed, and fill level. Also machine-to-FMIS-communication is covered by this team (AEF, 2017a).

2.3 AEF Plugfests

Plugfests are events for member companies to 'plug and play' with ISOBUS products and thus test compatibility against each other. Therefore they are an opportunity for manufacturers to test and adapt products before submitting them to the AEF ISOBUS Conformance Test.
They take place twice a year, alternately in Europe and USA. At the last plugfest in Bologna, Italy 215 attendees and 125 products amounted to more than 2200 individual terminal/implement combinations to be tested. Often necessary adjustments can be made on location to establish compatibility, while other issues require more work back home at the company. Over the past years the number of attendees has increased constantly. The next Plugfest takes plays from May 8th to 12th in Lincoln, Nebraska (AEF 2017a).

3. Results

The work of the AEF has resulted in three important 'tools', which will be explained in this section. However, they all link together and serve the aim of improving cross-manufacturer compatibility and establishing transparency towards customers.

3.1 The AEF ISOBUS Functionalities Concept

As a first step in order to provide clarity regarding the compatibility of ISOBUS products the AEF has developed the AEF ISOBUS Functionalities concept. Each functionality is specified in a guideline. To customers a functionality can be explained as an independent 'module' on the ISOBUS providing specific benefits. Figure 3 shows the functionalities that exist today. However, the concept is designed to be open, i.e. new ones can be added. In fact, a number of functionalities are currently being developed.
As mentioned in section 2.1, for the compatibility of ISOBUS systems the functionalities all components have in

common are decisive. For example, a customer will not be able to use section control with a sprayer, unless tractor, as well as terminal and sprayer support this functionality. The AEF Functionalities concept facilitates explaining the benefits of ISOBUS products in a clear and consistent way. Furthermore it is the basis for the AEF Conformance Test (AEF, 2012).

Figure 3: Overview of AEF ISOBUS Functionalities (AEF, 2017b)

3.2 The AEF ISOBUS Conformance Test and Certified Label

As described in the previous section, together with the ISO standard the AEF Guidelines should be the basis for developing ISOBUS products. But to ensure the highest possible degree of reliability for customers the AEF has developed the AEF ISOBUS Conformance Test. It is designed to prove that ISOBUS products actually support a specific functionality. Five independent test laboratories can carry out the test – ISOBUS Test Centre (ITC) and DLG Test Centre in Germany, Reggio Emilia Innovazione (REI) in Italy, Kereval in France and Nebraska Tractor Test Laboratory in the USA. Functionalities are tested separately, so manufacturers can choose which of them they would like to have tested.

If a product has passed a test it is 'AEF Certified' and allowed to bear the 'AEF Certified Label'.

With the release of a new functionality the necessary test protocols are integrated into the conformance test, i.e. each functionality can be certified.

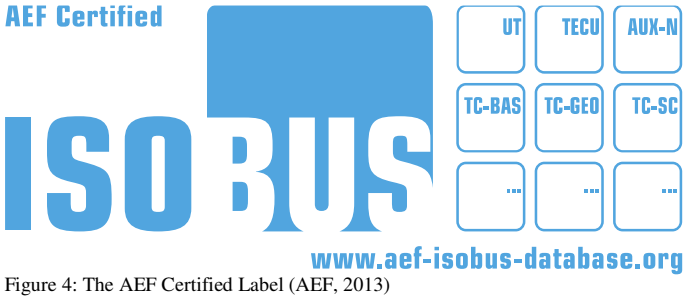

Figure 4: The AEF Certified Label (AEF, 2013)

The AEF Certified Label states that the respective ISOBUS product complies with the ISO 11783 standard and the additional AEF Guidelines. Only products that have passed the certification process may be advertised with the label. The three empty squares below the functionalities imply that the concept is extendable. However, regardless of the specific functionalities certified, the label will be the same, i.e. it does not indicate for which functionalities the product has passed a conformance test. This information can be found in the AEF ISOBUS Database (AEF, 2017a).

3.2.1 AEF Conformance Test for Farm Management Information Systems

Project Team 9 has been working on extending the AEF Conformance Test to include a test for Farm Management Information Systems. Then FMIS manufacturers could certify their products via this Conformance Test for the different functionalities, namely TC-BAS and TC-GEO.
AEF Certified FMISes could then be seen in the AEF ISOBUS database. This would allow the customer to search the database for compatible systems, for example: this green tractor, this red seeder, this yellow terminal and this blue FMIS show common functionalities. This information will give the customer piece of mind before making a new equipment purchase.
The test will check the functionalities of an FMIS system for both import and export of XML files.

3.3 The AEF ISOBUS Database

The AEF ISOBUS Database is the tool specifically developed for the agricultural public, and here is where all things come together – it shows all AEF Certified ISOBUS products.
'How can I be sure, that the implement I buy is fully compatible with my tractor on the farm? And what features can I use with this combination?' The database provides answers to these and other questions that users of agricultural equipment are confronted with. Thus the AEF seeks to clarify the compatibility of ISOBUS products towards customers, but also towards dealers and service technicians.
With a few mouse clicks users can check which functionalities a certain product supports and moreover, which functionalities a certain combination of tractor, terminal and implement supports.
The database offers three different options for checking compatibility.

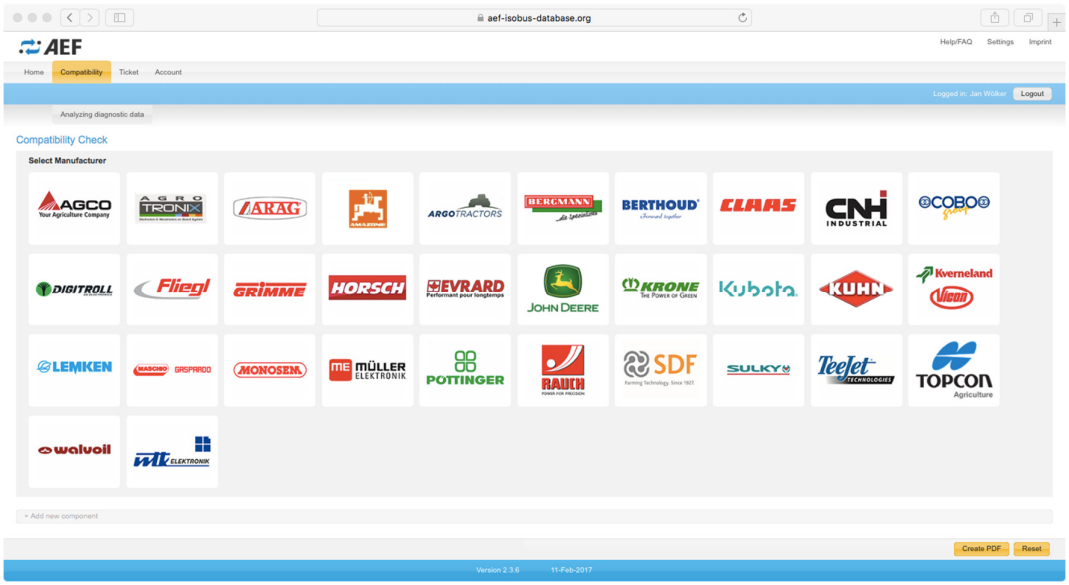

Figure 5: Manual Compatibility Check by Manufacturer (AEF, 2017c)

Figure 5 shows one of the options. A click on 'Manufacturer' shows all manufacturers that are currently represented in the database. Selecting one of them takes the user to an overview of the manufacturer's product range, such as tractors, drills or electronic components. If available a subcategory, e.g. precision drill, must be selected to see all matching products that are listed in the database. Clicking on one of the products will then show all available information regarding supported functionalities and certification.

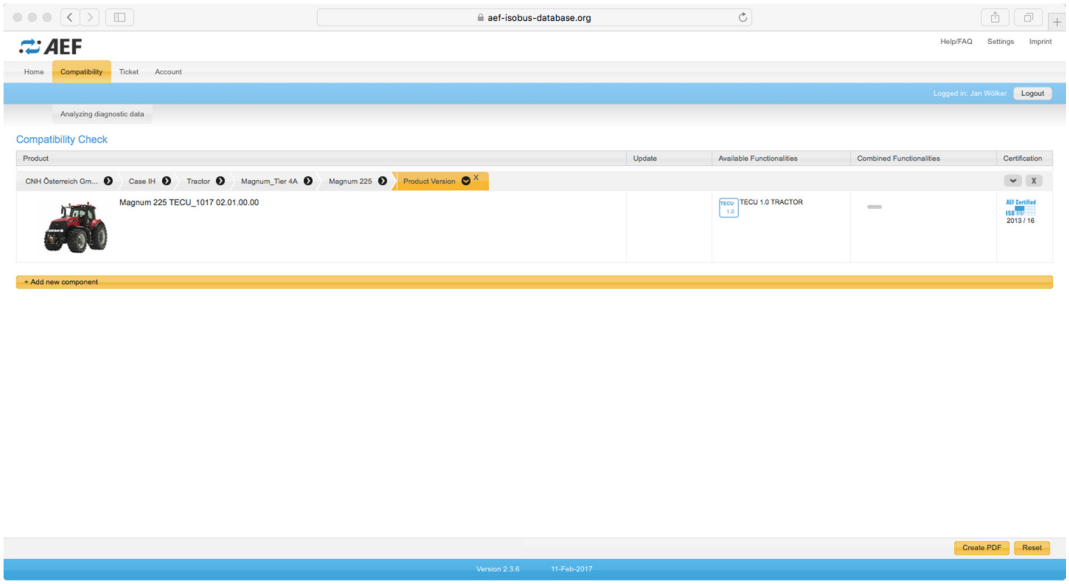

Figure 6: Product Selection (AEF, 2017d)

If a user wants to check the compatibility of products the next step would be to add another component, a precision drill, for example. After selecting the subcategory the user has to select a functionality they would like the product to support.

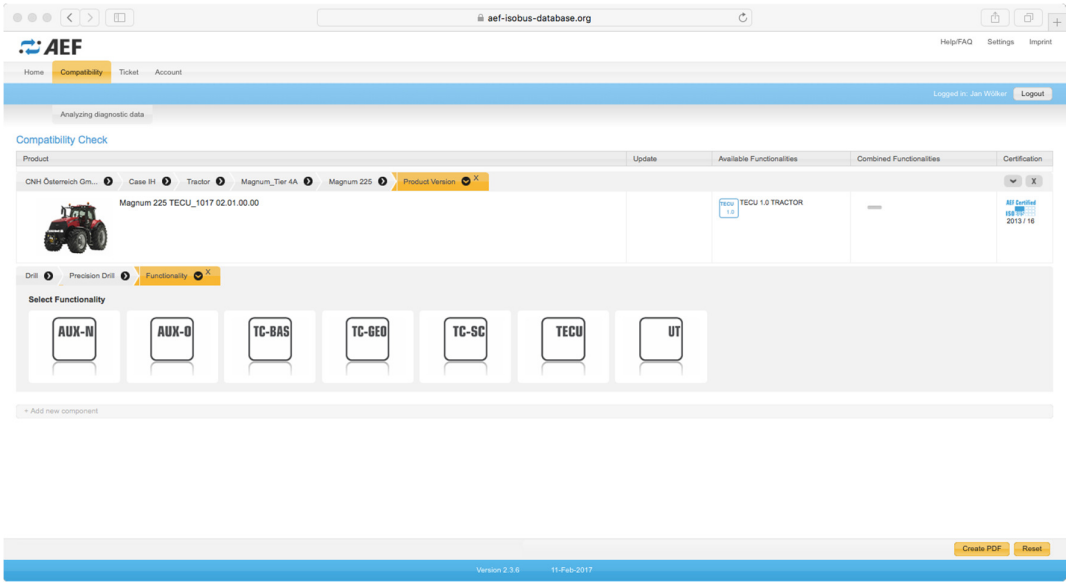

Figure 7: Selection of Functionality (AEF, 2017e)

In the next step manufacturer, product and product model must be chosen. The selected product will then be added to the compatibility check.

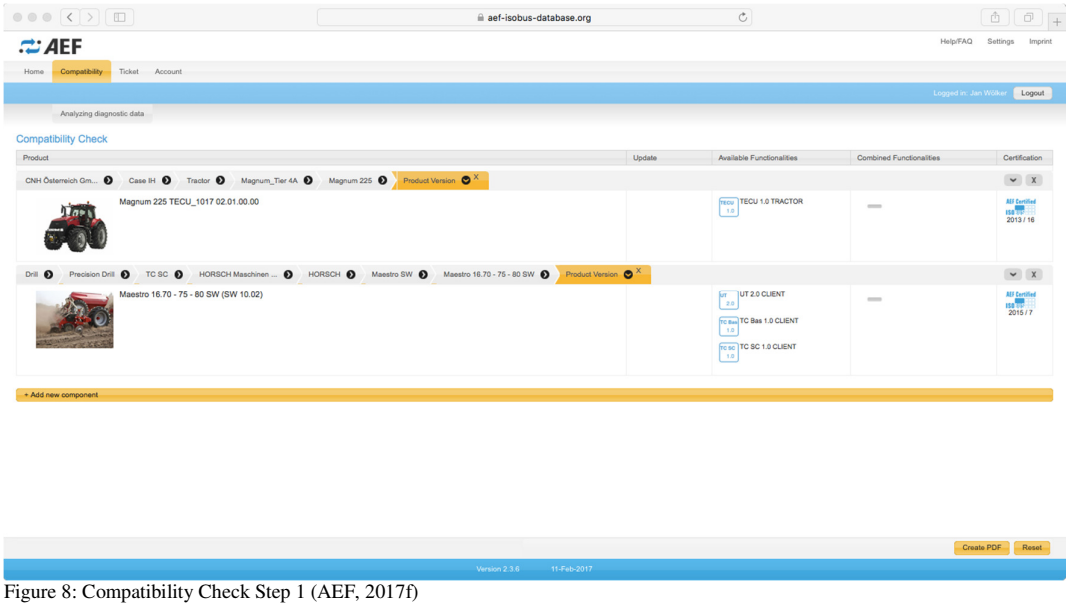

Figure 8: Compatibility Check Step 1 (AEF, 2017f)

Again the database shows which functionalities this specific product supports. But as can be seen in Figure 8 the row titled ‘Combined Functionalities’ is still empty, because an ISOBUS system requires a terminal. This can be added in the next step, again starting with the overview of manufacturers.
With the selected terminal also the combined functionalities appear in the compatibility check. These are the ‘lowest common denominator’, and only these can be used with this combination of ISOBUS products.

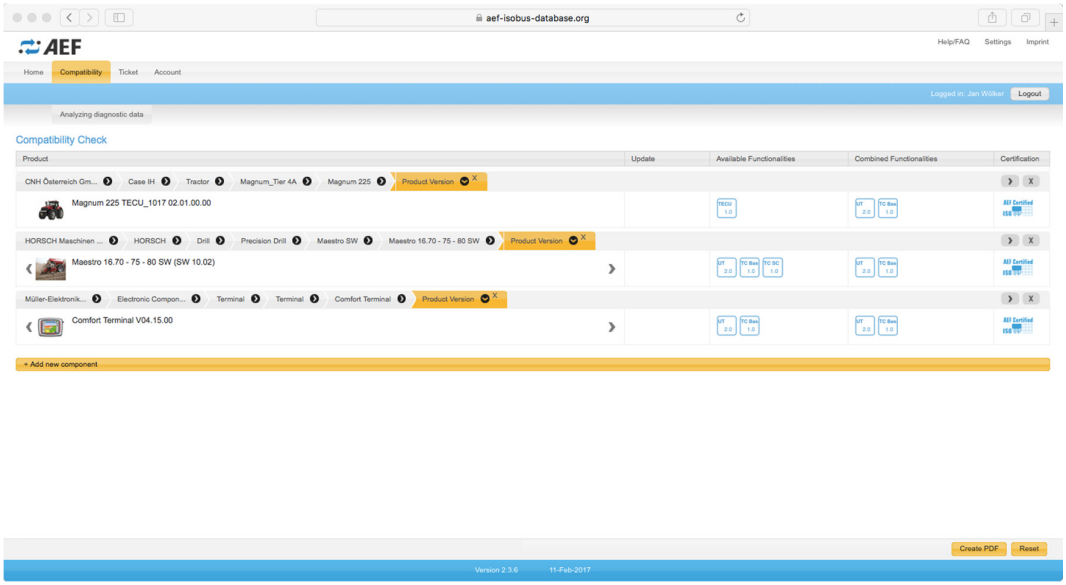

Figure 9: Compatibility Check Step 2 (AEF, 2017g)

As mentioned above the database offers additional ways of searching for products. One of them is to begin with selecting a product category. Then the functionalities available in this category will be displayed, and with a click on one of them the user can choose manufacturer and product.

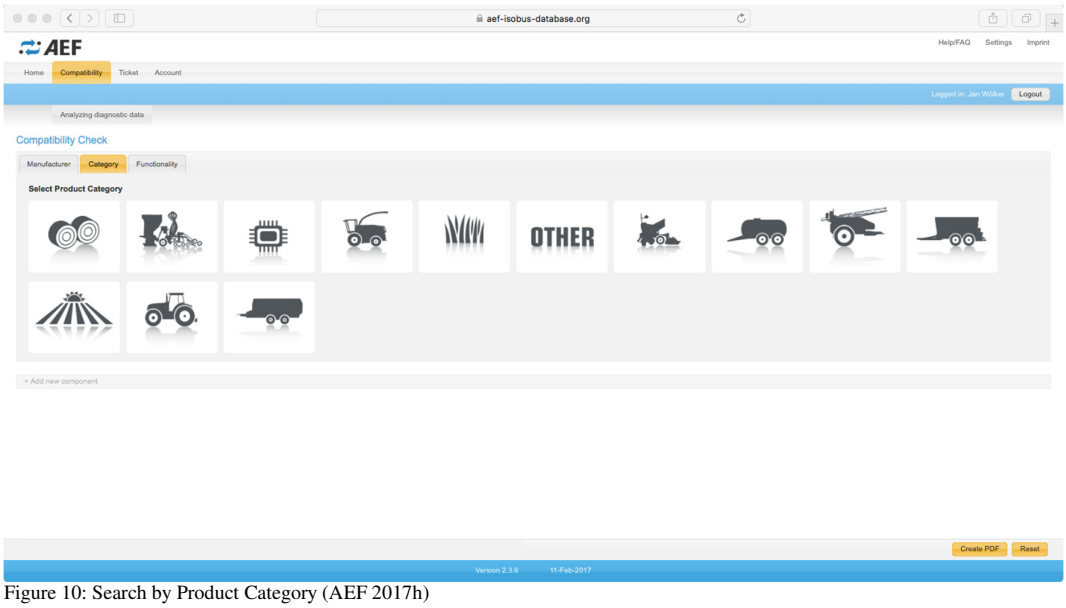

Figure 10: Search by Product Category (AEF 2017h)

A third way of searching for products in the database is to first select a functionality, and then product category and manufacturer.

Dealers can use the compatibility check to support sales conversations and advising customers, but also to speed up troubleshooting through customer service.
Lastly the industry collects reports about problems with ISOBUS systems and these remain available in the database as ISOBUS ‘knowledge’. Service technicians can use them to diagnose and find solutions for problems on the field more quickly (AEF, 2017a).

4.Conclusion

To face the challenges of agriculture today and in the future technical innovations by manufacturers of agricultural equipment are crucial. However, due to the great number of manufacturers and brands on the market, proprietary solutions will only benefit a very small percentage of farmers and contractors. At the same time, a lack of compatibility and usability and, moreover, reliable information about those issues tends to prevent customers from adopting new and innovative technologies.

With the ISOBUS Functionalities and Conformance Test the AEF has developed powerful tools that help customers to work as efficiently as possible and to comply with environmental regulations at the same time.

In the past customers had to purchase an additional terminal with every new implement to ensure there were no compatibility issues when working in the field. However with the AEF ISOBUS Database it is now up to the customer. Some might prefer to have a single terminal for every application, while others prefer to have more than one, maybe when using more complex applications, such as section control. However, with the information provided by the database customers can choose their supplier based on their individual needs and preferences.

Since both membership and the use of the AEF ISOBUS Conformance Test are voluntary, the success of the organisation and thus its contribution to agriculture as a whole depends on the joint effort of the industry.

References

AEF 2012. Hersteller-übergreifende ISOBUS Systemlösungen.

AEF 2013. AEF ISOBUS Certified Label.

AEF 2015a. AEF ISOBUS conformance test for farm management information systems.

AEF 2015b. Will exchanging data be easy?

AEF 2017a. http://www.aef-online.org Accesssed February 12th 2017

AEF 2017b. Overview of Functionalities.

AEF 2017 c-h. Compatibility Check. https://www.aef-isobus-database.org/isobusdb/login.jsf Accesssed February 12th 2017

IVA – Industrieverband Agrar, 2017. Nahrungsmittel für die Welt: Herausforderung für die Landwirtschaft. http://www.iva.de/moderne-landwirtschaft-sichere-versorgung-mit-hochwertigen-lebensmitteln/nahrungsmittel-fuer-die-welt-herausforderung. Accessed February 12th 2017

Aerial multispectral imagery for site specific weed management

Marine Louargant[a,b], Corentin Cheron[b]*, Nathalie Vigneau[b], Gawain Jones[a], Sylvain Villette[a], Christelle Gée[a]

[a] Agroécologie, AgroSup Dijon, INRA, Univ. Bourgogne Franche-Comté, F-21000 Dijon, France - 26, bd Docteur Petitjean BP 87999 21079 DIJON, France

[b] AIRINOV, 157 Bd Marechal Mc Donald, 75019 PARIS, France

* Corresponding author. Email: corentin.cheron@airinov.fr

Abstract

AIRINOV Company is offering its precision agriculture services to monitor agronomical variables of fields from experimental observations. The Unmanned Aerial Vehicle (U.A.V.) is automatically guided using a GPS and is loaded with a 4-band sensor (from 400 to 850 nm) offering a spatial resolution up to 6 cm/px. The resulting images allow a high precision mapping to characterize infield variability of weed infestation. We developed a method to detect inter-row weed in row-crop. It is based on a Fourier Transform to estimate row tilt, a Hough Transform to isolate crop rows and a connected component analysis to refine the discrimination. This method has been evaluated on sugar beet and maize fields. Prior testing has been conducted on images from a commercial service with a resolution of 6 cm/px to assess the weed detection potential of the U.A.V. Then, algorithm performances have been tested on higher resolution images (0.6 cm/px) to evaluate the possible improvements relying on spatial resolution. A test service has been conducted and prescription maps are presented and discussed. First results are promising but further work is required for them to be validated.

U.A.V., multi-spectral images, weed detection, map

1. Introduction

European regulations aim to reduce the environmental impact of agricultural practices. Diminishing chemical use is a major component in this matter and can also help improving the cost effectiveness of the production. New tools are required to characterize field heterogeneity for a site-specific management.

Regarding weeding operations, numerous researches have been conducted to detect weed occurrence from images acquired by sensors embedded on agricultural machines (Burgos-Artizzu et al., 2011). The very high resolution of the obtained images allows shape analysis and species recognition (Ahmed et al., 2012). However, the sensor proximity to the soil restrains to a small field of view and the resulting images are difficult to process due to perspective effect. Other studies showed that Quickbird satellite images can be used to detect big enough weed patches (Castro et al., 2013). In that case, the low resolution of these images prevents the detection of scattered weeds.

An Unmanned Aerial Vehicle (U.A.V.) with an embedded image acquisition system is a good compromise between these approaches as it allows the quick covering of big areas with high resolution images. With a proper image processing this acquisition vector have already been used for agricultural purposes such as water stress localization (Abuzar et al., 2009), some crop disease detection (Lan, 2009) or nitrogen needs (Goel et al., 2003). Concerning weed management U.A.V. can become an asset to detect and map weed occurrence, giving a global view of an infested field and allowing a temporal monitoring (Vioix, 2004).

AIRINOV is a French young company specialized in agronomical decision support tool using images acquired from U.A.V. (www.airinov.fr). Their services are dedicated to farmers (nitrogen application map for rape and wheat), seed companies, researchers or experimental platforms. Data produced by AIRINOV are relevant in different areas: phenotyping, nitrogen application, crop counting (sunflower, maize…) and weed localization.

Previous studies focused on weed detection from images acquired by embedded optical sensors to perform a site-specific spraying (Bossu, 2007; Jones et al., 2009). From these studies we developed a weed detection algorithm to process U.A.V. images. These images from a field are geometrically and radiometrically corrected and combined in a single orthoimage. The resulting orthoimage is not suffering perspective effect and is georeferenced so it can be easily overlapped over a field map.

In this paper we present a method to discriminate crop from weed in aerial images to provide weeding prescription map to farmers.

2. Materials and Methods

Provide sufficient details of the materials and methods to allow your work to be reproduced.

2.1. Materials

A multiSPEC 4C by AIRINOV multispectral digital camera, comprising of four 1.2 Mpix CMOS channels and an incident light sensor, is used to acquire images in four precise spectral bands: (550BP40, 660BP40, 735BP10 and 790BP40). The focal length is 3.6 mm and when combined with the CMOS pixel pitch of 6 µm, the resulting field of view is 67° by 54°. The sensor is comprised of an ARM CPU for acquiring a frame (the synchronous acquisition of the 4

bands) and a SD card slot for recording the frames. Optionally the sensor can be connected to an external GPS, for geotagging the frames in real time. The resulting physical weight is 165 g and 200 g, respectively without and with the GPS option.

For this experiment, two configurations where used in order to acquire the images. An eBee fixed-wing drone from senseFly was used to fly the camera at 55 m above ground and a mast was used for ground acquisition 3 m above ground with resulting resolutions of 6 cm and 0.6 cm respectively.

The senseFly eBee drone weighs 700 g and can fly up to 45 minutes with the multiSPEC 4C camera. Its nominal airspeed is 12 m/s making the highest resolution possible for mapping 6 cm at 55 m when keeping acceptable motion blur. It is programmed using the eMotion software provided by senseFly. The software allows grid mapping with specified lateral and longitudinal overlap. The acquisition density was around 20 frames per hectare. A field of 20 ha was acquired in a 20-minute flight.

A wooden mast was used to raise the camera 3 m above ground, and provide data at a very high resolution. The targeted resolution of 0.6 cm was achieved, even if the raw optical resolution was 3 mm. The camera was easily battery powered and the GPS option was used. The mast was moved by a human following an adapted flight plan with a defined pace and line spacing. The acquisition density was around 1.2 frames per square meter or 620 times more than the drone acquisition.

The images are processed in two steps: first a photogrammetric software (Pix4DMapper by Pix4D) is used to assemble the frames, register the four channels and create an orthomosaic, then different algorithms written in Python and MATLAB are used.

The acquisitions were performed on row crops mostly developed in France: maize and sugar beet. The row spacing goes from 35 to 80 cm. The acquisition date were selected at early stages (2-3 leaves), corresponding to the time to spray herbicide. At this stage, the rows of the crops can be clearly identified on the crops.

For this study, we focus on a maize field situated in the French Oise department, of a size of 16 ha. The field is infested by thistles (Cirsium arvense) from seedling to rosette stage and white goosefoot at stage seed leaf.

2.2. Methods

In the first part we present the pre-processing steps required to create the orthoimages, then we will focus on the algorithms developed to discriminate crop from weeds.

Image pre-processing:

a) Radiometric and geometric correction

Vignetting is a radiometric error produced by the sensor and optic used to acquire images. It leads to a light fall off for the pixels located at the periphery of the images. This error can be statistically corrected by computing the mean brightness of each pixel for the whole image set, resulting in “vignetting” map. The correction is obtained by subtracting this map to each image.

Geometric distortion is caused by the optic of the sensor; it can be corrected with a reverse distortion modelled from the camera intrinsic characteristics. In this case, the distortion is modelled with 3 radial distortion coefficients and 2 tangential distortion coefficients (Brown, 1965).

b) Orthoimage creation

To create the mosaic of the scene each image has to be georeferenced and the scene geometry needs to be assessed. The whole processing is automated: search of points of interest and pairing, beams adjustment to improve the shooting geometry, geometric reconstruction of the soil (Digital Surface Model, DSM) and images projection on this DSM (Hartley et Zisserman, 2004). These steps lead to the creation of an orthoimage picturing the whole studied area.

Image Analysis:

The flowchart presented in **Erreur ! Source du renvoi introuvable.** provides a global overview of the method used to process field orthomosaic images and deduce the corresponding weed infestation map.

Since the input orthomosaic image corresponds to a field of several hectares, this image is first divided in a set of small images in order to improve the efficiency of the image processing in terms of computer memory use and also to increase information homogeneity in each sub-image (e.g. soil colour, vegetation status). Moreover, reducing the size of sub-images ensures crop rows to be straight lines in the image. Nevertheless, the size of the sub-images needs to be large enough to show a sufficient number of crop rows.

The first step consists in obtaining a binary image corresponding to the vegetation. Considering the spectral properties of soil and vegetation, the NDVI (Normalized Difference Vegetation Index) value is first computed to enhance the contrast between soil and vegetation pixels in the NDVI image (figure 2a). The binary image (figure 2b) of the vegetation is then deduced from this NDVI image using the Otsu’s thresholding method (Otsu, 1979) which maximizes the inter-class variance.

The second step of image processing consists in segmenting the sub-image in homogenous region regarding the orientation of crop rows. This is obtained by transforming the sub-image into a frequency domain using the Fast Fourier

Transform. In the frequency space the presence of peaks reflects the spatial characteristics of the original image. Thus, filtering this space provides the segmentation of the image and the mean value of crop row orientation for each region.

Third, the locations the crop row axes are deduced from the binary vegetation image using the Hough Transform (Hough, 1962). Thus, the original image is transformed into a radius-angle parameter space (Duda and Hart, 1972) in which the location of peaks provides the location of the crop row axes (figure 2c) in the original image. The size of the parameter space is optimized thanks to the approximate value of the row orientation resulting from the previous Fourier Transform.

Forth, for each vegetation pixel, the discrimination between crop and weed is performed considering the location of the pixel with respect to the edge of crop rows and also considering the shape of the vegetation regions when they intersect crop rows. The borders of crop rows (figure 2d) are defined by linear interpolations through the side edge pixels of each vegetation regions lying along the row axes. Then, the vegetation pixels lying between the row borders are classified as crop pixels and the vegetation pixels lying in the inter-row space are classified as weed pixels. In order to improve the discrimination between crop and weed (figure 2e), some additional classification rules are taken into account. For each region of connected pixels which crosses a row, the area, the orientation and the minor axis length of the region are computed. The classification rules are then as follows:

- if the area is lower than the square of the row width, then the region is classified as crop,

- if the orientation is in a range of more or less 5° around the row crop orientation, and if the area is higher than the square of the row width, then the region is classified as unknown,

- for all other cases or if the minor axis length is higher than the inter-row space, then the region is classified as weed.

Concerning the unknown regions, the pixels remain classified as crop if they lie between the row borders and as weed if they lie in the inter-row.

These classification rules have been set empirically, considering results obtained on images of maize and sugar beet.

All sub-images are processed independently before being stored and put together to provide the final infestation map of the whole field.

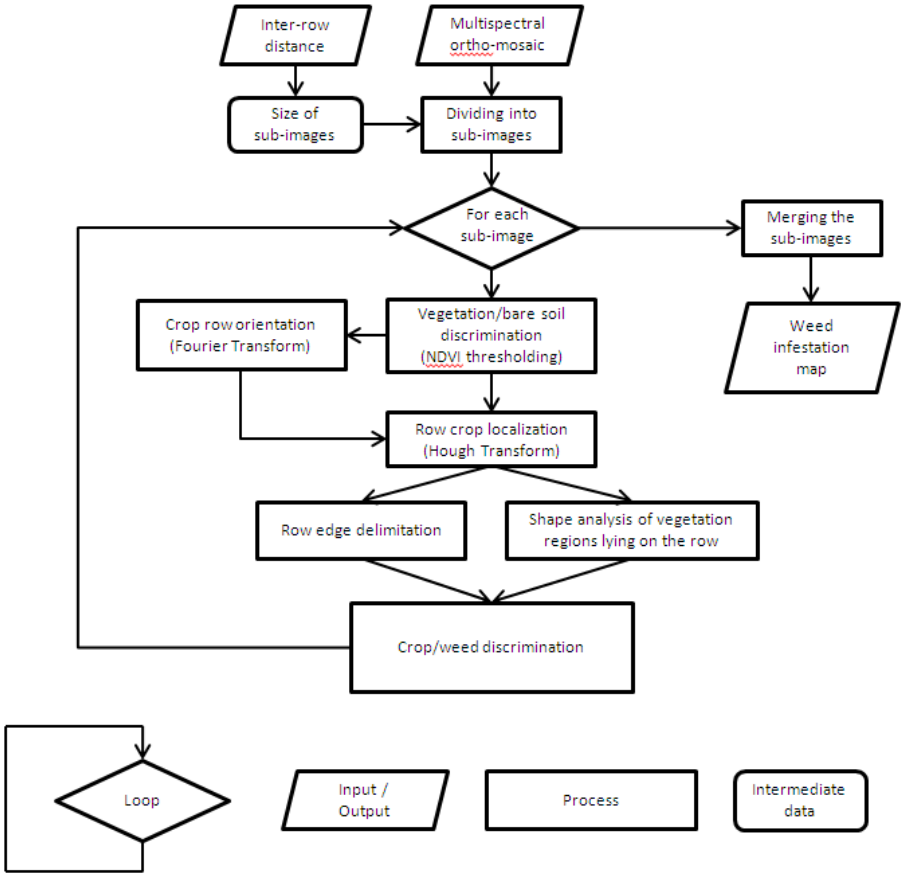

Figure 1: Flowchart of the image processing used to establish the weed infestation map.

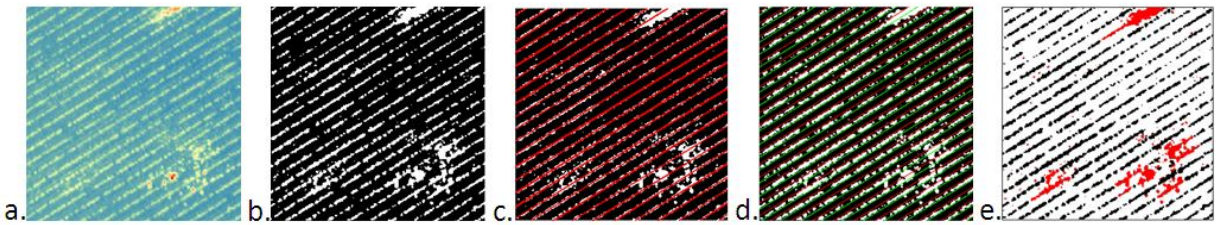

Figure 2: Successive steps of image processing: NDVI image (a), binary image of the vegetation (b), row axis detection (c), row edge determination (d), crop/weed discrimination (e).

3. Results and Discussion

This section first explores a pilot phase of site-specific weed management. Following these results, one sees limits of interpretation of these images (spatial resolution: 6cm) and new tests are realized with images of high spatial resolution (6mm).

3.1. A pilot phase

One of the applications is to offer a 'weed management' service for the farmer. Discussions with farmers and crop consultants were done in France and the service interest was validated. Flying over the crop field, an orthoimage is created and a weed infestation map is deduced. A first result of prescription map in is presented Figure 3 in the case of a maize field.

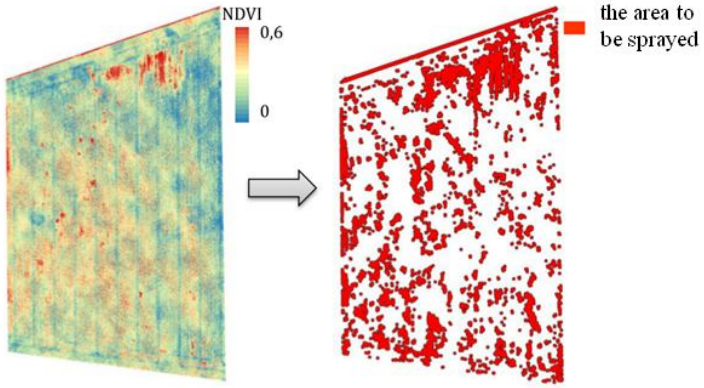

Figure 3: Orthoimage (left) of a maize field and prescription map (right).

The farmers' best wish is to have an application map compatible with their tractor GPS displays for remedial herbicide treatments. A pilot phase was run over two seasons in collaboration with farmers. Their feedback was positive in the correct detection of the weed areas. Some drawbacks in the application workflow were found: in order to take into account the relative positioning error between the application map and the tractor positioning system, round buffers of 5 m were created around every weed detected. This resulted in the application maps covering nearly 100% of the field is some cases. Moreover, the farmers experienced some difficulties with the compatibility and accuracy of the tractor GPS displays.

It could be possible to optimize the shape of the buffer to take into account multiple factors: the tractor GPS and drone GPS relative position error, the herbicide spraying accuracy and the direction of the crop rows and thus the moving direction of the sprayer. RTK GPS can be used for both the tractor and the drone (for example with the eBee RTK from senseFly) to get centimetric accuracy at an extra cost. The spraying precision can be assessed, for example, by placing paper band on the ground around a spot, Pérez-Ruiz et al. (2015). Then the buffer around each detected weed can be shaped as an ellipse with the major axis parallel to the tractor moving direction, see Figure 4.

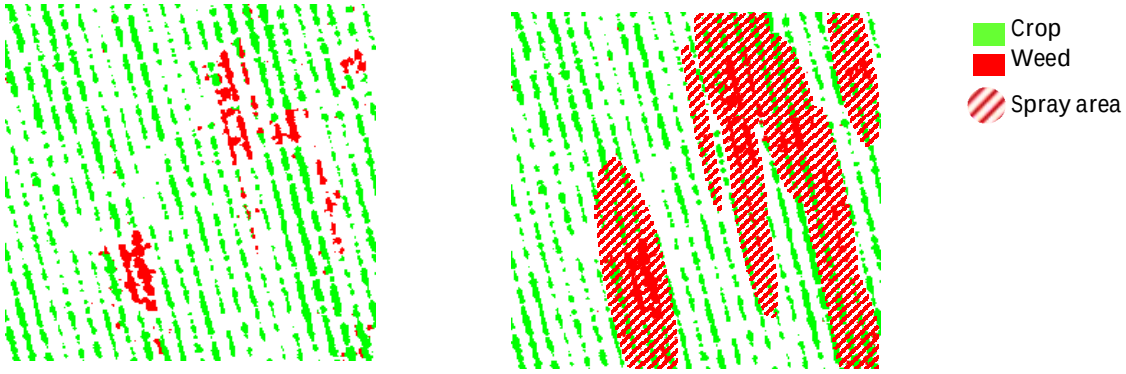

a. Weed detection using the spatial algorithm

b. Elliptic buffer generated with minor axis of 2.5m

Figure 4: Application map with optimized ellipse.

Finally, tests in collaboration with sprayer manufacturers could be done to further reduce the size of the spraying ellipse and reach significant herbicide saving.

3.2. Towards improved image quality

The classical AIRINOV flight height is 55 m above the ground that induces a 6cm/px spatial resolution of aerial images. Results about a sugar beet field are presented in Figure 5. As observed in Figure 5a and 5b, the weed infestation image informs farmers about areas with a strong weed pressure. NDVI sub-image (5 m x 5m) is rough image and the discrimination between crop and weed can be considered to a first general approach. According to the weeding context, the information may be sufficient for a specific application spraying, limited to a specific treatment such as weed patches for example. This type of images is very useful for farmers because the reduction of herbicides is obvious. But it is not sufficient to clearly discriminate the weed from the crop. To improved image quality, a mast was used for ground acquisition 3 m above ground with resulting resolution of 0.6 cm. The Figure 5c and 5d present NDVI image and crop/weed detection image. The results demonstrate the potential of a very high spatial resolution to improve the crop/weed discrimination and to obtain accurate weed detection. In this case, this type of images should be interesting for farmers for early detection of new weed plants or for monitoring weed plants.

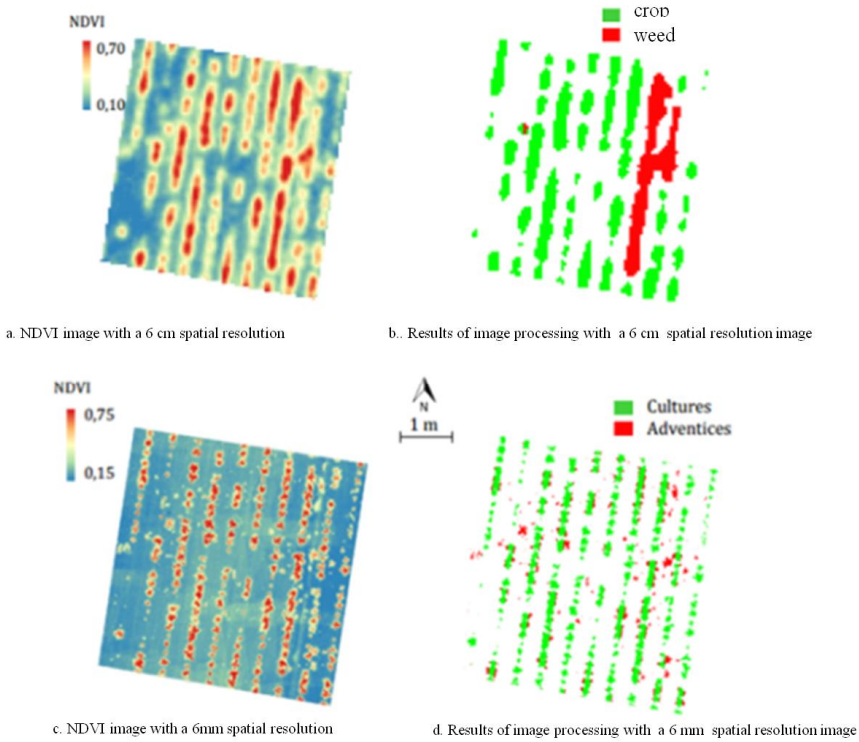

a. NDVI image with a 6 cm spatial resolution

b.. Results of image processing with a 6 cm spatial resolution image

c. NDVI image with a 6mm spatial resolution

d. Results of image processing with a 6 mm spatial resolution image

Figure 5 :. Effect of spatial resolution on crop/weed discrimination – (Crop: sugarbeet).

For both cases (Figure 5b and 5d), algorithm results are then compared with georeferenced floristic readings. A confusion matrix is used on different images to evaluate the quality of a classification and the Table 1 presents average results concerning the True Crop Rate (TCR) and the True Weed Rate (TWR). With a 0.6 cm spatial resolution, both rates (TCR and TWR) are clearly improved and the dispersion of measurements is obviously reduced (σ).

Table 1. Confusion matrix: results of True Crop Rate (TCR) and the True Weed Rate (TWR) for both image resolutions.

Spatial resolution	μ_{TCR}	μ_{TWR}	σ_{TCR}	σ_{TWR}
Images (6 cm/ pixel)	0.4738	0.7570	0.293	0.188
Images (0.6 cm/pixel)	0.877	0.7798	0.040	0.066

These results indicate that TWR is 75 % in the case of 6 cm/px resolution. This value has been slightly (78%) improved working with a 0.6 cm/px resolution. The conclusion is that weed detection is finally not too bad in with a spatial resolution of 6 cm/px. However, the TCR reveals a low value in the case of 6 cm/px resolution compared to 0.6 cm/px resolution.

The development of a weed management service is possible in both cases depending on the type of weeding. For a fine weed management, it requires a high spatial resolution and so a flight height of few meters. Therefore, the actual AIRINOV drone technology needs to be improved and adapted considering probably a UAV multi-rotor to deliver an infestation map of high quality. However, for a fine service, an economic study must be carried out to estimate the efficiency and cost in terms of technical and economic feasibility of such a service.

4. Conclusion

This study was dedicated to explore the feasibility of establishing a weed management service from UAV. Firstly, the multispectral aerial images have been processed to discriminate crop from weed using the classical AIRINOV flight technology: flying wing at a flight altitude of 50 meters. Then a mast was used for ground acquisition 3 m above ground. Developing a dedicated crop/weed discrimination algorithm for sugar beet and maize field, we demonstrate that a weed management service is possible depending on the image quality and so its spatial resolution (6cm/pixel or 0.6 cm/px). A 6 cm/px is sufficient for a global weed location and for detection weed patches and a 0.6cm/px will be more dedicated for early weed plants. In both cases, the TWR is up to 75% whereas the TCR is improved with images with 0.6 cm/px. It indicates that if AIRINOV wishes to continue this new service with a high quality, it needs to reflect on its technical innovations in order to maintain acceptable profitability.

This project is supported by AIRINOV Company and the ANRT (Association Nationale de la Recherche et de la Technologie). This study is also supported by the program “ANR CoSAC” (ANR-14-CE18-0007.

References

Abuzar, M., O’Leary, G., Fitzgerald, G., 2009. Measuring water stress in a wheat crop on a spatial scale using airborne thermal and multispectral imagery. Field Crops Research 112, 55-65.

Ahmed, F., Al-Mamun, H.A., Bari, A.S.M.H., Hossain, E., Kwan, P., 2012. Classification of crops and weeds from digital images: A support vector machine approach. Crop Protection 40, 98-104.

Bossu, J., 2007. Segmentation d'images pour la localisation d'adventices. Application à la réalisation d'un système de vision pour une pulvérisation spécifique en temps réel. Le2i - UP-GAP. Université de Bourgogne, Dijon.

Brown, D.C., 1965. Decentering Distortion and the Definitive Calibration of Metric Cameras. Annual Meeting of the American Society of Photogrammetric Engineering

Burgos-Artizzu, X.P., Ribeiro, A., Guijarro, M., Pajares, G., 2011. Real-time image processing for crop/weed discrimination in maize fields. Computers and Electronics in Agriculture 75, 337-346.

Castro, A., López-Granados, F., Jurado-Expósito, M., 2013. Broad-scale cruciferous weed patch classification in winter wheat using QuickBird imagery for in-season site-specific control.Precision Agriculture, 1-22.

Duda, R.O., Hart, P.E., 1972. Use of the Hough Transformation to detect lines and curves in pictures. Communications of the Association for Computing Machinery 15, 11-15.

Goel, P.K., Prasher, S.O., Landry, J.A., Patel, R.M., Bonnell, R.B., Viau, A.A., Miller, J.R., 2003. Potential of airborne hyperspectral remote sensing to detect nitrogen deficiency and weed infestation in corn. Computers and Electronics in Agriculture 38, 99-124.

Hartley, R. I., et Zisserman, A., 2004. "Multiple view geometry in computer vision" Cambridge University Press , ISBN: 0521540518.

Hough, P.V.C., 1962. Method and means for recognizing complex patterns.

Jones, G., Gée, C., Truchetet, F., 2009. Modelling agronomic images for weed detection and comparison of crop/weed discrimination algorithm performance. Precision Agriculture 10, 1-15.

Lan Y.H., Martin D. E., Hoffmann W. C., 2009. Development of an airborne remote sensing system for crop pest management: system integration and verification. Applied Engineering in Agriculture 25(4), 607-615.

Otsu, N., 1979. A Threshold Selection Method from Gray-Level Histograms. IEEE Transactions on Systems, Man, and Cybernetics 9, 62-66.

Pérez-Ruiz, M., Gonzalez-de-Santos, P., Ribeiro, A., Fernandez-Quintanilla, C., Peruzzi, A., Vieri, M., Tomic S., Agüera, J., 2015. Highlights and preliminary results for autonomous crop protection. Computers and Electronics in Agriculture 110, 150-161.

Vioix, J., 2004. Conception et réalisation d'un dispositif d'imagerie multispectrale embarqué : du capteur aux traitements pour la détection d'adventices. Le2i - UP-GAP. Université de Bourgogne, Dijon, p. 219.

Autonomous navigation of a platform with UVc-light to prevent crop infestation by powdery mildew

Andreas De Preter [a,*], Jan Anthonis [b] , Peter Melis[c], Jan Swevers[d], Goele Pipeleers[d]

[a] PhD Baekeland at Octinion, Interleuvenlaan 46, 3001 Leuven-Heverlee, Belgium

[b]Industrial supervisor at Octinion, Interleuvenlaan 46, 3001 Leuven-Heverlee, Belgium

[c] Research Centre Hoogstraten, Voort 71, 2328 Meerle, Belgium

[d]Scientific supervisor KU Leuven, Celestijnenlaan 300 - bus 2420, 3001, Leuven, Belgium,

* Corresponding author. The author is member of the MECO Research Group, which is an associated research lab of Flanders Make. Email: andreas.depreter@octinion.com

Abstract

Powdery mildew on strawberry plants is a constant menace wherefore growers have to spray up to three times every two weeks to keep the susceptible crop healthy. Trials at Research Centre Hoogstraten with vehicles carrying UVc-modules show a useful working rate of UVc-light in preventing infestation. An automation is necessary to reduce the labour cost of this treatment.

This paper proposes an autonomous platform for driving accurately between crop rows in greenhouses. It uses an Ultra Wideband system to position the vehicle instead of accurate GPS, which is unreliable indoors. The performance was improved by an extended Kalman filter (EKF).

To control the platform, a Model Predictive Controller is implemented. It looks forward to its future reference. With a mathematical model, a prediction of its desired behaviour is made. It will try to eliminate the deviation from its reference, without performing too aggressive actions.

A prototype platform was designed and tested to navigate in a greenhouse. Results show that the specifications regarding the accuracy and constant speed are met. More work has to be done on the positioning system, as it suffers from distortion when people or objects block the sight.

Keywords: MPC, EKF, UWB, greenhouse, indoor positioning

1. Introduction

1.1. Background and requirements

The strawberry industry in Belgium has gone through a serious transformation: it evolved from a local business to a modern organization with a yearround cultivation. This is possible by using multiple cropping systems and several plant dates in cooling cells. In order to stay competitive in the global strawberry-market, a research program was set up in the Research Centre Hoogstraten to optimize the techniques and plant performances in the future.

Nowadays strawberry plants suffer from numerous diseases and pests which causes damage to a developing crop. One of these diseases is powdery mildew. It is a constant menace and the disease pressure builds up towards summer and autumn. Growers have to spray regularly to keep the susceptible crop healthy. The spraying program is adapted to the disease pressure in the season, but can add up to three sprayings every two weeks. A total of 10 different active ingredients is not a curiosity in autumn cultivations to be sprayed on the developing crop. The use of pesticides, besides health concerns, means a big cost in labour for the grower.

Trials at Research Centre Hoogstraten show a useful working rate of UVc light in preventing crop infestation by powdery mildew. At least every 48 hours the plants have to be lighted with a UVc-treatment. The treatment proved to be highly effective and could suppress mildew on the crop with a 70-90% working rate. The harvested strawberries remained completely free from mildew infestation. The trials were done by pushing a vehicle carrying several UVc-modules to generate a sufficient intensity at crop level. Dealing with powdery mildew manually by using UVc-light, takes too much time and therefore automation is necessary in order to make it a competitive alternative to spraying.

The goal of this project is to introduce an autonomous platform that carries the UVc-modules. The platform has to navigate through the greenhouse at a constant speed. Maintaining a constant speed is very important: if the platform drives too fast, the mildew will be underexposed, while the plant will get burned when it drives too slow. Apart from the speed the accuracy of following a trajectory between the croprows is also very important. In order to not hit any objects or get too close to the plants the navigation accuracy has to be around 3 to 5 cm. Eventually the whole system has to be affordable and easy to install.

1.2. Research on autonomous navigation in agriculture

During the last decade a lot of research was done on the topic of autonomous navigation in agricultural environments. (Bakker, et al., 2010) proposes a systematic design approach for the development of an autonomous platform for robotic

weeding. This work gives an overview of sensors which can be used for navigating along the row. The device which provides the best absolute position, is the RTK-GPS. Commercial devices claim to have an accuracy of 25 mm. To determine the crop rows even better, this data has to be fused with some local information provided by machine vision (camera that identifies the crops), tactile sensors (touch the crops, which can cause damage), ultrasonic and optical sensors (both measure the distance of the robot to the crop).

(Dong, et al., 2011) developed a row guidance system for an autonomous robot for asparagus harvesting. The positioning of the vehicle is done by an RTK-GPS in combination with a vision system. It has a control scheme with traditional PID-controllers to follow one crop row. Experimental results show that a tracking accuracy of 0.5 cm is achieved.

(Kraus, et al., 2013) developed a combination of a moving horizon estimator (MHE) and a nonlinear model predictive controller (NMPC) for navigating a small tractor. The standard kinematic model was extended with slip parameters to cope with uncertain terrain conditions. The tractor is equipped with an RTK-GPS, wheel encoders and a potentiometer on the steering wheel. A similar research subject was covered in (Backman, et al., 2012), where a tractor with a trailer had to navigate autonomously in order to minimize the trajectory deviation of both the tractor and the trailer. The system consists of an extended kalman filter (EKF), which uses data from a GPS and IMU. For controlling the tractor an NMPC was also used.

1.3. Positioning in a greenhouse

The topics described above are all applications on large, outdoor fields. The application in this work concerns about navigating between crop rows in a greenhouse. Because of this restriction, a (precious) GPS system would have a reception of too bad quality in order to be useful in this type of environment. Therefore a local, indoor positioning system (IPS) has to be installed inside the greenhouse to simulate the outdoor GPS. This system needs to have an accuracy similar to an accurate GPS, needs to be installed easily and has to be affordable. (Deak, et al., 2012) provides a survey of commercial indoor localisation systems. The technologies used are Radio Frequency Identification (RFID), Ultra-wideband (UWB), Wireless LAN and Field Strength systems. The conclusion of this survey is that the ideal technology for indoor positioning does not exist, but the choice depends on the specifications required in each application. (Liu, et al., 2007) provides similar results.

Regarding the accuracy that is specified in 1.1**,** the UWB-technology has the right specifications to meet the requirements. This technology has a sufficient resolution without losing too much on signal range (Liu, et al., 2007). The UWB-system is an active IPS: minimum 4 modules, further called beacons, have to be put in the corners of the area that needs to be covered. One module, further called the tag, has to be installed on the vehicle. With the right settings and environmental conditions, these modules can range up to 200 meters. Compared to accurate GPS the cost of such system is very reasonable.

1.4. Goals and outline

The goal of this project is to investigate if it is possible to develop a mobile platform that can navigate in greenhouses using the UWB-technology with the requirements specified in 1.1 (these are: driving at a constant speed with an accuracy of 3 to 5 cm).

The outline of this paper is as follows: Section 2.1 discusses the mobile platform and how to model it, Section 2.2 and Section 2.3 provide a brief overview of the methods used for respectively on how the platform is positioned and controlled. Section 2.4 adds some remarks on the reference trajectory that was applied on the system. The results were shown and discussed in Section 3. Section 4 concludes the paper.

Figure 1: The robot used for testing: in the greenhouse (on the left) and schematically (on the right)

2. Materials and Methods

The autonomous navigation of a platform can be divided in two main parts: a. estimating the state of the platform and b. the control algorithm. Both algorithms are based on a vehicle model. This is discussed in Section 2.1. The state estimation algorithm is discussed in 2.2, the controller in 2.3. During the first tests a strange phenomenon was discovered in the UWB-positioning. Adjustments on the reference trajectory are explained in Section 2.4

2.1. Mobile platform

The two-wheel platform could be modelled with an advanced dynamic model where all forces acting on the vehicle are taken into account. However in order to have a good approximation about the interaction between the wheels and the soil, a tire-force model has to be included. Determining the parameters of this model is very difficult as they depend on many factors like weight-balance, type of soil and type of tire. In order to take these parameters into account, a lot of extra sensors are required for additional information. Eventually this also has complications for the control algorithm, as this results in a more complex control problem.

To avoid this inconvenience, a kinematic model was used. This model assumes that tire-ground contact is ideal and no slip occurs. The kinematic equations are as follows:

$$\begin{cases} \dot{X}_c = v_x \cdot \cos(\theta) \\ \dot{Y}_c = v_x \cdot \sin(\theta) \\ \dot{\theta} = \omega_z \\ v_x = \dfrac{v_l + v_r}{2} \\ \omega_z = \dfrac{v_r - v_l}{b} \end{cases} \tag{1.1}$$

In these equations, (X_c, Y_c) is the centre position between the two driving wheels in a global reference frame as shown in Figure 1. The other differential state is the yaw angle θ. The algebraic equations show the relationship between the wheel velocities v_l and v_r of respectively the left and right wheel, and the more general velocities v_x and ω_z, respectively the longitudinal and rotational velocity of the vehicle. The parameter $b = 0.65\ \text{m}$ is the length between the two rear wheels.

The motors of both wheels are controlled by a drive with its own control loop. The behaviour of the motor is described with a 2nd order function to model the voltage-speed transient.

The model of the system will be the base of both the estimation algorithm and the controller, which will be discussed respectively in Sections 2.2 and 2.3.

2.2. State estimation

The state estimation of the platform generates a decent value of the vehicle state vector. This state vector consists of the coordinates of the vehicle, its orientation and its corresponding velocities as discussed in Section 2.1**.** Only a part of these states are provided by sensors, which are also affected by measurement noise. In order to have a good estimate of all the elements a state estimation algorithm was implemented. The controller needs an accurate estimate of the state to avoid problems of stability.

The Kalman filter represents the probability of the state at time t with a mean and a variance. To update these parameters it requires the control outputs (coming from the controller) and measurements (from sensors, in this case: the UWB system). The estimation model and measurement equations of this algorithm are of the following form:

$$\begin{aligned} \hat{x}_{k+1} &= f_d(\tilde{x}_k, u_k) + w_k \\ \hat{y}_k &= h(\hat{x}_k) + v_k \end{aligned} \tag{1.2}$$

In these equations, f_d is the discretized version of the vehicle model described in section 2.1, h is the measurement function, $\hat{x}_k$ is the prediction and $\tilde{x}_k$ the final estimation of the new state at time k. It is assumed that the states and measurements are independently affected by White Gaussian Noise w_k and v_k. For more details the reader is referred to (Thrun, et al., 2006).

The UWB-system measures the time it takes to send messages between the tag and the beacons. With the Time Of Flight (TOF) and the speed of light, a distance can be calculated. These distances have to be recalculated to an absolute (X_d, Y_d) position of the tag. The distances represent a sphere around each beacon (whereof the coordinates are fixed and known). The intersection points of the spheres is the position of the tag. This is done by minimizing the sum of a nonlinear least-squares function (see (Liu, et al., 2007)):

$$\min_{X_d, Y_d} \sum_{i=1}^{4} \left(r_i - \sqrt{(X_i - X_d)^2 + (Y_i - Y_d)^2 + (Z_i - Z_d)^2} \right)^2 \tag{1.3}$$

In this equation (X_i, Y_i, Z_i) are the known coordinates of beacon i , r_i is the respective distance measurement and (X_d, Y_d, Z_d) are the coordinates of the tag, with Z_d the height of the tag which is fixed and known.

The measurement equation h in equation (1.3) is then:

$$\begin{cases} X_d = X_c + L \cdot \cos(\theta) \\ Y_d = Y_c + L \cdot \sin(\theta) \end{cases} \tag{1.4}$$

with L the distance of the tag with respect to the rear axis. One can see that putting the UWB-tag at a length L of the wheel axes benefits the observability of the orientation state.

2.3. Control algorithm

The control algorithm eliminates the deviation with respect to a given reference trajectory by imposing control outputs on the actuators, in this case the two motors. A promising technique is model predictive control (MPC). An introduction of this method is given based on (Grüne & Pannek, 2011).

MPC is an optimization based method for the feedback control of systems. On every time instant an optimization problem is solved, optimizing the control over a finite time horizon based on a prediction of the corresponding state trajectory. The first solution is then applied to the system, after which the state of the system is measured again. The whole cycle will then repeat.

The prediction of the state is done by a model of the system:

$$x(0) = \tilde{x}(t_n), \qquad x(k+1) = f_d(x(k), u(k)) \quad k = 0, \ldots, N-1 \tag{1.5}$$

with $\tilde{x}(t_n)$ the estimation of the current state at time t_n and $x(k)$ the prediction in the future on discrete time steps k. Here, f_d is the discretized form of the system model (1.1). A piecewise constant control $u(k)$ is assumed on each interval**.** The behaviour is predicted on the discrete interval $t_{n+1}, \ldots, t_{n+N}$, with N the horizon length.

The inputs $u(0), \ldots, u(N-1)$ are optimized such that the predicted state $x(k)$ lies as close as possible to a reference state $x_{ref}(k)$ for $k = 1 \ldots N$. Hence the difference between these two will be used as objective to be minimized in the optimal control problem. Typically also reference values for the control $u_{ref}(k)$ are defined.

To increase stability of the control problem, a terminal penalty term is also added (Kraus, et al., 2013)**.** This puts a higher weight on the final predicted state of the horizon to be sure it lies on its reference.

The cost-function that has to be minimized is a weighted quadratic sum of these three criteria and is of the following form:

$$F(x,u) = \sum_{k=1}^{N} \left\| x(k) - x_{ref}(k) \right\|_A^2 + \sum_{k=1}^{N} \left\| u(k-1) - u_{ref}(k-1) \right\|_B^2 + \left\| x(N) - x_{ref}(N) \right\|_C^2 \tag{1.6}$$

with A, B and C symmetric, positive-definite weighting matrices. The reference trajectory $x_{ref}(k)$ and reference control $u_{ref}(k-1)$ are assumed to be provided in advance for the whole horizon $k = 1, \ldots, N$.

In order to get optimal feedback, the first solution of the optimal control values $u(0)$ will be applied at the system.

This procedure is repeated at the next timestamps $t_{n+1}, t_{n+2}, \ldots$ with each time the new predicted state $\tilde{x}(t_{n+1}), \tilde{x}(t_{n+2}), \ldots$ as starting point.

In practice, there are also boundaries u_{min}, u_{max} on the control values due to hardware limitations (e.g. the maximum voltage applied on a motor). Also boundaries x_{min}, x_{max} on the system state can be defined (e.g. a restricted area where the

robot is not allowed to drive). To prevent this type of unsatisfactory behaviour, these boundaries are also included in the optimal control problem.

The whole problem is then formulated as follows:

$$\min_{x(\cdot),u(\cdot)} \; F(x,u)$$

$$\text{subject to: } \begin{cases} x(0) = \tilde{x}(t_n) \\ x(k+1) = f_d(x(k),u(k)) \\ x_{min} \le x(k) \le x_{max} \\ u_{\min} \le u(k) \le u_{max} \end{cases} \tag{1.7}$$

The optimization problem with a least squares objective function is solved with multiple shooting which is incorporated with a generalized Gauss-Newton method. In order to speed up the iterative method, the real-time iteration scheme of (Diehl, et al., 2002) was implemented. The main idea is to minimize the number of iterations to 1, in order to be able to generate quick process feedback. Each new optimization problem will be initialized intelligently with the solution of the previous one. This gives convergence results which are similar to classical solution methods, but with the advantage of very fast feedback (Kraus, et al., 2013).

The controller was implemented with the ACADO Code Generation toolkit. This software package exports customized real-time iteration algorithms (Houska, et al., 2011) by self-contained C-code which can run on embedded hardware. The tool is as open-source software under the LGPL license and can be downloaded at http://www.acadotoolkit.org

2.4. Trajectory

When the first tests were analysed, the results showed that the platform drove very accurately on the reference trajectory. However a men's eye could perfectly see that the vehicle was performing one big curve. Further investigation of the positioning system showed that the UWB distance measurements contain a constant bias, which was different for each beacon. This bias deforms the coordinate system.

In order to eliminate this effect, a curved trajectory was programmed which compensates the deformation. This was done with the following procedure: the platform was put manually on different points on the line in the middle of the crop rows. For each point the calculated UWB position (the result of equation (1.3)) were averaged out and a polynomial was fit through. The resulted new reference trajectory is shown in Figure 2.

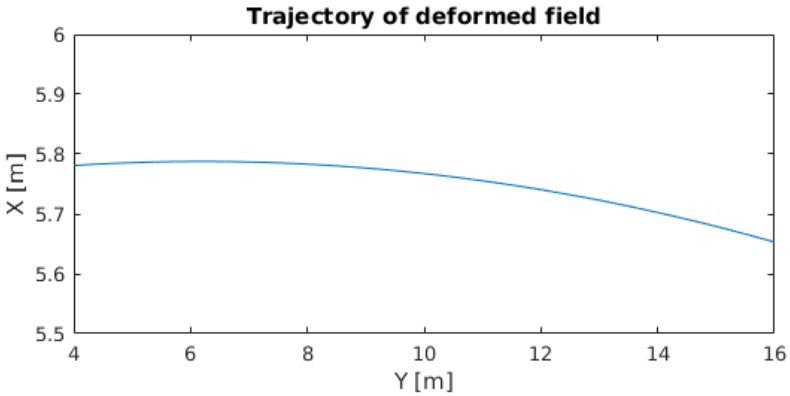

Figure 2: Identified curve for driving a straight line

3. Results and Discussion

3.1. Experimental setup

The mobile platform is a differential two-wheel robot as shown in Figure 1. It is a custom design made by Octinion. It is actuated with two BLH5100KC-30 motors from Oriental Motors. These motors are controlled with a drive delivered by the manufacturer. The drives have a proper control loop for the motor speed.

The UWB-devices used for positioning are the EVB1000-modules of Decawave (Dublin, Ireland). They were configured so they had a maximum range of 30 meters at a frequency of 35 Hz. The beacons were mounted on tripods. To preserve a maximum direct visibility (which benefits the performance of this technology), the devices were placed below the crop rows and heating tubes, at approximately the same height as the tag on the vehicle.

The computer that runs the algorithms is a development pc with the following characteristics: It has an Intel® Core™ i5 2.7 GHz processor with 2Gb memory on an Intel® Q67 motherboard. The algorithms run in Robot Operating System (ROS, sd). It is an open source set of software libraries and tools that are very useful while developing robot applications.

3.2. Results

The vehicle was put between two rows in a greenhouse and had to drive the trajectory described in section 2.4, both forward as backwards. The UWB-beacons were put in a rectangle that covered a couple of rows. The length of one row is around 17 meters. The reference velocity was constant at 0.5 m/s.

The results are shown in Figure 3 (forward driving) and Figure 4 (backwards driving). The figures represent the deviation of the vehicle from respectively its reference curved line and its reference velocity (which is constant). The statistical results of these tests are summarized in Table 1.

Table 1: Test results in statistical form

	Mean lateral error [m]	Standard deviation lateral error [m]		Mean velocity error [m/s]	Standard deviation velocity error [m/s]
Forward	0.019	0.014		0.021	0.015
Backwards	0.017	0.013		0.019	0.015

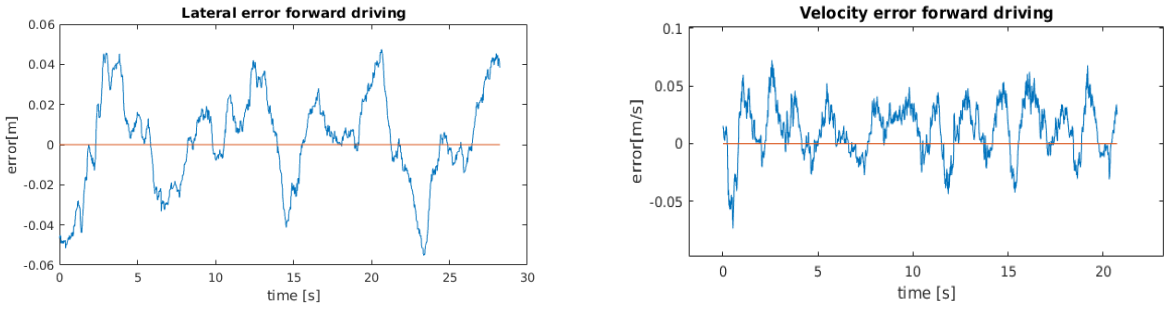

Figure 3: deviation from reference forward driving: lateral error (left) and velocity (right)

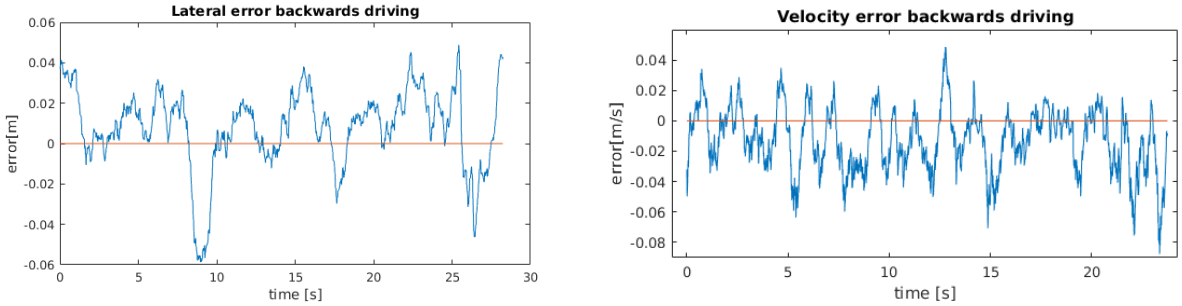

Figure 4: deviation from reference backwards driving: lateral error (left) and velocity (right)

3.3. Discussion

The goal of this project was to drive a platform autonomously between two rows in a greenhouse by using UWB-technology for positioning. The precision targeted was 3 to 5 cm at a constant speed. The results are quite sactisfactory. However the adjustment on the trajectory as explained in section 2.4 is not a sustainable solution for the further use of UWB-technology for positioning. A proper identification of the bias on UWB-measurements has to be done.

A second problem of the UWB-system is the requirement that the tag on the vehicle needs to be in the line of side (LOS) of the beacons at anytime. Experiments showed that, when objects are between the robot and the beacon, an additional bias was added on the measured distance. This is too restrictive for applications in greenhouses because objects like pillars are unavoidable. More specific research showed that a more thorough analysis of the signals can solve this issue.

The concept proposed in this paper meets the requirements of the application. The UWB-system has overall a sufficient accuracy for good navigation. The side effects described in this section undermine the trust that can be put on it. To create more robustness, a technology for local positioning should be added, as also was suggested in (Bakker, et al., 2010). Adding other sensors will be crucial in order to create a system that is more robust.

4. Conclusions

This paper investigated the programming of a mobile platform that will carry UVc-modules for combating powdery mildew on strawberry plants. The goal was to see if UWB-technology is applicable for accurate positioning between croprows in a greenhouse.

Apart from the modification on the trajectory, the platform was able to navigate forward and backwards as accurate as required. This means that UWB-technology has a future for indoor positioning. However, the constant bias on the distance measurements and the restriction of LOS-operation withhold the technology for immediate application. Further investigation in this specific technology needs to be done in order to get rid of these side-effects.

Because of these effects, it will be useful to investigate whether the integration of local sensors will improve the performance and robustness of positioning the platform.

Acknowledgements

Special thanks to Marijn Goossens (colleague at Octinion) for all his work and help with the practical implementation on the robot and the recording of the curved reference trajectory.

Grateful thanks to VLAIO (Vlaams Agentschap voor Innoveren en Ondernemen) for the financial support of this doctorate (Baekeland PhD Grant 150712).

References

Backman, J., Oksanen, T. & Visala, A., 2012. Navigation system for agricultural machines: Nonlinear Model Predictive path tracking. *Computers and Electronics in Agriculture,* Volume 82, pp. 32-43.

Bakker, T. et al., 2010. Systematic design of an autonomous platform for robotic weeding. *Journal of Terramechanics,* Volume 47, pp. 63-73.

Deak, G., Curran, K. & Condell, J., 2012. A survey of active and passive indoor localisation systems. *Computer Communications,* Volume 35, pp. 1939-1954.

Diehl, M. et al., 2002. Real-time optimization and Nonlinear Model Predictive Control of Processes governed by differential-algebraic equations. *Journal of process control,* 12(4), pp. 577-585.

Dong, F., Heinemann, W. & Kasper, R., 2011. Development of a row guidance system for an autonomous robot for white aspargus harvesting. *Computers and Electronics in Agriculture,* Volume 79, pp. 216-225.

Grüne, L. & Pannek, J., 2011. *Nonlinear Model Predictive Control: Theory and Algorithms.* sl:Springer.

Houska, B., Ferreau, H. & Diehl, M., 2011. An Auto-Generated Real-Time Iteration Algorithm for Nonlinear MPC in the Microsecond Range. *Automatica,* Volume 47, pp. 2279-2285.

Kraus, T. et al., 2013. Moving horizon estimation and nonlinear model predictive control for autonomous agricultural vehicles. *Computers and Electronics in Agriculture,* Volume 98, pp. 25-33.

Liu, H., Darabi, H., Banerjee, P. & Liu, J., 2007. Survey of Wireless Indoor Positioning Techniques and Systems. *IEEE Transactions on systems, man, and cybernetics - part C: applications and reviews,* Volume 37, pp. 1067-1080.

ROS, sd *What is ROS?.* [Online] Available at: http://www.ros.org, [Opened on 25 01 2017].

Thrun, S., Burgard, W. & Fox, D., 2006. *Probabilistic Robotics.* sl:Massachusetts Institute of Technology.

Multi-sensor fusion method for crop row tracking and traversability operations

Bernard Benet, Roland Lenain
IRSTEA, UR TSCF, 9 avenue Blaise Pascal, 63178 Aubière, France
Email : bernard.benet@irstea.fr

Abstract

Precision agriculture vehicles need autonomous navigation in cultures to carry out their tasks, such as planting, maintenance and harvesting in cultures such as vegetable, vineyard, or horticulture. The detection of natural objects like trunks, grass, leaf, or obstacles in front of vehicle in crop row is crucial for safe navigation. Sensors such as LiDAR devices or Time Of Flight cameras (TOF), allow to obtain geometric data in natural environment, using information of an Inertial Measurement Unit (IMU), for measurement accuracy. Fusion of geometric information with a color camera data improves the natural object identification, using some color classification technique, such as Support Vector Machine (SVM), considering two object classes, either solid objects such as crop or tree branch, and other elements like grass, leaf and soil. Agricultural vehicles can use these geometric and colorimetric data in real time, to follow crop rows and detect obstacles while executing various precision agriculture operations. In this application, perception sensors embedded on a light mobile robot were used to detect and identify natural objects in agricultural crops, working in various fields, with or without soil perturbation, with different speeds and several vegetation levels to achieve crop row tracking tasks, from a desired lateral deviation between robot and crop line, or traversability operations which consisted to take a decision in vehicle navigation, according to the size and nature of the detected objects, in front of vehicle. The vehicle could cross or avoid the object, or it must stop, for big solid obstacles.

Keywords: sensor fusion, crop row tracking, traversability, mobile robot navigation

1. Introduction

The development of Precision Agriculture, with respect to social needs, requires proposing new tool for food production, especially in the fields. Progresses achieved in robotics permitted to consider mobile robots as a promising solution to actually apply new methodologies. Nevertheless, in order to be fully autonomous, such device needs to be accurately and safely controlled, while using relatively low cost sensors. This problem is particularly pregnant considering the crop row tracking operations, obstacle detection and avoidance in natural environment. Autonomous vehicle guidance to perform farming operations such as planting, maintenance and harvesting in cultures such as vegetable, vineyard, horticulture, can be achieved using many kinds of sensors which can locate some crops and other natural objects, either in absolute mode with GPS devices or in relative mode using sensors like LiDAR or Camera device. Research works about automatic guidance for agricultural vehicles were achieved (Keicher and Seufert, 2000) and (Ming et al., 2008). As example, robotic technology evolution, with the use of these absolute or relative perception sensors for detecting and locating weeds could reduce dependency on herbicides, improving sustainability and reducing environmental impact. Various automatic systems have demonstrated the potential of this technology in the field, for various crops. GPS and machine vision fused together, and also with others technologies, are the trend for agricultural vehicle guidance systems. As most crops are cultivated in rows, an important step towards this long-term goal is the development of a row-recognition system, which allows a robot to accurately follow a row of plants. About GPS sensors, losses of GPS signal, as example if the vehicle penetrates in an environment with many trees, prevent to perform autonomous tasks with accuracy. In many applications, acceleration data given by an IMU device is used, to correct GPS signals, during a short time (Takai et al., 2014). For different crops, like for example citrus groves, the tree canopy frequently could block the satellite signals to the GPS receiver. So, in this case, perception relative sensors, such as LiDAR or Camera device, embedded on a vehicle such as a tractor, can be employed, to detect and follow crop rows (Subramanian et al., 2006). Among relative perception sensors, Time of Flight cameras (TOF) or LiDAR 3D, such as the celebrated Velodyne (Haselick et al., 2012), permit to get 3D information, in order to obtain environment maps, for terrain classification, with detection of various objects such as crop, grass, leaf, soil, but the cost of some of them does not appear to be compatible with the design of agriculture tool. As a consequence, cheapest sensors have to be used, even if they provide less accurate data. To get information of a set of crops, to realize a crop row tracking operation, a simple LiDAR 2D associated or not with a camera, can be sufficient for this task. Both LiDAR sensor and vision systems used separately or in fusion mode, permit to achieve many crop row tracking tasks, for sugar beet (Åstrand and Baerveldt, 2002), cotton crops (Billingssley and Schoenfisch, 1995) or rice rows (Choi et al., 2015).

Finding guidance information such as known crop row spacing is a solution for achieving accurate control of the vehicle (Han et al, 2003). In the application presented in this paper, a LiDAR device, a TOF camera, a IMU sensor and a color camera, were used in a fusion mode, to get the natural object positions, in real time, in various crops. Sensors were embedded on a light mobile robot. Soil perturbations affected the autonomous navigation in cultures. In a first stage, IMU data permitted to correct position of LiDAR or TOF points detected in robot environment. Then a fusion method was applied between these corrected points and a color camera, in order to identify and classify each point. Using a color database corresponding to two pixels classes (class crop and others (grass, leaf, soil), identification with the Support Vector Machine classic algorithm (Hyeran and Seong-Whan, 2002), permitted to identify objects and carry out some measurements on these ones. For crop row tracking task, from identified crop points, after removing noise, two methods were tested and compared, Hough method and Least Square (LS) technique, to obtain geometric information on the line, in order to choose the most adapted for crop row tracking tasks, to get the best ground truth. Automatic control/command operations were then applied to follow crop rows, after setting a lateral distance between the vehicle and the crop row. Various applications use fusion methods between LiDAR and a color camera device, for example for detecting tree trunks (Shalal et al., 2013), or for autonomous tractor guidance in some crops (Garcia-Alegre et al., 2011). The aim was to develop a system able to track crop rows, with accuracy, working in different fields, in various working conditions: soil perturbations, different speeds, various vegetation levels. For traversability operation, the estimation of 3D information in front of a vehicle, was investigated through the fusion between one sensor giving geometric information in the environment such as a low cost LiDAR 2D or a TOF camera and a color camera which brings color information on natural objects. The measurement achieved on detected objects, were used to take a decision in robot navigation. The vehicle crossed or avoided the obstacle in front of him, or must stop for big ones. In various applications, TOF camera and color cameras are used to make measures on agricultural products, for plant recognition to achieve robotic weeding (Gai et all, 2015), and for mobile robot locomotion (Joachim et all, 2008). The fusion algorithm proposed aims at controlling an autonomous robot in crop row and detecting the presence of obstacle in order to preserve safety (for both robot and environment). Such a point of view permits to achieve several kind of task, such as environment monitoring tasks, planting, maintenance or harvesting, with accuracy, in agricultural environment, from detection, localization and physical characterization information obtained on naturel objects, in various cultures. From these geometric and colorimetric data given by TOF camera, LiDAR devices and color cameras, in fusion mode, the farmers can achieve agricultural tasks, either in real time, like for example weeding, taking into account the data for each crop, or in differed time, using the recorded databases for a culture. These information can also be used to detect and locate some illnesses in crops, or to make comparisons between natural objects in cultures.

2. Materials and methods

2.1. Mobile robot and sensors

The light mobile robot used in the experimentations is presented in Figure 1. Four sensors were embedded on this vehicle, to acquire and compute data, in order to achieve traversability or crop row tracking operations in fields, in various crops: a TOF camera (IFM PMD O3M151), a GigaEthernet camera, with a resolution of 1022x1022 pixels (Baumer VLG 40C), a LiDAR device (SICK TIM551), an Inertial Measurement Unit (IMU) (Xsens).

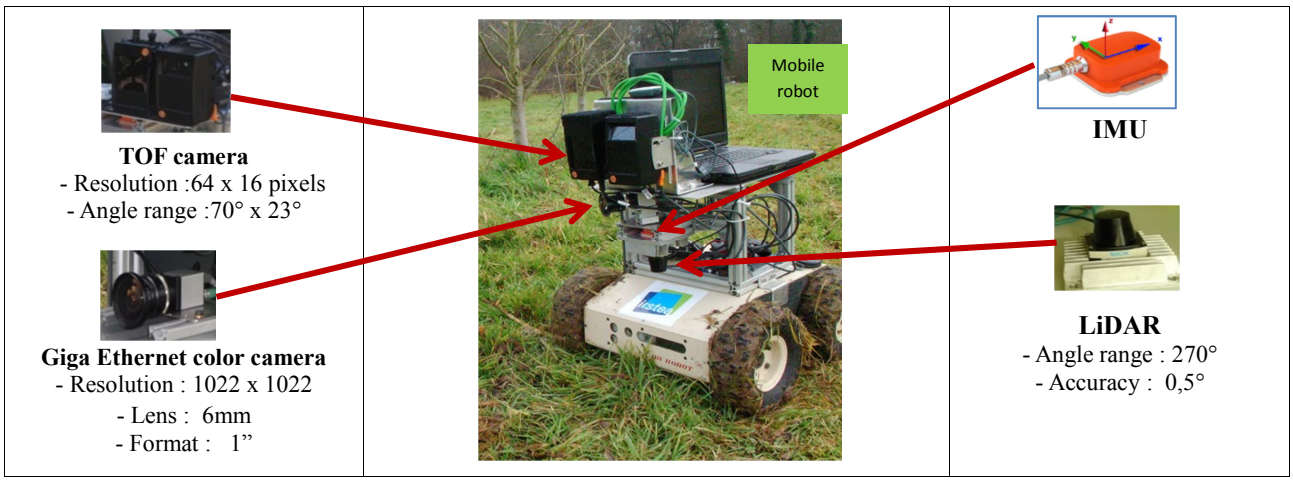

Figure 1. Mobile robot and embedded sensors

The TOF camera model chosen is insensitive to brightness variation, so it can be used for outdoor applications, in agricultural fields, in various lighting conditions, to make 3D geometric measures, unlike other 3D cameras, such as Kinects models, which can only be used in indoor conditions. Comparative studies for TOF cameras were conducted to analyse the measures accuracy, the sensitivity to lighting conditions (Piatti and Rinaudo, 2012). This camera was used in various mobile robotics applications (Hussmann et al, 2009), including the monitoring of borders (Montella and all, 2012). It can be used to produce map scenes both inside and outside, using the fusion mode with a color camera to identify objects. Figure 2 presents examples of outdoor data acquired with this camera: (a) 3D map in a crop field and (b) detection and identification of crop points (red color), by fusion with color camera data.

(a) 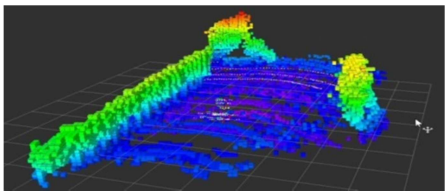 (b) 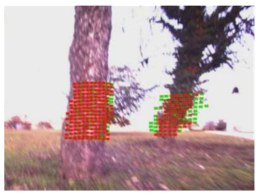

Figure 2. Outdoor data with IFM PMD O3M151 TOF camera

In the field of agricultural machinery, this type of sensor can be used to perform automated steering operations in different cultures to realize various applications such as the monitoring board, the harvesting, recognition swath, self-monitoring line cultures, in particular in the vineyard, to ensure the automatic steering along a vine row.

2.2. Model of mobile robot with sensors

LiDAR device and TOF camera enabled to obtain 3D points in the environment. These ones were corrected using pitch (β) and roll (α) angular data given by IMU device. Figure 3 presents the robot model, with different geometric parameters, considering only LiDAR device positioning (T).

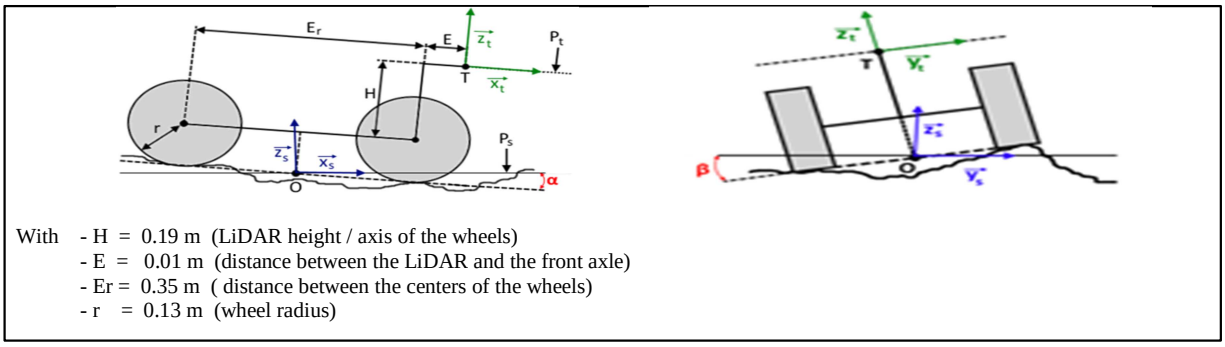

With - H = 0.19 m (LiDAR height / axis of the wheels)
- E = 0.01 m (distance between the LiDAR and the front axle)
- Er = 0.35 m (distance between the centers of the wheels)
- r = 0.13 m (wheel radius)

Figure 3. Robot model

2.3. Fusion Imu/(LiDAR and TOF)

The aim was to compute the point coordinates $P_{LiDAR}(x,y,z)$ and $P_{TOF}(x,y,z)$, in environment, taking into account IMU data angles (roll (α), and pitch (β)). Figure 4 a) and b) present, respectively, the equation to obtain P_{LiDAR} corrected points, from LiDAR data points ((ρ, Θ), and P_{TOF} corrected points, with the application of both rotations with (roll (α) and pitch (β) angles. From corrected points, it was so possible to remove all points outside a desired search place, particularly points situated under a height limit. As example all points situated under a grass height parameters eg 100 mm) were eliminated.

(a) P_{LiDAR}

$$x = \rho.\cos(\theta).\cos(\beta) - (E + 0{,}5.E_r).\cos(\beta) + (r + H).\cos(\alpha).\sin(\beta)$$
$$y = \rho.\sin(\theta).\cos(\alpha + \pi) + (r + H).\sin(\alpha).\cos(\beta)$$
$$z = \rho.(\sin(\theta).\sin(\alpha + \pi) + \cos(\theta).\sin(\beta)) - (E + 0{,}5.E_r).\sin(\beta) + (r + H).\cos(\alpha).\cos(\beta)$$

(b)
$$\begin{bmatrix} \cos(\beta) & \sin(\beta) & 0 \\ -\sin(\beta) & \cos(\beta) & 0 \\ 0 & 0 & 1 \end{bmatrix} \begin{bmatrix} \cos(\alpha) & 0 & \sin(\alpha) \\ 0 & 1 & 0 \\ -\sin(\alpha) & 0 & \cos(\alpha) \end{bmatrix} \rightarrow P_{TOF}$$

Figure 4. Computation of corrected LiDAR and TOF points

2.4. Calibration Camera/(LiDAR and TOF)

Figure 5 presents the geometric model of the robotic system, with sensor position, which enabled to calibrate the complete sensor device, necessary for fusion operations. From these sensor positions, computation of distance between robot and detected natural objects, in front of vehicle, in fields, and also height of these objects, could be achieved.

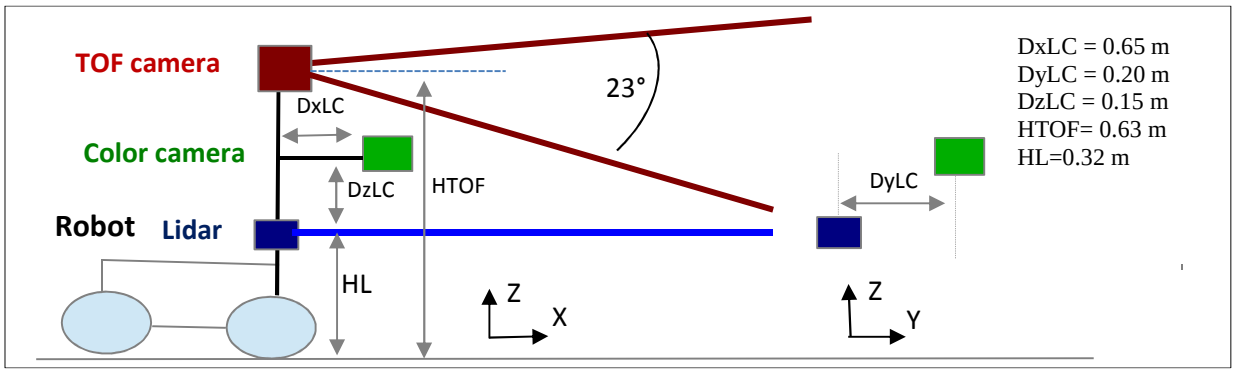

Figure 5. Calibration Camera / (LiDAR and TOF)

2.5. Fusion Camera/ LiDAR and TOF

The camera calibration, taking into account its characteristic parameters, and the information about relative position of LiDAR, TOF and color camera, embedded on robot, permitted to get intrinsic and extrinsic parameters of the multi sensor device, in order to realize the fusion between sensors, In our application, after fusion with IMU data, two sensor fusion types were considered: a first one between LiDAR device and color camera and a second one between TOF camera and the color camera. Figure 6 shows the mathematical method used to compute the geometrical position of points given by LiDAR and TOF device, inside a color image.

$$\begin{pmatrix} su \\ sv \\ s \end{pmatrix} = \underbrace{\begin{bmatrix} k_u & s_{uv} & c_u \\ 0 & k_v & c_v \\ 0 & 0 & 1 \end{bmatrix} \begin{bmatrix} f & 0 & 0 & 0 \\ 0 & f & 0 & 0 \\ 0 & 0 & 1 & 0 \end{bmatrix}}_{\text{intrinsic parameters}} \underbrace{\begin{bmatrix} & R_{3\times3} & & t_x \\ & & & t_y \\ & & & t_z \\ 0 & 0 & 0 & 1 \end{bmatrix}}_{\text{extrinsic parameters}} \begin{pmatrix} X \\ Y \\ Z \\ 1 \end{pmatrix}$$

Figure 6. Mathematical model for positioning LiDAR and TOF points inside color image

Figure 7 shows the positioning of LiDAR points (a) and TOF points (b) inside a color image, by fusion. For each point, to take into account the inaccurate information provided by LiDAR and TOF devices, a window (10 x 10 pixels) was considered around each point on color image, to determinate, in a next step, the class of each point (crop, grass,…).

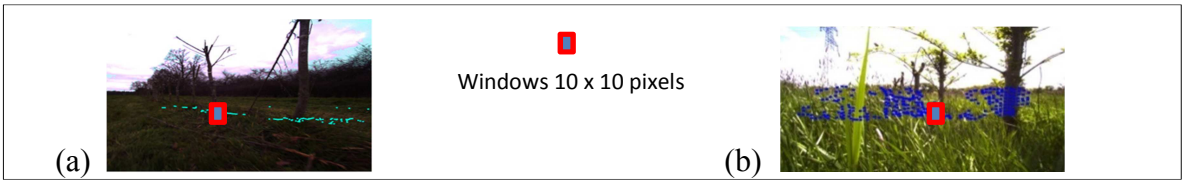

Figure 7. Positioning of LiDAR (a) and TOF (b) data on color images

2.6. Pixel classification and identification

Merging 3D LiDAR systems with camera was the subject of various works by identifying points or 3D zones in the environment for different classes of color properties (Laible et all, 2013). Point classification by SVM methods (Support Vector Machine) was carried out focusing on two element classes: solid objects such as crop, or tree branch, and noise such as grass, leaf, soil, working in different lighting conditions, in environment. The aim was to compute the mean color in windows associated to each point (Figure 8), in order to classify each point, after applying a SVM method which consisted to determinate a hyperplane for separating both classes, from databases corresponding to RGB color of both classes. Figure8 presents some color samples for both selected color classes for our application. Pixel identification stage consisted to work in every window around the geometric points detected with the TOF camera (PT) and LiDAR (PL), and classify each point using the SVM method, taking into account the mean color inside windows.

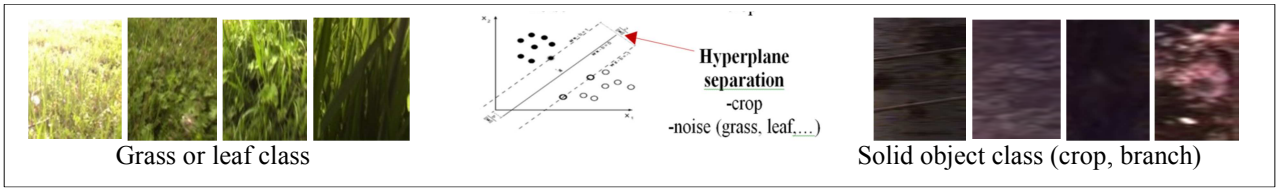

Figure 8. Selected images for object classification by SVM method

Examples of SVM classification results, to discriminate both object classes, are presented in figure 9, in white and black color, respectively for grass and solid object classes.

Figure 9. SVM classification result

2.7. Crop row tracking operation

The chart below (Figure 10) shows the various stages carried out to realize the crop row tracking task. First, LiDAR device enabled to obtain 3D points in the environment. These ones were corrected using data given by IMU device. All the geometric points situated outside a desired region, were eliminated. Then a second fusion operation between corrected LiDAR data and color camera information enabled to get the desired color points, corresponding to objects that must be tracked by robot. For vineyard, the aim was to detect trunk points and to eliminate the green ones corresponding to grass and leaf. One method like Hough or LS technique was then applied to obtain at the end, the line geometric information used for crop row tracking operation. Finally, the robot control algorithm was launched, using the line information, the desired lateral deviation and taking into account also the robot angular deviation, the temporal aspect, and the variable spacing between natural objects in crop rows.

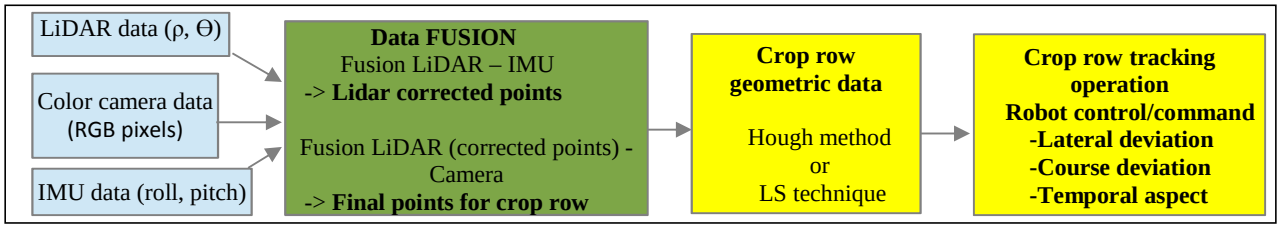

Figure 10. Crop row tracking operation

For each P_{LiDAR} point (called Gi in Figure 11), if this point, was identified as a crop point, with SVM method, then the P_{LiDAR} point was kept in next stage (final points Fi), for obtaining, in next stage, the geometric parameters of the crop line. Otherwise, P_{LiDAR} point was eliminated.

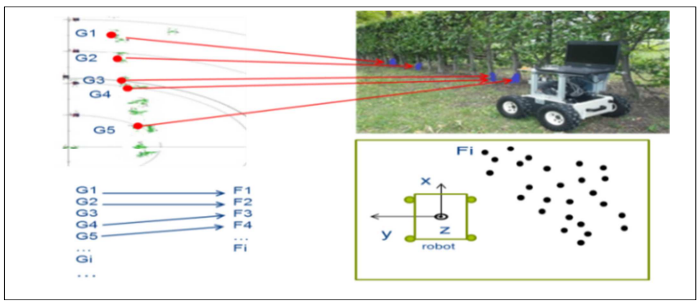

Figure 11. Detection by fusion of crop row points

Two methods were tested to obtain, from the final points Fi obtained by fusion methods, the crop row geometric information used for tracking operation (Figure 12): the LS technique with the crop line computation presented in (a) and the Hough method (Duda and Hart, 1972) (b). Hough method consisted of working in (r,Θ) space in which a point characterizes a line, and to increment a matrix accumulator, considering all points Fi, and with variations of both variables r $[r_{min};r_{max}]$ and Θ $[\Theta_{min};\Theta_{max}]$. The maximum value of the matrix corresponded to the desired crop line.

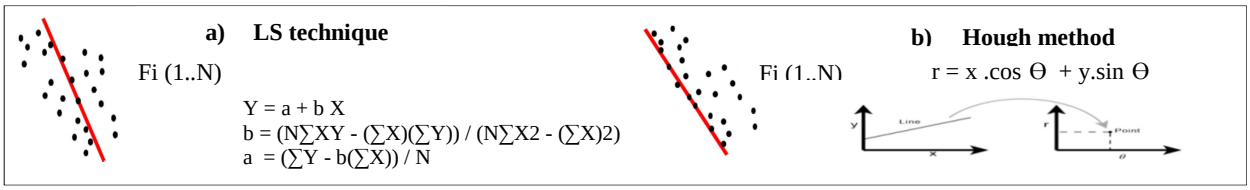

Figure 12. Crop row detection

Finally, the robot control algorithm was launched, using the line information (Y=a+ bX), the desired lateral deviation (DELat) and taking into account also the robot angular deviation and the temporal aspect (Figure 13), in order to avoid high robot movements, during navigation.

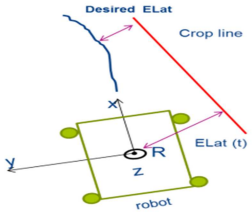

Crop line Y = a + b X (perception)

Robot Jaguar control/command for crop row tracking operation

Lateral command: ELat (t) = DELat - distance (R - Crop line) = DELat - (abs(a) / sqrt(b^2+1))

Angular command: Course deviation (t) = PI/2 - atan(-1/b)

Time filtering: ELat (t) = c x ELat (t) + (1-c) x ELat (t-1) c € [0;1]

Figure 13. Robot control for crop row tracking

2.8 Traversability principle

The aim was to detect objects at a distance between 0 and 5 meters from robot, and take a decision in the robot mobility control. LiDAR device gave planar information with high resolution (one point each 0.5°) whereas with TOF camera used, a low resolution image (64 x 16) was obtained. TOF cameras can be used for traversability operations in different environments, such as PMD Camcube camera model embedded on farm vehicles, civilian or military (Balta et all, 2013). Detecting solid obstacles such as trees, relatively large is an easy task to achieve with TOF cameras and facilitates autonomous navigation of mobile robots. In our application, solid objects, in front of vehicle, such as branches or trees were considered as obstacles to avoid, while grass-type objects were traversable objects. The charts below (Figures 14 and 15) show the various operations carried out to obtain the final decision stage, for a traversability application in a culture. In real time, the mobile robot, according to the data obtained with three sensors (color camera, TOF camera and LiDAR) adapted its mobility. Grass and solid objects were considered separately. In real time, the Grass (G) and Solid (S) point numbers above two height values Gheight and Sheight, respectively for grass and solid objects, were computed. These points could be obtained with LiDAR or TOF camera. For these point numbers, the maximum value obtained with both sensors was taken into account for traversibility decision. The distance values between robot and objects were also considered in this operation, respectively DGrass and DSolid for grass and solid objects. According to the information obtained for grass and solid detected objects, the vehicle could move at normal speed, at reduced speed, must avoid solid objects or must stop, if obstacle was very near it. Several thresholds values T1...T5 were defined for traversability decision.

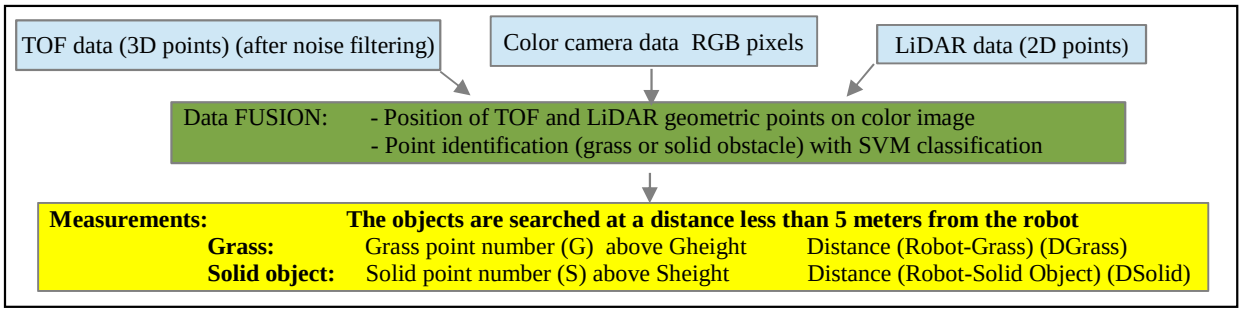

Figure 14. Data acquisition and measurements for traversability

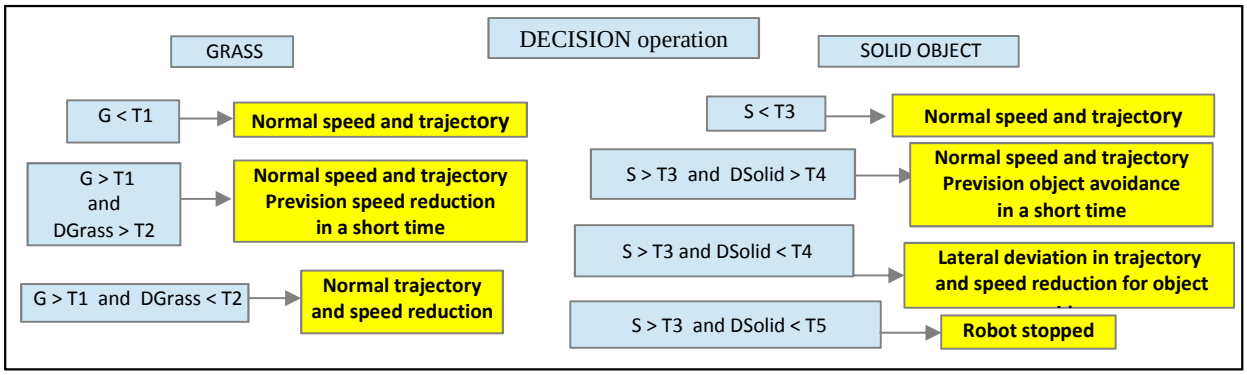

Figure 15. Traversability decisions

3. Results and discussion

Experimentations were achieved in different crops (Figure 16), particularly in vineyard environment, in order to study the capability of the developed fusion method, to realize crop row tracking operations, with accuracy, working with various robot speeds between 1 and 3m/s, various vegetation levels and ground perturbations such as holes, bumps, or mud. For traversability operation, various grass heights and solid obstacles, in these fields, in front of vehicle, were taken into account, to realize some measurements in order to take some traversability decisions, for robot navigation, to modify speed and trajectory of mobile robot.

Figure 16. Test fields for crop row and traversability operations

3.1. Crop row tracking operation

Figure 17 presents results images with the LiDAR points put on images. Black and red color points are respectively the crop points that will be tracked by vehicle and noise points corresponding to either points which have not crop color (grass, leaf, soil,…) or points outside the desired place, where we are looking for tracking points. The colorimetric discrimination achieved with SVM method enabled to eliminate noise, to keep only, finally, crop elements (set of points characterized by geometric position in 3D environment).

Figure 17. Fusion result for crop points detection

A study was carried out to compare two methods (Hough and LS) to get, from crop points, the crop line geometric parameters which must be tracked by vehicle. The standard deviation differences, between both methods, in lateral deviation values, presented in Figure 18 (manual navigations, working without (a) or with (b) fusion mode with camera, near a crop line), showed that Hough method was less sensitive to noise, gave more stable information and permitted to get less oscillation, in the robot navigation than LS technique.

(a) 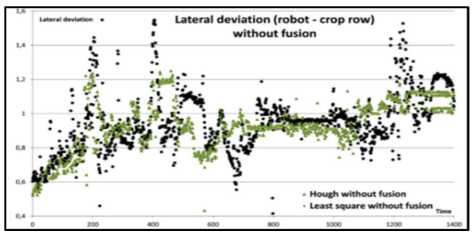

(b) 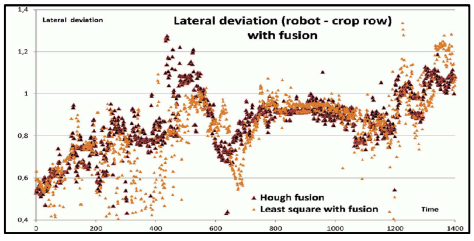

	Without fusion		With fusion (camera)	
	Hough method	LS technique	Hough method	LS technique
Standard deviation of lateral deviation	0,145 m	0,209 m	0,143 m	0,172 m

Figure 18. Comparison between LS technique and Hough method

Hough method with fusion (LiDAR, IMU and Camera) was the most stable, to detect and follow crop rows, particularly in a noise environment. Anyway, Hough method is much slower (processing time) than LS technique, so for high speed applications, with a few noise points detected by LiDAR device in one crop, it could be better to use this last one.
Figure 19 presents crop row autonomous tracking result examples, without (a) and with (b) soil perturbations. In these tests, Hough method was carried out, the fusion with IMU and Camera was used, the control/command speed was 1m/s and the navigation distance was 50 meters. The **c** coefficient for temporal filtering was 0,8. The desired lateral deviation value (DELat) was 1.5 m.

(a)

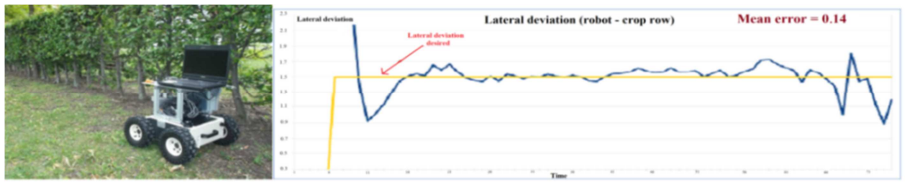

(b)

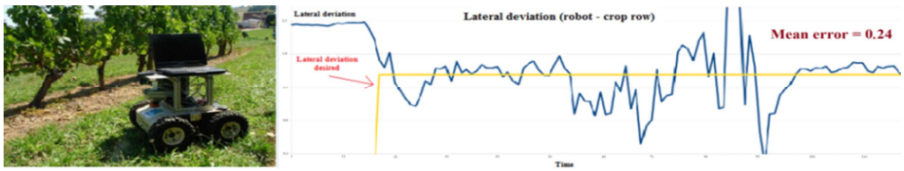

Figure 19. Crop row tracking on soil without and with perturbations

For all tests carried out, the mean error for lateral deviation between robot and crop row, varied in the range [0.1 - 0.2m] and [0.2 – 0.3m] respectively for soil without and with perturbations such as vines. Figure 20 presents crop row autonomous tracking result examples, without (a) and with (b) soil perturbations (vines), working with a speed of 1.5m/s. As example, the difference between mean absolute error for two robot speeds 1m/s and 1.5m/s, was about 0.06m and 0.11m, respectively for tests without and with soil perturbations, working in the same crops, modifying only speed value. For many tests, mean error for lateral deviation was about 0.25 m and 0.4m, respectively for soils without and with perturbations, with a speed of 1.5 m/s.

(a)

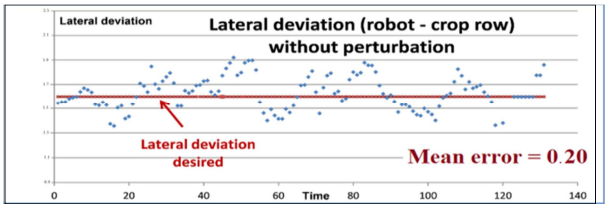

(b)

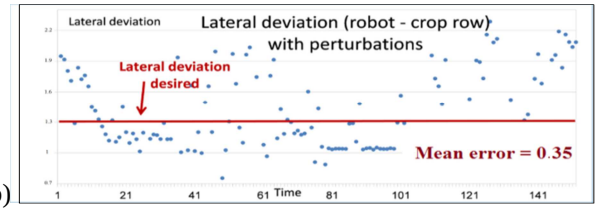

Figure 20. Speed influence on crop row tracking accuracy

3.2. Traversability operation with LiDAR and TOF device

The fusion method consisted to put the LiDAR and TOF data inside the color image, and to make some colorimetric and geometric measurements on the detected objects in front of the vehicle, for identifying these ones. For each image, the computation of grass and solid point numbers (G and S), above respectively the threshold values chosen for grass height (Gheight) and for solid objects height (Sheight), and the mean distance between robot and these objects (DGrass and DSolid) characterized the height and position of these ones. From this information, some decision could be taken in the traversability operations, for crossing or avoiding objects, and in extreme case the robot must stop, if a solid object was in front of it, near it. In the experimentations, the aim was to detect grass points above Gheight=0.32m (=HL) and Solid points above Sheight=0.25m. The threshold values chosen for traversability decision were the following:

T1 = 100 points, T2 = 3 m, T3 = 100 points, T4 = 4 m, T5 = 1 m

In Figure 21 and 22, grass and solid objects detected by LiDAR and TOF device, in front of robot, were put by fusion on color image. Pixel classification results by SVM are presented in red and blue color, respectively for grass and solid objects, for LiDAR device (A) and in green and red color, respectively for grass and solid objects, for TOF camera (B).

Measurement results and traversability decisions, taking into account the nature and size of detected objects are presented under each image. For LiDAR, object were detected at fixed height (HL=0.32m from the ground).

A	 **G = 27 < T1 S=20<T3**	 **G = 133 > T1 S =8<T3 DGrass=3.4 >T2**	 **G = 158 > T1 S = 12<T3 DGrass < T2**
Traversability decision	Robot continue moving without any modification in trajectory and speed	Robot continue moving without any modification in trajectory and speed**, but will have to reduce speed "in a short time"**	Robot continue moving keeping trajectory **at reduced speed**

Figure 21. Object detection and identification by fusion with LiDAR

B	 **G = 213 > T1 S = 9 < T3** **DGrass = 4,2m > T2**	 **G = 156 >T1 S = 2 <T3** **DGrass = 2.6m <T2**	 **G =121 > T1 S = 328 > T3** **DGrass = 2.9m <T2 DSolid = 3.5m <T4**
Traversability decision	Robot continue moving without any modification in trajectory and speed**, but will have to reduce speed "in a short time"**	Robot continue moving keeping trajectory **at reduced speed**	Robot moves **at reduced speed** and **avoids solid object** (tree and branches) (lateral deviation)

Figure 22. Object detection and identification by fusion with TOF

The application of the fusion method developed to detect and identify objects in front of the vehicle, using the geometric data obtained with the LiDAR device and the TOF camera, merged with color camera data, has shown that the mobile robot can improve and optimize its mobility, adapting its speed and trajectory, in real time, taking into account, the sensor data, which bring information about the nature and size of objects in front of it. Both grass and solid objects like tree and branches were considered separately. A supposition was made to consider that both object types were not superposed, but sometimes solid objects were hidden by grass. In these experimentations, LiDAR and TOF camera were embedded on mobile robot with a horizontal position. But depending of the application and of the object type which must be detected, the position and orientation of both sensors can be modified. In various crops, LiDAR devices data were used to detect if grass height was higher than its height from ground (HL). From this information, agricultural vehicles could reduce speed. But this planar information given by this sensor was not sufficient to detect with accuracy solid objects (like tree or branches), whereas TOF camera, which gave geometric information in 3D space, with low resolution (64x16 pixels) permitted, in various lighting conditions, the detection by fusion of both object types (grass and solid objects), in front of vehicle, at different heights from ground. From TOF data, solid objects detected could be avoided by vehicle, and grass detection permitted to reduce vehicle speed. The main problem with this sensor is to choose correctly its position and orientation, in order to be able to detect objects with various heights and various distances from vehicle.

4. Conclusions

A fusion method has been developed, taking into account data from perception sensors such as a color camera, a LiDAR and a TOF camera, and also the ones coming from a IMU device, in order to improve agricultural tasks such as crop row tracking and traversability in the fields. This method consisted in the detection and identification of natural objects such as crops, grass, leaf, soil or other elements in front of vehicle, using the combination of the rich and colored representation provided by the images with the geometric data given by the LiDAR or TOF device. For crop row tracking operation, the results obtained working with a light mobile robot in different navigation conditions, in various crops, showed the robustness of developed fusion method, for realizing stable autonomous navigation for crop row tracking, particularly in the vineyards, with many perturbation and speeds up to 2m/s. Hough method enabled to obtain a better ground truth and less oscillations in navigation than LS technique, because it permitted to detect the exterior points of trees. The mean lateral error between desired and obtained trajectory varied between 0.1 and 0.4m, depending of speed and soil perturbations. Over than 2m/s, the robot could not navigate with stability, particularly in vineyards environment. This developed system, with three aspects (perception/fusion/control) will be carried on heavier vehicles or other mobile robot less sensitive to soil perturbations, to be able to work with high speeds over than 2m/s. For traversability task, both tested sensors LiDAR and TOF camera bring complementary information: LiDAR sensor could detect objects above its height (0.32m in our experimentations) at various distances between vehicle and objects, and TOF camera could detect objects at different heights but this detection depended of the distance. The longer the distance is great plus it can detect objects of low height. Information obtained in real time, by both sensors, was used to detect objects in front of vehicle, at various distances. Despite the low resolution of the TOF camera (64 x 16) objects with different heights from ground and various sizes, such as grass and tree branches, were detected, with accuracy, with this sensor. Image information given by TOF camera permitted to obtain better detection of obstacles (solid or grass) in front of robot than plane information given by LiDAR device. With this TOF camera, 3D maps, in agricultural fields, could be also performed. This should allow having more accurate information on terrain, and on obstacle geometry, allowing considering traversability maps on areas expected to be crossed by the robot. The accuracy of sensor data for autonomous navigation and obstacle detection/avoidance has been investigated under different lighting conditions and various vegetation levels. From the obtained results in the developed fusion method for both operations presented in this paper, traversability and crop row tracking, next works will consist to realize in the same time both operations, with the fourth sensor, working with many perturbations (mud, bumps, a lot of grass) for both operations.

LiDAR data will be used for tracking task, in order to identify crop points with camera, and TOF data will be used for obstacle detection and identification with color camera, in front of vehicle, using a light robot or a bigger vehicle. On main problem, in this work, will be to choose the right height for LiDAR device, in order to be able to detect crop points, every time, without being perturbed by grass height and leaf area. This fusion method which gives geometric and colorimetric information in crops, could be applied, in various fields, in different agricultural tasks, such as environment monitoring tasks, planting, maintenance or harvesting. For safety operations, for detecting people, near agricultural vehicles, or in dangerous areas, in order to avoid accidents, the use of a TOF camera associated with a color camera, could also be used.

References

- Åstrand B and Baerveldt AJ 2002. An Agricultural Mobile Robot with Vision-Based Perception for Mechanical Weed Control. Autonomous robot, July 2002, Vol. 13(1), pp 21–35.
- Billingssley J and Schoenfisch M 1995. Vision-Guidance of Agricultural Vehicles. Autonomous Robots, Vol. 2(1), pp 65–76.
- Balta, H., De Cubber, G., Doroftei, D., Baudoin, Y., Sahli, H., 2013.Terrain Traversability Analysis for off-road robots using Time-Of-Flight 3D Sensing. Royal Military Academy of Belgium (RMA), Belgium.
- Choi KH, Han SK, Han SH, Park KH, Kim KS and Kim S 2015. Morphology-based guidance line extraction for an autonomous weeding robot in paddy fields. Computers and Electronics in Agriculture 113, pp 266–274.
- Duda RO and Hart PE 1972. Use of the Hough transformation to detect line and curves in pictures. ACM, Vol.15(1), pp 11–15.
- Gai, J., Tang, L., Steward, B., 2015. Plant Recognition through the Fusion of 2D and 3D Images for Robotic Weeding. Agricultural and Biosystems Engineering Conference Proceedings and Presentations.
- Garcia-Alegre S, Martin D, Garcia-Alegre G and Guinea Diaz D 2011. Real-Time Fusion of Visual Images and Laser Data Images for Safe Navigation in Outdoor Environments. Center for Automation and Robotics Spanish Council for Scientific Research, Spain.
-Han, S., Zhang, Q., Ni, B., Reid, J.F., 2003. A guidance directrix approach to vision-based vehicle guidance systems. Computers and Electronics in Agriculture 43 (3). pp 179-195.
- Haselick M, Arends M, Lang D and Paulus D, 2012. Terrain Classification with Markov Random Fields on fused Camera and 3D Laser Range. DataVision Group, AGAS Robotics, University of Koblenz-Landau, 56070 Koblenz, Germany.
-Hyeran B and Seong-Whan L, 2002. Applications of Support Vector Machines for Pattern Recognition: A Survey
-Hussmann S., Schauer D., MacDonald B., 2009. Integration of a 3D-TOF camera into an autonomous mobile robot system. I2MTC 2009 - International Instrumentation and Measurement.Technology Conference.Singapore, 5-7 May 2009.
- Joachim, C., Roth, H., 2008. Development of a 3D Mapping using 2D/3D Sensors for Mobile Robot Locomotion. Institute of Automatic Control Engineering Department of Electrical Engineering and Computer Science, University of Siegen Hoelderlinstr 3 57068, Germany.
- Keicher R and Seufert H 2000. Automatic guidance for agricultural vehicles in Europe. Computers and Electronics in Agriculture, Vol. 25, pp 169–194.
-Laible, S., Niaz Khan, K., Zell, A., 2013. Terrain Classification With Conditional Random Fields on Fused 3D LIDAR and Camera Data. European Conference on Mobile Robots (ECMR), Barcelona, Spain, September 25-27, 2013.
- Ming L, Kenji I, Katsuhiro W and Shinya Y, 2008. Review of research on agricultural vehicle autonomous guidance. International Journal of Agricultural and Biological Engineering Vol2, N°3.
- Montella, C., Pollock, M., Schwesinger, D., Spletzer, J.R, 2012. Stochastic Classification of Urban Terrain for Smart Wheelchair Navigation. Department of Computer Science and Engineering Lehigh University.
- Piatti, D., Rinaudo, F., 2012. SR-4000 and CamCube3.0 Time of Flight (ToF) Cameras: Tests and Comparison. Remote Sens. 2012, 4, pp 1069-1089.
- Shalal, N., Low, T., McCarthy, C., Hancock, N., 2013. A preliminary evaluation of vision and laser sensing for tree trunk detection and orchard mapping. Proceedings of Australasian Conference on Robotics and Automation, 2-4 Dec 2013, University of New South Wales, Sydney Australia.
- Subramanian V, Burks TF and Arroyo AA 2006. Development of machine vision and laser radar based autonomous vehicle guidance systems for citrus grove navigation. Computers and Electronics in Agriculture 53, pp 130–143.
- Takai R, Barawid O, Ishii K and Noguchi N 2014. Development of Crawler-Type Robot Tractor based on GPS and IMU. Engineering in Agriculture, Environment and Food, Vol.7 (4), pp 143–147.
- Zhang X., LI, L., Tu, D., 2013. Point Cloud Registration with 2D and 3D Fusion Information on Mobile Robot Integrated Vision System. Proceeding of the IEEE International Conference on Robotics and Biomimetics (ROBIO) Shenzhen, China, December 2013.

Low cost active devices to estimate and prevent off-road vehicle from rollover

Dieumet Denis[3*], Benoit Thuilot[1,2], Roland Lenain[3], Michel Berducat[3]
[1]Clermont Université, Université Blaise Pascal, Institut Pascal, BP 10448, 63000 Clermont-Ferrand, France
[2] CNRS, UMR 6602, Institut Pascal, 63177 Aubière, France
[3]Irstea, 9 avenue Blaise Pascal, 63172 Aubière, France
[*] Corresponding author: dieumet.denis@irstea.fr

***Abstract*— This paper proposes to investigate the use of active devices, able to anticipate for hazardous situations, by using low cost sensors. In this approach, the risk of rollover is considered thanks to the Lateral Load Transfer (LLT) metric, able to characterize gradually the dynamic mass repartition on the vehicle, without using expensive cell forces. In order to account for variable conditions, an observer algorithm is used in order to adapt on-line the grip conditions thanks to a dynamical yaw model. Once adapted, this model supply the dynamic variable influencing the evolution of LLT. This metric can then be estimated thank to a second partial dynamic model considering the roll plane. Thanks to the vehicle parameters (mass, elevation of centre of gravity), the risk of rollover may be accurately computed.**

Keywords: Robotics in Agriculture, Hydraulic Actuators, Active Security Devices, Rollover, Dynamics, Grape Harvester.

I. Introduction

Nowadays, mobile robotics perfectly fits in the notion of technological progress, either for intervening in extension or instead of humans by releasing them of repetitive, laborious or dangerous activities. Areas benefiting from the growth of robotics are legion, notably in the field of agriculture. Indeed, thanks to a certain repeatability that they can bring in the work, mobile robots represent a coherent answer to the current bets of the agricultural sector (increased acreages cultivated, quality, productivity, yielding, etc.). However, because of the continued increase in the size and the speed motion of agricultural machinery [1] combined to variable and bad grid conditions associated to a large diversity of terrains, driving vehicles in off-road environnement remains a dangerous and harsh activity. Driving difficulties may be also encountered when considering huge machines with possible reconfiguration of their mechanical properties (changes in mass and centre of gravity height for instance). As a consequence, for the sole agriculture sector, several fatal injuries are reported per year in particular due to rollover situations [2], [3], [4], [5].

In order to reduce accident consequences, passive protections such as ROllover Protective Structures - ROPS [6] or Slope Correction Systems are installed on tractors. However, protection capabilities of these structures are very limited [7] and the ROPS cannot be embedded on bigger machines due to mechanical design limitations.

Therefore, active safety devices allowing either to warn the operator or to act directly on vehicle control variables are promising solutions to reduce risks and avoid hazardous situations. Nevertheless, if driving assistance systems (such as ESP [8] or ABS [9]) have been deeply studied for on-road vehicles and successfully improve safety, development of control stability systems dedicated to off-road vehicles is still being in its infancy [10], [11], [12].

Besides reducing the accident statistics in the agriculture field, the economic benefits of these systems would be also very important provided such new solutions are at a reasonable cost for the purchaser [13]. Thus, given the limited number of sensors required to evaluate the Lateral Load Transfer (hereafter denoted LLT), its physical meaning and its relative computational simplicity, this metric has been here chosen as a relevant stability criterion among several rollover indicators described in the literature [14].

This paper presents a control stability system to assess and avoid rollover risk in reconfigurable agricultural vehicles. In such platforms, stability assessment needs to be robust to intrinsic property changes such as vehicle load and elevation of center of gravity. Therefore, in Section IV, relying on a sensitivity based steepest descent algorithm, the estimated LLT in Section III and its intermittent measurement in Section II are coupled in order to adapt the vehicle parameters. Thereby, the estimated LLT supplies relevant values when the measured one is unavailable and allows then to monitor the stability of the vehicle whatever the state of the slope correction system, the soil type and the load of the machine. In Section V, the efficiency and the capabilities of the proposed algorithm are investigated through full scale experiments on an hazardous field by using a grape harvester equipped with exteroceptive and proprioceptive sensors. The experimental vehicle considered in this paper (a grape harvester) can be geometrically reconfigured according to terrain slope and mass changes as the grape receptacle is progressively filled.

II. Vehicle rollover propensity measurement

A. Rollover Metric Formulation and Interpretation

The Lateral Load Transfer is a stability metric based on the distribution of the normal wheel-terrain contact forces, that indicates nearness to wheel lift-off. More precisely, it is defined as the difference in normal forces on the left and right sides of the vehicle ([15], [16], see also Figure 1) and normalized with the overall normal contact forces.

$$LLT = \frac{F_{n1} - F_{n2}}{F_{n1} + F_{n2}} \quad (1)$$

The LLT range of variation is comprised in $[-1\ \ 1]$, the extreme values meaning that the wheels of one side of the vehicle lift off. In practice, it is considered that the rollover is imminent when $|LLT|$ reaches 0.8, i.e., 80% of the sprung mass is then distributed on one side of the vehicle. For

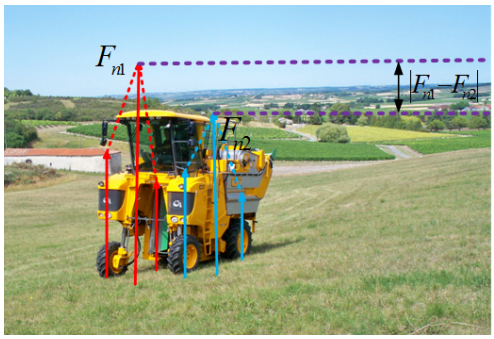

Fig. 1. Representation of the lateral load transfer

convenience purpose, hereafter the measured value and the estimated one will be denoted respectively $\overline{LLT}$ and $\widehat{LLT}$.

B. Rollover metric measurement

The hydraulic cylinders of the harvester used for slope correction are equipped with pressure sensors in order to enable force control. It is here proposed to use these sensors to obtain an indirect measurement of the actual LLT. More precisely, the pressure sensors located at the inlet and outlet chambers of the hydraulic actuators enable to measure the differential pressure in each cylinder connecting each axle to the suspended mass. Let us denote P_{ij} the differential pressure in the cylinder, where ij denotes the wheel, rr for **r**ight **r**ear wheel for instance. The normal forces at the surface of contact of each wheel can be inferred from the differential pressure measurement in the cylinders as follows:

- The normal forces are $K_{lf}P_{lf}$ and $K_{rf}P_{rf}$ for respectively **l**eft and **r**ight **f**ront wheels,
- They are $K_{lr}P_{lr}$ and $K_{rr}P_{rr}$ for respectively **l**eft and **r**ight **r**ear wheels

where K_{ij} are constant parameters that can be inferred from the diameter and the orientation of the cylinders. Since the rear (respectively the front) cylinders have the same diameter and a symmetric orientation, then $K_{lr} = K_{rr} = \chi K_{lf} = \chi K_{rf}$ (where χ is a constant) and in view of (1) the actual LLT value is eventually available from the pressure measurements according to:

$$\overline{LLT} = \frac{P_{lf} - P_{rf} + \chi(P_{lr} - P_{rr})}{P_{lf} + P_{rf} + \chi(P_{lr} + P_{rr})} \tag{2}$$

Nonetheless, this measurement of wheels-ground contact forces obtained by exploiting the actuators state is not permanently available. Indeed, when actuators are in end stops or in slope correction, pressures are not representative of the suspension forces. As a result, in order to monitor the degree of stability of the vehicle whatever the state of the slope correction system, in the next section, we will develop an observer to estimate permanently the vehicle rollover risk in real time.

III. Rollover metric estimation

A. Dynamics Vehicle model

It appears that the use of a complete 3D dynamic model may be hardly tractable and time consuming from an observation point of view [17] and with a low cost perception system. Hence, in order to allow control law developments, a multi-model approach, where the vehicle dynamics is split into two $2D$ frames, see Fig. 2, has been preferred.
In the yaw projection, the vehicle is considered as a bicycle (each axle is viewed as a wheel) and its motion is described perpendicularly to a plane defined by the wheel/ground contact points. The influence of the vehicle inclination is accounted via the addition of a component of the gravity force $P_y = mg\sin\alpha$. The velocity v of the rear axle and the steering angle δ_F are the variables controlled by the driver. The other parameters and variables are:

- L_F and L_R are respectively the front and rear vehicle half-wheelbases,
- ψ is the vehicle yaw angle,
- u is the linear velocity at the roll center O',
- β is the global sideslip angle.

In the roll frame, the vehicle is viewed as a $2D$ system whose mass is suspended. In order to account for damping and stiffness, a restoring force F_a depending on the roll angle φ and the roll rate ($\dot{\varphi}$) of the sprung mass is introduced as:

$$\overrightarrow{F_a} = \frac{k_r\varphi + b_r\dot{\varphi}}{h}\vec{y}_2 \tag{3}$$

where h is the distance between the roll center O' and the vehicle center of gravity G. The roll damping b_r and stiffness coefficient k_r are obtained thanks to a preliminary calibration using weight measurements at each wheel in different conditions. In addition, the following variables are used:

- c is the vehicle track,
- α is the bank angle of the terrain,
- $\gamma = \varphi + \alpha$ is the overall bank angle in the roll frame,
- I_x, I_y and I_z are respectively the roll, pitch and yaw moments of inertia,
- $P = mg$ is the gravity force attached to the suspended mass in the roll projection (where g is the gravitational constant),
- F_{n1} and F_{n2} are the normal components of the wheel/ground contact forces at the vehicle left and right sides.

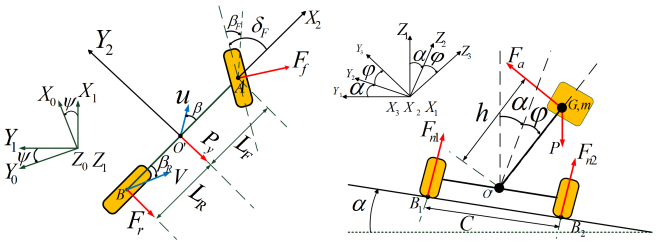

(a) Yaw Projection (b) Roll Projection

Fig. 2. Vehicle modeling into two frames

B. Wheel/Ground interaction model

As illustrated in Figure 2(a), lateral contact forces at each wheel F_f and F_r are solely considered since this paper is only interested in the lateral risk of rollover. In order to avoid the use of complex tire/soil interaction models such as [18], these forces are assumed to be in linear relation with corresponding sideslip angles β_F and β_R, such as:

$$\begin{cases} F_f &= C_f \beta_F \\ F_r &= C_r \beta_R \end{cases} \tag{4}$$

with $C_f,\ C_r > 0$, cornering stiffnesses for the front and the rear axle. However, in order to account for the non-linear behavior of the tire and grip conditions variations, the cornering stiffnesses are adapted online relying on the backstepping observer proposed in previous work [19] and recalled below.

C. Observer for grip conditions reconstruction via the Yaw model

The lateral dynamics observer is based on both the linear tire model (4) and the yaw model depicted in Fig. 2(a) and its general scheme is shown in Fig. 3. As detailed in

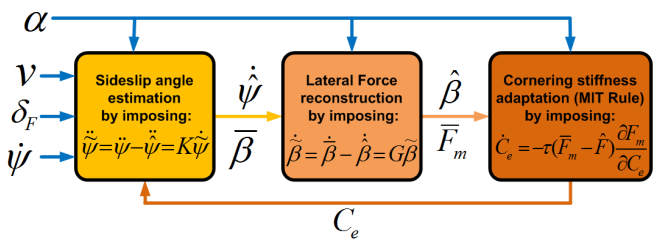

Fig. 3. Observer overview

Section V-A, the yaw rate ($\dot{\psi}$), the rear axle linear velocity (v) and the steering angle (δ_F) are measured. The terrain inclination (α) is estimated thanks to the measured lateral acceleration of the vehicle. These only four variables do not permit to estimate C_f and C_r separately. Thus, for observability reasons, they are supposed to be equal to a global virtual cornering stiffness C_e, i.e., $C_f = C_r = C_e$. The backstepping observer is divided into three parts:

- The first one consists in computing a virtual measurement of the global sideslip angle (noted $\bar{\beta}$ in Fig. 3). More precisely, $\bar{\beta}$ is derived by imposing the convergence of the estimated yaw rate $\hat{\dot{\psi}}$ to the measured one $\dot{\psi}$. This virtual global sideslip angle $\bar{\beta}$ is then treated as a reference to be reached by the observed angle $\hat{\beta}$.
- In the second step, lateral contact forces are reconstructed by treating the global lateral contact force $F_m = C_e(\beta_F + \beta_R)$ as a control variable (denoted $\overline{F_m}$ in Fig. 3). More precisely, $\overline{F_m}$ is obtained by imposing an exponential convergence on the observation error of the global sideslip angle $\tilde{\beta} = \bar{\beta} - \hat{\beta}$. Thereafter, $\overline{F_m}$ is treated as reference to be reached by the observed one $\widehat{F}$.
- Finally, since C_e is a slow varying parameter of force model (4), it has been obtained by imposing the convergence of the estimated force $\widehat{F}$ to $\overline{F_m}$ by using the MIT rule adaptation law as presented in [20].

As mentioned in previous work [19], the observer is stable and ensures asymptotic convergence except when the vehicle is at stop ($v = 0$), which is not considered here because at ($v = 0$) there is no risk of rollover or when $L_R = L_F$ which is never met on commercial tractors [21].

D. Rollover Metric Estimation via the Roll Model

As detailed in [14], the fundamental principle of dynamics applied on the roll model depicted in Fig.2(b) yields motion equations (6) in the roll frame. From the first equation of the roll model (6), the roll angle value (φ) is derived and thereafter, the rollover risk (1) is estimated thanks to the two last equations of system (6). Figure 4 summarizes the process of LLT estimation relying on the partial dynamic approach used for modeling the vehicle. Indeed, thanks to the observer described previously, all the variables of the roll model are known, so that the LLT can be estimated from (1) and (6).

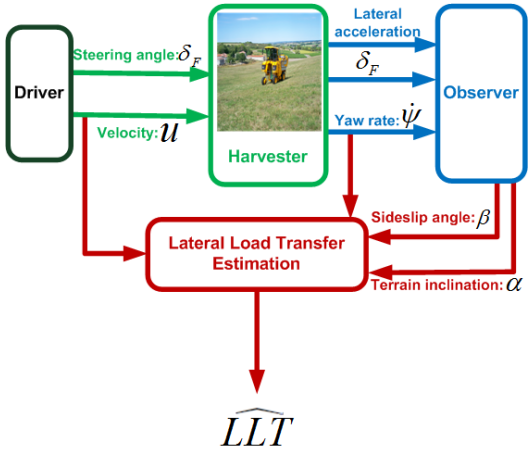

Fig. 4. Lateral Load Transfer Estimation Scheme

IV. PARAMETRIC ADAPTATION FOR THE RELEVANCE OF THE ESTIMATED $\widehat{LLT}$

As pointed out before, the LLT estimation proposed in Section III requires the knowledge of several parameters that may be varying, such as the mass and the elevation of the center of gravity. Some off-road machines such as the experimental vehicle considered here, i.e., a grape harvester, can be geometrically reconfigured according to the terrain slope and its heaviness changes gradually when the grape receptacle is filled. Indeed, its heaviness may change in real time as the grape receptacle is progressively filling for instance. As a result, the estimated LLT may diverge from its actual value.

Hence, the aim of this section is to combine, when it is available, the discontinuous measurement of the LLT detailed in Section II with its estimation presented in Section III-D in order to update the vehicle varying parameters so that

the estimation algorithm can always deliver relevant $\widehat{LLT}$ values. This then enables to monitor the stability of the vehicle whatever the state of the slope correction system, the soil type and the load of the machine.

A. Comparison and Coupling of measured and estimated Lateral Load Transfer

The idea is to update the height h and/or the mass m in order to ensure the convergence to zero of the error e between the measured and the estimated LLT. The general scheme is shown in Fig.5. More precisely, at each instant, the procedure is as follows:

1) Lateral Load Transfer measurement, according to equation (2),
2) If it is available,
   - Computation of the derivative of the height (respectively of the mass) according to equation (5) in order to ensure the convergence of the error e to 0,
   - Update of the height parameter (respectively of the mass) as: $h = h + \dot{h}dt$ (respectively, $m = m + \dot{m}dt$) where dt is the sampling period,
3) If $\overline{LLT}$ measurement is not available, then h and m remain unchanged.

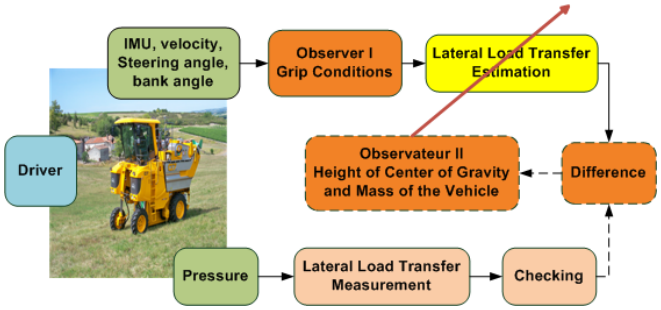

Fig. 5. Synopsis of the Estimator herein proposed

B. Adaptation of the vehicle suspended mass and of the height of the center of gravity

Provided that h and m are slow-varying parameters, which is a relevant assumption in the considered application, they can be adapted on-line, relying on a sensitivity based gradient search algorithm, in order for $e = \widehat{LLT} - \overline{LLT}$ converges to 0. Then h and m should be adapted according to equations (5).

$$\begin{cases} \dot{h} &= -\tau_1(.)\ e\ \frac{\partial \widehat{LLT}}{\partial h} \\ \dot{m} &= -\tau_2(.)\ e\ \frac{\partial \widehat{LLT}}{\partial m} \end{cases} \tag{5}$$

where $\tau_1(.) > 0$ and $\tau_2(.) > 0$ are two varying gains controlling the dynamics of the convergence of the adapted parameters.
As it can be seen in the roll model (6), h and m have a similar influence on the estimated LLT. Nevertheless, mechanical constraints limit their evolution. Hence, in order to compel the adapted values of the parameters to stay within their physical limits, $\tau_1(.)$ and $\tau_2(.)$ are designed as two sigmoid functions. Indeed, as depicted in Figure 6, $\tau_1(.)$ is zero when h reaches its extreme values. $\tau_2(.)$ is similarly defined. In the sequel, the height of the center of gravity is more likely to vary, for instance when the driver uses the slope correction system. Conversely, the vehicle weight is very slow varying parameter when the grape receptacle is being filled. Consequently, $\tau_2(.)$ has been designed so that the adaptation of the height has a higher priority than the adaptation of the mass.

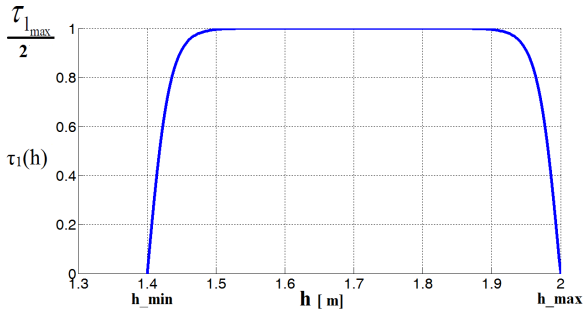

Fig. 6. Varying gain function of the height

V. Experimental results

In order to highlight the efficiency of the proposed approach, some results obtained with a grape harvester are presented and discussed below.

A. Experimental vehicle and on boarded sensors

The experimental vehicle used to validate the proposed algorithm is a grape harvester manufactured by Gregoire SAS, depicted in Figure 1. As it can be seen, it is equipped with slope correction systems. The maximal inclination that can be imposed by this device is 16.5°. The total machine weight and the height of the center of gravity can vary during work respectively from 9 tons to 12 tons and from 1.4 m to 2 m and the maximal speed is 2 m/s.
The main sensors on-board, to be used by the algorithms described in this paper, are:

- a low cost IMU (Xsens), providing accelerations and angular velocities in three dimensions. Thanks to the lateral acceleration, the vehicle inclination (α) can also be known,
- a Doppler radar, supplying the vehicle velocity (v) at the center of the rear axle,
- an angular sensor providing the steering angle δ_F,
- pressure sensors located at the inlet and outlet chambers of the hydraulic actuators, providing the differential pressures.

B. Validation of the proposed algorithm

The conditions of the test carried out to demonstrate the capabilities of the proposed algorithm are listed in Table I. The grape harvester moves on a sloping field (around 10°), perpendicularly to the slope. As shown in Figure 7, the

$$\begin{cases} \ddot{\gamma} & = \frac{1}{h\cos\varphi}(h\dot{\gamma}^2\sin\varphi + h\dot{\psi}^2\sin\gamma\cos\alpha + u\dot{\psi}\cos\beta\cos\alpha + \dot{u}\sin\beta + u\dot{\beta}\cos\beta - \frac{F_a}{m}\cos\varphi + g\sin\alpha) \\ F_{n1}+F_{n2} & = m(-h\ddot{\gamma}\sin\varphi - h\dot{\gamma}^2\cos\varphi + g\cos\alpha - \frac{F_a}{m}\sin\varphi - h\dot{\psi}^2\sin\gamma\sin\alpha + u\dot{\alpha}\sin\beta - u\dot{\psi}\cos\beta\sin\alpha) \\ F_{n1}-F_{n2} & = \frac{2}{c}(I_x\ddot{\gamma} + (I_z - I_y)\dot{\psi}^2\sin\gamma\cos\gamma - h\sin\varphi(F_{n1}+F_{n2})) \end{cases} \quad (6)$$

trajectory followed is composed of a straight line, a half turn and a straight line to go back to the starting point.

TABLE I
TESTS CONDITIONS

Vehicle load	10.3 tons
Velocity	1.35 m/s
Grip conditions	Wet soil
slope correction system	On
Height of the Center of Gravity	1.7m

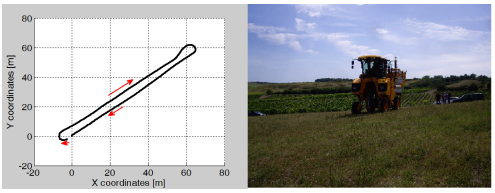

Fig. 7. Vehicle path

Figure 8(a) compares the estimated LLT (see Section III-D) and measured LLT (see Section II). The green graph was obtained by feeding the algorithm with the real values of the suspended mass and height of gravity, (i.e., $m = 10.3$ tons and $h = 1.7$ m, see Table I). It can be noticed that the estimated LLT is properly superposed with the measured LLT (black graph) when this latter is available. This demonstrates the relevance of the estimation algorithm on difficult soil.
The red graph was obtained when the estimation algorithm is fed with incorrect values for h and m and when these latter are not adapted (as it can be seen in Figures 8(c) and 8(d)). More precisely, the height ($h = 1.4$ m) and the mass ($m = 9$ tons) values are incorrects but they are realistic since they both belong to the admissible ranges (9 tons to 12 tons for m, 1.4 m to 2 m for h). Fig. 8(a) shows in this case, the estimated LLT is not representative of the actual one and consequently could not be used to detect imminent rollover. This result demonstrates that the knowledge of the vehicle mass and height of the center of gravity is necessary for a relevant estimation of the LLT.
The graph in blue was obtained when initializing the estimation algorithm with the previous incorrect parameters values (i.e., $h = 1.4$ m and $m = 9$ tons) but this time they were adapted on-line according to the gradient descent method (5). As soon as a measured LLT is available, the adaptation of the mass and of the height (see blue graphs in Fig. 8(d) and 8(c)) allows the estimated LLT to converge to its actual value. This demonstrates that the algorithm meets the expectations and allows to overcome the discontinuous availability of the LLT measure, even if h and m are poorly known.
As illustrated in Fig. 8(c), when the measure is not available (as a matter of fact between 124 and 141 seconds), the parameters adaptation is stopped as expected but the proposed algorithm continues to provide a reliable indicator of the risk of rollover. Indeed, when the LLT measure is again available at 141 seconds, i.e. just before the parameters are again adapted, the estimated LLT is still superposed with the measured one. This result demonstrates the algorithm robustness with respect to changes in vehicle geometry: as shown in Fig. 8(b) and 8(a), the driver used the slope correction system when he took the half-turn between 124 and 141 seconds. Thereafter, the overlap between the estimated and measured LLT is instantaneous. On many tests, it was found that the LLT measurement through the pressure sensors is often unavailable, showing the interest of the estimation presented in this paper.
Finally, it is relevant to notice in Fig. 8(c) and 8(d), that the variation of h and m stays within their physical values. Indeed, the mass adaptation starts at 49 seconds, and 19 secondes later the real value of the mass is reached (i.e., $m = 10.3$ tons). Then, the adaptation of m is definitively stopped at its correct value. And without exceeding its correct value ($h = 1.7$ m), the height adaptation continues to ensure the convergence of the estimated LLT to the measured one. As a result, the adaptive method described here can also be used as an indirect measurement of the variation of the vehicle mass which has an important interest in the agricultural field.

VI. CONCLUSION AND FUTURE WORK

This paper has presented a control stability system based on-line estimation of the LLT metric continuously. Moreover, the latter can also be intermittently measured from the pressure sensors equipping the slope correction system of the grape harvester. The coupling of these discontinuous measurements with the estimated LLT allows the adaptation of vehicle parameters relying on a sensitivity based gradient search algorithm, so that the estimated LLT can always be relevant. This then allows to monitor the stability of the vehicle whatever the state of the slope correction system, the soil type and the load of the machine. As demonstrated in experiments, the multi-model approach chosen for modeling the vehicle is validated by the representativeness of the estimated LLT compared with the measured one. This online estimation method is implemented for the lateral load transfer evaluation, but it could also be applied similarly to evaluate the longitudinal load transfer. Hence, current work aims at extending the estimation method described here to the longitudinal risk of rollover. This work is also developed

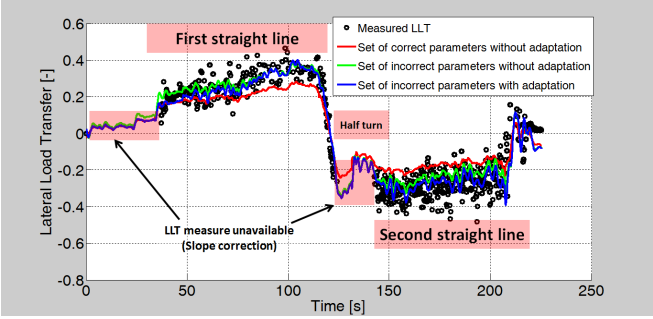

(a) Estimated and Measured Lateral Load Transfer

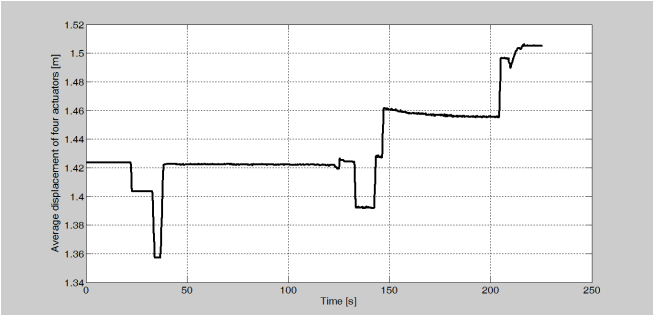

(b) Actuators displacement

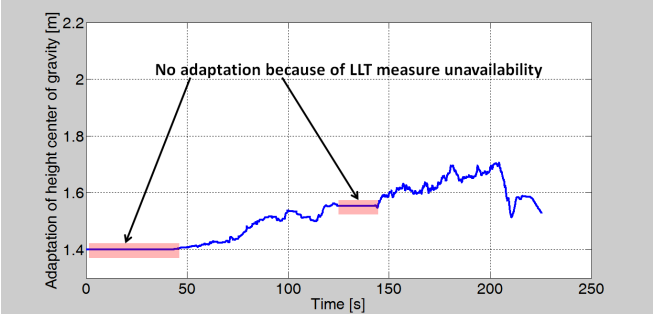

(c) Height adaptation

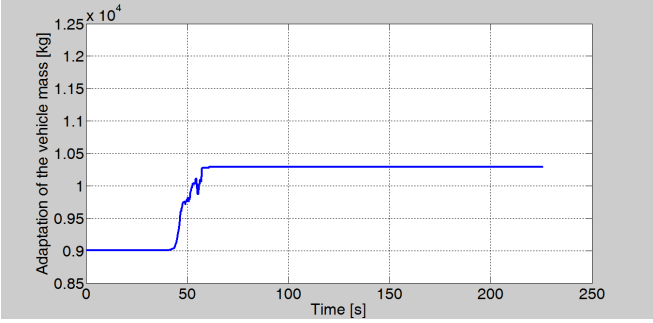

(d) Mass adaptation

Fig. 8. Parameters adaptation for a relevant Lateral Load Transfer Estimation

further in order to anticipate the rollover risk by predicting the LLT values relying on the proposed vehicle models.

ACKNOWLEDGMENT

This work is supported by French National Research Agency (ANR) under the grant ANR-10-VPTT-008 attributed to ActiSurTT project. It also received the support of French Agricultural Social Insurance (CCMSA) and French Ministry of Agriculture.

REFERENCES

[1] S. Blackmore, B. Stout, M. Wang, and B. Runov, "Robotic agriculture - the future of agricultural mechanisation," *5th European Conference on Precision Agriculture (ECPA), Upsala (Sweden)*, 2005.

[2] CCMSA, "Accidents du travail des salariés et non salariés agricoles," Observatoire des risques professionnels et du machinisme agricole, Paris, France, Tech. Rep., 2006.

[3] M. Personick and J. Windau, "Self-employed individuals fatally injured at work," *United States Bureau of Labor Statistics, Washington, DC*, pp. 55–62, 1997.

[4] N. S. Council, "Accident facts," National Safety Council, Chicago, IL, Tech. Rep., 1999.

[5] J. M. Stellman, *Encyclopédie de santé et de sécurité au travail*. Bureau International du Travail, Genève, Suisse, 2000, vol. 4.

[6] ASAE, "standards: roll-over protective structures (ROPS) for wheeled agricultural tractors (iso compatible)." *ASAE S519 DEC94*, 1997.

[7] H. Cole, M. Myers, and S. Westneat, "Frequency and severity of injuries to operators during overturns of farm tractors," *Journal of Agricultural Safety and Health*, vol. 12, no. 2, pp. 127–138, 2006.

[8] F. Tahami, R. Kazemi, and S. Farhanghi, "A novel driver assist stability system for all-wheel-drive electric vehicles," *IEEE Transactions on Vehicular Technology*, vol. 52, no. 3, pp. 683–692, 2003.

[9] B. Guvenc, T. Bunte, and D. Odenthal, "Robust two degrees-of-freedom vehicle steering controller design," *IEEE Transactions on Control Systems Technology*, vol. 12, no. 4, pp. 627–636, 2004.

[10] B. Paggi and M. Ribaldone, "Braking control system for agricultural tractors." *Same Deutz-Fahr: Italy*, 2000.

[11] M. Kise and Q. Zhang, "Sensor-in-the-loop tractor stability control: Look-ahead attitude prediction and field tests." *Computers and Electronics in Agriculture*, vol. 52, no. 1-2, pp. 107–118, 2006.

[12] J. Powers, J. Harris, J. Etherton, K. Snyder, M. Ronaghi, and B. Newbraugh, "Performance of an automatically deployable rops on asae tests," *Journal of Agricutural Safety Health*, vol. 7, no. 1, pp. 51–61, 2001.

[13] K. Owusu-Edusei Jr, "Net monetary benefit of cost-effective rollover protective structures (crops): An estimate of the potential benefits of the crops research project." *Journal of Agriculture Safety and Health*, vol. 14, no. 3, pp. 351–363, 2008.

[14] D. Denis, "Contribution à la modélisation et à la commande de robots mobiles reconfigurables en milieu tout-terrain. application à la stabilité dynamique d'engins agricoles," Ph.D. dissertation, Université Blaise Pascal, Clermont-Ferrand II, 2015.

[15] D. Odenthal, T. Bünte, and J. Ackerman, "Nonlinear steering and braking control for vehicle rollover avoidance," *Proc. of European Control Conference (ECC), Budapest (Hongrie)*, 1999.

[16] B. Chen and H. Peng, "Differential-braking-based rollover prevention for sport utility with human-in-the-loop evaluations," *Vehicle System Dynamic*, pp. 359–389, 2001.

[17] G. Genta, "Motor vehicle dynamics: Modeling and simulation," *World Scientific*, 1997.

[18] H. Pacejka, *Tire and vehicle dynamics*. Society of Automotive Engineers, 2002.

[19] M. Richier, R. Lenain, B. Thuilot, and C. Debain, "On-line estimation of a stability metric including grip conditions and slope: Application to rollover prevention for all-terrain vehicles," *in Proceedings of IEEE/RSJ International Conference on Intelligent Robots and Systems, IROS'11, San Francisco, U.S.A*, pp. 4569–4574, 25-30 Sept. 2011.

[20] K. Åström and B. Wittenmark, "Adaptive control (2nd edition)," *New-York, Addisson-Wesley*, 1994.

[21] D. Denis, A. Nizard, B. Thuilot, and R. Lenain, "Slip and cornering stiffnesses observation for the stability assessment of off-road vehicles," *in Workshop "Transports, Mobility and Vehicles" at Mediterranean Green Energy Forum (MGEF), Marrakech (Morocco)*, 2015.

Narrow tractor development: emissions, mother regulation, comfort and precision farming. All in the same space

Massimo Ribaldone[a,*], Stefano Dominoni [b]

[a] Executive Vice President and Head of Tractors & Combines development, SDF group, Treviglio, 24047, Bergamo, Italia

[b] Vehicle Systems Analyst, SDF group, Treviglio, 24047, Bergamo, Italia

* Corresponding author. Email: massimo.ribaldone@sdfgroup.com

Abstract

Nowadays not only the big open field tractor has to fulfill the EU regulations such as engine emissions level and mother regulation but also the narrow tractors.

Moreover comfort and driveability are becoming important for improving the efficiency in the daily work. So kind of tractor has also to be fit with the implements with high flow hydraulic circuits.

Precision farming and connectivity have the same level of requirements like the open field tractor.

Keywords: narrow tractors, efficiency in the daily work, precision farming and connectivity.

1. Introduction

The open field tractors have to fulfil several requirements in terms of EU regulations (such as emissions level and mother regulation) and performance like fuel consumption, driveability, comfort and hydraulic flow rate. Precision farming and connectivity are well known topics, and they will be much more important with the development of the new technologies.

All these goals do not change moving from tractors of big size to the narrow ones, but the challenge become much more interesting due to the small size and the complexity of the possible working conditions. Special tractors for orchard and vineyard have to fulfil much more requirements, that are strictly related to their own mission profile. Among all the constraints, the most important are the tractor dimensions, in particular the short wheelbase and a very high steering angle (higher than 55°) in order to achieve very low steering radius. The wheel-track is a big item for several reasons, it is suitable for all the operations in the narrow row spacings, but in the same time it's dangerous in some manoeuvres, like turning in field both uphill and downhill due to the low stability.

The tractor mass distribution is another very important point which affects stability, handling and traction. A low centre of gravity height means a lower load transfer, and namely an higher stability and a better handling not only in field, but even in transport at high speed. A proper weight distribution between the two axles is very important for having always good traction, in particular in field. It is easy to understand the importance of this matter with different implements coupling, which can be placed in lateral position, in front or at the rear.

All these aims are satisfied by means of high technology solutions which affect the design of many tractor components like powertrain, axles, cab, hydraulic circuit, electronic control, etc., but above all the design methodology, with the necessity to find the optimal result by means of very sophisticated analysis and advanced simulation tools. This optimization process is based on the design of experiments (DOE), where the tractor performance are evaluated as a function of the design variable, in order to achieve the best possible performance among several objective functions. This process is much more suitable as the input data are reliable, for this reason it is very important to collect data from the field and to know the real tractor mission profile.

For instance, the cooling system has been developed starting from the data recorded in field in different conditions of engine power exploitation and/or hydraulic power absorption. Transmission has to be developed according to the engine, and with the right number of speeds around the working speed for properly managing power and sprayer implements. All the implements used have to be analyzed and monitored in field because the collected data are helpful for the transmission re-sizing.

All these information have to be managed by a very detailed electronic control, with the purpose to manage signals coming from different devices, giving back the best control law depending on the goal to achieve, for instance, the best powertrain work condition, or the proper damping level of the front suspension to increase the comfort felt by the driver.

Most of the tractors are sold to big professional farmers, where the vineyard are cultivated through intensive agricultural methodology, this requirement goes very well with new technologies currently available like drones and sensors of temperature, humidity, infrared pictures, etc.. All these thing connected each other could help the farmer to take the right decision for getting high product quality at fair cost. Monitor, antenna, connectivity module and TIM (Tractor Implement Management) interface need to be installed on narrow tractor in order to ensure the performance required.

Nothing can be forgotten.

2. Materials and Methods, Results and Discussion

2.1. History and main features

SDF design and manufacture tractor for orchard and vineyard since approximately 1970, with the first model called "Atlanta". That tractor was not entirely designed as special tractor, but it was a sort of open field tractor with reduced wheel-track and an higher steering angle. SDF quickly realized the necessity to design a specific tractor with lower steering radius, better handling for all the operations in the narrow row spacings, and suitable for working on the hills. For these reason SDF introduced new front and rear axles, with reduced wheel-track and wheelbase, equipping the tractor with tyres of small size to reduce the bonnet height and the tractor centre of gravity. Another very important point was the height from the ground.

These were the main feature of the models "Minitauro", "Delfino", "Aurora" and "Corsaro", and in 1979 SDF started the production of the first tractors properly designed for orchard and vineyard applications: the "Vigneron", see Figure 1.

Figure 1. Vigneron, 1979 - 1997.

"Vigneron" was designed to face the demand of the French vineyard market. This model was characterized by new transmissions, front axle with wheel-track lower than 1m, and higher engine power (70hp instead of 45hp of the "Atlanta" model). From 1991 to 2011 SDF started the production of the "Frutteto" model with a new comfortable cab and a further step in terms of stability, lightness, compact dimensions and engine power (reaching 110hp).

All these tractors were equipped by a front rigid tilting axle, but in 2014 SDF started the design on a new front axle with the purpose to improve the tractor comfort, handling, road holding and safety both in field and during transport, and increase traction and operative speed. The matter was very challenging because SDF wanted to design a plug and play solution without carry over from the current production, and with the purpose to start the production of a new front axle layout in parallel to the usual rigid tilting axle. There were some technical constraints like reduced steering radius, low centre of gravity, stability and compact dimensions, and last but not least time limit and a certain target cost. SDF identified the double wishbone suspension as best solution among several layout and in 2016 started the production of this new front axle, called "Frutteto Active Drive". See Figure 2 (for a detailed description about the design methodology see paragraph 2.2).

Figure 2. Frutteto Active Drive, 2016.

All the models previously described represent an evolution not only in terms of size or engine power, but even from the transmission and hydraulic point of view. The transmission plays a fundamental role both in terms of efficiency and working speed. The introduction of range gear, creeper and super creeper have allowed to define much more working speed for properly manage the power and the speed with sprayer implement.

The transmission design will be very close to the engine, and the goal will be the optimization of all the powertrain reducing the fuel consumption and increasing the efficiency. In the meantime the engine will be undergone to further steps in terms of emission. Special tractors are currently moving from stage 3A to stage 3B, and the stage 5 is very close.

The data coming from the field are fundamental to design and develop the powertrain; the main example is for sure represented by the cooling system, because the experimental data allow to define the conditions of engine power exploitation and/or hydraulic power absorption.

A very detailed analysis of the under bonnet fluid dynamic allows to optimize the cooling system by means of the CFD analysis. This is a very important topic because all the devices positioned under bonnet have to be smallest than possible, otherwise the bonnet would be bigger with a reduction of steering capacity and visibility, see Figure 3.

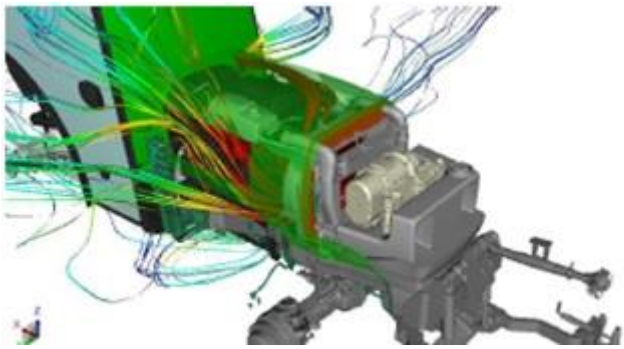

Figure 3. Under bonnet CFD analysis.

The cab has been undergone to different improvement steps that are not only ergonomics (noise, vibration, visibility, etc.) or safety (ROPS), but even for the air healthiness. The last improvement is represented by the cab 4 category with active carbon filter able to block the entrance of dangerous substances (not only the dust but also aerosol and gas).

An evolution has occurred not only on the tractor but even on the implements, with higher flow power rate required; for instance, the "Vigneron" had a flow power rate of 24l/min, while nowadays it is much more than double. The development of new implements will increase this requirements in the future technical specifications. This is a very important point, SDF is developing a new system able to increase the front hydraulic flow rate and to manage it in a smart way. SDF entirely design the overall powertrain and the hydraulic circuit, this is an advantage respect to the other competitor because we can manage two pumps drive: one on the transmission and one on the engine, increasing the number of pump, the number of SCV's couplers way (a maximum of 12 instead of 7) and the hydraulic flow rate. An higher hydraulic flow rate means additional requirements in terms of cooling capacity, for this reason a smart management of the flow rate is needed. The smart management of the new hydraulic circuit, called high flow, will allow to manage directly from the cab the flow rate distribution between the front and the rear as a function of the implement

coupled with the tractor, and the request of flow rate.

The coupling between tractor and implement will be much more important because a smart cultivation will allow to optimize the vineyard productivity. The TIM (Tractor Implement Management) allow to the implement to "talk" with the tractor requiring for instance to increase/decrease the speed or the hydraulic power flow. Connectivity and precision farming will represent a step further.

2.2. Tractor development

A tractor is a complex system made by different subsystems which have to be taken under control, communicating each other, and influencing the overall tractor performance. In a special tractor all these things are much more important because of the small size and all the requirements previously described, for this reason it is necessary to adopt a new design methodology with the necessity to find the optimal result by means of very sophisticated analysis and advanced simulation tools.

A good example of this new methodology is represented by the double wishbone front axle suspension developed by SDF. The guideline of the project have been represented by a very detailed risk assessment analysis which has underlined the main functionalities to achieve in order to satisfy safety and functional requirements. This analysis played a fundamental role because the weakness point of the risk assessment have been the main focus during the design of the suspension.

One of the critical point was the stability on hill, because the wrong chosen of suspension stiffness could lead to tractor rollover at a slope lower than the tractor currently in production, but this situation was absolutely to avoid because it would represent a not acceptable loss of performance respect to the tractor with rigid axle. In addition to this scenario we identified other working conditions useful to assess tractor comfort, handling and road holding, which are affected by suspension stiffness and damping. It was clear that we were facing an optimization process and for this reason we decided to approach the problem by means of a design of experiment (DOE). This approach has been followed considering the tractor with front rigid tilting axle as reference, and comparing the performance of several front axle layout (double wishbone suspension, suspended rigid axle, etc.) with that of the reference.

We made two different optimization processes, the first one for the definition of the kinematic points of the suspension, and the second one for the definition of the suspension parameters in terms of stiffness and damping. The second optimization was the most challenging because we have analysed several possible manoeuvres representative of the tractor behaviour in field and during transport, at different tractor speed and for different tractor mass distribution (front or rear implement, lateral pruner). For each of these scenario we summarized the results in graph as shown in Figure 4.

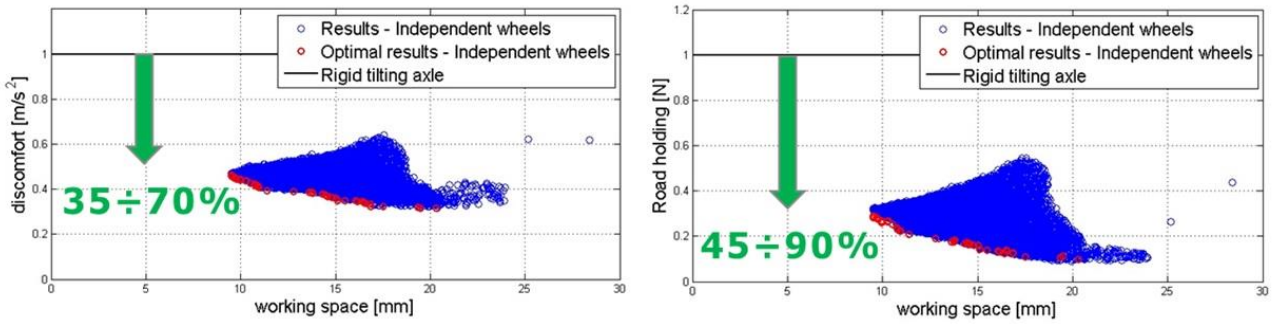

Figure 4. Optimization results.

Figure 3 shows two of the possible objective functions (discomfort and road holding) as a function of the suspension working space for a specific manoeuvres (symmetrical and asymmetrical obstacles). The black line represents the performance of the rigid tilting axle, while each of the blue circle represents the performance reached by the double wishbone suspension depending on the values of stiffness and damping. The Figure 3 shows, in this manoeuvre, a clear improvement (at least 35% for the discomfort index and at least 45% for the road holding index) respect to the rigid tilting axle, but this is not enough because among all these solutions we have chosen just the optimal one. Optimal solutions are represented by the red circle and they mean optimal among all the scenario analysed with a certain tractor mass distribution. As result of our simulations we have defined the technical specification in terms of stiffness and damping as a function of the tractor mass.

Following this methodology there is, as consequence, a different relationship with our suppliers, which are involved since the beginning in the definition of the component suitable for our device. Even our own internal work organization

was changed as a function of the new methodology, because colleagues from different departments (hydraulics, electronics, virtual and experimental validation, etc.) are involved since the beginning in a work team with the purpose to achieve all the technical specifications, integrating the components provided by our suppliers in the whole suspension device.

Another example of application of this new methodology is represented by the DTC (Differential Traction Control), which has the purpose to split the traction force on the wheel in contact with the ground avoiding problems due to the loss of traction, see Figure 5.

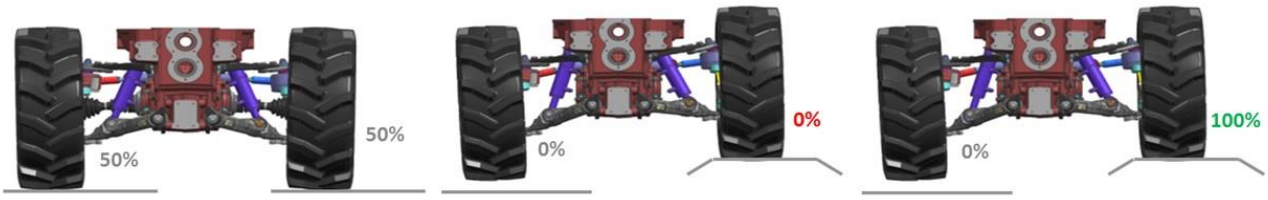

Figure 5. DTC (Differential Traction Control).

In this case the simulation tools have been very helpful for the detection of the problem and how to manage it. The simulations have allowed to design the software able to manage the signals which come from the sensors, detecting the loss of traction with the automatically closing of the front differential without loss of traction.

2.3. Precision farming and connectivity

Most of the tractors are sold to big professional farmers, where the vineyard are cultivated through intensive agricultural methodology and with the help of other technologies currently available like drones, ISOBUS devices, sensors of temperature, humidity, infrared pictures, etc.. All these thing connected each other could help the farmer to take the right decision for getting high product quality at fair cost. Monitor, antenna, connectivity module and TIM (Tractor Implement Management) interface need to be installed on narrow tractor in order to ensure the performance requested.

Connected Vineyard is a system designed to improve, integrate, automate and make an easier management of the vineyard and the work in the vineyard itself, by means of an integration among several well-known technologies like ISOBUS devices, drones, weather stations and sensors. In particular, Connected Vineyard is a system cloud based, which offer to the farmer the possibility to manage all the process, including the planning of the drone fly, the mapping of the vineyard, the monitoring of the cultivation and the delivery of the final report after work. Everything is allowed by a cloud platform where all the devices, machines and sensors are continuously connected each other in a constant bi-directional exchange of data. Connected Vineyard objectively support all the decisions that the agronomist have to take in his vineyard management, see Figure 6.

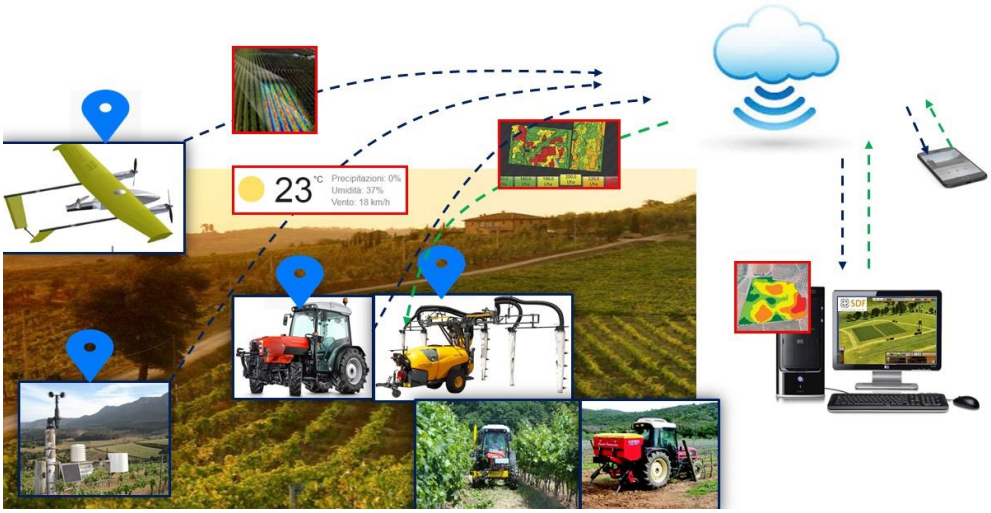

Figure 6. Connected Vineyard.

Figure 6 shows how the system works, with all the data measured by the sensors that are stored in a cloud and managed in order to help the agronomist to take his decisions. One of the most interesting point is represented by the weather station because it can forecast the possible weather conditions and optimize when to work in field depending on the weather condition itself. Everything is managed by the monitor placed ahead of the steering wheel, see Figure 7.

Figure 7. Connected Vineyard.

Another very important point is the mapping of the vineyard and the monitoring of the cultivation, because with the data coming from the field it is possible to estimate a model of the cultivation health, with a forecasting about when and where the vineyard can become ill.

3. Conclusions

The open field tractors have to fulfil several requirements in terms of EU regulations (such as emissions level and mother regulation) and performance like fuel consumption, driveability, comfort and hydraulic flow rate.

All these goals do not change moving from tractors of big size to the narrow ones, but the challenge become much more interesting due to the small size and the complexity of the possible working conditions. Special tractors for orchard and vineyard have to fulfil much more requirements, that are strictly related to their own mission profile. Among all the constraints, the most important are the tractor dimensions, in particular the short wheelbase, the very high steering angle and the narrow wheel-track suitable for all the operations in the narrow row spacings.

All these aims are satisfied by means of high technology solutions which affect the design of many tractor components like powertrain, axles, cab, hydraulic circuit, electronic control, etc., but above all the design methodology, with the necessity to find the optimal result by means of very sophisticated analysis and advanced simulation tools. This optimization process is based on the design of experiments (DOE), where the tractor performance are evaluated as a function of the design variable, in order to achieve the best possible performance among several objective functions. This process is much more suitable as the input data are reliable, for this reason it is very important to collect data from the field and to know the real tractor mission profile. These data are very important for the development of new subsystems like the cooling system and the transmission re-sizing.

Most of the tractors are sold to big professional farmers, where the vineyard are cultivated through intensive agricultural methodology, this requirement goes very well with new technologies currently available like drones and sensors of temperature, humidity, infrared pictures, etc.. All these thing connected each other could help the farmer to take the right decision for getting high product quality at fair cost. Monitor, antenna, connectivity module and TIM (Tractor Implement Management) interface need to be installed on narrow tractor in order to ensure the performance required.

References

Journal articles:

R. Demaldè, Frutteto S 90.3 ActiveDrive: tra i filari col comfort di un campo aperto, Macchine Agricole Domani, Settembre 2016, 36 – 43.
http://www.macchineagricoledomani.it/ita/provemadscheda.asp?ID=2372
http://www.macchineagricoledomani.it/same_frutteto_90_3_activedrive

Same Frutteto S 90.3 Active Drive, Trattori, Febbraio 2016, 26 – 31.

Conference proceedings papers and book sections:

M. Ribaldone, F. Galli, S. Dominoni, S. Tremolada, *Development of an innovative suspension and traction system for compact tractor*, 4th International VDI Conference Transmission in mobile machines, Friedrichshafen, VDI Berichte 2276 pp.743 – 753, 21 and 22 June 2016

Patents:

L. Heraudet, L. Stucchi, *Sistema a singola ruota sospesa sterzante comprendente un dispositivo sensore di rotazione*, 2015, Patent application BG2015A000017

L. Heraudet, L. Stucchi, *Gruppo giunto con dispositivo sensore di rotazione*, 2015, Patent application BG2015A000016

Tools and methods to develop and validate soil-wheel interaction model and knowledge.

P. Heritier [a,*], D. Miclet [a], E. Piron [a], M. Chanet [b], R. Lenain [b]

[a] Irstea, UR TSCF, Centre de Clermont-Ferrand, Domaine des Palaquins, F-03150 Montoldre, France

[b] Irstea, UR TSCF, Centre de Clermont-Ferrand, F-63178 Aubière, France

* Corresponding author. Email: philippe.heritier@irstea.fr

Abstract

The development of high efficiency off-road tyre aims at obtaining high economic and ecological gain during agricultural works, thanks to reduction of soil compaction and reduction of energy consumption. It appears necessary to design new measurement devices in order to optimize tyre performances and limit environmental impact on agricultural fields. This paper introduces a package of tools and methods available or/and recently developed to measure agricultural tyre performances regarding tyre efficiency and soil compaction minimization. An overview of measurement devices dedicated to the analysis of tyre soil interaction is proposed. Developed in the TSCF research unit of Irstea, such a package permits to investigate the impact of tyre on the efficiency of agricultural tasks and the environmental impact. Such tools allow improving the design of tyre and adjust their tuning to improve off-road works efficiency.

Keywords: tyre efficiency, soil compaction, soil-wheel interaction.

1. Introduction

The role of the tyre in vehicle dynamics is fundamental, because it transmits all forces, which are acting on the vehicle. On soft soil and mostly on agricultural soil, the tyre role is even more important because of its direct impact on soil fertility. Agricultural productivity is closely linked to soil compaction, and its preservation allows to avoid decompaction work which is both energy and time-consuming. So, in order to help design and evaluation of tyre performances, regarding satisfaction of environmental and economic stresses, tools and methods should be available.
This paper presents a set of tools to evaluate performances regarding efficiency losses and impacts on soil compaction. A first part describes a package of available tools. It includes a single-wheel tester equipped with sensors allowing measurement of tyre deformations and efficiency, a scattering measurement device, an automatic penetrometer and a 3D scanner to measure soil compaction and deformation. A second part highlights results obtained using these tools, particularly regarding the development of a tyre sensor allowing tyre deformation measurements and empirical carcass tyre deflection model development. An overview of parameters which are extracted from the single-wheel tester, and an application of these parameters to compare tyres and to determine optimum tyre setting is given. Finally a comparison regarding soil compaction of two tyres using two different technologies is introduced. This last study requires 3D laser scanner and automatic penetrometer.

2. Materials and Methods

2.1. Single-wheel tester

Irstea developed from several years a specific device named "single-wheel tester" to perform experimental studies regarding soil-wheel interaction. It's linked to the three-point linkage of an agricultural tractor. It can be divided by three different parts:

- a deformable parallelogram enabling to transmit only the gravity vertical force to the tested wheel. By this way, a metallic frame allows to apply a constant static load to the wheel;
- a hydraulic control unit, electronically driven, provides power to the wheel (Figure 1);
- a mechanical frame for the linkage with the tractor, sensor equipped to provide net traction power.

The single-wheel is equipped with several types of sensors, which can be used for electronic control of the single-wheel, but also for power measurements, tyres efficiency evaluation, etc. Three force sensors are integrated into a double linkage, allowing to measure the net traction force noticed "NT". They provide only the horizontal force and are not affected by the vertical force. A centimetric DGPS, placed vertically on the axle of the tyre under test, measures continuously real travel displacement or speed ("V"), allowing instantaneous net power calculation ("NP"). For the gross power measurement, torque ("T") and angular velocity "Ω" are measured directly at the tyre hub: the rotation degree of freedom of the hydraulic motor is blocked using a sensor force in order to get the torque, and an incremental encoder measures the angular velocity of the wheel.

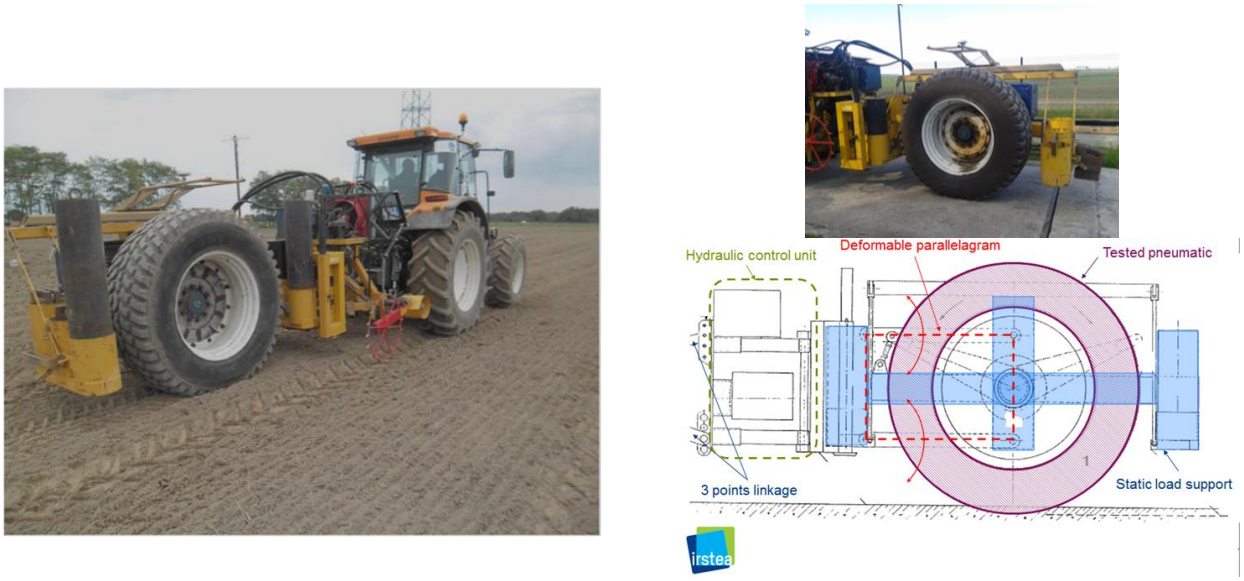

Figure 1: Single-wheel tester description

Two different regulation ways can be used during measurements: constant traction force or constant torque on the hub. In case of experimentation using constant traction coefficient, this one can be set between $0 < CT = \frac{NT}{W} < 0{,}5$ where W is the vertical load applied on the wheel. In case of experimentation using constant torque on the hub, this one can work in the range 0 < T < 2000 daN m. Most of the time, for practical reasons, the single-wheel forward speed is set to around 1 $m.s^{-1}$ during measurements and sensor data are registered using 100 Hz frequency. This bench can be easily coupled with deformation measurement system developed just after. A synchronization signal recorded by both acquisition devices allows synchronization between signals coming from the single-wheel bench and tyre-sensor devices.

Irstea is part of the ENTAM network in the working group "Agricultural Tyre Energy Efficiency". The aim is to develop a common test method for agricultural machinery and equipment on the basis of international standards. The aim was to find a compromise between easiness and representativeness of the measurements, with reproducible records carried out on real agricultural fields, in standardized soil conditions everywhere in Europe (Figure 2).

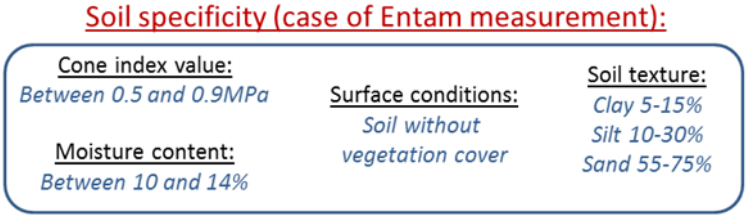

Figure 2: Soil specificity in case of Entam tyre efficiency measurement

Two dimensionless performance indices can then be computed: The Pull Loss Index (PLI) and the Carry Loss Index (CLI) after tyre test in a field.

Case of pulling (NT > 0):

$$\text{Pull\_Loss\_Index} \equiv \text{PLI} = \frac{\text{T}\times\Omega}{\text{NT}\times\text{V}} - 1 \qquad (1)$$

Case of self-propelling (NT = 0):

$$\text{Carry\_Loss\_Index} \equiv \text{CLI} = \frac{\text{T}\times\Omega}{\text{W}\times\text{V}} \qquad (2)$$

The smaller the indices' values are, the better the energy efficiency of the tested tyre is. In case of PLI (with traduces traction losses), for instance a value of 55% means that if the implement behind the tractor requires a drawbar power of 100 kW, the needed power at the wheel axle of the tractor will be 155kW. The advantage of this index is that tyres can be compared on a given delivered basis (the 100 kW in above example, transmitted by drawbar to implement), like if they had to "work the same field". However, other indices can also be calculated (like the "tractive efficiency") using the same

input physical sizes (T, NT, Ω and V). In case of CLI, the values are close to the motion resistance ratio, in case the "free rolling" and the "self-propelling" modes are very comparable to each other, on the given soil.

2.2. Sensors embedded on rim to measure tyre deformation

This principle is based on deformation sensors integration inside tyres. Sensors allow obtaining the tyre carcass deflection at a point "M" at the level of the tread centre. Typical sensors used for these measurements are potentiometric linear displacement sensors and laser range finder. Signals are converted, transmitted and recorded by an electronic box located on the rim. Potentiometric linear displacement sensors are mounted in "trilateration" mode. This technical implantation allows finding the deformations on the Oi (longitudinal), Oj (lateral) and Ok (radial) axis as illustrated in figure 3. The laser range finder only provides deformation on the Ok axis. Sensors are fixed on rigid brackets themselves fixed on hatches. The hatches ensure the rim sealing (by means of O-rings). Deflections dX, dY and dZ are referenced using the rotating reference frame (P, X, Y, Z) described in figure 3, where P is defined as the origin of the reference frame when no force is applied to the tyre. It should be noted that the point P position in the reference frame (O, i, j, k) depends on tyre pressure (If pressure increases, OP distance increases).

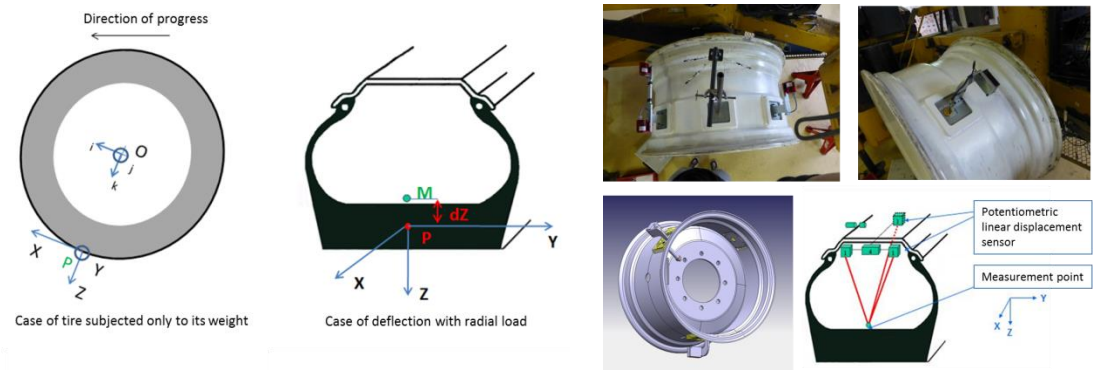

Figure 3. Sensors embedded on rim to measure tyre deformation

2.3. Scattering measurement device

On soft surface, consequences of soil compaction after machine works can be measured. In addition to the tools typically used to characterize hardness soil such as penetrometers, Irstea's TSCF laboratory developed a scattering measurement device which allows measurement on a large area (unlike penetrometer which allows more localized measurement). This device is made of three different steel blades (equipped by force sensors) which cut the soil at three different depths (10, 20 and 30 cm). The global tool is linked to the three-point system of an agricultural tractor (cf. figure 4). A possible method to measure and compare soil compaction is the following: Successive runs are done into a large field, following a random distribution in order to minimize natural soil field effects. Perpendicularly to the machine following parallel runs, a soil hardness resistance measurement is performed using this scattering measurement device. Displaced into the field, this device allows measuring the hardness force. Values are registered using 100 Hz frequency. Both of these field operations are geo-localized using a DGPS allowing a very precise spotting of 1 cm. Figure 5 propose a field organization example of the agricultural compaction evaluation.

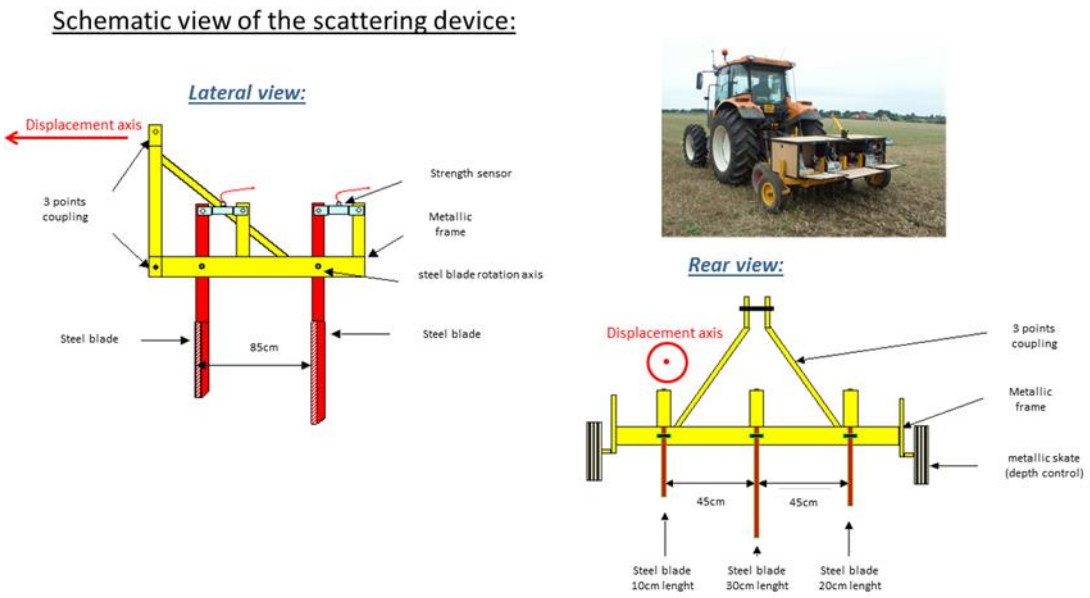

Figure 4. Scattering device used to measure the soil hardness everywhere in the field

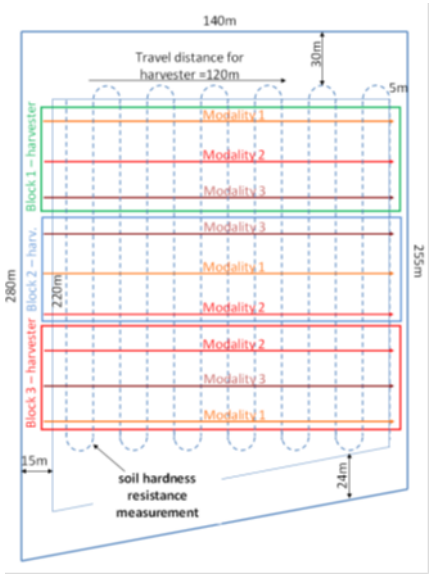

Figure 5. Field organization example of an agricultural compaction evaluation following an agricultural work

2.4. Automatic penetrometer

Unlike the scattering device described in the section before, automatic penetrometer can be used in order to describe precisely soil hardness region at different level of the footprint. This automatic penetrometer performs local measurements, with high accuracy and high resolution. It allows recording force during the lowering of the rod. The lowering number and the distance between each lowering can be set with a minimum of 2 cm. The maximum section that can be achieved is (width × height) 120 cm×115 cm. The force measurement is made using a cone surface equal to 0.4 cm2. The figure 6 shows automatic penetrometer operation principle.

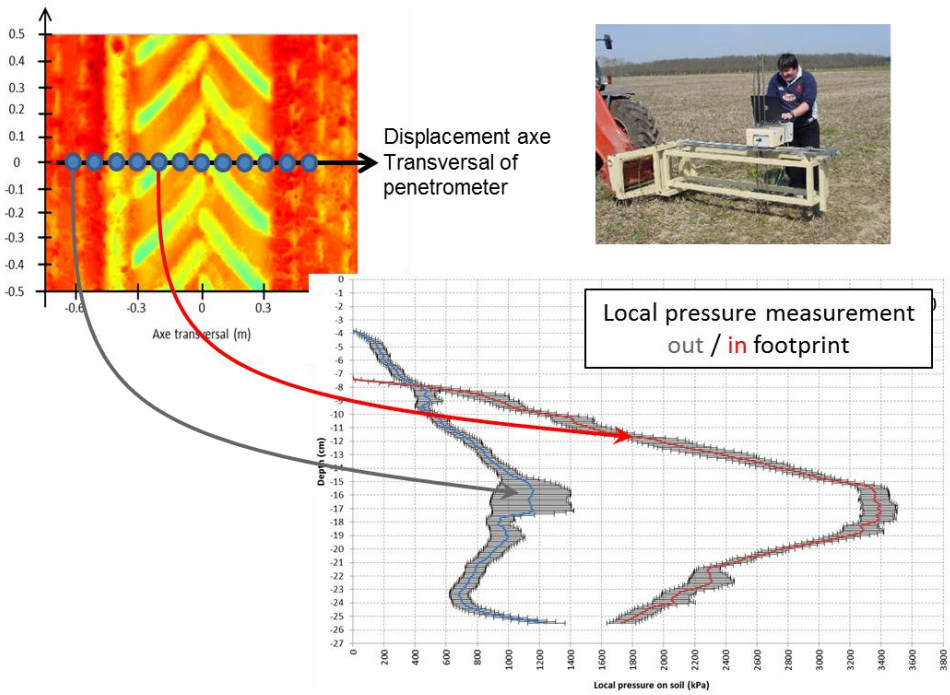

Figure 6. Operation principle of automatic penetrometer

2.5. 3D laser scanner for footprint characterization

In many cases, a strong correlation has been found between vehicle track depth and soil penetration resistance [7]. So, the precise sinkage measurement is interesting to provide soil compaction indicator. For a fine and complete characterization of the sinkage in a given area, a laser scanner type FARO focus 3D is used, it permits obtaining the footprint dimensions in 3D with one millimeter accuracy. Vertically positioned above the footprint by means of a telescopic lifting device, the 3D scanner measurement is launched in static mode (figure 7). The flexibility and the robustness of modern commercial 3D laser scanner makes easy and quick the operation.

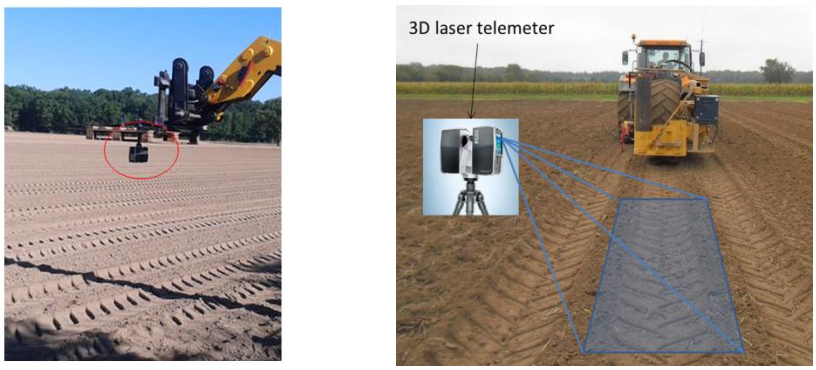

Figure 7. Scanner position above the sinkage

Obtained data from the scanner are post-processed: a division of the relevant zones is carried out. Several illustrations are then available and statistical processing is realized to obtain synthetic information of the scans. For example, in the case of agricultural tyres, the average depth of the tyre bars can be extracted from the height measurements distribution of the footprint.

3. Results and discussion

Results shown in this part are a partial illustration of possible investigation that can be realized with this tools and methods pack.

3.1. Tyre efficiency measurement

This part deals with an example of tyre displacement on an agricultural soil with a tyre subjected to four traction levels and a constant vertical load W = 3700 daN. The wheel runs on a soil prepared using ENTAM referential conditions.

The graph of figure 8 presents signals registered thanks to single-wheel sensors described in the first part.

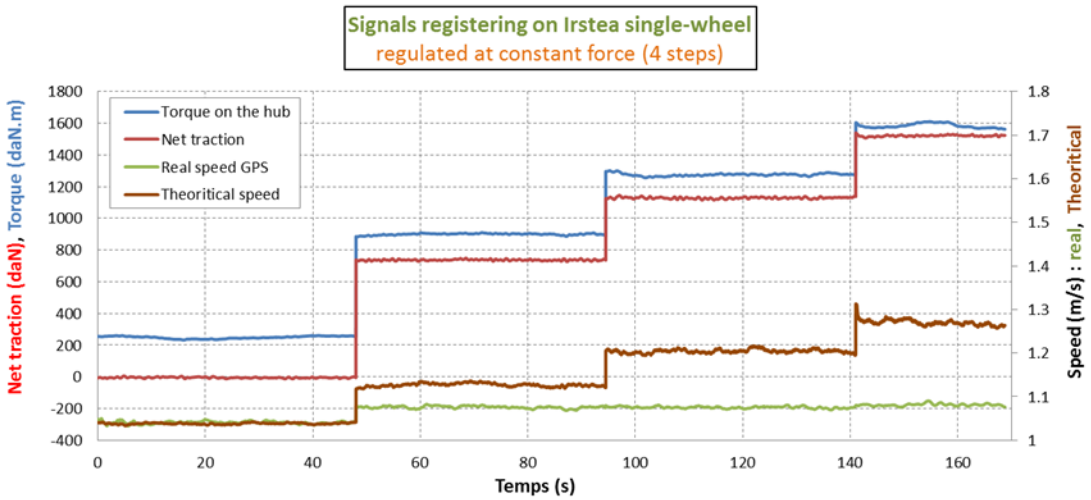

Figure 8: Signals registered on single-wheel tester when submitted to four traction levels

PLI indices (traction losses) are calculated in case of tyre pulling, when NT > 0. The graph of figure 9 presents an example of PLI calculation for 2 different tyre set under three different inflations pressures (0.7, 1 and 1.6 bar) and submitted to 3700 daN vertical load. For this study case, traction losses decrease when traction coefficient increases and when the inflation pressure decreases.

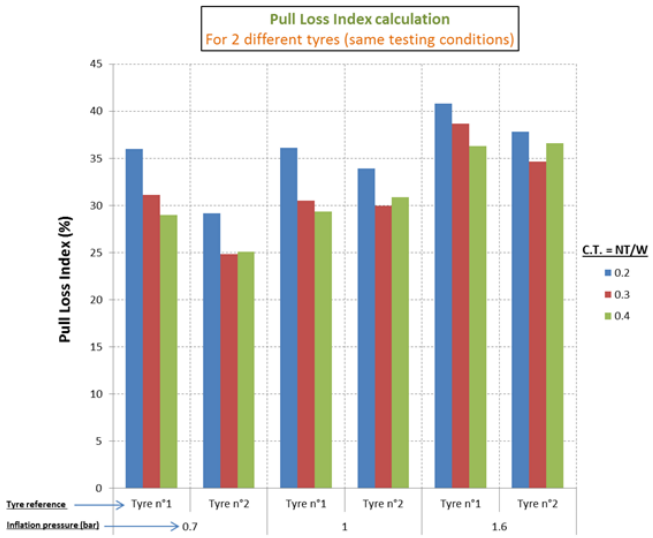

Figure 9: Pull Loss Index for 2 tyres according to inflation pressure and traction coefficient

3.2. Empirical models of tyre deformation and tyre-sensor

Even if forces are generated by the tyre tread, the tyre carcass transmits all those forces to the rim and to the vehicle. Consequently, carcass deflections of a rolling tyre contains interesting informations about tyre operating state, which would be beneficial for active safety systems [8]. In this part, deformation measurements results performed on a grape harvester tyre are presented. They were realized in the research project ANR ActiSurTT. The aim of this project task on innovative sensor is to determine tyre stresses by means of deformation measurements. More precisely, settings to access are torque, lateral and radial loads. To achieve this relation, empirical models linking deformations and stresses should be established. Deformation measurements are obtained by embedded measuring system on rim presented previously. In a non-exhaustive list, the forces influencing the deformations are the torque, the lateral (Y axis), the longitudinal (X-axis),

and the radial (Z-axis) forces, but also the pressure inside the tyre. Other factors can impact tyre deformations: like steering angle, speed, camber (angle between tyre and vertical), tyre stiffness, soil texture, soil moisture, soil inclination (longitudinal and transverse), temperature, etc. [9].

3.1.1. Deformation overview

A typical deformation overview recorded thanks to sensors is given in figure 10. The wheel is subject to a vertical load of 3335 daN, the inflation pressure is set to 2.8 bar and roll on flat and hard soil.

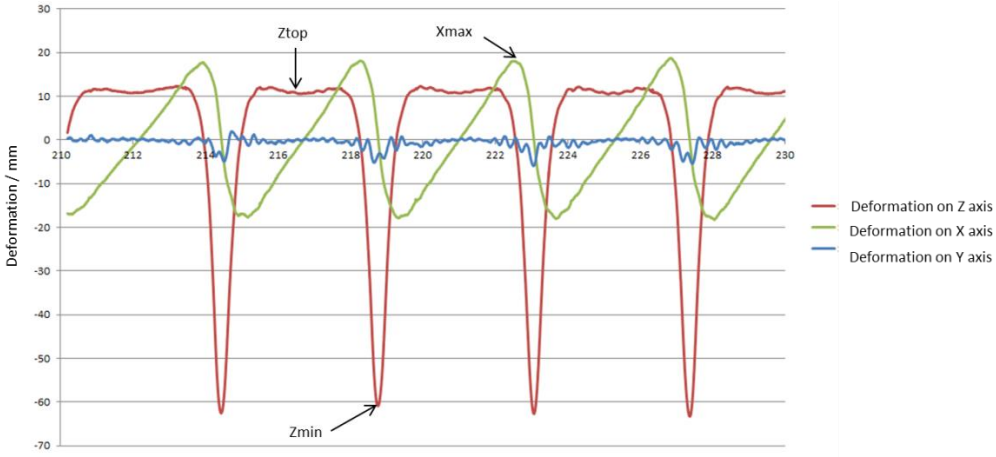

Figure 10. "P" point deformation on XYZ axes without torque applied to the wheel

Physical analysis of deformation during tyre rotation:

For Z-axis (red colour on previous graph), each rotation of the wheel presents a peak corresponding to the tyre arrow. Except in the tyre contact area, which corresponds to Z-deformations lower than zero, values are positive. The tyre crushing in the contact area induces an increase of tyre radius outside the surface in contact with the ground. For X-axis (green colour on previous graph), when the point P leaves the contact area, the deformation increases until P re-enter in the contact area. This corresponds to the de-radialization: during the crushing of the tyre, the bows of its carcass are de-radilised with low values at the output of the contact area which progressively increase throughout the circumference of the tyre until they become maximum at the input of contact area. For Y-axis (in black), the deformation is maximum in the contact area to return close to zero outside of it. This is explained by the fact that when the point P enters in the contact area, the tyre deforms laterally, these deformations returning to zero when the point P leaves.

3.1.2. Remarkable points in deformations

Three remarkable points can be highlighted when a tyre is placed in contact with the ground in various situations (slope: the maximum tyre deflection corresponds to the peak and is called Zmin in this paper. A mean value Xmean of deformation on X axis can be calculated for each tyre revolution. This parameter is very sensitive to the torque applied to the wheel. The deformation on Y axes measured at the same time than Zmin is chosen to be linked to lateral forces.

3.1.3. Experimental modelling of radial, lateral load and torque

Only the factors pressure, lateral force, load, torque and their combinations are taken into account for this modelling. A battery of tests (variations in pressure, radial force, torque, etc.) defined in the experimental design are carried out using the single-wheel tester. From the analysis of the experimental plan, the relations between the deformation criteria and the influencing factors are deduced. For example, for the parameter Zmin, the relationship obtained is:

$$Zmin = 186{,}5 - 80{,}5 \times p - 0{,}0166 \times W + 11{,}34 \times p^2 + 6{,}04.10^{-6} \times W^2 \qquad (3)$$

where W is the load in kg, p is the inflation pressure in bars. By inversion of the model, it is possible to evaluate the load from pressure and Zmin measurements in mm. Thus, load estimation is given for each revolution of the wheel. Same method is applied on other parameters (Xmean, Ymax) and allows accessing to a torque and lateral force model. Subsequently, only the results obtained for the load will be presented not to overload the paper.

3.1.4 Load estimation results obtained in test package of ActiSurTT project

The tyre-sensor device is installed on the grape harvester dedicated to the test. To compare stress information, grape harvester is equipped with a six axes load sensor at level of wheel hub. Mobility tests are performed. Figure 11 is a measurement extract which shows a comparison of the radial force given by the tyre-sensor and by the six axes sensor. In this test, as shown in figure 12, the machine moves on an irregular terrain with a slope part of 10 depicted by the yellow strip on the trajectory. The effect of the slope on the machine is shown on the right in the same figure. The trajectory has been achieved at a speed of 2 m/s. The machine is set to a low elevation without relative inclination. The vehicle mass is equal to 11t.

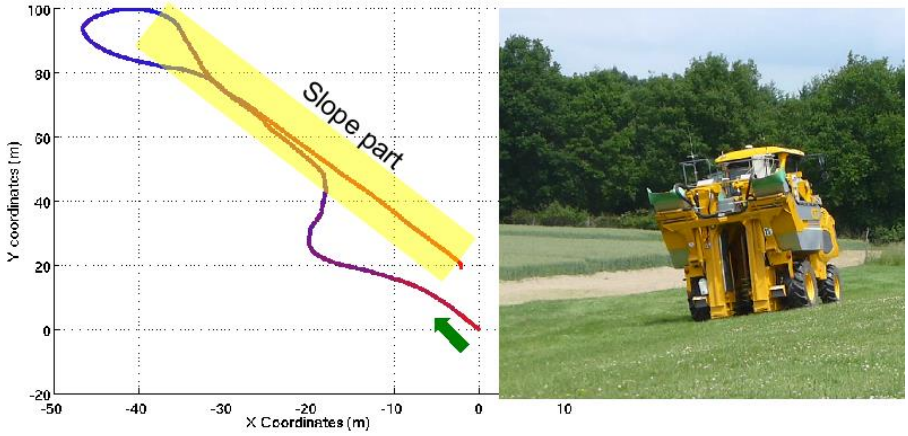

Figure 11. Test background

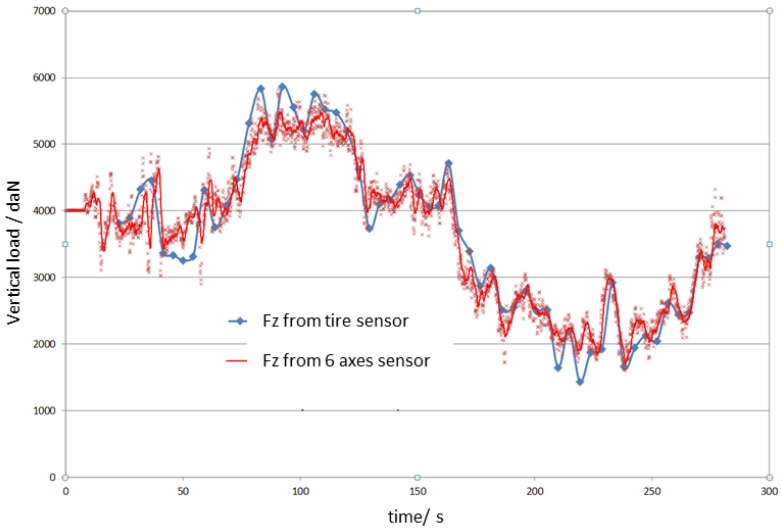

Figure 12. Vertical load measured by 6 axes load sensor versus tyre sensor measurement

As show in figure 12, it can be noticed that the estimated vertical load by tyre sensor is properly superposed with the vertical load by six axes load sensor. This demonstrates the relevance of the vertical load supplied by sensor embedded on rim on difficult soil.

3.3. Soil compaction comparison of two tyres

This part presents results of soil compaction characterization obtained in experimentation whose purpose was to raise awareness agricultural machine users to choose good tyre. In this paper, the aim is to illustrate the relevance of soil characterization tools to evaluate soil compaction. In the same agricultural soil, two different tyres identically loaded (2700 daN) roll on a field. They are both inflated with each recommended pressures by manufacturer. Figure 13 and 14 present scan and penetration results for the two tyres. More precisely, the figure 14 shows the statistical distribution of footprint depths.

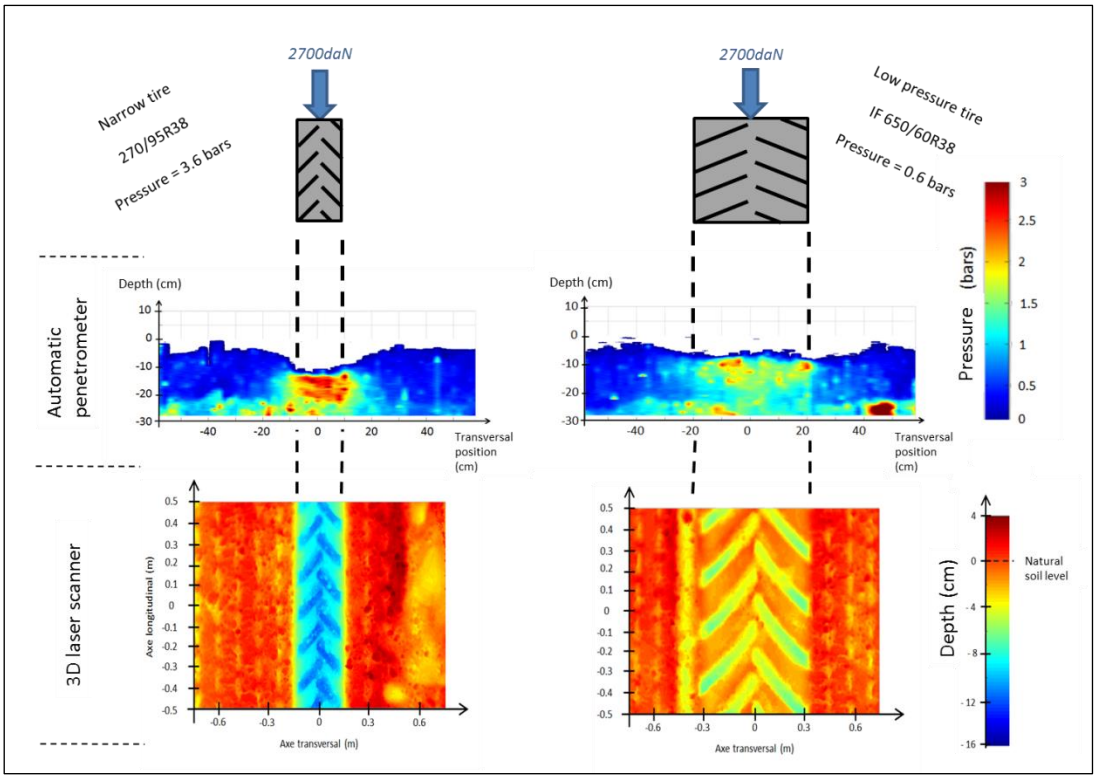

Figure 13. Soil compaction of two tyres

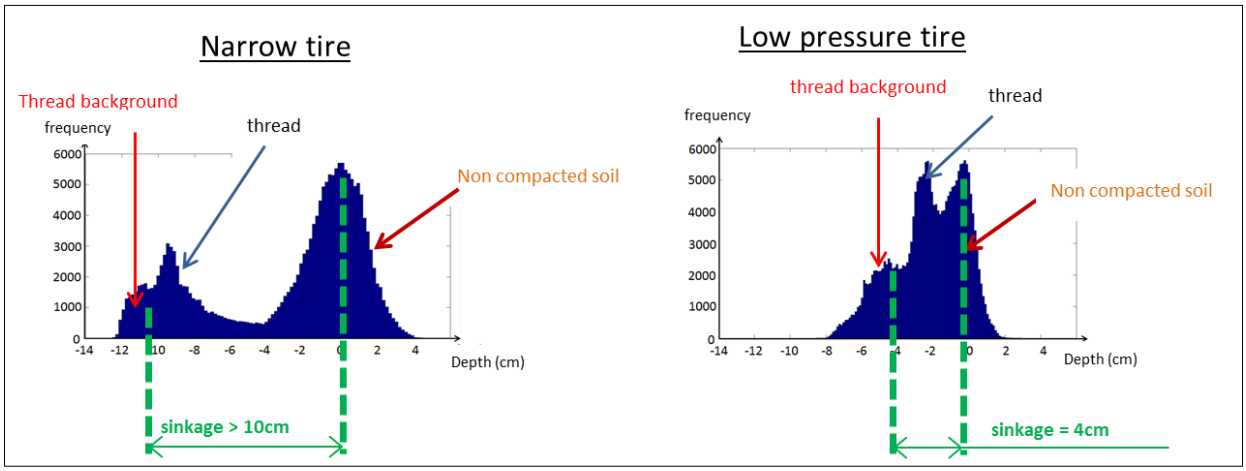

Figure 14. Distribution histogram of depth

Without any surprise, the narrow tyre with high pressure has a strong impact on soil compaction. Pressures which are recorded from automatic penetrometer are important under the narrow tyre regarding pressure under low pressure wide tyre. Concerning scans, three populations of depth can be identified in the histogram (thread background population, thread population and non-compacted soil population). Means of depth for these populations can be extracting. The footprint depths confirm penetration results: values for narrow tyre are more than two times those obtained with wide tyre. It confirms the importance to choose the appropriate tyre for the specific agricultural operation.

4. Conclusion

This paper presents a set of characterization technics, from tyre behaviour investigation with sensors equipped wheel to tyre efficiency evaluated by single-wheel tester, state of soil constation by scattering, penetration and laser technics. Results show that tools and methods presented can be used to compare tyre regarding efficiency, soil compaction, but also to get the experimental data needed to feed numerical simulations and models which are developed. Sensors or sensitive part integration in research work must allow to test and develop these technics in order to access to connected wheel or intelligent wheel.

Due to significant soils heterogeneities, even in case of standardized ENTAM tests for which consequent works are dedicated to soil preparation, it is interesting and necessary to use continuous soil characterization solutions in oder to access to large measurements number and obtain a representative characterisation sample in same way as the scattering measurement device introduced in this paper. Coupling continuous measurement technics, less voluminous but more frequent, with high resolution technics is relevant because it allows obtaining information with good representability and high accuracy.

Acknowledgements

Work introduced in 3.1 part is supported by French National Research Agency (ANR) under the grant ANR-10-VPTT-008 attributed to ActiSurTT project. It also received the support of French Agricultural Social Insurance (CCMSA) and French Ministry of Agriculture.

References

[1] ENTAM TWG: Energy efficiency of agricultural tyres, 2010.

[2] ISO 25177:2008 Soil quality — Field soil description

[3] NF ISO 11465-1994 Soil quality. Determination of dry matter and water content on a mass basis.

[4] ASABE; EP542 (R2009): "Procedures for using and reporting data obtained with the soil cone penetrometer"

[5] ASABE; S313; "Soil Cone Penetrometer"

[6] G. Fancello M. Szente L. Kocsis K. Szalay E. Piron, A. Marionneau, 2013. “New experimental method for measuring the energy efficiency of tyres in real condition on tractors”, VDI AgEng

[7] J. S. Nam, Y. J. Park, K. U. Kim, 2010. “Determination of rating cone index using wheel sinkage and slip”, Journal of Terramechanics, vol. 47.

[8] D. Denis, B. Thuilot and R. Lenain, 2016. “Online adaptive observer for rollover avoidance of reconfigurable agricultural vehicles”, Computers and electronics in agriculture, vol. 126.

[9] A. J. Tuononen 2011, “Laser triangulation to measure the carcass deflections of a rolling tyre”, IOP Publishing Ltd, http://stacks.iop.org/MST/22/125304

Innovative Field Test Methods for Tillage Tools

Christian Rechberger [a,*], Peter Riegler-Nurscher [b], Johann Prankl [b], Franz Handler [a]

[a] BLT Wieselburg, HBLFA Francisco Josephinum, 3250 Wieselburg, Austria

[b] Josephinum Research, 3250 Wieselburg, Austria

* Corresponding author. Email: christian.rechberger@josephinum.at

Abstract

Accurate field testing of agricultural tillage equipment is still challenging due to the uncertainties of measurements caused by inhomogeneities of soil properties on a field. To cope with changing soil conditions, a holistic approach is needed which also takes the soil properties as well as the outcome of a tillage activity into account. Josephinum Research developed in collaboration with BLT Wieselburg several methods for advanced field testing of tillage tools in recent years. Along with the conventional force measurements, methods based on image analysis and stereo vision are used to quantify the quality of the tillage process. This makes it possible to compare different machines and tools for soil tillage in a more objective way. A stereo vision system is used to evaluate the real working depth, the tilled volume of soil per square meter, the increase of the pore volume through tillage and the roughness of the soil surface and of the working horizon. An image analysis method based on machine learning is used to estimate the amount of soil covered by living plants, plant residues and stones before and after tillage. In this paper, some exemplary results of those methods are presented.

Keywords: soil coverage, soil roughness, stereo vision, image analysis

1. Introduction

Nowadays, the agricultural production is facing the challenge to efficiently provide high quality and save food and raw materials. At the same time, the competitiveness and sustainability must be ensured through responsible use of resources. Tillage is one of the most energy consuming processes in agricultural production. Higher efficiency can be reached either by reducing the intensity of tillage or by increasing the effectiveness of tillage tools.

Wear of tillage tools is a great issue and a cost driver as well. To expand the lifetime of tillage tools and thus reduce the service costs, agricultural equipment manufacturers offer tools with wear-resistant coatings. State of the art is the processing of tools by application welding. For this purpose, metal matrix layers with a thickness of several millimetres are deposited with embedded hard materials, such as, for example, tungsten carbides. This thick-film technology, however, leads to the loss of the dimensional accuracy, in particular of the cutting geometry. The associated negative effects are the increase in the pulling force requirement or a poorer pull-in behaviour of the tools. In order to be able to determine such differences in the tractive force objectively, it is necessary to use a sophisticated testing technique, which also considers the tillage outcome and accordingly the quality of work.

2. Materials and Methods

2.1. Force measurement devices for tillage tools

For the force measurement on a single tine, a special cultivator frame was built, which is equipped with a multiaxial force transducer unit on the centre tine, two reference tines and two depth wheels (Figure 1). The multiaxial force transducer unit enables the independent detection of the horizontal und the vertical component of the resulting force as well as side-forces acting on the coulter point.

Figure 1. Cultivator frame for single tine force measurements

The reference tines are each equipped with strain gauges and placed in the same row side by side with the centre tine and the depth wheels. They are also adjustable in height so it can be assured, that the reference coulter points are working at the same depth as the tested coulter point. The values measured by the reference tines are later used as covariates for the statistical analysis. In this way, the influence of spatial changing soil properties within the field can be removed to some extent. Nevertheless, it is still necessary to have a large number of repetitions per variant to get high sensitivity which is needed for instance to compare non-coated and coated coulter points. An example of a test plot with 16 repetitions is illustrated in Figure 2. A randomization of the track order is usually not necessarily required, since there are no interactions between the variants if there is enough space between the tracks. To avoid a too high influence of compacted soil in existing traffic lanes, the test tracks are applied in an angle of 30 to 90 degrees to the main driving direction.

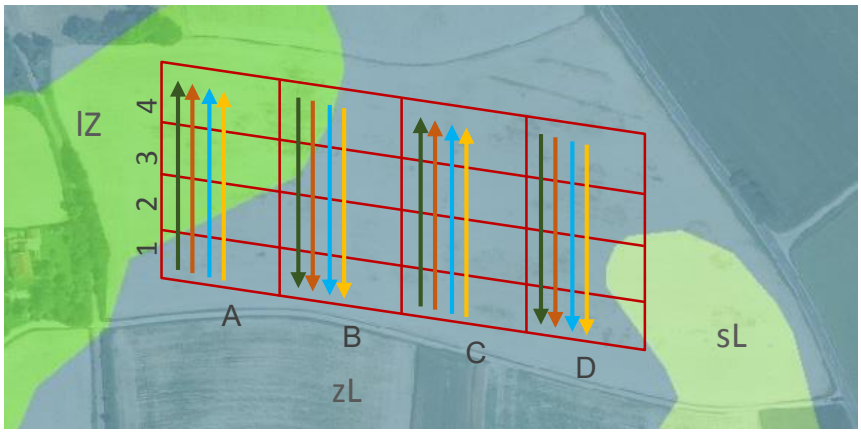

Figure 2. Test plot for experiments with the single-tine cultivator

For the force measurements with complete tillage machines at the tractor's 3-point -linkage, two different systems are available (Figure 3). The older system (Figure 3a) consists of two force transducers for the lower linkage and a special upper link, which is also equipped with a strain gauge type force transducer. The force sensors are limited to 5,000 kg m s^{-2} in each direction each lower linkage and 100,000 kg m s^{-2} at the upper linkage. For dynamic measurements, this system has to be additionally equipped with angle sensors. For heavier machinery, a new force-measuring frame was built which is equipped with six independent force transducers (Figure 3b). These are limited to 100,000 kg m s^{-2} and 200,000 kg m s^{-2} for lower and upper linkage respectively. In addition, side forces up to 50,000 kg m s^{-2} can be sensed with this new unit.

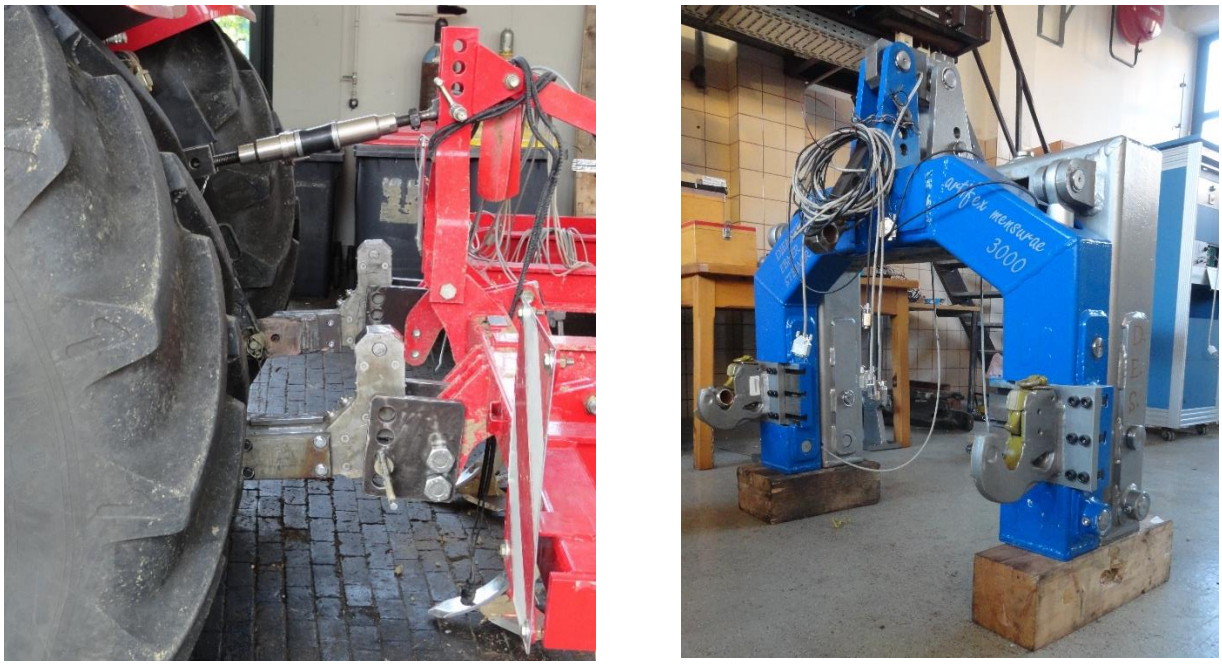

(a) (b)

Figure 3. Force measurement units for the 3-pont-linkage

2.2. 3D surface evaluation

For the evaluation of the quality of work of a tillage implement, a 3D-scanning system, based on a stereo vision camera and a linear motion frame, was developed. With its help, it is possible to determine parameters for soil surface roughness after tillage, actual working depth over the full working with, tilled volume per square meter and the increase of pore volume through tillage. The system is described in Riegler et al. (2013)

Figure 4. Linear motion 3D scanner

2.3. Soil coverage

Depending on the purpose of the processing, either as much plant material as possible should be mixed in or left behind at the soil surface. The estimation of the soil cover by residues and living plant material is also a fundamental issue for the sustainable cultivation of arable land. Especially, the percentage of soil covered by material is one of the main factors to protect soil from erosion. Conventional methods for the measurement are either subjective, depending on an educated guess or time consuming, e.g., if the image is analysed manually at grid points.

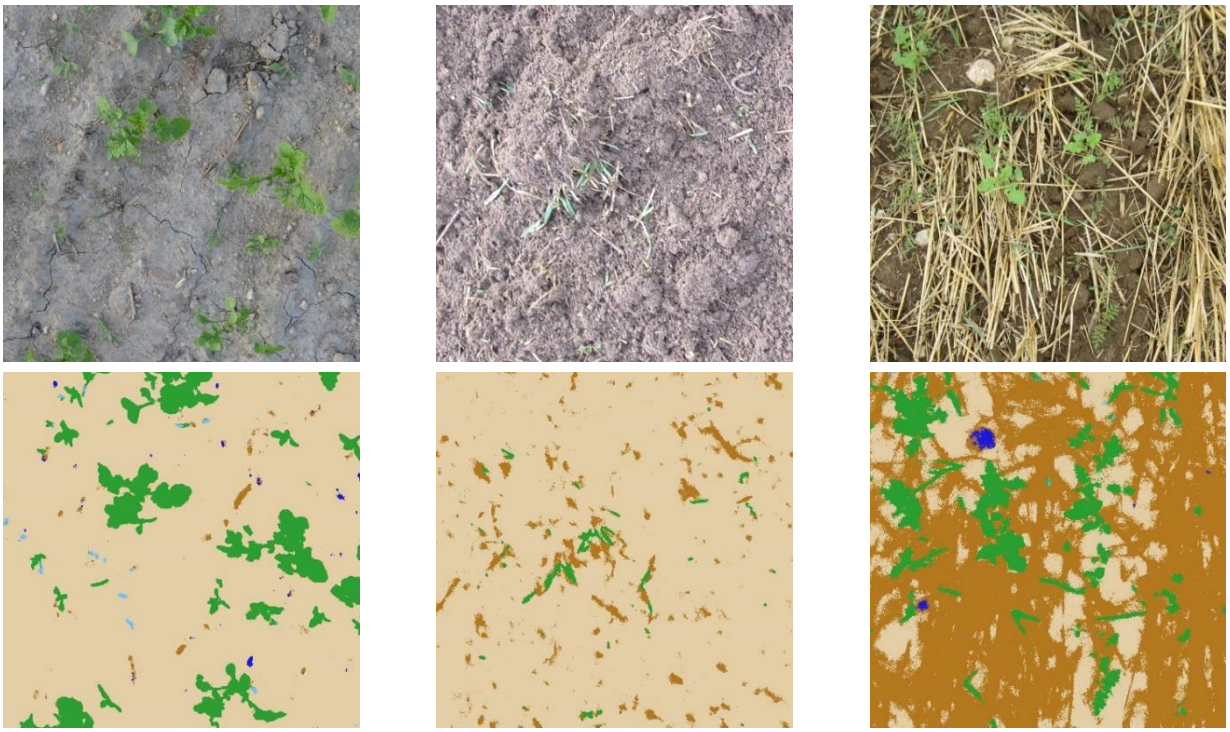

(a) (b) (c)

■ living plant, ■ residue, ■ soil, ■ stone, ■ biofilm

Figure 5. Examples for evaluated pictures by the “SoilCover” method.

First approaches using automatic segmentation of objects and classification into soil, residue and plants show promising results, but they rely on a manual adjustment of parameters. Therefore we introduced novel pixel-wise features to a special variant of machine learning technique – namely the entangled forest – in order to improve the robustness and the generalisation of the classification of individual image pixel into soil, living plants and residues.

A classical machine learning approach consists of different computer vision steps, e.g., segmentation into homogeneous patches, patch description (with colour, contour, texture ...), classification and a smoothing step. In contrast, the entangled forest, a variant of random decision forest, classifies individual pixel using simple pixel-wise comparisons to neighbouring pixels with a trained offset and in addition, smoothing is achieved by maximum a posteriori features, where the decision in a specific node depends on the a posteriori label probability of a neighbouring pixel of the previous decision tree layer. The full description of the method can be found in Riegler-Nurscher et al. (2016). We compared our system with a data set, which was manually annotated at grid points. The images have been taken in different lighting conditions of soil covered from 0% up to 100% with different materials, such as living plants, residues, straw material and stones (Figure 5). The results indicate that our method is as accurate as the manual annotation with a mean deviation of 6% to the grid method.

For the purpose of field testing and comparison of tillage equipment, large numbers of sample images are needed to be able to conduct a satisfactory statistical analysis. Therefore, it is planned to use a UAV (drone) for shooting images along a defined path at future experiments. The method will be also available via web service and smartphone-app.

3. Results and Discussion

3.1. Force measurement on single tine cultivator

As mentioned in the introduction above, geometry changes by welded wear coatings on tillage tools can influence the required draft force. A number of experiments were carried out to quantify such effects on a single tine. Figure 6 (a-e) shows the five coulter points used in the experiment: (a) standard coulter point, (b) lengthwise welding bead, (c) crosswise welding bead, (d) tool tip coated on backside and (e) tool tip coated on front side.

(a)	(b)	(c)	(d)	(e)
Standard	Lengthwise	Crosswise	Backside	Front side

Figure 6. Tested variants of coulter points

The tests were carried out in summer after harvest of wheat under very dry conditions on a silt soil (Table 1). The working depth was set to 10 centimetres for all variants and the forward speed was constant at 10 km/h (2.78 m s^{-1})

Table 1: Conditions for the experiment with coated coulter points

Soil type	Silt
Preceding crop	Wheat
Water content (db)	16% (s=0,7)
Bulk density	1,327 kg m^{-3} (s=50.6)
Forward speed	2.78 m s^{-1} (10 km/h)
Number of repetitions	n = 18
Working depth	10 cm

The results of a one-way ANOVA with Tukey HSD post hoc test of the values from the force measurements are listed in Table 2 and illustrated in Figure 7. With a +/- limit of 64.92 kg m s^{-2}, the difference for the required draft force is significant between all tested variants. This result indicates the high sensitivity of the proposed method.

Table 2: Draft force Fx

Type	Count	Mean Fx in kg m s-2	Stnd. error (pooled s)	Homogeneous Groups
Standard	12	1,577.11	16.2779	X
Lengthwise	12	1,726.13	16.2779	X
Crosswise	12	1,797.49	16.2779	X
Backside	12	1,874.67	16.2779	X
Front side	12	2,015.62	16.2779	X
Total	60	1,798.20		

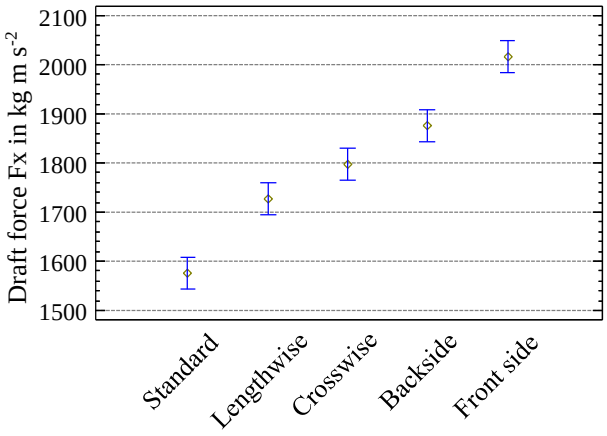

Figure 7. Means and 95% Tukey intervals for Fx

3.2. Tillage system comparison: Compact disc harrow vs. stubble cultivator

As an example for the application of the force measurement system on the 3-point-linkage in combination with the 3D-scanning method, a short summary of the results of a tillage system comparison between a compact disc harrow and a stubble cultivator is presented here. The stubble cultivator was equipped with wing shares and standard coulter points. Both machines with a working width of 3 meters have been delivered by one manufacturer and were equipped with the same packer roller. The target of the experiment was to compare the required draft force and the tillage result at the same mean working depth at different speeds. Figure 8 illustrates the differences in draft force requirement and the resulting down force at the tractor's three-point for the two tested machines at different speeds.

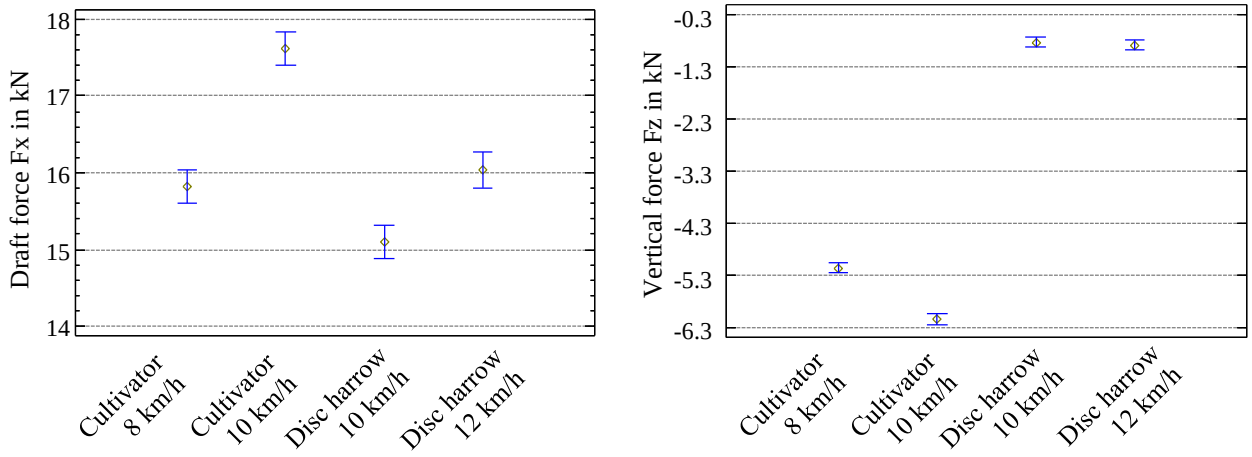

Figure 8. Means and 95% Tukey HSD intervals for draft force and vertical force for cultivator and compact disc harrow

At a forward speed of 10 km/h, the stubble cultivator requires about 17% higher draft force as the compact disc harrow. In contrast to the the disc harrow, the downforce increases along with the draft force at the cultivator. However, to be sure, that the two results are comparable, also the values for the mean working depth of the two implements had to be checked. For this purpose, four test spots for each variant where scanned before and after tillage. In a 3rd step, the loosened soil was removed to be able to scan the working horizon. Figure 9 shows coloured point cloud reconstructions of those scans for the cultivator (a) and the disc harrow (b).

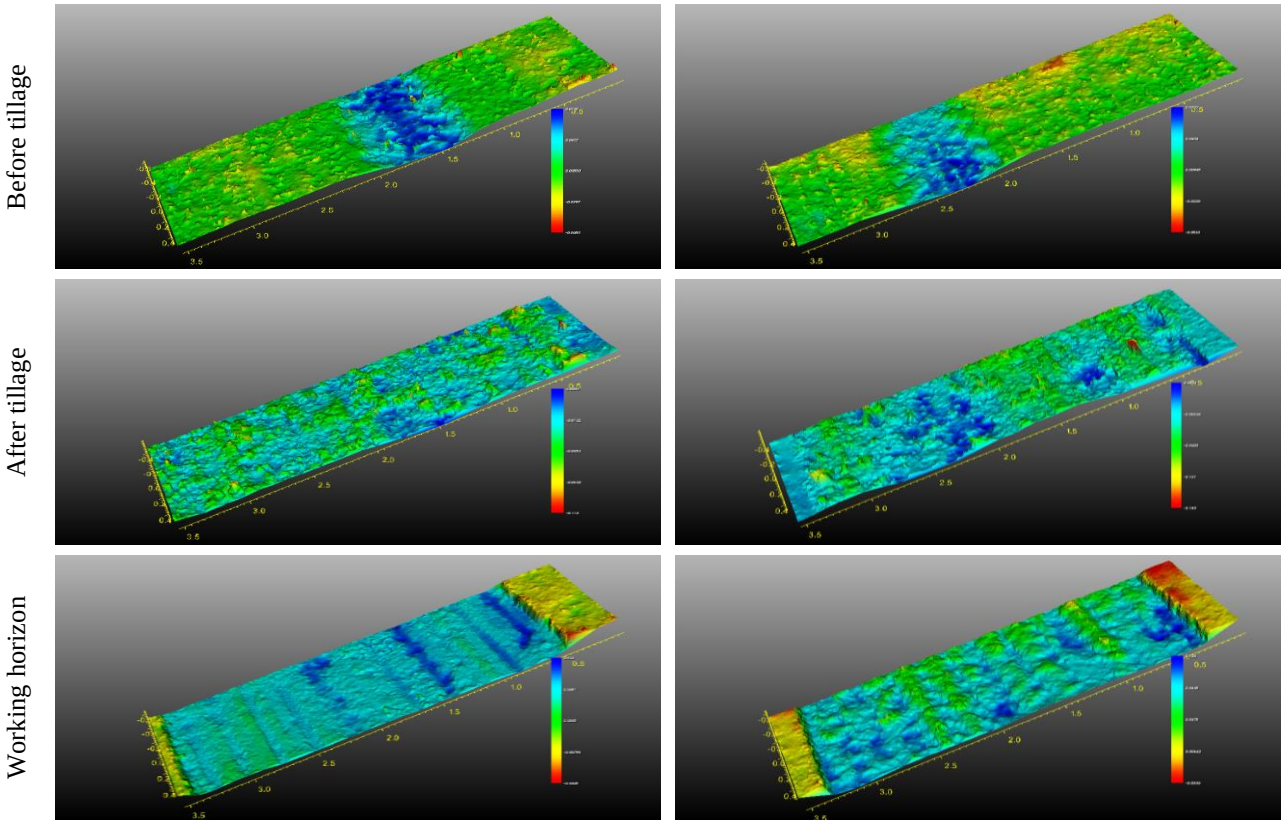

(a) (b)

Figure 9. Scans before tillage, after tillage and working horizon for cultivator (a) and disc harrow (b)

In both scans before tillage, an existing tractor track is clearly visible. After tillage, the scans of both variants look quite similar. In addition, the evaluation of several roughness indices derived from the surface scans after tillage showed no significant differences. Figure 12 shows for example a comparison of the roughness index RC, introduced by Currence and Lovely (1970). The scans of the working horizon demonstrate clearly the differences of the tillage result of the tested machines. Although the mean working depth was comparable (Figure 10), the disc harrow leaves a much more uneven working horizon. This means, that in practical use, the disc harrow must be set to a deeper working depth than the winged cultivator to ensure, that all plant roots are cut across the entire working width.

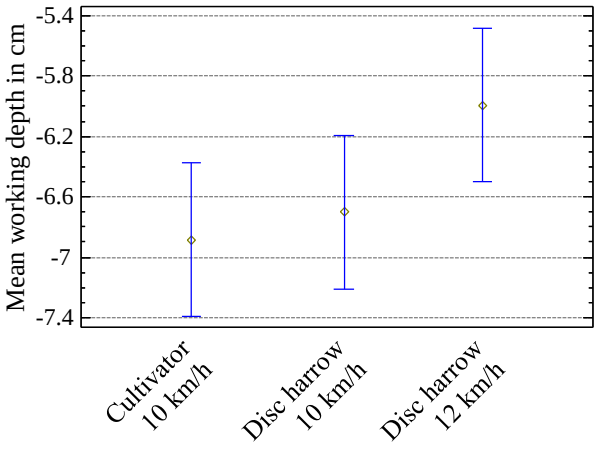

Figure 10. Means and 95% intervals of the working depth

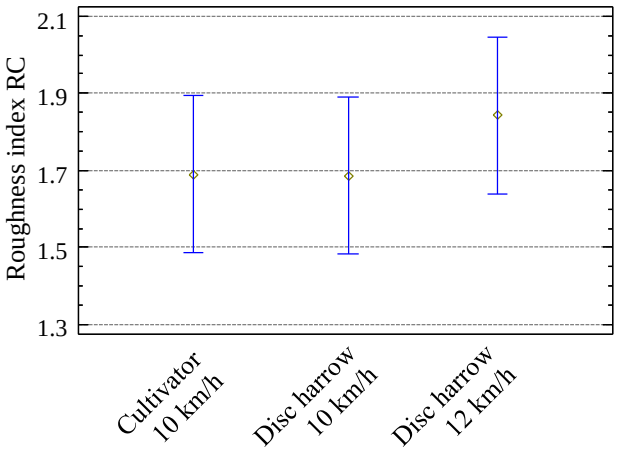

Figure 11. Means and 95% int. of the roughness index RC

For better illustration of the differences, the 3D-point-clouds are reduced to a line diagram with a smoothed line (Figure 12). The comparison of the lines “after tillage” attest the cultivator a better levelling effect than the disc harrow, especially in the area of the tractor track.

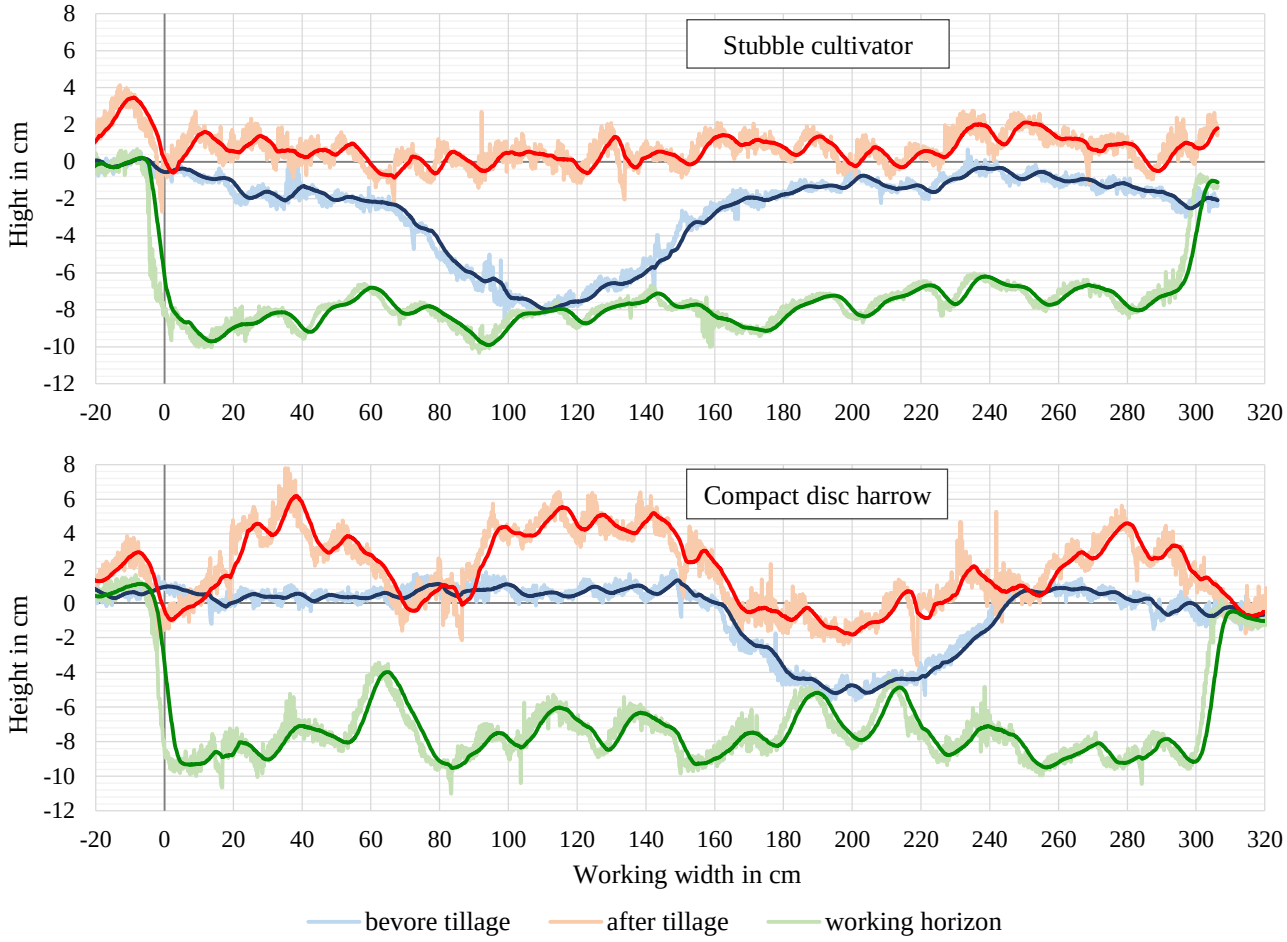

Figure 12. Smoothed line diagrams of the 3D-scans

3.3. Soil coverage

The „Soil-Cover" method was used to evaluate the differences of compact disc harrow (Amazone Catros^{+} 5002-2TS), a seedbed cultivator (Güttler SuperMaxx 50) and a stubble cultivator (Kerner Stratos 500) in terms of mixing winter greening crop residues (Charlock, 1,500 kg dm/ha) into soil. The soil type at the test site was loamy sand at a gravimetric water content of 17,9% (dry basis). The forward speed was 2.9 m s^{-1} for all three machines. An example image of the amount of soil cover is shown in Figure 13a, the corresponding analysis in Figure 13b.

(a) (b)

Figure 13. Soil coverage before tillage

After Tillage, the percentage of soil covered by organic mass was significantly reduced. Figure 14 shows an example image of the soil after tillage by the compact disc harrow, which left the lowest amount of plant residues on the surface.

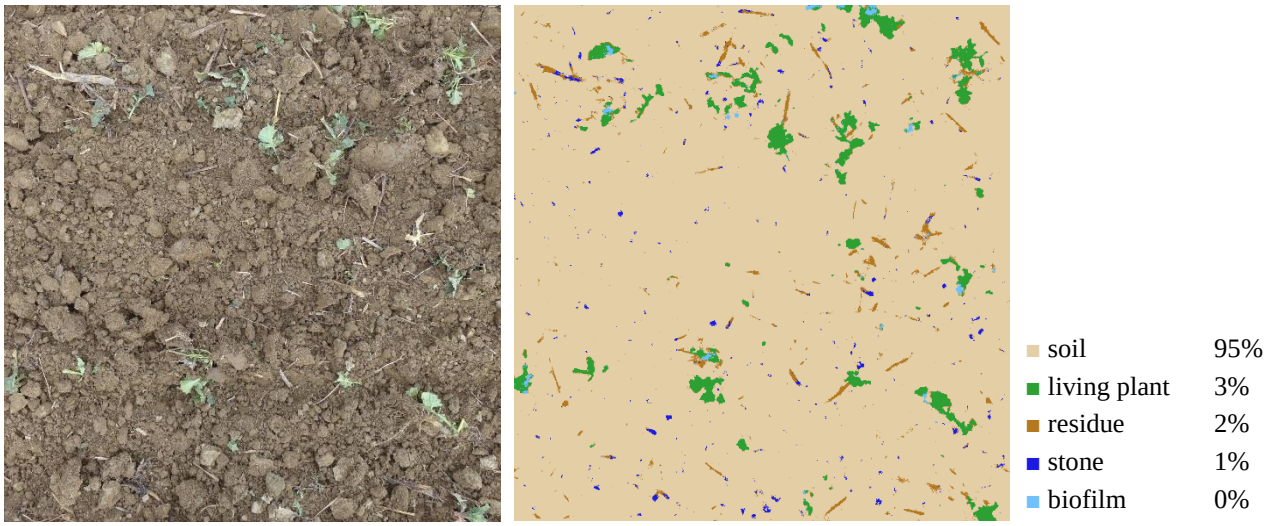

(a) (b)

Figure 14. Soil coverage after tillage

Table 3 and Figure 15 show the results of the statistical analysis. For each variant, 96 images were taken across the field with a compact camera. There was a highly significant reduction of crop residues on the surface at all three variants. The seedbed cultivator left the highest amount of organic mass on the surface, although not significantly different to the stubble cultivator.

Table 3: Soil coverage by organic mass before and after tillage

Machine	Count	Mean	Stnd. error (pooled s)	Homogeneous Groups
Before tillage	96	0.377714	0.005738	X
Disc harrow	96	0.047400	0.005738	X
Seedbed cult.	96	0.121047	0.005738	X
Stubble cult.	96	0.101826	0.005738	X
Total	384	0.161997		

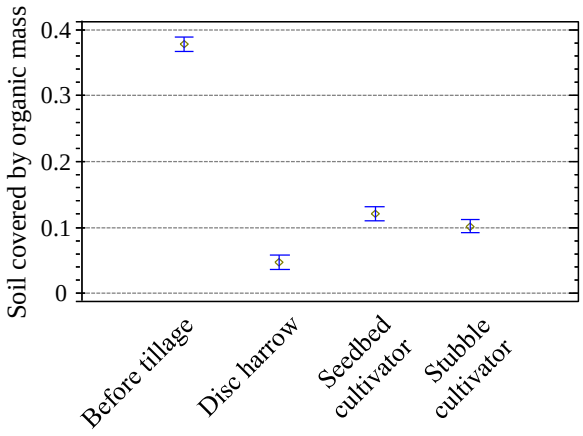

Figure 15. Means and 95% Tukey HSD intervals

4. Conclusions

With the proposed optical inspection methods, it is possible to quantify the quality of work of tillage implements in an objective way. Thus, in combination with the force measurement devices, an integrated test procedure is available for comparative tests of tillage systems as well as for different tool geometries. Furthermore, these optical methods have capabilities to be applied inspection of the tillage outcome directly on the machines. In this way, real time adjustments of tillage parameters and adaption of tillage intensity for precision farming applications will be possible in future.

Since some of the methods were still in evaluation, results from different test scenarios were presented here. For upcoming season, a complete test scenario is planned, where all methods will be applied at the same time.

Acknowledgements

The research leading to this work was enabled by funding from The Austrian Research Promotion Agency (FFG) and the Lower Austrian government.

References

Currence, H., & Lovely, W., 1970, The analysis of soil surface roughness, Trans. ASAE, 13, 710–714.

Riegler, T., Rechberger, C., Handler, F., Prankl, H., 2013. Characterizing quality of work for tillage by image data processing. In *Conference Agricultural Engineering AgEng 2013*. Hannover, Germany, Nov. 8-9, 2013, VDI-Berichte Nr. 2193, ISSN 0083-5560, ISBN 978-3-18-092193-8. 315-325

Riegler-Nurscher P., Prankl J., Bauer T., Strauss P., Prankl H., 2016, An Integrated Image Analysis System for the Estimation of Soil Cover. CIGR-AgEng conference, Aarhus, Denmark, Jun. 26–29, 2016.
http://conferences.au.dk/uploads/tx_powermail/2016cigr_ageng_full_paper.pdf

Experimental justification of the conveying parameters for the air-seeders

Andrii Yatskul [a,*], Jean-Pierre Lemière [b]

[a] UniLaSalle – 19, rue Pierre Waguet, 60000 – Beauvais – France

[b] UMR PAM, Agrosup Dijon, 26 boulevard Docteur Petitjean, BP 87999, 21079 Dijon Cedex, France

* Corresponding author. Email: andrii.yatskul@unilasalle.fr

Abstract

Air-seeder is a solution for a fast seeding: seeds are conveyed from the high-capacity seed hopper to the coulter-bar by an air-stream. Taking into account the complexity of this type of seed drills, they stay little-studied. The chief point for air-seeders design is the pneumatic conveying system. The flow of seeding material must be high and regular for a high speed seeding. There are two parameters ensuring the conveying of seeding material in a pipe: air velocity and pipe diameter. We show that the outlets of divider heads are the most critical part of the conveying system. The outlet pipes have a relatively small diameter and must admit the highest seeding rates without clogging. We made the hypothesis that the air velocity in outlet pipe may be used as an input data for the design of the totality of conveying system. This paper discloses i) a minimal air velocity per type of seeds relatively to a pipe diameter ii) a method to measure the air velocity of the loaded flow, which could be used to optimize existing seeders from an energy point of view, iii) a global design methodology for air-seeders' conveying systems. Trails were made for wheat/barley seeds, starter fertilizers and for a wheat-fertilizer mixture, for three current pipe diameters (20, 25 and 30 mm).

Keywords: air-seeder, distribution system, pneumatic conveying, flow concentration, conveying velocity.

1. Introduction

Agricultural practices are becoming more demanding for increased yields, a high quality of crops and a reduction of energy input. Satisfying these demands is important for a farm operation, especially for the seeding. The agricultural machinery manufacturers must provide an equipment that allows an accurate seed placement in a fast and efficient manner. Air-seeder is a solution for a fast seeding: seeds are conveyed from the high-capacity seed hopper to the coulter-bar by an air-stream (Weiste, 2013). Taking into account the complexity of this type of seed drills, they stay little-studied.

The key point for designers of pneumatic seed drills is the design of the pneumatic conveying system. It must be precise in terms of uniformity in order to achieve the agro-technical objectives. It must also allow high flows without causing damage to the seeds.

Pneumatic conveying of solids is well known for a long time in the fields of chemistry, mining, food processing and pharmaceuticals industry (Destoop, 1999). To design a conveying system, it is necessary to set the working air velocity. There is a high discrepancy between theoretical calculating and practical measurements (Binsirawanich, 2011; Astahov, 2007). This discrepancy exists because of non-steady conveying (caused by the many bends, variations of the pipe diameter, the distribution heads, stop and restart of seeding in headlands...). Existing calculation methods for conveying systems don't take into account the specificity of seeds and air seeders (risk of clogging) or seed damage.

The distribution system of the air-seeders is the network of pipes of variable diameters and cross-sections. Furthermore, the stationary pneumatic conveying installations work with constant material flowrates of agricultural seeds is between 8 and 10 kg s^{-1} and an air velocity from 10 to 30 m s^{-1}. However, for the air-seeders, the material flowrate rarely exceeds 1 to 1.2 kg s^{-1}, with a higher range of air velocities between 20 and 39 m s^{-1}.

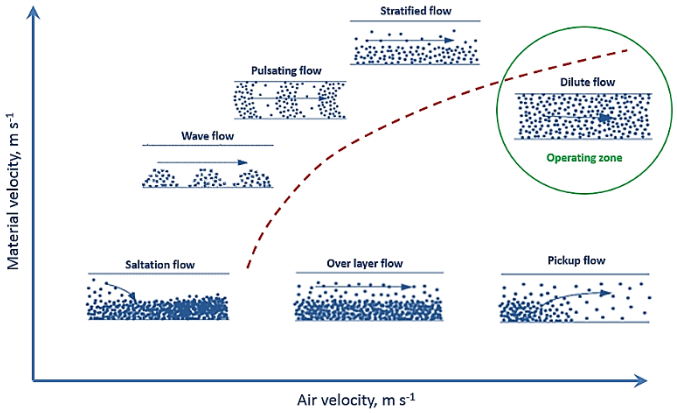

Figure 1. Flow regimes for air-solid mix as the function or the air velocity (Source: Binsirawanich, 2011; Barbosa et Seleghim, 2003).

In the world patent database, we found quite a few of interesting technical solutions to avoid any clogging risk in the air-delivery system as well (Clochard et Leveille, 2008). Bibliography survey revealed a noticeably poor database of a previous researches especially touching an energy consumption aspect.

So, very often, conveying system parameters are chosen intuitively and incorrectly, which leads to a clogging of pipes or to unjustified energy losses (excessive pressure drops and use of oversized fans...).Thus, the air velocity values for the steady state industrial processes cannot be accepted for air-seeders design. As the theoretical definition of theses parameters is impossible, we developed a rational method of experimental definition of the optimal air velocity for various seeds and fertilizers for the air-seeders.

Depending of an air/solid ratio we could distinguish two conveying regimes: the dilute phase and the dense phase conveying (Figure 1). The choice of conveying phase is mainly defined by the dimensions of the particles, their aerodynamic properties and the feeding stability requirements (Li et Tomita, 2000; Destoop, 1999; Zuev, 1976). According to the graph the air velocity decreasing triggers off the pulsating regime, which transforming into packet flow. The packets movement is performed only by the air static pressure in the spaces between the packets. The further air velocity decrease causes gradual sedimentation of seeding material and the ridges formation which clog the cross section of the conveying pipe. Then material conveying stops. From standpoint of the energy consumption, the dense phase conveying is preferable (Kunii & Levenspiel, 2013; Sanchez et al., 2003; Zuev, 1976; Razumov, 1972). Nevertheless, the dense phase pneumatic conveying is inapplicable on seeders for few reasons.

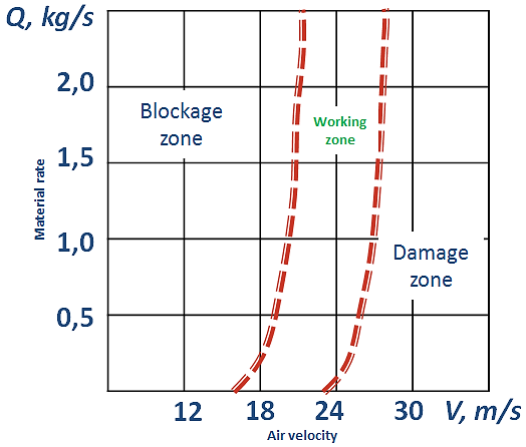

Figure 2. Range of acceptable air-velocities for pneumatic conveying of wheat and barley according to Segler (1951).

Firstly, the agricultural seeds, because of their dimensions and density are hardly fluidizable (Eskin et al., 2004; Levy and Kalman, 2001; Destoop, 1999; Gorial and O'Callaghan, 1990) and their fluidization velocity is high. Secondly, agronomically, to ensure homogeneous seeds germination, it is necessary to ensure a stable seeds supply to the soil openers (Spaar, 2008; Vilain, 2012; Buzenkov and Ma, 1976). Any pulsation or packets at this point are unacceptable. We can see from the diagram that air-seeding must run in the dilute phase only.

Besides, during the air-seeder working the conveying pipes are susceptible to the risk of a sudden clogging. The clogging could be caused in particular by the hygroscopic properties of fertilizers, by the delivery system overloading, foreign bodies or by the air velocity shortage. First of all, it concerns the outlet pipes, situated just after divider devices. These pipes have a small diameter (average 20-30 mm) but they represent a larger overall cross-section than that of the feed lines. So, the air velocity is usually reduced comparatively to the air velocity in the upstream in the divider head.

However there is a need to note that a very high air-velocity is also unwanted (Figure 2). A very high air-velocity could provoke a seed damage, inciting decreasing of a germinating power and resistance to diseases. All these factors could impact the future yield.

From a design point of view, after the classic methods of pressure drops determination it will be necessary to provide two interconnected parameters: flow concentration and conveying velocity, known from the literature. The pressure drops value will be used to define ne needs in the static pressure, required from the fan.

The volumic air-flow rate required from a fan unit is given by:

$$Q'_g = \frac{Q_s}{\mu \rho_a}, \text{ [m}^3 \text{ s}^{-1}\text{]} \qquad (1)$$

where Q_s is mass material rate, in kg s^{-1}; μ is mass flow concentration, kg kg^{-1} (Eq 8); ρ_a is volumetric mass density

of air.

The difficulty is in correct interpretation of the machine structure and in detection of all controversial areas causing energy losses and flow perturbations. At this point, it is important to notice that the conveying of particles in air-seeders is assumed to be assimilated to a dilute phase conveying. The total system pressure drop is a totality of losses, Mills (2004). We can distinguish horizontal conveying losses $\sum \Delta P_h$, vertical lift losses $\sum \Delta P_v$, losses in bends $\sum \Delta P_c$ and losses in accessory equipment (distribution heads, loading units), $\sum \Delta P_{ac}$:

$$\Delta P = \sum_1^n P_i = \sum \Delta P_h + \sum \Delta P_v + \sum \Delta P_c + \sum \Delta P_{ac} \quad (2)$$

Horizontal conveying losses can be presented as:

$$\Delta P_h = \Delta P_l + \Delta P_{tr} + \Delta P_a \quad (3)$$

where ΔP_l is linear pressure losses, Pa; ΔP_{tr} is pressure losses dues to material conveying, Pa; ΔP_a is pressure losses dues to material acceleration.

These losses could be calculates (Srvvastava et al. 2006; Zuev 1976; Razumov, 1972):

$$\Delta P_l = \lambda \frac{L}{D} \cdot \frac{\rho v_a^2}{2} = (0.0056 + \frac{1}{2Re^{0.32}}) \frac{L}{D} \cdot \frac{\rho v_a^2}{2} \quad (4)$$

where L, D are the length and diameter of the conveying pipeline, in m; λ_a is resistance coefficient; Re is Reynolds number: $Re = \frac{V_a D}{\nu}$; where ν – kinematic viscosity of the air (1.33 10^{-5} m^2 s^{-1}); V_a is the air velocity, m s^{-1} .

$$\Delta P_{tr} = \lambda' \frac{L}{D} \cdot \frac{V_m^2 \rho \mu}{2} \quad (5)$$

where λ' - resistance coefficient, for agricultural seeds: $\lambda' = 0.0037$, Zuev (1976); V_m is the material velocity, m s^{-1}.

$$\Delta P_a = \lambda_a \mu \frac{\rho_a V_a^2}{2g} \quad (6)$$

Vertical conveying is subordinated to the same principles as in horizontal areas, except that in vertical conveying we consider an influence of gravity and an impermanence of flow concentration. Pressure drop can be described as Srivastava et al. (2006):

$$\Delta P_v = \mu \frac{V_a \rho}{V_m} g \Delta H \quad (7)$$

where ΔH is height of lifting, m.

The losses in bends $\sum \Delta P_c$ are generally equated to some equivalent linear losses. In the case of particles conveying, losses in accessory equipments $\sum \Delta P_{ac}$ can be determined experimentally.

According to Zuev (1976), the theoretical definitions of flow concentration and of optimal air velocity, relatively to a pipe diameter, are very difficult or are impossible. So, we had to develop a rational method for the experimental definition of flow concentration for various seeds and fertilizers in the case of air-seeders.

Moreover, as several conveying velocities and several pipe diameters are possible, it is proposed in this paper to choose the most energy efficient solution. The conveying system design involves the definition of a pipe internal diameter, the calculation of pressure drop and the assignation of a fan unit. The power of the fan must be lower as possible and depends both of the pressure loss and the volumic air-flow rate.

It remained to be seen what part of the conveying system should be designed first. To make this choice, observations and field measurements were carried out to find which was the part of the system that suffered the most frequently problems

of clogging or flow heterogeneity.

The long-term experience of air-seeding, testified about numerous stagnations and clogging between the distribution head and openers. The trouble areas showed inflections of the flexible pipe and low initial air velocity. For these reasons we propose to define the maximum flow-concentration and the minimum air-velocity in the outlets of distribution heads for different cultures and pipe diameters. These values must avoid the clogging of the system. Searched parameters will be used as input data for the design of the pneumatic conveying. These values will lead (according to the mass conservation law) the design of the previous part of the conveying system (in which air velocity is higher because of a total lower section of feeding pipes).

2. Materials and Methods

2.1 Experimental setup

Testing was made on a specific experimental setup (Figure 3, a) within the company Kuhn SA in Saverne in France. This setup used for the testing of metering units in the case of small seeds and fertilizers was modified after our needs. It was reequipped with the metering unit of already manufactured air-seeder in order to simulate flows equivalent to real flows in the outlet of distribution head.

The seeds, provided by the metering unit (1) from the pressurized hopper (6), are picked-up by the air flow provided by the fan (2). They are conveyed in the flexible pipe (3) toward the plastic box (4) through a cyclone (5). The airflow was controlled using a primary control valve (8) and a fine control valve (7). The material flowrate was controlled by the electronic terminal ISOBUS VT50 of Kuhn (9), used on the manufactured machines compatible with the ISOBUS standard.

Air velocity was measured using Venturi tubes, according to Lefebvre (1986), by acquiring the kinetic energy of airflow in the form of pressure difference between the different sections separated by converging area (Figure 3, a). Pressure difference was taken by micro-manometers Testo 512 (11) laterally to air and material flows and in a straight area with a stabilized flow.

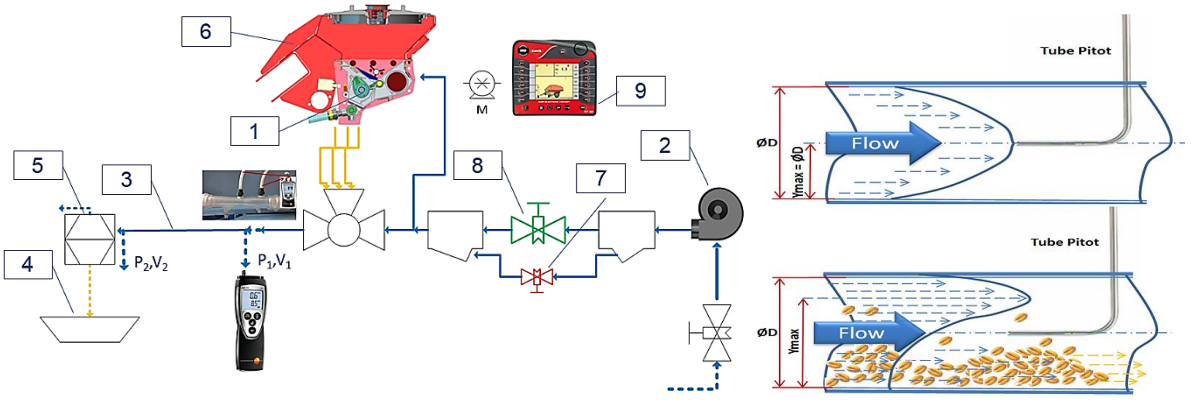

a) b)

Figure 3: (a) - Experimental setup. (b) – Air velocity profiles and velocity measurement in a horizontal pipe. (Idle air flow; loaded flow).

The first measurements of air velocity were made with a Pitot-tube but they didn't give adequate results. The Pitot-tube introduced in the middle axe of the straight pipe (far from the impermanent flow area) provided values corresponding to some local air-velocity (Figure 3, b). Ideally the maximum value is in front of the Pitot-tube but in a horizontal conveying this value represents a random and accidental velocity of a flow layer in a point of velocity profile. The value of air velocity reduces towards the walls of the pipe (and in practice it is very problematic to locate the Pitot-tube precisely on the pipe axis). Furthermore when air-flow is loaded with particles, the velocity profile is ousted on the top because of particles concentrated in the bottom of pipe. So the core of velocity profile moves up relatively to the axis of pipe, depending on loading (Figure 3, b). This phenomenon makes impossible a correct utilization of Pitot-tube.

2.2 Test procedure and data collection

Three current diameters (20, 25, 30mm) of flexible pipes were tested. The trail was made for the seeds of wheat, barley, starter fertilizers and a barley-fertilizer mixture (with a mass proportion 60/40). The material flowrate was calculated after agro-technical requirements for the ground speed of 10 km h^{-1}, a coulter-bar width of 12 m with 6 divider heads, 11 outlets per head. The established material flowrate was equal to material flowrate in a one outlet of distribution head. The flowrate then was changing from 3 to 30 g s^{-1}. Sometimes for the higher rates the metering unit overflowed and material flowrate could not be respected (with the smallest pipe diameters).

Each test was realized for horizontal and vertical pipes upon the following sequence: the metering unit was set to a precise material flowrate. The fan flowrate was set to a high and sufficient level to ensure material conveying. The airflow decreased by progressive closing of the valve, waiting at each position that flow stabilizes, until particles begin to subside and stagnate in the bottom of the pipe. Just as we visually detected material stagnation, the data from micro-manometers were collected. To ensure the most accurate results, a first manipulation was devoted to define the range of air velocities corresponding to particles stagnation. As soon as the velocity range is known and when approaching the stagnation air velocity, we start closing the valve more slowly and precisely, fixing air velocity to a clogging beginning. Each trail was replicated 5 times.

After the known material flowrate and measured stagnation velocity, the maximum flow concentration was calculated as:

$$\mu = \frac{Q_s}{Q_g} = \frac{Q_S}{V_{ast}\pi\frac{D^2}{4}\rho_a} \qquad (8)$$

3. Results and Discussion

3.1 Vertical and horizontal conveying comparison

Stagnation air velocity corresponds to the minimum quantity of energy necessary to the air to move materials and itself. Stagnation air velocity during vertical conveying of wheat is always higher than during horizontal one (Table 2). Stagnation air velocity during vertical conveying is about 25 % higher than during horizontal conveying whatever pipe diameter. It can be explained by the influence of gravity forces which are single forces opposing velocity vector. That's way vertical conveying needs greatest air velocity. This value will be specific for the each type of material according to its physical properties (weight, shape *etc*.). The vertical stagnation air velocity is then the critical parameter which should be used for the design of air-seeders pneumatic conveying system.

Stagnation velocities for high concentrated flows in horizontal and vertical pipes are similar regardless of pipe diameter (each point is the mean of 5 measurements and values are very closed to mean value). But pipe diameter probably influences the horizontal stagnation air velocity, especially when flowrate of grains is low. Physically a low rate of grains permits the use of less energy for the conveying and so the use of a lower air velocity. On the contrary practically we may suppose that seeds' deposit (when air velocity can be lower) occurs more easily and has more easily consequences on air flow homogeneity (a deposit generates a pressure drop and a deflection of the air flow) in wide pipes than in thinner ones (cf. Figure 3, b). This probably explains why, unexpectedly, horizontal stagnation air velocity seems to be lower in thin pipes than in wider ones.

These data about fluidization and pick-up velocities can be compared to literature data (*cf.* Table 1) taken from Buzenkov et Ma (1976). Our experimental values of stagnation velocities are in the top of fluidization threshold for a vertical conveying and in the top of pick-up threshold for a horizontal one. Similar results were obtained for wheat, barley and fertilizers.

Table 1. Physical characteristics of tested grains (Afonso Júnior et al. 2007; Buzenkov et Ma 1976.

Type of crop	Length, mm		Width, mm		Height, mm		Seeding rate, (kg ha-1)		Fluidization velocity (m s-1)	
	min.	max.	min.	max.	min.	max	min.	max.	min.	max.
Wheat	4	8.6	1.6	4	1.4	3.8	60	250	8.9	11.5
Barley	7	14.6	2	5	1.2	4.5	90	350	7.6	10.7
Fertilizers	0,25	7	sphere				100	250	3	11

3.2 Mixture conveying

There are ambiguous observations about barley-fertilizer mixture conveying. The results obtained with barley, fertilizers and their mixture are grouped on the same diagram. In the smallest pipe (diameter 20mm) stagnation velocity of mixture is identical to barley one (green curves, Figure 5). The ratio 60/40 by weight implicates that barley volume is double than fertilizer's volume in one volume of air. We could suppose the behavior of the fertilizer is masked by the behavior of barley: Barley has a tendency to “carry” fertilizers in the manner of a "broom".

In the pipe of 25 mm the effect of fertilizer presence is more perceptible. The curve of mixture stagnation is just between the barley (green) and fertilizer (red) curves (Figure 5). We can suppose that as air could circulate freely between the particles, heavier particles (fertilizer and heavier barley seeds) subside easily at the bottom of the pipe. In spite of the superior volume of the barley seeds have a less influence on the fertilizer stagnation because of the wider diameter of the pipe. We can suppose that a bigger content of fertilizer in the mixture will increase the stagnation limit velocity.

However, increasing of pipe diameter to 30 mm (black curves), we observed the same result than for the 20 mm pipe. So further experiments and statistical analysis will be done in order to conclude. In a first approach, we will use the higher stagnation velocity of one part of the mixture (here fertilizer) to design the system of conveying.

Table 2. Test results for the seeds of wheat in the pipes of 25 mm.

Material flowrate per second, g s^{-1}	Horizontal conveying				Vertical conveying			
	Pressure difference, hPa	Stagnation velocity, m/s	Average stagnation velocity, m s^{-1}	Maximal flow concentration, kg kg^{-1}	Pressure difference, hPa	Stagnation velocity, m/s	Average stagnation velocity, m s^{-1}	Maximal flow concentration, kg kg^{-1}
	0.8	7.01			1.50	9.57		
	0.7	6.55			1.40	9.25		
3.3	0.9	7.43	7.09	0.79	1.40	9.25	9.37	0.60
	0.8	7.01			1.40	9.25		
	0.9	7.43			1.50	9.57		
	0.9	7.43			1.60	9.91		
	0.9	7.43			1.50	9.59		
4.6	0.9	7.43	7.47	1.05	1.60	9.91	9.78	0.80
	0.85	7.22			1.50	9.59		
	1	7.83			1.60	9.91		
	1.05	8.03			1.60	9.91		
	1	7.83			1.70	10.21		
6.3	1	7.83	7.87	1.36	1.70	10.21	10.09	1.06
	1	7.83			1.60	9.91		
	1	7.83			1.70	10.21		
	1.1	8.21			1.90	10.80		
	1.2	8.58			1.90	10.80		
9.2	1.2	8.58	8.51	1.84	2.00	11.08	10.91	1.43
	1.2	8.58			1.90	10.80		
	1.2	8.58			2.00	11.08		
	1.25	8.76			2.00	11.08		
	1.2	8.58			2.00	11.08		
11.3	1.3	8.93	8.79	2.18	2.00	11.08	11.02	1.74
	1.25	8.76			1.90	10.80		
	1.3	8.93			2.00	11.08		
	1.3	8.93			2.00	11.08		
	1.3	8.93			1.90	10.80		
12.1	1.34	9.07	8.99	2.29	1.90	10.80	10.96	1.87
	1.3	8.93			2.00	11.08		
	1.35	9.10			2.00	11.08		
	1.4	9.27			2.00	11.08		
	1.35	9.10			2.10	11.35		
14.2	1.35	9.10	9.23	2.61	2.00	11.08	11.24	2.15
	1.45	9.43			2.10	11.35		
	1.4	9.27			2.10	11.35		
	1.5	9.59			2.10	11.35		
	1.5	9.59			2.10	11.35		
16.3	1.5	9.59	9.66	2.87	2.20	11.62	11.46	2.42
	1.6	9.91			2.10	11.35		
	1.5	9.59			2.20	11.62		
	1.7	10.21			2.40	12.13		
	1.8	10.51			2.30	11.88		
20	1.7	10.21	10.33	3.29	2.30	11.88	11.93	2.85
	1.8	10.51			2.30	11.88		
	1.7	10.21			2.30	11.88		
	1.9	10.80			2.50	12.38		
	1.9	10.80			2.40	12.13		
25	1.9	10.80	10.80	3.93	2.30	11.88	12.13	3.50
	1.9	10.80			2.30	11.88		
	1.9	10.80			2.50	12.38		

3.3 Flow concentration and pipe diameter

For the dilute phase conveying, the oversizing of pipes' sections is not a solution. Particles present in the bottom part of wide pipes offsets the maximum of air velocity towards the upper part of the pipe. The subsiding of grains then creates a "brake" for the air (Figure 3, b). The air arriving in this section of pipe has the tendency to "avoid" the pressure loss created by obstacles. So the largest diameter will always create an "avoidance" of seed clusters instead of pushing the whole flow of seeds toward the right direction. Therefore, when the section size decreases, air circulation between particles will be more homogeneous, so fan energy will be more efficiently used. The oversizing of diameter will also lead to increase airflow rate (for a constant air velocity) and increases the energy consumption (to a power 3). The power consumption can be expressed as:

$$\frac{N_1}{N_2} = \left[\frac{Q_{a1}}{Q_{a2}}\right]^3 \qquad (9)$$

where Q_{a1}, Q_{a1} – the air flowrates before and after changing, in $m^3\ s^{-1}$; N_1, N_2 are fan shaft horse powers before and after changing, in kW.

It is necessary to create good conveying conditions, ensuring local velocities are greatest than the critical velocity.

The first parameter to determine is the air velocity in the pipes after divider heads. It is proposed to set this value from Figure 1 as a function of the flow of seeds (here in the case of wheat). This value may be 15% higher than the limit of stagnation velocity in vertical conveying for more safety. This velocity value sets the maximum conveying concentrations (plotted in Figures 4 and 5). In Figure 4 we realize that the diameter of 20 mm would be sufficient to conveying the flow concentrations in the case of air seeders. In addition, this pipe diameter reduces the energy cost of the operation. In practice we do not choose smaller diameter because seeder must be versatile and must also sow large seeds.

Previous calculations were made for pipes after the distribution head. In an air-seeder, the sum of the sections after the distribution head is greater than the section before it. According to the matter conservation law, the airflow velocity before distribution head will so be higher and air velocity before head of distribution will be high enough to avoid particles stagnation.

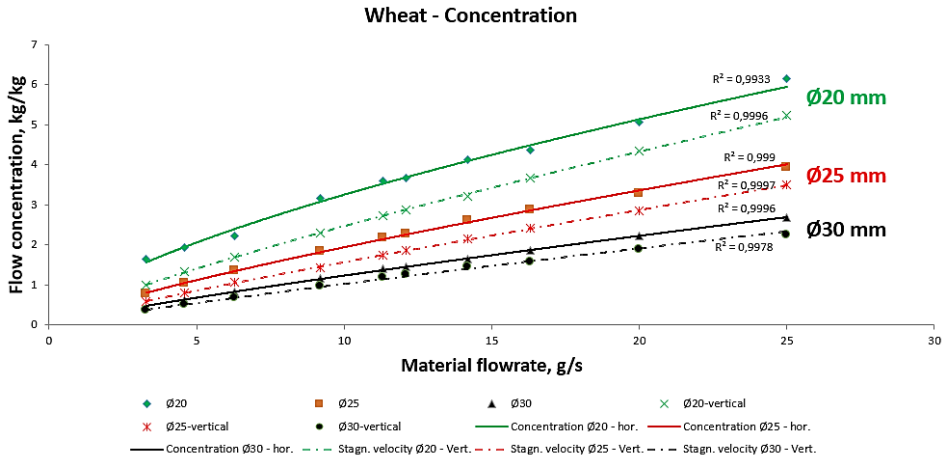

Figure 4. Maximum flow concentration of wheat. Each point is the average of 5 measurements.

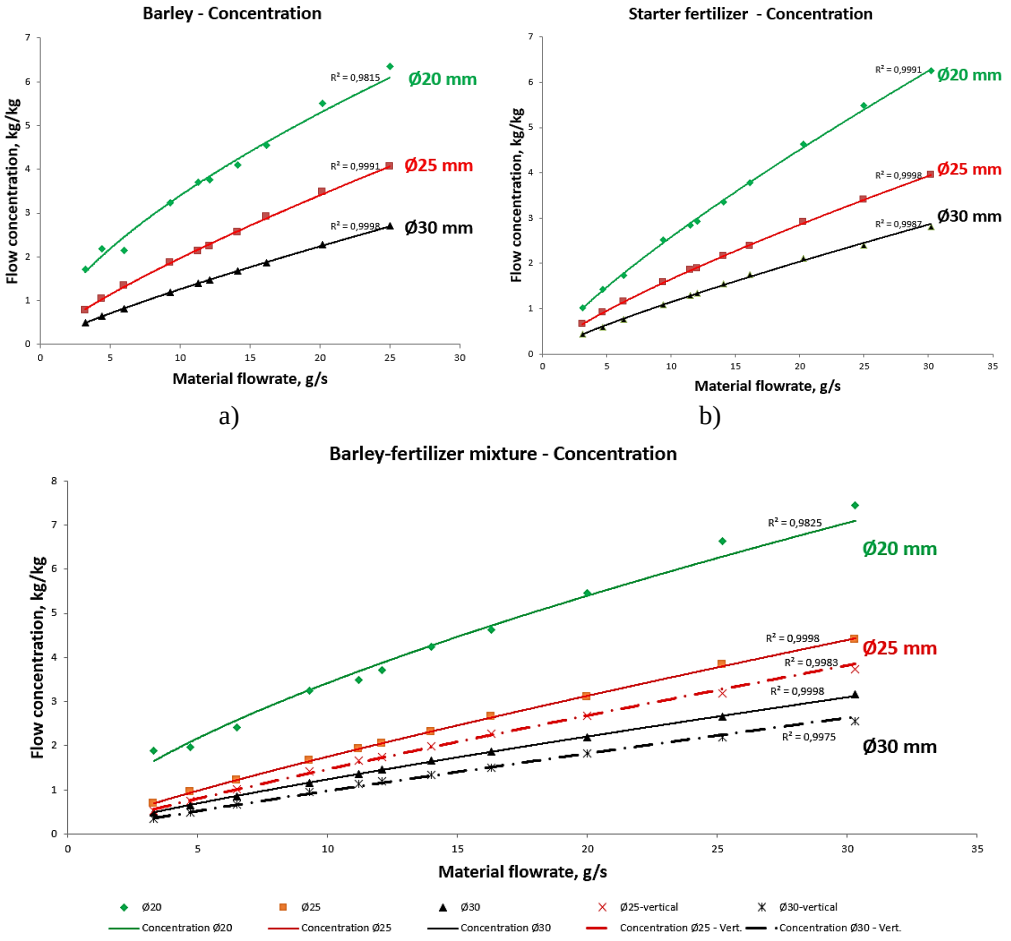

Figure 5. (Each point is the average of 5 measurements): a - Maximum flow concentration of barley; b - Maximum flow concentration of starter fertilizers; c – Maximum flow concentration, barley-fertilizer mixture.

4. Conclusions

According to this work, about pneumatic conveying in the case of an air-seeder, it was found that:

1. Starting point of design must be the optimization of conveying after distribution head's outlets. The design of the rest of the conveying system will result from this first step
2. An experimental set up was design to obtain experimental values for the maximum flow concentration and the minimum air velocity suitable for pneumatic conveying. The results obtained are usable but it was necessary to develop an innovative sensor system because the pitot probes are unsuitable for this work. Further development of this experimental set-up could use image analysis in order to correlate pressure measurements and seeds clusters formation.
3. Experimental curves of minimum air-velocity can be used to define conditions of conveying for a type of seeds. It is proposed to set this value from Figure 1 as a function of the flow of seeds (here in the case of wheat). This value may be 15% higher than the limit of stagnation velocity in vertical conveying for more safety.
4. It is recommended to use the pipe sections as lower as possible to favor a homogenous airflow and to reduce the energetic cost of conveying.
5. In order to develop knowledge on the conveying of mixtures other experiments could be requested for several proportions of fertilizers and seeds.
6. Same work must be made for other species of seeds, and for different qualities of seeds inside a species (regarding to humidity, size homogeneity...) in order to study the robustness of our results.

Acknowledgements

This work was performed as a part of research collaboration of National Institute of Higher Education in Agronomy, Food and Environmental Sciences of Dijon (AgroSup Dijon) and company Kuhn SA.

References

Afonso Júnior, P. C., Corrêa, P. C., Pinto, F. A. C., & Queiroz, D. M. 2007. Aerodynamic properties of coffee cherries and beans. *Biosystems Engineering*, 98(1), 39-46.

Astahov V.S. 2007. Mechanical and technological fundamentals of the air-seeding having a centralized distribution system. In Russian. (Астахов В.С. Механико-технологические основы посева сельскохозяйственных культур сеялками с пневматическими системами группового дозирования: Дис. докт. техн. наук. Горки) D. of Science thesis. Gorki, Byelorussia, 377 p.

Barbosa, P. R., & Seleghim Jr, P. 2003. Improving the power consumption in pneumatic conveying systems by a daptive control of the flow regime. *Journal of the Brazilian Society of Mechanical Sciences and Engineering*, 25(4), 373-377.

Binsirawanich P., 2011. Mass flow sensor development for an air seeding cart. M.Sc thesis. University of Saskatchewan.

Buzenkov G. M. et Ma S.A. 1976. Crop seeding machines. In Russian. (Бузенков Г.М., Ма С.А. Машины для посева сельскохозяйственных культур. Машиностроение) Moscow, 270p.

Clochard, D., et Leveille L., 2008. Automated particle-distribution system for agricultural machine, and corresponding method. Patent EP 2409559 (B1).

Destoop, T. 1999. *Manutention pneumatique de produits en vrac*. Ed. Techniques Ingénieur.

Eskin, D., Leonenko, Y., & Vinogradov, O. 2004. Engineering model of dilute pneumatic conveying. *Journal of engineering mechanics*, *130*(7), 794-799.

Gorial B.Y., & O'Callaghan J.R. 1990. Aerodynamic properties of grain/straw materials. *Journal of Agricultural Engineering Research*, 46(4), 275-290.

Klinzing, G. E. 2003. Dilute-Phase Pneumatic Conveying. HANDBOOK of FLUIDIZATION and.

Lefebvre, J. 1986. Mesure des débits et des vitesses des fluides. Masson.

Levy, A., & Kalman, H. 2001. Dilute-phase pneumatic conveying problems and solutions. Handbook of Conveying and Handling of Particulate Solids, 10, 303.

Li, H., & Tomita, Y. 2000. Particle velocity and concentration characteristics in a horizontal dilute swirling flow pneumatic conveying. *Powder Technology*, 107(1), 144-152.

Mills D. 2004. Pneumatic Conveying Design Guide. Second Edition Butterworth-Heinemann.

Razumov, I. M. 1972. Fluidization and pneumatic conveying of bulk materials. In Russian. (Псевдоожижение и пневмотранспорт сыпучих материалов М.: Химик). *Khimiya, Moscow*.

Sanchez, L., Vasquez, N., Klinzing, G. E., & Dhodapkar, S. 2003. Characterization of bulk solids to assess dense phase pneumatic conveying. *Powder Technology*, *138*(2), 93-117.

Segler, G. 1951. *Pneumatic grain conveying*. National Institute of Agricultural Engineering, Wrest Park-Silsoe, Bedfordshire.

Spaar, D., 2008. Crops: cultivation, harvesting and processing. (Зерновые культуры. Выращивание, уборка, доработка и использование. ООО ≪DLV АГРОДЕЛО≫,) Moscow, Russia, 656 p.

Srivastava A. K., Goering C. E., Rohrbach R. P., Buckmaster D. R., 2006. Conveying of Agricultural Materials Chapter 14. In *Engineering Principles of Agricultural Machines*, 2nd ed., pp. 491-524 St. Joseph, Michigan: ASABE. (doi: 10.13031/2013.41476).

Weiste, H. 2013. The ACCORD PNEUMATIC-System: From invention to worldwide application, Landwirtschaftsverlag GmbH, Münster-Hiltrup. Germany, 224p.

Vilain, M. 2012. Méthodes expérimentales en agronomie: pratique et analyse. Lavoisier.

Zuev, F.G., 1976. Pneumatic conveying on crop processing industries. In Russian. (Зуев Ф.Г. Пневматическое транспортирование на зерноперерабатывающих предприятиях.- М.: Колос). Moscow, 344p.

Centrifugal fertilizer spreader : control of working width and fertilization quality

Tien-Thinh LE[*1], **Emmanuel PIRON**[1], **Denis MICLET**[1], **Alaa CHATEAUNEUF**[2], **Michel BERDUCAT**[3], and **Phillipe HERITIER**[1]

[1]Irstea, UR TSCF, Centre de Clermont-Ferrand, Les Palaquins, F-03150 Montoldre, France
[*] Corresponding author. Email : `tien-thinh.le@irstea.fr`
[2]Université Blaise Pascal, Institut Pascal, BP 10448, F-63000 Clermont-Ferrand, France
[3]Irstea, UR TSCF, Centre de Clermont-Ferrand, F-63178 Aubière, France

Abstract

This research deals with the control of working width and fertilization quality when using centrifugal fertilizer spreader. From such spinning disc spreader, the stationary spatial distribution of fertilizers is described, in the cylindrical coordinate system, by radius and angle (average and standard deviation). Because of the variability of fertilizer's physical characteristics, the landing position and drop angle of particles typically exhibit a strong variation. Indeed, the latter has been demonstrated by both experimental investigations, such as using the Cemib device at Irstea, and numerical modeling. In this work, we address the construction and identification of a prediction model for controlling the spatial distribution of fertilizers from spinning disc spreader. The proposed model is based on (i) the operating parameters of machine and (ii) the physical characteristics of fertilizer particles. To this aim, we first perform the characterization of particle size and shape by using image analysis. The morphology of particle is characterized by various shape parameters, scaled to values between 0 and 1, describing the changes with respect to a reference geometry (circle or ellipse for instance). The image-based method provides a quantitative, representative and reproducible description of the fertilizer morphology, hence allowing for the study of particle aerodynamic properties in the ballistic flight and the construction of a suitable prediction model for the drag coefficient of fertilizers. This model is subsequently identified through a inverse problem involving experimental data of Cemib. The model also helps calibrating which fertilizer's physical characteristics best describe the spreading pattern of centrifugal spreader. The impact of such prediction on transverse distributions, working widths and fertilization quality (CV curves) is finally characterized by using sensitivity analysis.

Keywords : Centrifugal spreader ; Fertilizer ; Working width ; Drag coefficient ; Spread pattern ; Morphology

1 Introduction

In Europe, the solid inorganic fertilizers are often applied onto agricultural fields by a centrifugal spreader (Hofstee, 1995; Olieslagers et al., 1996). The spatial position of particles on the ground depends on three types of parameters : the operating distributor (such as the rotational speed of the disc), the physical characteristics of fertilizers (such as their size, shape and density), and other external conditions (such as weather). The spatial distribution of fertilizers is examined in test benches, for instance the collection trays equipped with sensors (Piron et al., 2010; Coetzee & Lombard, 2011). There are two main steps in centrifugal spreading process : the first one is the motion of particles on the disc and the second one is concerned with the flight of particles in

the air (Mennel & Reece, 1963). When thrown out, the particle surface interacts with the air and generates a mechanical force like the drag (Clift et al., 1978; Haider & Levenspiel, 1989). The morphology of particles defines their aerodynamic behavior, which in turns determines the landing position of fertilizers on the ground (Hoerner, 1965). Several works were proposed to determine the drag coefficient of fertilizers in laboratory conditions (for instance, Grift et al. (1997); Haider & Levenspiel (1989); Dioguardi & Mele (2015) measured fall time or terminal velocity of irregular particles in a sealed cylinder). In order to increase the accuracy of predicted landing distribution, the drag coefficient has been investigated in real conditions of the spreading process.

The purpose of this article is to establish a quantitative characterization of aerodynamic properties of particles in the ballistic flight. The drag coefficient of fertilizers has a potential application to predict numerically the spread pattern compared to that from test benches.

The paper is organized as follows. Section 2 presents the considered fertilizers and image analysis method to characterize particles. In this section, our particle analyzer is described together with several methods to calibrate photographic and statistical conditions. The modeling of spreading process involving particle aerodynamic behavior is also considered. The results of characterization and identification are finally presented in Section 3.

2 Material and methods

2.1 Characterization of physical characteristics of particles

2.1.1 Samples of fertilizers

In this work, several solid inorganic fertilizers are characterized by image analysis, which exhibit a wide range of shapes. Sieve analysis is also applied in accordance with the standard in CEN (1995). Image analysis method introduced in Section 2.1.2 provides also particle geometrical information, which helps better understanding of the results of size from sieve tests (Le et al., 2016a). The summary is presented in Tab. 1.

Fertilizer	Mass density (kg/m^3)	Sieve analysis	D_{50} (mm)
F1	1895	80% ∈[2, 4]	2.64
F2	1265	84% ∈[2, 3.2]	2.58
F3	1594	91% ∈[2.5, 4]	3.46
F4	1307	83% ∈[2, 4]	2.94
F5	2056	81% ∈[2.5, 4]	3.26
F6	1792	85% ∈[2.5, 4]	3.40
F7	1681	85% ∈[3.2, 5]	3.69
F8	1706	79% ∈[2.5, 4]	3.00
F9	1672	90% ∈[3.2, 5]	3.74
F10	1543	77% ∈[3.2, 5]	3.66

TABLE 1 – Notation, mass density and sieve analysis results of the fertilizers considered in this study.

2.1.2 Image analysis method

Regarding number of particles, cost, acquisition, processing time and limitation of instruments, 2D image analysis is chosen to characterize fertilizer particles (Liu et al., 2015; Hryciw et al., 2016). In our case, Dynamic Image Analysis is applied to handle the measurement of particle size and shape (Le et al., 2016a). The method is well defined and standardized in ISO (2006). Photographic and statistical conditions are also taken into account, particularly in terms of image resolution and number of particles.

We present in Fig. 1 our video-granulometer equipment. A flow of particles is driven in front of a high-speed camera. Multiple images are taken and then processed by our developed software to extract the desired dimensional characteristics (using Matlab Image Processing Toolbox (MATLAB, 2004)).

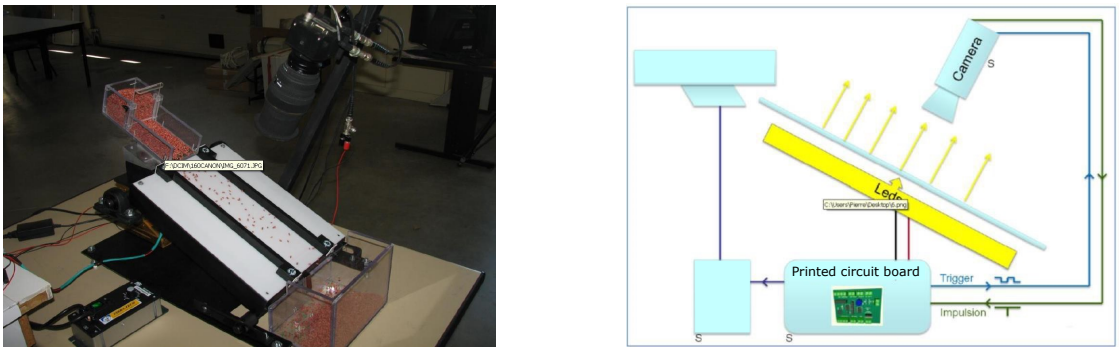

FIGURE 1 – The video-granulometer developed at Irstea.

There are several shape factors which could be defined to characterize the morphology of particles (with respect to a reference geometry). In this paper, the circularity parameter is presented (Bouwman et al., 2004; Hryciw et al., 2016; Liu et al., 2015) :

$$C = \frac{4\pi A}{P^2}, \tag{1}$$

where A and P are the area and perimeter of the projection surface, respectively. When C = 1, the particle is circular.

Taking photos of moving irregular particles requires special photographic and statistical conditions. In our case, image resolution, exposure time and number of particles are optimized. The calculation of shape factor depends strongly on the resolution of captured images. An optimal value of image resolution is identified through convergence analysis of shape factor calculation. The condition of exposure time is described by the indicator ε as follow :

$$\varepsilon = \sqrt{1 + \frac{A_{meas}}{A_{real}}}, \tag{2}$$

where A_{meas} is the area of moving particle and A_{real} is the area of static particle in regard to the direction of motion. The convergence analysis must be taken into account to obtain the required accuracy of the measurement, in this case, the number of particles. The statistical estimator for the mean value of the real-valued random variable is defined as (Le et al., 2016b).

$$n \mapsto \text{ConvMean}\,(n) = \frac{1}{n}\sum_{i=1}^{n} T\,(\omega_i), \tag{3}$$

where n is the number of realizations, $T\,(\omega_i)$ is the i value of the observed data T.

2.2 Measurement of spread pattern : Cemib device

The Cemib bench, invented by Irstea in 2006, allows to measure the spatial distribution of fertilizers from spinning disc spreader with high accuracy (Piron et al., 2010). Its main advantage is the reduction of the necessary space in the hall to make acquisitions : a hall of 45m×10m is sufficient (450m^2) whereas the traditional bench requires 90m×60m (5400m^2). An image of Cemib and its operation of measurement are presented in Fig. 2.

2.3 Aerodynamic behavior of fertilizers

2.3.1 Modeling of spreading process

There are two main steps in the spreading process. The first one is the motion of particles on the disc. The second step deals with the flight of particles in the air. For a given particle, the following ballistic equation was

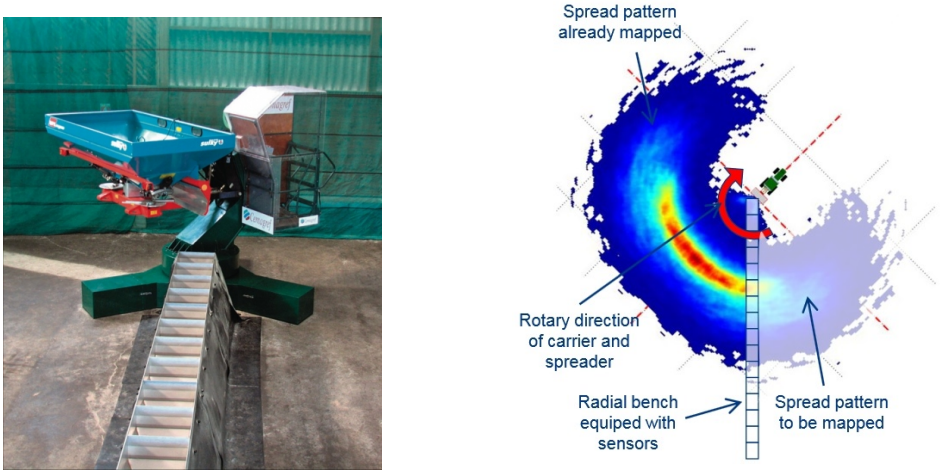

FIGURE 2 – An image of Cemib bench (on the left) and its operation of measurement, schematized in the polar coordinate system (on the right).

used to model the particle trajectory in the air based on its initial positions and velocities (measured at the outer extremity of the vane) (Mennel & Reece, 1963; Dintwa et al., 2004; Villette et al., 2005) :

$$m\boldsymbol{a} = -\frac{1}{2}C_d S \rho_f ||\boldsymbol{v}||\boldsymbol{v} + m\boldsymbol{g}, \tag{4}$$

where m is the mass, $\boldsymbol{a}$ is the acceleration, C_d is the drag coefficient, $\boldsymbol{v}$ is the velocity and S is the reference area of the particle ; ρ_f is the air density. All parameters in Eq. (4) are known through the characterization of particle's physical characteristics (Section 2.1.2), except the drag coefficient. We present in the following sections the identification of this aerodynamic coefficient involving experimental data of Cemib.

2.3.2 Determination of drag coefficient

For a given fertilizer, on the one hand, the Cemib device provides experimental spatial distribution, and on the other hand, a numerical model based on the drag coefficient is constructed to simulate a virtual spatial distribution (Eq. (4)). An identification procedure (using Matlab optimization toolbox (MATLAB, 2004)) is then used to minimize error between the experimental spread pattern and virtual one. Optimal drag coefficient of the given fertilizer is finally deduced from the identification program. The inverse identification problem is well detailed in Le et al. (2017a).

The identified drag coefficients can be used in models of prediction and control of the fertilization procedure. An example is presented in Section 3.3 for fertilizer F10 : use of drag coefficient identified at 800 rpm to predict spread pattern at 1000 rpm.

3 Results and discussion

3.1 Particle characterization : optimal photographic and statistical conditions

As introduced in Section 2.1.2, we investigate now photographic and statistical conditions when using image analysis method. The calibration of optimal image resolution for our fertilizer particles is shown in Fig. 3 while the optimal number of particles is shown in Fig. 4 on the left. The condition of exposure time is also calibrated (but not shown). Under optimal photographic and statistical conditions, the characterization of particles is quantitative, representative, repetitive and reproducible (see Fig. 4 on the right).

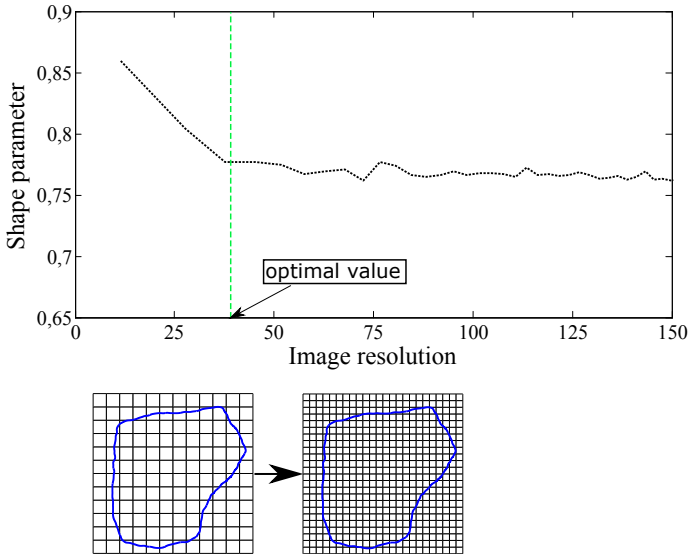

FIGURE 3 – Calibration of optimal image resolution (optimal value : 34 px/mm) (see Eq. (1)).

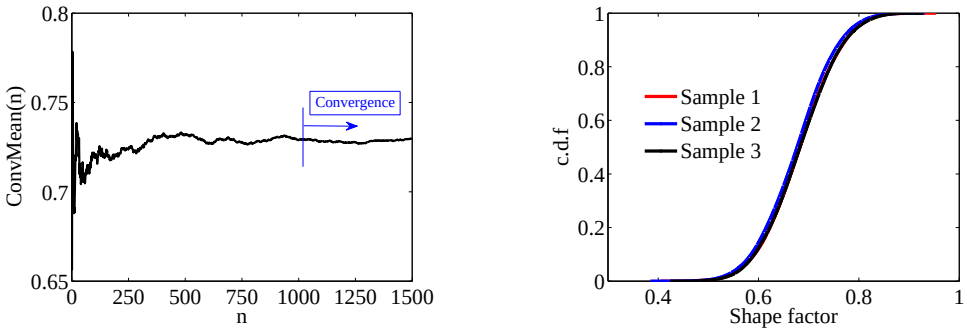

FIGURE 4 – Figure on the left : statistical analysis to determine the convergence of observations as a function of number of particles (see Eq. (3)). Figure on the right : strong repetition of measurement under optimal conditions.

3.2 Prediction model based on identified drag coefficients

In this section, a prediction model of spread pattern is proposed (schematized in Fig. 5). The model is based on the identified drag coefficients from the optimization program (Section 2.3.2). The first input of the model is the operating parameters of the centrifugal spreader, such as the rotation frequency of the disc. The second input of the model is physical characteristics of particles (drag coefficient identified previously). We obtain the virtual spatial distribution of fertilizers as well as the curve of fertilization quality in the output of the model. An example of use of the model is presented in the following sections.

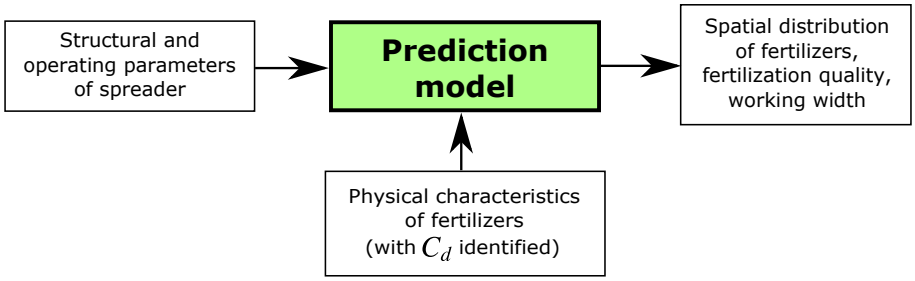

FIGURE 5 – Prediction model based on identified drag coefficients.

3.3 Use of identified drag coefficients

Considering now the case of fertilizer F10, its drag coefficient identified at 800 rpm is used to simulate a virtual spatial distribution at same structural parameters of spreader but 1000 rpm. Fig. 6 presents the measured spatial distribution of fertilizer F10 from the Cemib device (on the left) and from the numerical model (on the right). Fig. 7 presents the corresponding fertilization uniformity at different working widths for two cases : measurement and simulation. We observe a very strong statistical correlation between the CV curve of measurement and the one from numerical model. From the results of Cemib, an optimal working width of 32m is deduced (CV = 2.42%). Values of CV measured and simulated at several working widths near 32m are detailed in Tab. 2.

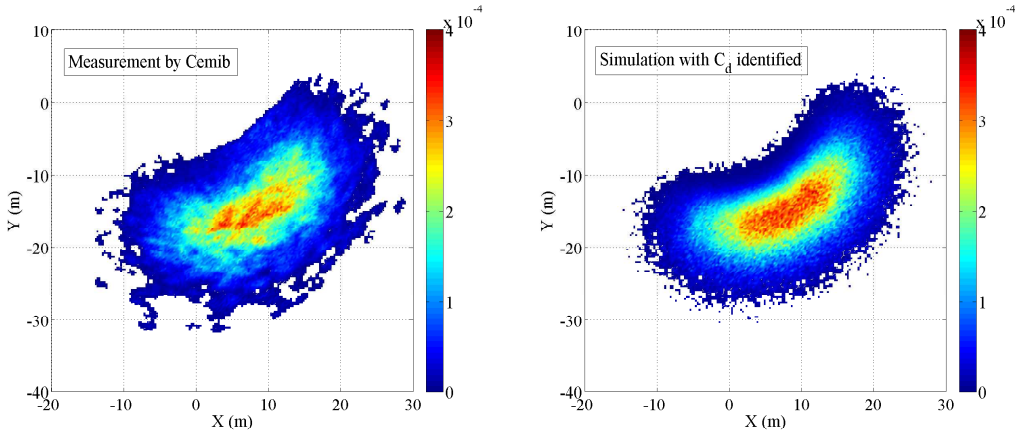

FIGURE 6 – Use of C_d identified at 800 rpm to estimate the 3D spread pattern at 1000 rpm, case of fertilizer F10. The vane angle on the disc is 14 deg, particles leave the vanes at 0.8m above the ground, the center of the disc is located at (0, 0).

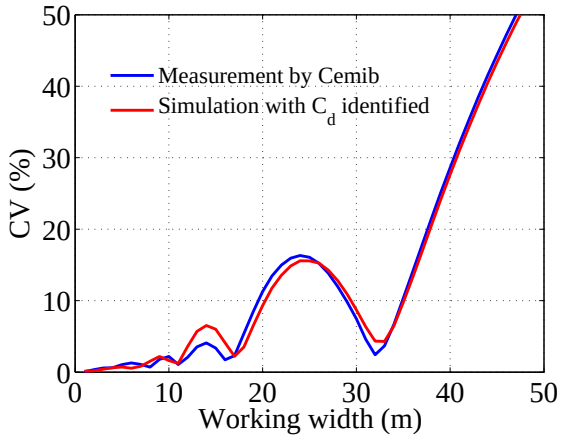

FIGURE 7 – Use of C_d identified to estimate the coefficient of variation, case of fertilizer F10. The rotation speed of the disc is 1000 rpm, the vane angle on the disc is 14 deg, particles leave the vanes at 0.8m above the ground, the center of the disc is located at (0, 0).

As shown in Fig. 6–7 and Tab. 2, the numerical model shows a potential application to predict the spread pattern in real conditions. More details on the effects of spread pattern shapes obtained in both measurement and simulation could be found in Le et al. (2017b).

CV measured (%)	Working width (m)	CV simulated (%)
11.98	28	12.81
9.86	29	10.94
7.46	30	8.71
4.59	31	6.34
2.42	32	4.34
3.67	33	4.29
6.70	34	6.49
10.36	35	9.78
14.06	36	13.24

TABLE 2 – Values of measured and simulated coefficient of variation at several working widths (from Fig. 7).

4 Conclusion

In this work, we presented a numerical strategy to predict the spread pattern of fertilizers when using centrifugal spreader. The proposed model was based on an identification of aerodynamic behavior of fertilizers in the ballistic flight. We first characterized the physical characteristics of fertilizers by using image analysis method. Photographic and statistical conditions were also optimized. Second, the spreading process was modeled through ballistic equation involving drag coefficient of particles. The latter was identified by an inverse procedure. A numerical simulator using identified drag coefficient was finally constructed to predict the spread pattern of fertilizers. A very strong statistical correlation between measurement and simulation was found. In the future, the proposed numerical model is potentially applicable to control the fertilization procedure.

Acknowledgements

This work was supported by the French National Research Institute of Science and Technology for Environment and Agriculture (Irstea). We would also like to acknowledge the grant of the European Regional Development Fund (FEDER) through the Auvergne Region of France.

References

Bouwman, A. M., Bosma, J. C., Vonk, P., Wesselingh, J. H. A., & Frijlink, H. W. (2004). Which shape factor(s) best describe granules ? *Powder Technology*, *146*, 66–72. doi :10.1016/j.powtec.2004.04.044.

CEN (1995). NF EN 1235 *Solid fertilizers - Test sieving*. European Committee for Standardization.

Clift, R., Grace, J. R., & Weber, M. E. (1978). *Bubbles, Drops, and Particles*. Academic Press.

Coetzee, C. J., & Lombard, S. G. (2011). Discrete element method modelling of a centrifugal fertiliser spreader. *Biosystems Engineering*, *109*, 308–325. doi :10.1016/j.biosystemseng.2011.04.011.

Dintwa, E., Tijskens, E., Olieslagers, R., De Baerdemaeker, J., & Ramon, H. (2004). Calibration of a spinning disc spreader simulation model for accurate site-specific fertiliser application. *Biosystems Engineering*, *88*, 49–62. doi :10.1016/j.biosystemseng.2004.01.001.

Dioguardi, F., & Mele, D. (2015). A new shape dependent drag correlation formula for non-spherical rough particles. experiments and results. *Powder Technology*, *277*, 222–230. doi :10.1016/j.powtec.2015.02.062.

Grift, T. E., Walker, J. T., & Hofstee, J. W. (1997). Aerodynamic properties of individual fertilizer particles. *Transactions of the Asae*, *40*, 13–20.

Haider, A., & Levenspiel, O. (1989). Drag coefficient and terminal velocity of spherical and nonspherical particles. *Powder Technology*, *58*, 63–70. doi :10.1016/0032-5910(89)80008-7.

Hoerner, S. F. (1965). *Fluid-Dynamic Drag*. Published by the author.

Hofstee, J. W. (1995). Handling and spreading of fertilizers .5. the spinning disc type fertilizer spreader. *Journal of Agricultural Engineering Research*, *62*, 143–162. doi :10.1006/jaer.1995.1073.

Hryciw, R. D., Zheng, J., & Shetler, K. (2016). Particle roundness and sphericity from images of assemblies by chart estimates and computer methods. *Journal of Geotechnical and Geoenvironmental Engineering*, . doi :10.1061/(ASCE)GT.1943-5606.0001485.

ISO (2006). ISO 13322-2 *Particle size analysis - Image analysis methods, Part 2 : Dynamic image analysis methods*. International Organization for Standardization.

Le, T., Miclet, D., Heritier, P., Piron, E., Chateauneuf, A., & Berducat, M. (2016a). Morphology characterization of irregular particles using image analysis. application to solid inorganic fertilizers. *submitted to Computers and Electronics in Agriculture*, .

Le, T., Piron, E., Miclet, D., Chateauneuf, A., & Berducat, M. (2017a). Construction and identification of a numerical model to predict the spatial distribution of fertilizers from spinning disc spreader : take into account the physical characteristics of particles. *submitted to Biosystems Engineering*, .

Le, T., Piron, E., Miclet, D., Chateauneuf, A., & Berducat, M. (2017b). Sensitivity analysis to assess the performance of numerical prediction when using centrifugal fertilizer spreader. *submitted to Biosystems Engineering*, .

Le, T. T., Guilleminot, J., & Soize, C. (2016b). Stochastic continuum modeling of random interphases from atomistic simulations. application to a polymer nanocomposite. *Computer Methods in Applied Mechanics and Engineering*, *303*, 430–449. doi :10.1016/j.cma.2015.10.006.

Liu, E., Cashman, K., & Rust, A. (2015). Optimising shape analysis to quantify volcanic ash morphology. *GeoResJ*, *8*, 14–30. doi :10.1016/j.grj.2015.09.001.

MATLAB (2004). *version 7.0.1 (R14SP1)*. Natick, Massachusetts : The MathWorks Inc.

Mennel, R., & Reece, A. (1963). The theory of the centrifugal distributor iii : Particle trajectories. *Journal of Agricultural Engineering Research*, *8(1)*, 78–84.

Olieslagers, R., Ramon, H., & DeBaerdemaeker, J. (1996). Calculation of fertilizer distribution patterns from a spinning disc spreader by means of a simulation model. *Journal of Agricultural Engineering Research*, *63*, 137–152. doi :10.1006/jaer.1996.0016.

Piron, E., Miclet, D., & Villette, S. (2010). Cemib : an innovative bench for spreader eco-design. *Int. Conf. on Agr. Eng., Clermont-Ferrand, France*, .

Villette, S., Cointault, F., Piron, E., & Chopinet, B. (2005). Centrifugal spreading : an analytical model for the motion of fertiliser particles on a spinning disc. *Biosystems Engineering*, *92*, 157–164. doi :10.1016/j.biosystemseng.2005.06.013.

A virtual spreader to overcome experimental limits: Example of use to deepen the meaning of the transverse coefficient of variation

Sylvain Villette [a,*], Emmanuel Piron [b], Denis Miclet [b]

[a] Agroécologie, AgroSup Dijon, INRA, Univ. Bourgogne Franche-Comté, 26, bd Docteur Petitjean, F-21000 Dijon, France

[a] Irstea, TSCF, Centre de Clermont-Ferrand – Montoldre, 40 Route de Chazeuil, 03150 MONTOLDRE France

* Corresponding author. Email: sylvain.villette@agrosupdijon.fr

Abstract

A virtual spreader was modelled by combining the use of theoretical motion equations and statistical distributions of input parameters. These parameters were deduced from experimental measurements using a custom-made spreader, an imaging system, a particle impact recording device and a rotating test bench. Using this model, each spread pattern was computed using a random selection of values following the statistical distribution of each input parameter. Using simulations, we quantified how the CV value was affected by application rates and measurement protocols whatever spreader settings. Simulations showed the CV value and its measurement variability increased when the application rate decreased. The CV value also increased when the collection tray surface (used for spreader tests) decreased. The model was also used to analyse the CV value of blended fertilisers.

Keywords: Fertiliser spreading, modelling, transverse test, fertiliser ballistic properties.

1. Introduction

Centrifugal spreading is a widely used method to apply fertiliser in fields. During last decades, considerable efforts and regular innovations improved the accuracy of spreaders and the quality of fertiliser applications. Nevertheless, numerous machine design improvements are still technical challenges owing to materials being spread (*e.g.* blended fertilisers), field conditions (*e.g.* wind, uneven field relief, guidance error), and availability or performance of spreading measurement devices (*e.g.* collection tray method according to various standards). Thus, the need for difficult, costly or unrealistic experiments hinders the ability to develop new technical solutions especially when problems of interactions between parameters occur or when high numbers of test replications are required. Moreover, since the transverse coefficient of variation (CV) is used to assess the quality of the spreading, a deep understanding of the CV value is required to avoid erroneous interpretation. This understanding is also of great interest when the CV value is considered from an agronomical point of view to reflect the fertiliser spatial variability in fields (i.e. for use in agronomical model).

Using traditional experiments, it is particularly difficult to study how the test protocol, the application rate or the fertiliser ballistic properties affect the CV value. To overcome the limits of practical experiments and explore the meaning of the CV value, we chose to carry out virtual experiments based on numerical simulations.

Numerous works already described and modelled the motion of fertiliser on the spinning disc considering individual fertiliser particles (Villette et al, 2008) or taking into account particle interaction (Van Liedekerke, 2009). Some works also addressed the particle ballistic motion (Grift et al). Nevertheless, at the present time, no model is sufficiently advanced to compute the fertiliser spread pattern deposition by considering only theoretical relationships to describe the fertiliser motion from the hopper to the ground. Moreover, there is no model in the literature to reflect the variability observed from run to run in practical spreader tests.

The aim of this study is to model a virtual spreader by combining the use of theoretical motion equations and statistical distributions of input parameters. The paper presents how these parameters are deduced from experimental measurements and how the model is calibrated using the measurement of an actual spread pattern deposition. It also presents how spread pattern are computed using a random selection of parameter values following statistical distributions. Examples of results are then provided to illustrate the output information that can be derived from the approach concerning the meaning of CV values.

2. Materials and Methods

The virtual spreader combined the use of theoretical relationships to describe the motion of the fertiliser particles (when they leave the spinning disc and during their ballistic flight) and the use of experimental data to provide a realistic calibration of the model.

2.1. Model parameters and experimental devices

The virtual spreader approach required the use of the statistical distributions of four input parameters.

The first statistical distribution described the particle size distribution. This was deduced from a sieving test according to the European standard EN 1235/A1 (2003).

The second statistical distribution described the horizontal outlet angle of the fertiliser particles when they leave the vane. This information was measured using an imaging system developed to capture the motion of the particles in the vicinity of the disc. The acquisition technique consisted in setting the exposure time of the camera long relative to the velocity of the fertiliser granule, so that the particle trajectories appeared as streaks across the image. A specific image processing allowed the outlet angle to be deduced. The distribution was then fitted with a Gaussian curve.

Concerning the vertical outlet angle, its mean value was derived from the horizontal outlet angle using a theoretical relationship. To complete the information concerning this parameter, the dispersion around the mean value was deduced from fertiliser impacts recorded on a vertical screen placed in the vicinity of the spinning disc (Villette et al 2013). Then, the statistical distribution of the vertical outlet angle was deduced and fitted with a Gaussian curve.

The last statistical distribution described the angular mass flow around the spinning disc (i.e. the fertiliser mass fraction leaving the vane at its extremity with respect to the angular location of the vane). These data were deduced from the knowledge of the spread pattern deposition combined with the knowledge of the horizontal outlet angle. The spread pattern deposition was measured using the rotation test bench of IRSTEA called CEMIB (Piron and Miclet, 2005).

In this study, the experimental measurements were carried out with a custom-made spreader. It consisted of a single concave disc equipped with two radial vanes. The vane radius was 0.395 m and the vertical angle of the vanes was 13.5°. The fertiliser was ammonium nitrate and the particles were assumed to be spheres.

2.2. Virtual spreader modelling

The model considered a twin disc spreader and assumed that each disc was fed by the same constant mass flow. We assumed that the setting of the spreader was obtained by changing the angular location of the feeding point on each disc, involving the rotation of each spread pattern around the corresponding disc axle.

The static spread pattern deposition was computed using a Monte Carlo process so that the motion of each fertiliser particle was computed with input values randomly drawn from statistical distributions.

A set of particles is first generated by random selection following the diameter distribution derived from the fertiliser particle size distribution. The number of particles is so that the sum of all particle masses was the total mass defined for the spread pattern deposition.

The angular location of the vane at the ejection time (i.e. when the particle leaves the vane) was then randomly selected following the angular mass flow distribution. Thus, the location of each particle at the beginning of the ballistic flight was computed.

The value of the horizontal outlet angle and the value of the vertical outlet angle were randomly selected for each particle considering the normal distributions pre-established for these parameters. Then, combining these values with the angular location of the vane, the three-dimensional components of the outlet velocity vector were computed.

After having generated all these parameter values for all particles, the landing point of each particle was computed by solving the ballistic flight equations.

In practice, the spread patterns were computed independently for each disc. Consequently various spreader setting could be simulated by rotating the right and left spread patterns before analysing the final resulting spread pattern deposition.

At the end of the simulation process, the landing point of each particle was perfectly known in a Cartesian coordinate system. Since each particle was also known in terms of diameter and mass, various analyses of the fertiliser spatial distribution could be performed.

When the model was used to study the transverse distribution, the total mass of fertiliser used in the simulation was computed as the product of the target application rate and the collection surface on the whole working width (product of the working width and the length of the collection tray).

3. Results and Discussion

3.1. Comparison between simulated and actual spread patterns

The comparison between simulated and measured spread patterns was carried out for a single disc. The aim of the comparison was to ensure that the constant values and the statistical distributions used for the inputs parameters allowed the simulation of realistic spread pattern depositions. Figure 1 shows that the simulated spread pattern is in good accordance with the measured spread pattern. Figure 1.a presents the simulated spread pattern computed on a Cartesian grid (0.25x0.25 m) by summing the particle masses in each cell. Figure 1.b presents the experimental spread pattern derived from polar data measured with the rotating test bench CEMIB. In order to improve the visual comparison, figure 1.b represents the spread pattern when some sampling and interpolating transformations were applied on simulated data to reflect the CEMIB polar data processing.

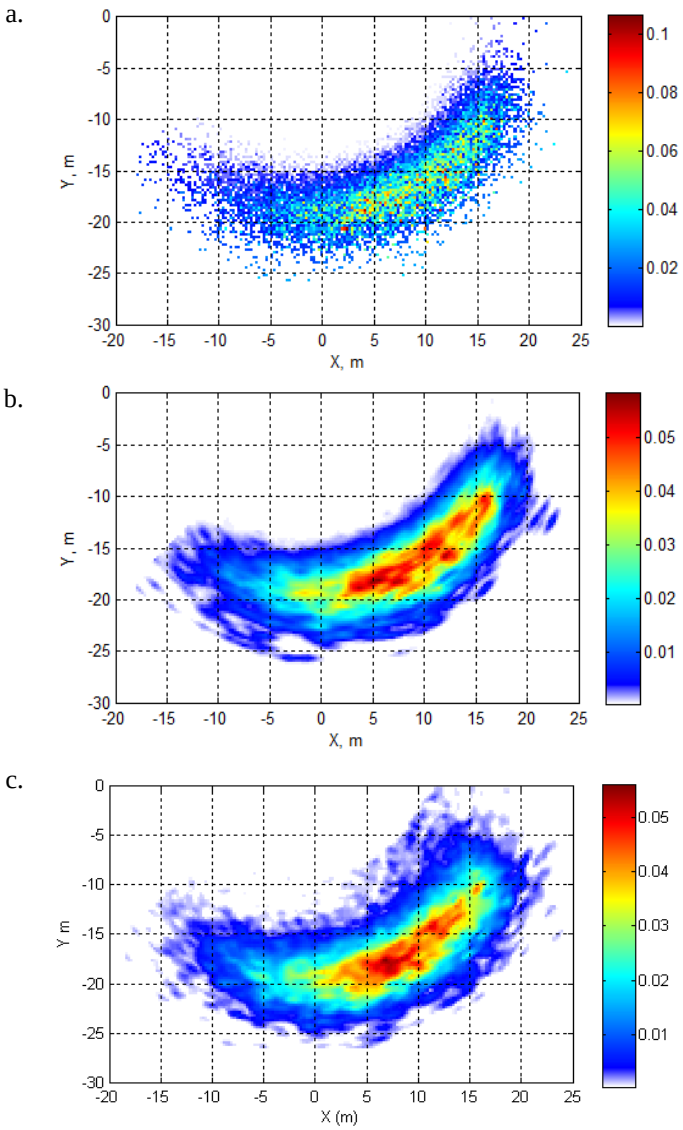

Figure 1: Comparison of the simulated spread pattern (a: raw Cartesian representation, b: after polar and cartesian transformation to reflect the experimental data processing) with the measured spread pattern (c).

3.2. Use of the virtual spreader to study how the Coefficient of Variation is affected by application rate and measurement method

For a specified setting and a specified working width, the virtual spreader was used to compute simulated transverse distributions for various application rates. Figure 2 illustrates the transverse distributions obtained at 100 kg/ha and 500 kg/ha. For these particular examples, the CV values were respectively 13.7 % and 5.7%.

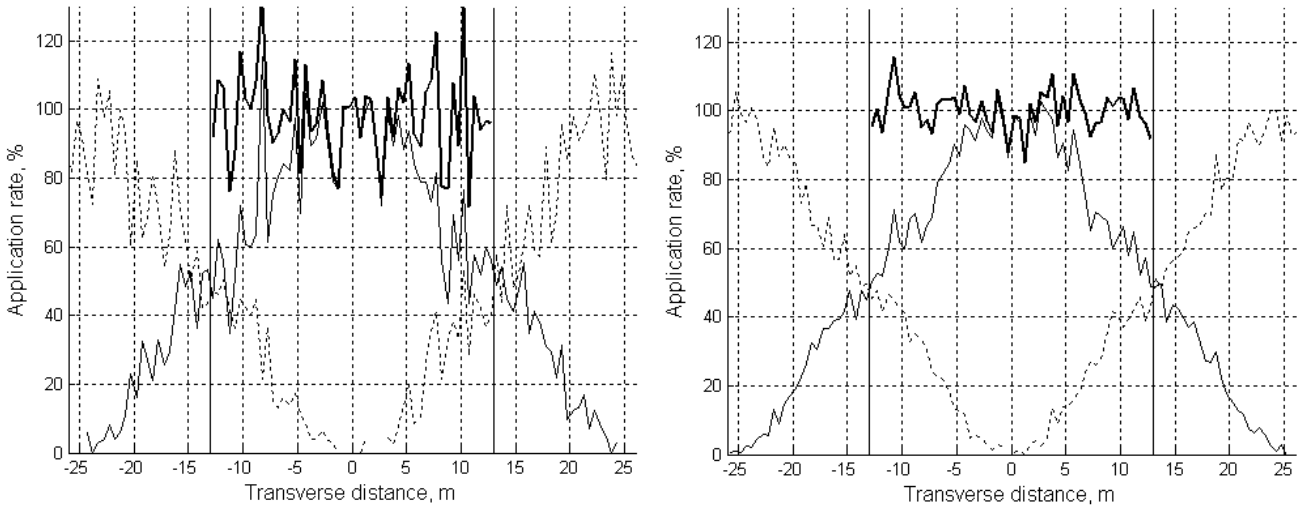

Figure 2: Transverse distributions computed with the virtual spreader for the same setting, the same working width and two different application rates: 100 kg/ha (left) and 500 kg/ha (right). The application rate is expressed as a percentage of the target rate. Transverse distributions after overlapping: bold line; central pass: continuous line, adjacent passes: dashed line.

Considering the same setting and the same working width, a high number of transverse distributions have been computed for various application rates and for four surfaces of collection trays. The corresponding CV values are presented in Figure 3. This figure demonstrates that the CV value increases when the application rate decreases. It also shows that the CV value increases when the collection tray size decreases.

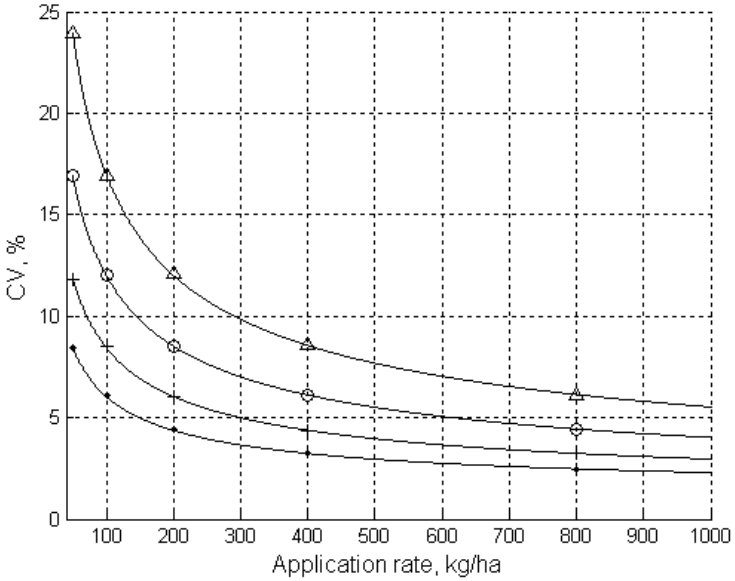

Figure 3: Mean value of the CV with respect to the application rate, when it is measured with various collecting surfaces (• 1 m^2, + 0.5 m^2, ○ 0.25 m^2, △ 0.125 m^2).

Simulations make also possible the study of the impact of the measurement method on the CV value. For example, figure 4 presents results obtained for the same setting and the same working width when the CV is measured following the standard method (EN 13739-2, 2011) and when it is measured with the same collection trays in field. Figure 4 shows that the values of the in-field CV are significantly higher than the CV values deduced from the standard method although no additional disturbance (vibration, wind, guidance error, landform…) are taken into account in simulations.

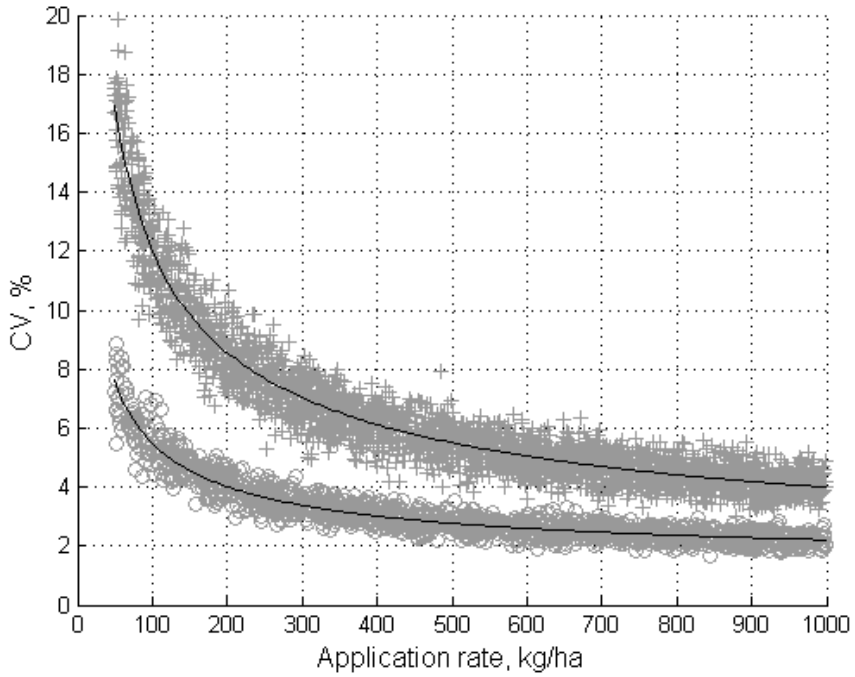

Figure 4: CV values obtained for the same setting and the same working width when the CV is measured in field (+) or following the standard method (o) described in EN 13739-2 (2011).

3.3. Use of the virtual spreader to study how the Coefficient of Variation is affected by fertiliser properties

The virtual spreader can also be used to study how fertiliser properties affect the CV value. For example, figure 5 presents the CV maps of the virtual spreader with respect to the setting and the working width for blended fertilisers and its two components when they are considered independently. In the simulation, the two fertilisers only differ in their drag coefficient *Cd* (0.47 and 0.6). Thus, in this simulation, the difference in fertiliser behaviour only concerns the ballistic flight. Other parameters of the simulation (horizontal angle, etc) were considered identical (same hypothesis than Piron, AFCOME, 2015). Figure 5 shows that selecting the best CV value considering the blended fertilisers do not ensure to obtain good CV value for each fertiliser components. For example, when the working width is 24 m the best CV value is 1.2% for the blended fertilisers and is 3.4% and 2.6% for its two components. When the working width is 38.5 m the best CV value is 5.7% for the blended fertilisers while the CV value reaches 13.6% and 14% for its two components. This shows that increasing the working width, the quality of the spreading can be much more deteriorated than what could be expected regarding the CV value computed for blended fertilisers. Same conclusions than Piron, AFCOME, 2015 can be noticed: one of both fertilisers is under-applicated at the rear of the spreader while the other one is over-applicated in this area.

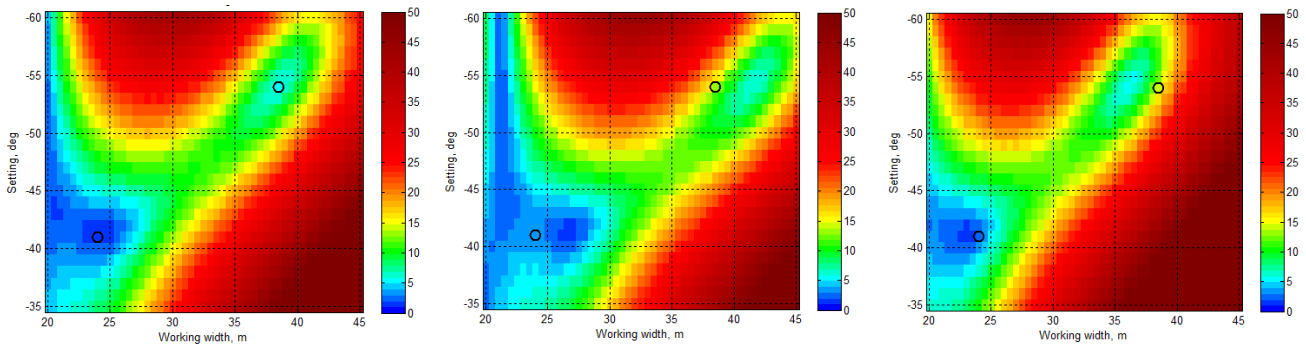

Figure 5: Maps of the CV values with respect to setting and working width for blended fertilisers (left), for the first fertiliser component for which the drag coefficient was 0.47 (middle) and for the second component for which the drag coefficient was 0.60 (right).

4. Conclusions

The quality of fertiliser spreading is traditionally assessed by the transverse coefficient of variation (CV). This CV reflects the spreader performance but remains difficult to interpret in the context of agronomic models. The study of the spatial distribution of the fertilizer is available thanks to a centrifugal distribution model which takes into account statistical distributions of the input parameters in a Monte Carlo simulation. It allows to overcome limits of practical experiments and to explore the meaning of the CV value.

Simulations show the influence of the application rate and the measurement protocol on the CV value. They also allow the analysis of the ballistic segregation on the transverse distribution and the calculation of the probability of obtaining a dose on a surface defined at the scale of the plant. Simulations reproduced the well-known random variability observed in actual spreader tests. Moreover, they provide the statistical characterization of the output variables. More specifically, the work of the virtual spreader is a useful tool.

References

EN 13739-2, 2011. Agricultural machinery - Solid fertilizer broadcasters and full width distributors - Environmental protection - Part 2: Test methods. European Committee for Standardisation.

EN 1235/A1, 2003. Solid fertilizers – Test sieving. European Committee for Standardisation.

Piron, E, Miclet D, 2005. Centrifugal fertiliser spreaders: a new method for their evaluation and testing. The International Fertiliser Society, Proceedings 556.

Villette S, Piron E, Cointaut F, Chopinet B, 2008. Centrifugal spreading of fertiliser: Deducing three-dimensional velocities from horizontal outlet angles using computer vision. Biosystems Engineering. 99, 496-507.

Villette S, Piron E, Martin R, Miclet D, Jones G, Paoli JN, Gée C, 2013. Estimation of two-dimensional fertiliser mass flow distributions by recording granule impacts, Biosystems Engineering, 115, 463-473.

Van Liedekerke P, Tijskens E, Dintwa E, Rioual F, Vangeyte J, Ramon H, 2009. DEM simulations of the particle flow on a centrifugal fertilizer spreader. Powder Technology 190 (2009) 348–360.

Grift T. E., Hofstee J. W., 2002. Testing an online spread pattern determination sensor on a broadcast fertilizer spreader. Transactions of the ASAE, Vol. 45(3): 561–567, 2002.

Piron E, 2015. Evaluation des performances des épandages des engrais de mélange. 14ème rencontres internationales de l'AFCOME, Reims, 22 octobre 2015.

Centrifugal spreader eco-evaluation method: Sulky Econov example

E. Piron[a,*], D. Miclet[a], N. De-Freitas[a], L. Leveillé[b], T. Juhel[b], Y. Guyomarch[c]

[a] Irstea, Centre de Clermont-Ferrand – Montoldre, 40 Route de Chazeuil, 03150 MONTOLDRE France

[b] Sulky, Les portes de Bretagne, P.A. de la Gaultière, 35220 CHATEAUBOURG France

[c] KEREVAL, 4 rue Hélène Boucher, 35235 Thorigné Fouillard, France

* Corresponding author. Email: emmanuel.piron@irstea.fr

Abstract

The study shows how it is possible to evaluate spreader performances when it is really used in the field. The study deals with the new Econov section control evaluation. It shows first the followed methodology and its three steps, from continuous data acquisition of spreader parameter states to spread pattern characterization, and finally distributed rates into the field. Obtained maps results are given as well for spreader parameter states as for final obtained field rates. Performed in many cases of field shape, fertilizer types, with section control or not, the study gives some quantified results about induced spreading defaults and also on benefits to use section control devices. It particularly highlights the first order importance of field shape and the regularity of spaces between tramlines importance, firstly to obtain the desired rate (global gain) and secondly to minimize fertilizer rate dispersion and maximize crops yield and quality. In a second level, fertilizer performance is also presented, mainly by the dispersion reduction it allows when transverse curves are triangular. In a more precise analyze, benefits to use section control is also evaluated regarding the position in the field (main field application vs boarder application).

Keywords: Section control, Isobus, Evaluation, Simulation

1. Introduction

Fertilizer spreading stays in agriculture a key-point for plants growing development. Regarding the work rate which is required nowadays to perform it, the most powerful device is the centrifugal spreader. The major proportion of them are double–disc spreaders with maximum working width always growing, reaching more than 50m nowadays and keeping a very satisfactory Variation coefficient (VC) under 5% when most performant fertilizers are used. In these cases, total spread pattern covered area is more than $^1/_3$ ha. As it is a centrifugal projection, the spread pattern is semi-circular and irregularly distributed regarding fertilizer density. When machines are used on regular and known spaced paths, they allow very good homogeneity distributions thanks to correct overlapping, especially when transverse curves present triangular tendencies. For a long time, methods have been established, standardized, and corresponding benches developed to evaluate spreader performances. The given evaluation is correct as long as paths are regularly spaced, in both main field and longitudinal border spreading scopes. VC and transition coefficient (TC) are then good criteria. However, Fields are neither regular nor proportional to the set working width but present specific shapes. Final spreading uniformity in the field is also a compromise using successive spread pattern placement along followed trajectories. In the five recent years, specific adjustment devices have been developed on spreaders in order to optimize this best possible compromise. Named section control devices, they allow optimizing local overlapping everywhere in the field. Depending the spreader manufacturer, these devices control, in a dynamic way, fertilizer flow as well as optimal working width settings.

In this new context, spreading evaluation standard isn't suitable. Even if it has already been used (Le Gal – 2013 / 2014 and AB - 2015), field experiments are neither adapted because of complexity, heaviness of the method, and provide not representative results (too much cases to evaluate, etc.).

Figure 1: Picture from Profi test 2015 using in-field measurements in order to evaluate Sulky Econov device.

Before this study, there were some initiatives (Fig. 1 shows the complexity of such test in real field conditions) regarding spreader section control evaluation. Unfortunately, none of them has been enough representative regarding field sizes and different conditions that could occur during spreading.

However, it seems important to give objective evaluations about these new devices to farmers and methods have also to be adapted in order to evaluate spreader global performances when it's used in real field conditions.

The purpose of this article is to present a real case study where a significant number of parameter have been explored. It has been carried out at Irstea's place: Sulky Econov section control evaluation. After a presentation of the method (data acquisition process in the field, spread pattern acquisition, method to evaluate real local amounts everywhere in the field), results are presented as well in terms of dynamic spreader actuator states as for local induced rates in the field. Section control benefits are presented for different field cases and fertilizer formulations.

2. Materials and Methods

Section control devices now equipped many spreaders and their goal is to locally minimize fertilizer under and over-applications. It can be view as an automatic control unit which optimize everywhere in a field the spreader distribution parameters. The spreader must be equipped with a georeferenced module (GPS for example) and must be electronically driven (continuous flow and working width adjustments). For Sulky Econov spreader (cf. Fig. 2), flow rate can be controlled using gate adjustments (one for each disc, coupled with a real mass flow control) and working width is set using the fertilizer drop zone variation on the disc, inducing an angular adjustment of the spread pattern position regarding the driving direction.

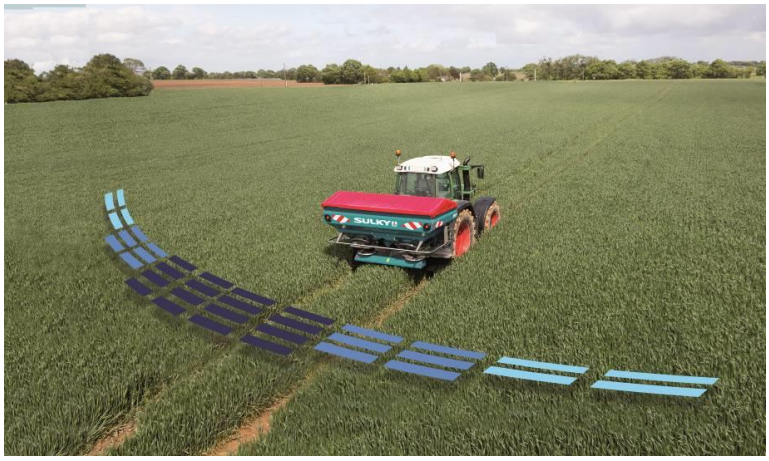

Figure 2: Sulky Econov spreader, electronically driven and section controlled.

Eco-evaluation is used in this article with a restrictive scope and means spreader performances evaluation when used in real environment (neither real elevation variations of the ground level nor wind effect are taken into account in this study, but it should be possible to do it). As it performs a post-evaluation of the spreading performance, the method requires many inputs to calculate the final fertilizer field distribution. The method consists in calculating, everywhere in the field, local fertilizer amounts brought by all successive overlapping during spreading. The computing program also requires time-referenced knowledge regarding spreader distribution parameter states, and 3D spread pattern distribution induced. Fig. 3 explains successive steps which were followed for the experimentation.

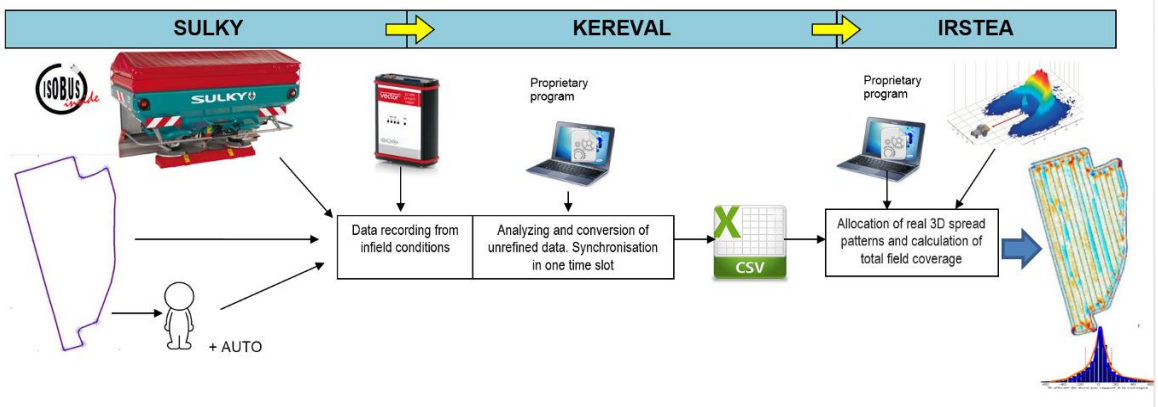

Figure 3: General overview of followed steps during Econov performance evaluation.

2.1. Spreader distribution parameter states acquisition

Acquisition must be coupled from three different origins (Fig. 4):

- informations coming from ISOBUS bus for the data transfer between the task controller and the spreader (information about section control)
- informations coming from proprietary CAN bus for "in live" data of all spreader sensors and actuators. For example, information of the real target rate, working width adjustment, etc.
- informations from GPS to localize precisely the spreader. As GPS frames were proprietary messages, frames which display the value on the UT were intercepted and registered.

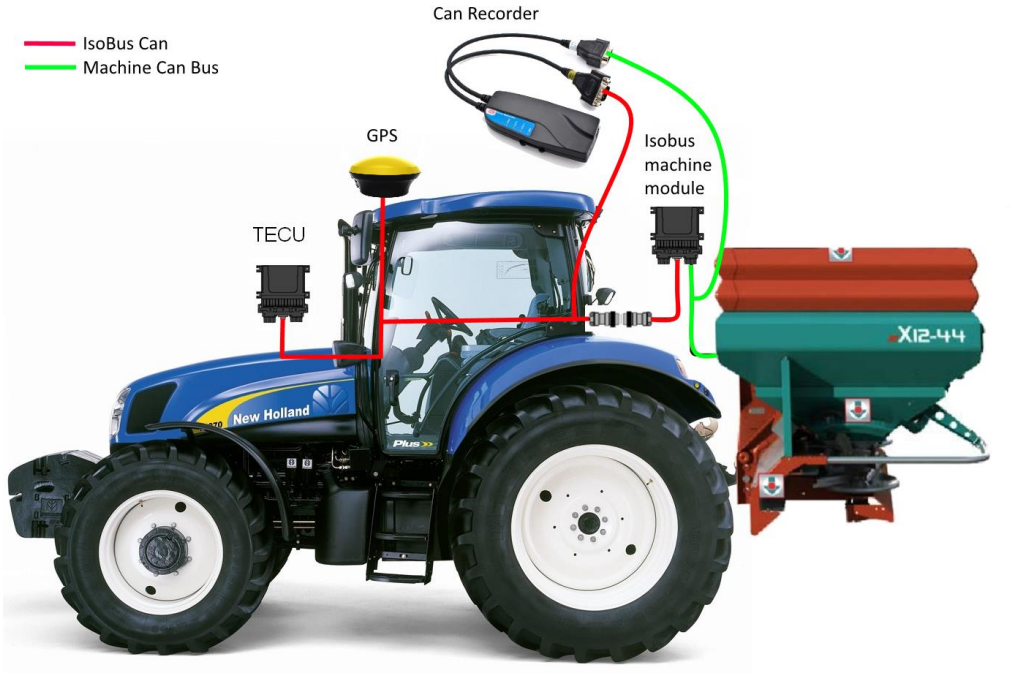

Figure 4: Global picture of information origins during data acquisition.

A Matlab® program has been developed to compute all valuable datas registered from all frames (more than 1.5 million frames per bus saved). This Matlab program also allows obtaining the same timeslot for each data type.
One of the difficulties is the multiplexor. Per example for the working width adjustment, right frame with the right command has to be detected, with the right element number and the right DDI (Data Dictionary Identifier). Fig. 5 shows an example of the obtained file after this step.

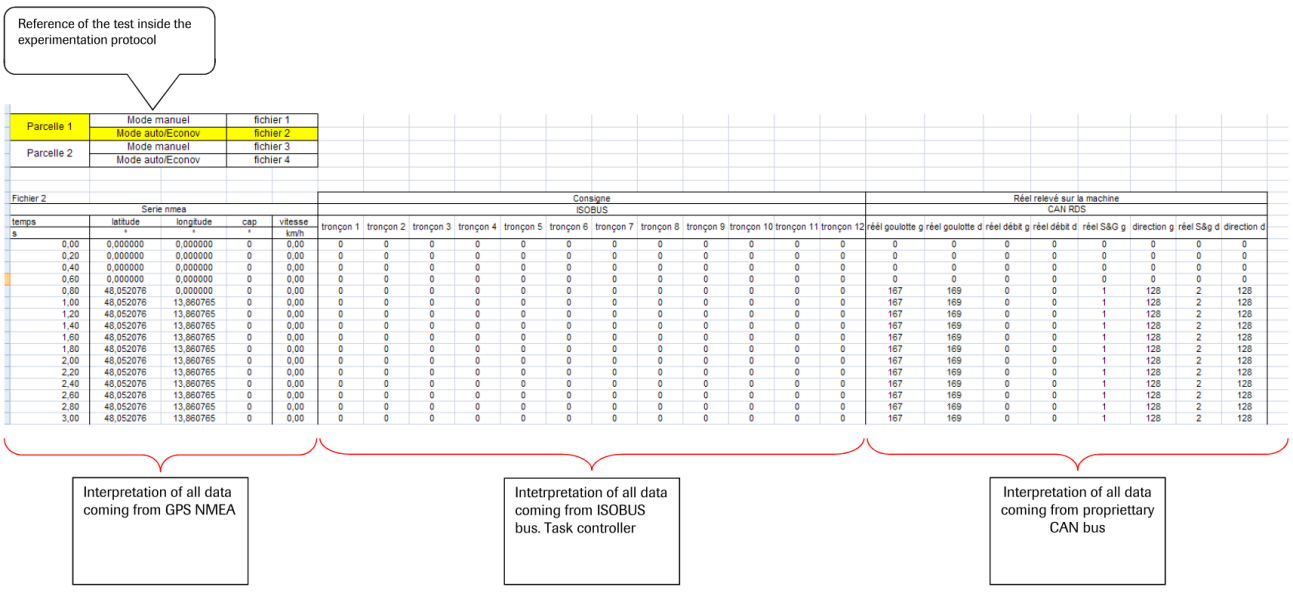

Figure 5: Example of obtained file after first Matlab processing step.

2.2. Spread pattern acquisition

Sulky distribution device uses an angular drop zone variation to set the working width. The induced consequence on the spread pattern is an angular variation of the spread pattern position regarding the driven direction. Also test bench measurements have been performed in order to register spread patterns in many adjustment cases, using as well the working width and the flow rate setting. Fit laws were then calculated in order to get the spread pattern distribution characteristics whatever the flow rate and the working width setting could be, even during stabilized phases or during transition phases between two settings. Border spread pattern were also acquired.

CEMIB test bench (Piron, Miclet, 2010) has been used in order to acquire 3D spread pattern (cf. Fig. 6).

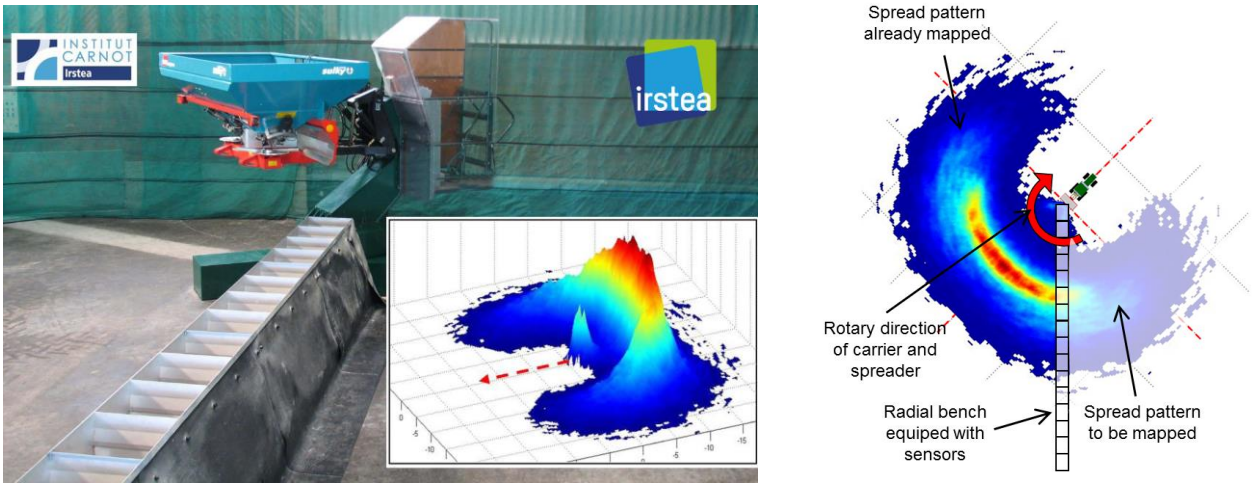

Figure 6: Left: CEMIB test bench developed by Irstea, Montoldre, France. Right: 3D CEMIB spread pattern way of measurement. Spread pattern is slowly angularly positioned above the row of sensitive trays, allowing the entire spread pattern to be measured, whatever the covered area size can be.

Using the NF EN13739-2 standard recommendations, 3D spread pattern are acquired with a high accuracy and a very small noise in the mapped fertilizer densities. A consistent and represented spread pattern is also registered in all tested configuration cases allowing a fit calculation between tested points, and field simulation edition. An example of obtained spread pattern is presented on Fig. 7.

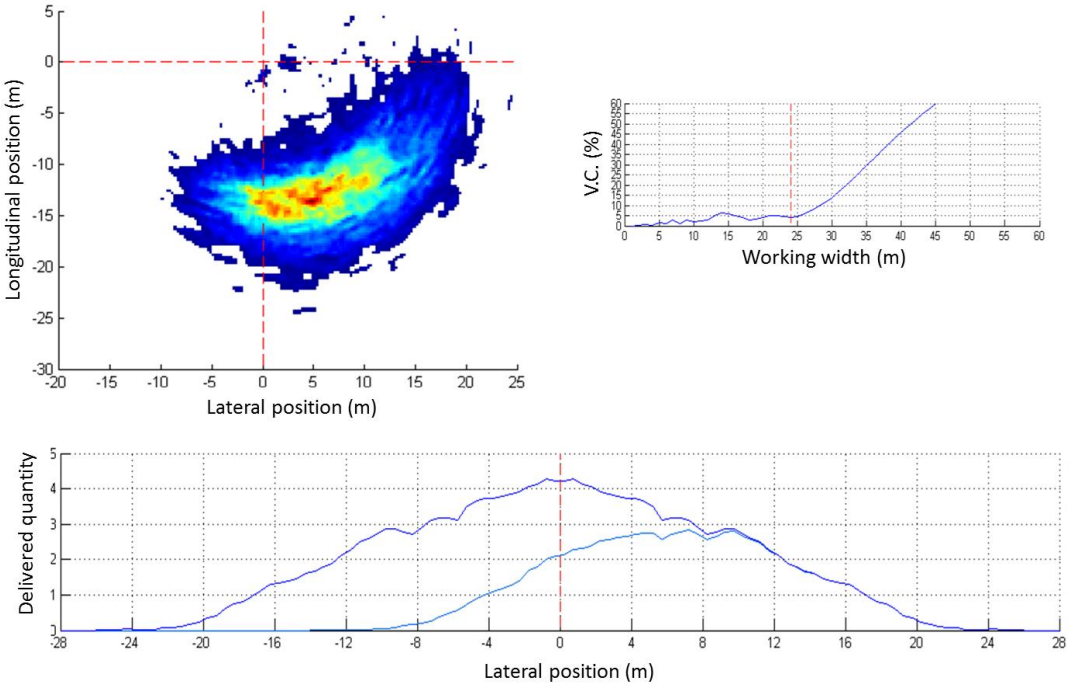

Figure 7: Top left: Example of spread pattern obtained using one disc spreader (in right position) and fertilizer configuration. Bottom: in light blue, the transverse curve calculated from the registered spread pattern, in dark blue, the global transverse curve when both disc are used. Top right: the V.C. curve.

2.3. Simulation in the field

Using all information obtained as well during spreading as with CEMIB tests, simulations are performed in order to calculate fertilizer accumulations at all field positions. The method used is a Monte Carlo simulation: particles are randomly distributed around the spreader trajectory. As the SULKY spreader generates around 14 fertilizer spreading projections each second (810 RPM) and is equipped with 2 vanes each disc, 30 spread patterns for each disc were generated by second, allowing the real phenomena to be really well represented. Particles are distributed regarding the 3D spread pattern density considered at each successive trajectory points (real flow rate, fertilizer size, densities, spread pattern distribution, driven direction, … are input parameters for the computer to calculate the number of particles to deliver and their landing position).

Fertilizer quantities are then accumulated in a given field grid measuring 1 square meter size. Filed map are also obtained, representing fertilizer densities delivered everywhere in the field. Visual evaluation can be done between different spreading configurations, but also synthetic analyses can be performed in order to mathematically estimate the distribution quality. For example, rate distribution histograms, global amounts, mean rate value and its standard deviation if pertinent, etc… are edited and calculated.

3. Results and Discussion

3.1. Tested configuration evaluations

In order to evaluate section control benefits, two main spreader control modes have been studied: manually driven spreader and Econov driven spreader. Great ligns of these modes are described in table 1.

Table 1: evaluated Configurations

Considered setting	Manual control mode	ECONOV control mode
Working width setting	Optimized one time before beginning of the spreading	Auto-adjustment along the trajectory by Econov
Flow opening (gates)	Manually driven by the spreader user	Automatically driven by the Econov calculator
Flow modulation	Automatically adapted by the computer (Flow rate adjustment to the speed / Based on an fixed working width for all the field)	Automatically adapted by the computer (Flow rate adjustment to the speed / Take the real working width everywhere in the field in the calculation)
Main field / Border spreading mode	Used	Used

Two different field types have also been used in order to estimate real benefit tendencies: (1) a big rectangular field N.1 following very regular spaced tramline during the spreading, and (2) a field N.2 with a complex form, with non-regular and non-well defined paths during spreading (cf. Fig. 8).

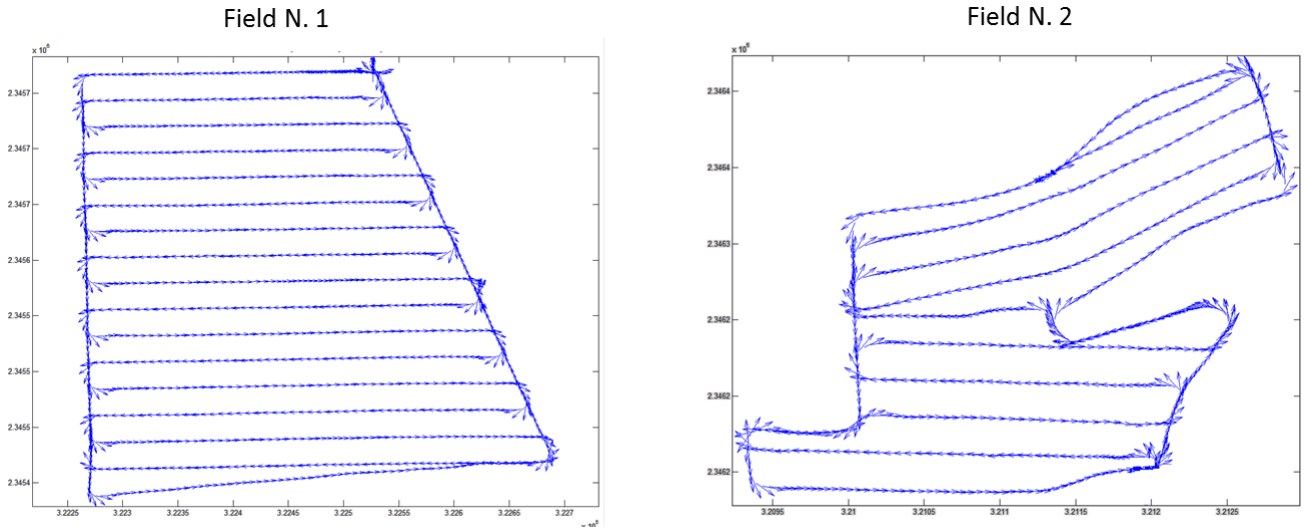

Figure 8: Trajectories followed by the spreader on both field used for evaluation. Trajectories are totally represented, whatever the spreader was spreading or not. For each field, the trajectory is exactly the same for Manual and Econov driven modes.

3.2. Example of obtained spreader parameter states using georeferenced maps

Spreader parameter states are presented in this paragraph for spreading using section control case and Field N.2.

3.2.1.Working width setting

Figure 9 shows working width settings which have been finally used in the case of field N°2. As there isn't any interest in the affected working width values when gates are closed they were not represented on these maps.

It can be seen only a few adjustments for these settings in the south part of the field, where regular tramlines do not induce setting adjustments. At the opposite, the north part presents complex field morphology which induces variable tramline distances and brings on working width setting adjustments, differently on the right and on the left.

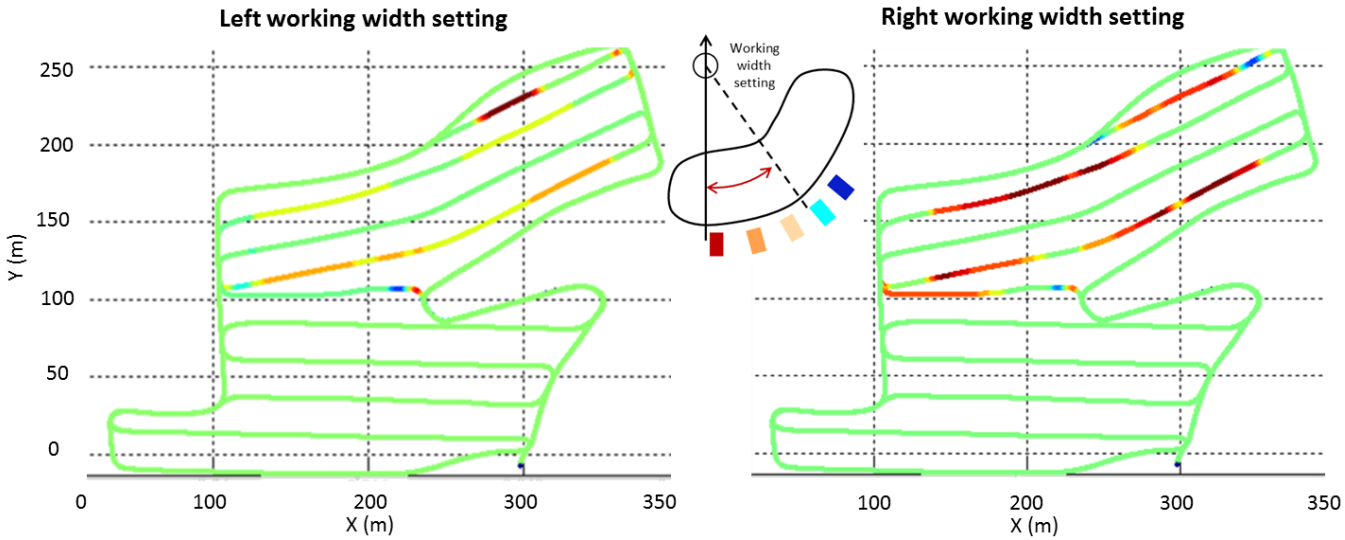

Figure 9: Working width settings on left and right discs registered when fertilizing Field N.2.

3.2.2.Flow settings

Using the same methodology, Fig. 10 shows successive left and right flow values which were automatically used spreading field N.2. As the affected values calculated by the spreader computer depend on each local real working width as well as on real speed, left and right states values have been represented using two different maps, not juxtaposed.

Due to this double factorial dependence, the simple analyze is quasi impossible.

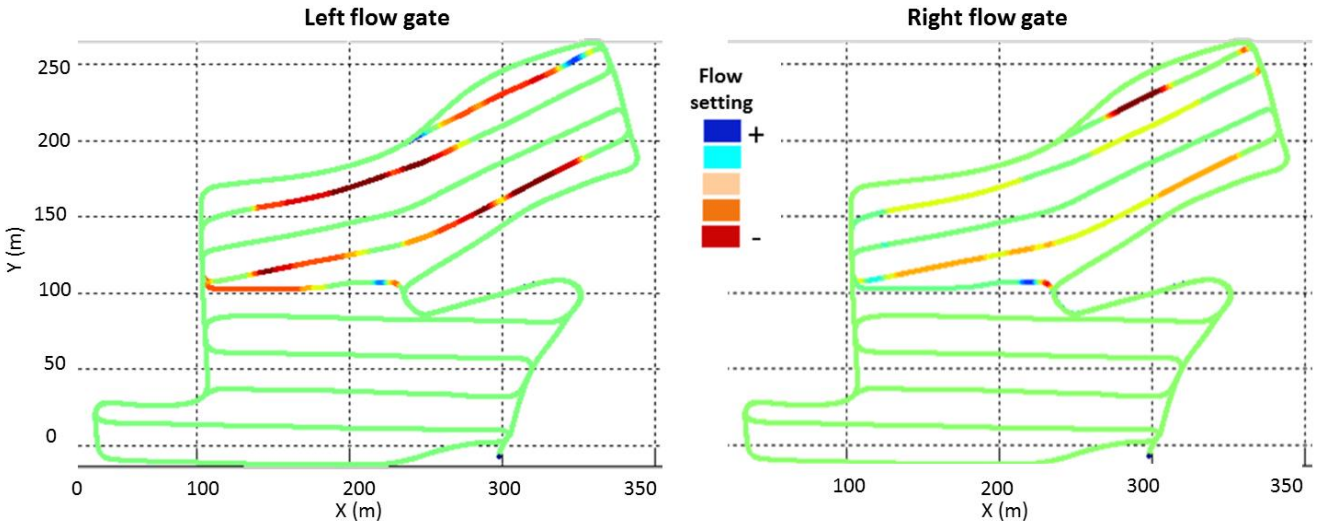

Figure 10: Flow gates states for field N.2 and both spreader sides.

3.3. Rate maps obtained

3.3.1.Field rate maps

As it has been seen in the previous maps, obtained local rates in the fields are polyfactorial. For this reason, each parameter state map analyze is very difficult. Maps which present final applied rates everywhere in the fields show directly the spreading quality and can be directly interpreted (Fig. 11).

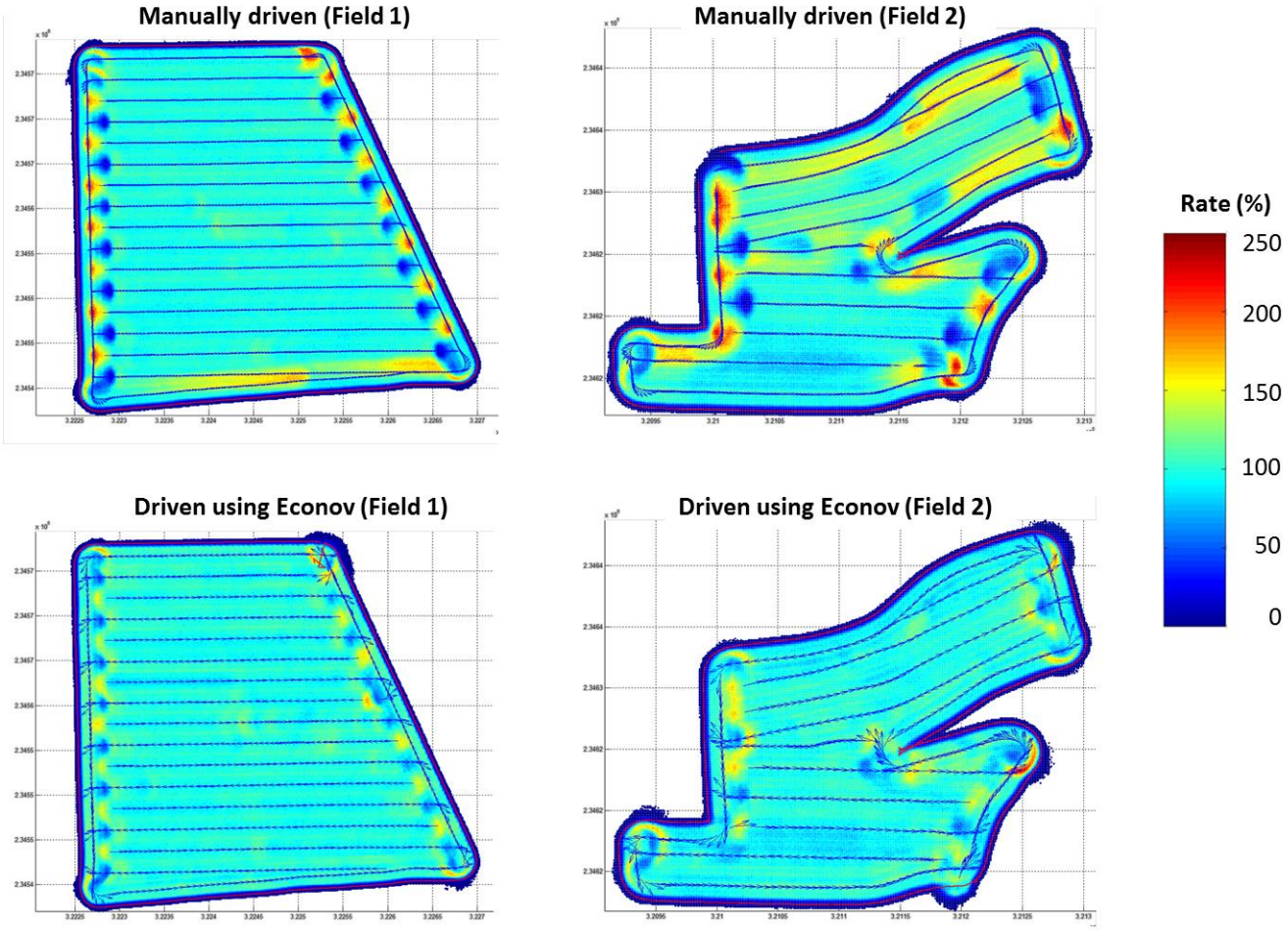

Figure 11: Final rate maps obtained in both fields, with or without Econov section control device.

Well-known local over and under-application can be seen on these maps when spreading is manually controlled: each start and end-point or each wrong spaced path mean local errors, as well traduced as under or over-applications. Using section control allows reducing a lot of these local defaults, even if reaching the absolute perfect application is quasi impossible since the game consists in combining together semi-circular with variable density shapes into complex geometric field shapes and in order to obtain an homogeneous density!

3.3.2.Rate histograms

The global analyze of the distributed rates (Fig. 12) shows the benefit of using section control devices. Whatever the considered area in the field is (all field or only the internal part), the rate homogeneity using section control is highly better when control is operated by the electronic device. Benefits are lower for very low delivered fertilizer densities since it represents mainly the border spreading (really along the field limit), which isn't affected by section control. As the travelled distance in the field using this mode is very high, it's an important part of the final histogram. Even in the internal part of the field (right part of the Fig.12), the dispersion is highly better and decreased, due to quite suppression of under and over-application as soon as tramlines are irregular. Globally in the field, over-applications are highly decreased, particularly due to removal of earlier gate opening at each spreading main field part (red spot each new tramline).

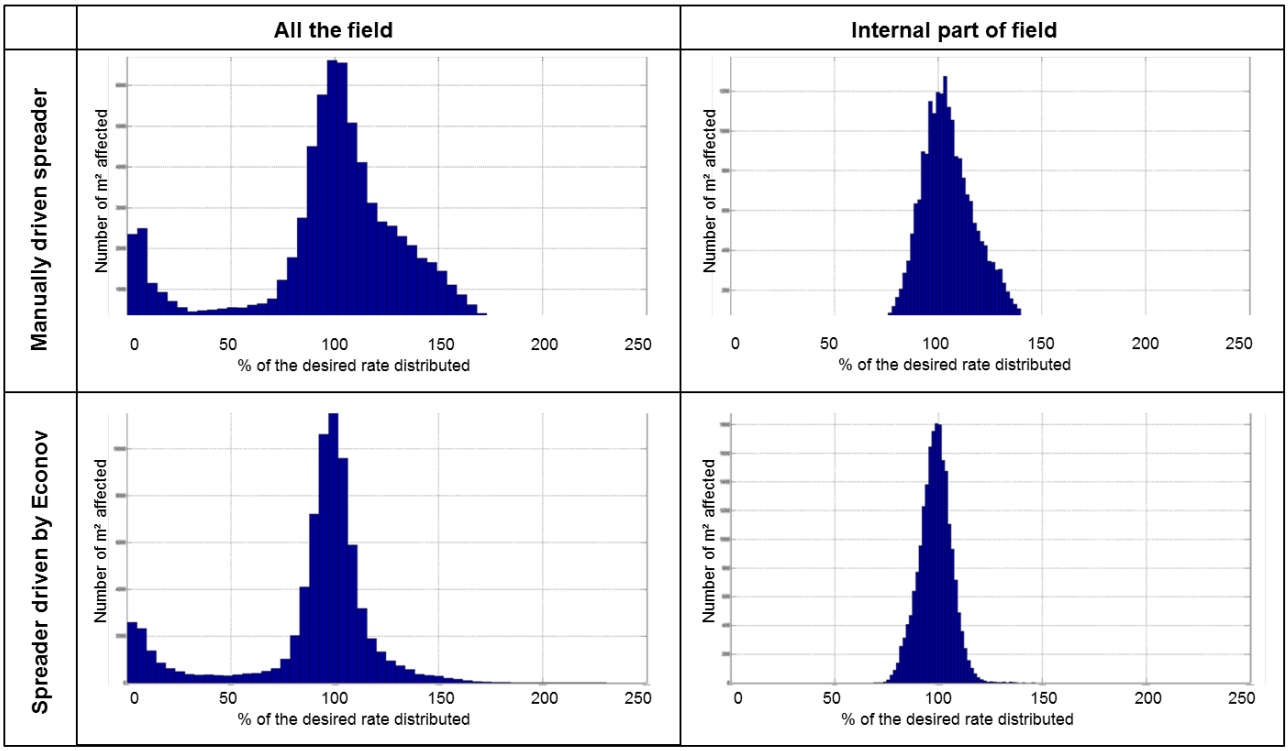

Figure 12: Rate histograms for Field number 2, when spreading is performed using a manually driven method (upper part of the picture) and using an Econov control (low part of the picture). Two evaluations were calculated, the first considering all the field (left part of the figure), the second considering only the internal part of the field (right part of the figure).

3.4. Global results

Global results must be taken with care since they are highly configuration dependent (field configuration and size, etc.). They must not be considered as general and absolute values. Nevertheless, following elements were found.

3.4.1.- Regarding the global distributed amount

Globally, using section control allows minimizing the total applied fertilizer amount. Nevertheless, gains are variable regarding many parameters:

- The field shape configuration: in the configuration of field N. 1, where the shape and the tramlines are both regular, it was noticed a global fall-off around 1% using section control while a more consequent value of 8% was observed in field N. 2, where shape and tramlines are not regular. It was especially the case in the north part of this field.
- The place in the field:
  - the internal part of the field benefits fully from section control as soon as tramlines are not regularly spaced (Field N. 2, 6% less fertilizer distributed in this part) while the interest is quite null where tramlines are regular (Field N. 1, same quantities delivered with and without section control).
  - Boarder spreading part in the field benefits fully from section control whatever the geometrical shape of the field. The explanation comes from the automatic spreader switching at the beginning and at the end of each tramline. The gain is nevertheless the most important when fields are irregular (nearly 10% less fertilizer spread in Field N. 2 in the boarder part, between 3 and 6% gain in Field N. 1).
- The nature of the spread fertilizer, i.e. the nature of the spread pattern, doesn't affect a lot the global fertilizer application gain.

3.4.2.- Regarding the rate dispersion in the field

Section control always allows benefits regarding the fertilizer rate dispersion, i.e. the local under and over-applications, whatever the analyzed parameter (field shape, size, fertilizer used, etc.). Nevertheless, as it has been shown in the case of global amounts, the fertilizer rate dispersion intensity is highly dependent from many parameters:

- From a very small effect (practically negligible) in the internal part of the field when tramlines are regular (Field N. 1) to a significant interesting two-fold decrease of the fertilizer rate distribution standard-deviation when tramlines are variable-spaced (Field N. 2).

- A systematic fall-off around 10 point on the standard-deviation in the boarder application part, with a great part which comes from the automatic spreader switching at the beginning and the end of tramlines, and another part from under or over-applications due to non-standardize distances between tramlines at the end of spreading (particularly visible on Fig. 11-Field N.1 in its south part and on Fig. 11-Field N. 2 in its north part).
- An identified effect of the spread fertilizer (i.e. shape of the transverse curve), not shown in this article but also studied. The section control gives increasing benefits when it is used with fertilizer inducing trapezoidal transverse curves at the mean working width of the field. It allows in this case the continuous adjustment of the spread pattern to place the V.C. crew at the optimum working width. Something which is less important when the transverse curve is triangular and the fertilizer over or under-application diluted on the all spreading width.

4. Conclusions

This study showed it is possible to evaluate spreader performances regarding all the technical points. It allows testing devices which should be very difficult or even impossible to test in reality. In this scope, section control has been investigated here, but it should also be possible to evaluate spreader regarding their precision agriculture performances. The followed methodology is easiest to follow than real field test and gives more representative results. It requires a couple of competencies and tools, from data registering of both spreader ISOBUS informations and spreader state parameters, to spread pattern measurements, and finally simulations. Obtained results are very consistent and allow performing precise analysis, minimizing random effects which should occur if a real field experiment was envisaged to evaluate these types of performances. It could represent, for example, the base for a global analyze about bringing gains induced by the different devices which equipped spreaders.

Section control which have been evaluated (Econov) allows to improve significantly the fertilizer distribution quality. It allows, regarding fields shape and size, a variable decrease of the global fertilizer delivered amount (between 1 and 8 or 9%). The most important information is the attached benefit it allows on the fertilizer rate dispersion minimization. In the same way, field shapes, position in the field, fertilizer used, are important factors which play a role.

Coupling the given study conclusions leads to establish the fundamental role section control devices plays nowadays for spreading. Effectively, sizes always greater of spread patterns, in a context of constant field sizes, incite these types of spreading auto-adjustments. Thus equipped, spreaders allow increasing yields and its quality, because of the loss decrease (decrease cereal sensitivity in case of over-application for example), but also because of the protein induced increase.

References

AB (2015). GPS section control, Sulky X50 Econov spreader: Sulky's slice 'n' dice. Profi Electronics. 3/2015

Le Gal, C., Knuivers, M. (2013). La coupure de tronçons GeoSpread de Vicon à l'essai. La France Agricole 3494, 5 juillet 2013.

Le Gal, C., Huiden, F. (2014). La coupure de tronçons Sulky Econov à l'essai. La France Agricole 3525, 7 février 2014.

NF EN 13739-2 (2011). Distributeurs d'engrais solides en nappe et centrifuges – Protection de l'environnement. Partie 2 : Méthodes d'essai.

Piron, E., Miclet, D., Villette, S. (2010). Cemib : an innovative bench for spreader eco-design. Int. Conf. on Agr. Eng., Clermont-Ferrand, France.

Reliability approach for fatigue design on mechanical structure in agricultural domain

F. Lefebvre*, I. Huther, P. Letort
Cetim, 52 avenue Félix Louat, 60304, Senlis, France
* Corresponding author. Email: Fabien.lefebvre@cetim.fr

Abstract

The reliability approach described in this paper is based on the "Stress-Strength Interference Analysis" where the criterion for acceptability complies with a reliability objective, i.e. a required maximum probability of failure. This study carried out for several agricultural industries aims to promote the methodology through different case studies: brush cutter, charger or plough with the tractor. This paper aims at demonstrating the necessary steps to validate a reliable probabilistic analytical design approach for fatigue in the agricultural domain.

Concerning the Stress analysis, database has been created for the tractors and his tools trough specific instrumentations. A loading mix strategy is adopted. The mission profile consists of "elementary situations of life" as field/road working, speed, etc... At the end, the Stress statistical distribution is calculated.

The work consisted of:

- studying, supplying, preparing and installing the instrumentation and the sensors necessary for carrying out the tests,
- setting up the acquisition equipment on the tractor and tools (brush cutter, loader, plough),
- defining the mission profile (% situation of life),
- making the recordings,
- processing data to obtain the distribution of in-service loads,
- analysing the data with respect to fatigue.

For the Strength distribution analysis which integrates material and manufacturing variability, sufficient fatigue test results up to failure on representative specimens and components are considered. Fatigue strength statistical distribution is developed on these experimental fatigue data on the one hand, and sensitivity analysis performed on the model and material law on the other hand.

Finally, the estimation of the "component of interest" failure rate is calculated, enabling a comparison to the defined reliability objective.

The interest of a probabilistic approach for the fatigue design in the agricultural domain has been demonstrated. This non-deterministic approach can help the traditional design approach and can also provide a better management of uncertainties and risks. This method could be used to realise acceptance files for waivers in production. It could be useful to obtain the necessary changes in the engineering know-how in order to manage industrial projects by mastering their technical risks and at the same time to develop an engineering probabilistic culture in a project team.

Keywords: Reliability approach, Fatigue.

1. Introduction

In the scope of the Stress-Strength approach for fatigue design, it is necessary to know the loadings applied to the structures or parts. The work presented in this study has been conducted for the Agricultural Machinery committee who asked to perform in first instance recordings of various measurement signals during functional tests for several assemblies [1-9], tractor + brush cutter, tractor + loader, and tractor + plough. Furthermore, the stress-strength approach was applied to the case of the plough.

2. Stress-Strength interference method

The reliability approach described in this paper is based on the "STRESS-STRENGTH" interference analysis represented graphically in Figure 1 [10-12].
The STRESS represents, for all possible service loading of the structure, the statistical distribution of the loading severity in terms of fatigue damage that is to say the loading' variability defined by μ_C and σ_C.
The strategy for the reconstitution of an operating assembly is based on the coupling of targeted measurements carried out during basic life situations that are representative of the fatigue changes and operating surveys at the clients' (basic life situations) for the system. Mission profiles are elaborated from these basic life situations.
The STRENGTH represents the statistical distribution of the fatigue strength for the fabricated products defined by μ_R and σ_R. Analysing the fatigue results from various origins (rupture fatigue tests for various products or test specimens

from a same family or for a same product tested in various configurations) will help determine a variation coefficient (CV_R) for a given material-process pair. The CV_R coefficient is a good indicator of the manufacturing quality.

So the failure probability in the probability approach may be visualised by means of the overlapping of both distributions, that is to say the variability of the loading in service and the variability of the part manufacturing (**Erreur ! Source du renvoi introuvable.**). It is therefore advisable to determine an acceptance criterion for part subject to fatigue so as to ensure the target reliability.

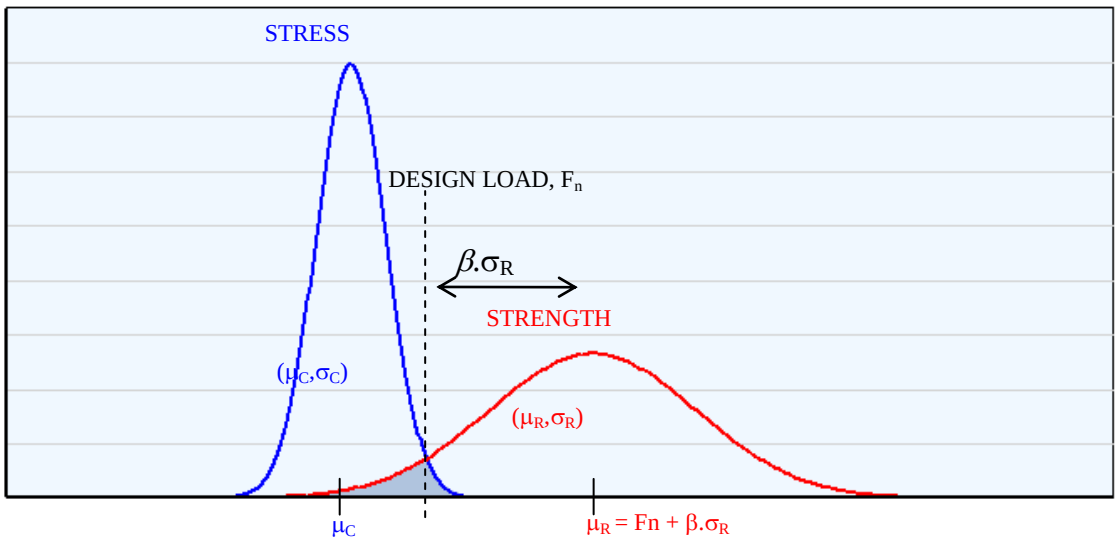

Figure 1 – STRESS-STRENGH interference method.

Given a distribution that describes the stress levels experienced in service by a structure and a distribution that describes the fatigue strength of this structure (*e.g.* material/process properties), the analyst can assess an objective reliability for this unit, *i.e.* the probability that the STRESS exceeds the STRENGTH:

$$P(x_2 \geq x_1) = \int_0^{\infty} f_{strength}(x) \cdot R_{stress}(x) dx$$

At this stage of conception, a design load "F_n" is defined as a given severity (cf. Figure 1). The objective is to define the minimum requirement on the Strength to guaranty the reliability target. The probabilistic analysis gives $\mu_{R = Fn +} \beta.\sigma_R$, with β a function of the severity of Fn, the reliability target and the confidence level. Therefore in any point of the structure, the fatigue indicator (stress, plastic strain, dissipated energy,...) should be lower than the mean value of the fatigue strength minus β x standard deviation.

As a general rule, a component in service is subject to random loadings corresponding to a succession of cycles whose magnitude and average level vary.

The notion of ***equivalent loading*** comes down to looking for the sinusoidal cycle which, repeated N_{eq}, will generate a damage equivalent to the one resulting from the in-service loading considered for a given operating period. The characteristics of this equivalent loading are as follows:

- a constant average level (for instance $F_m = 0$),
- a constant magnitude F_{eq},
- applied a cycle number N_{eq}.

The rule for damage accumulation used here is Miner's rule [13].

The whole loading applied to the structure for a given operating period is discretised then represented by means of a Rainflow matrix [14]. This matrix contains the number of repetitions of the pair (F_{ai}, F_{mi}).
As a reminder, the Rainflow counting allows the complete load-unload cycles to be counted from a time recording of loading.

The procedure to analyse the loading is as follows: from the Rainflow matrix (F_{ai}, F_{mi}, n_i) of a random loading measured or simulated, the Fatigue Equivalent F_{eq}, is defined by means of an iterative process so that the studied loading damage accumulation is equal to one.

- ***First step***

  Correction of the average as required:

$$F'_{ai} = \frac{F_{ai}}{\left[1 - \left(\left|F_{mi}\right| / K.F_{eq}\right)^c\right]}$$

  where c = 1 Goodman correction, c = 2 Gerber correction

- ***Second step***

  Calculation of the acceptable cycle number for each loading level

$$N_i = N_0 . \left(\frac{F_{eq}}{F'_{ai}}\right)^b$$

- ***Third step***

  Research by iteration of the F_{eq} value leading to a Miner sum equal to **1** [13].

$$\sum_i \frac{n_i}{N_i} = 1$$ (value different from 1 may be used depending on the experience)

where:

N_0: number of reference cycles (***in order of magnitude close to the number of events that generate most part of the damage***, which represents at best the operation of the structure and minimises the influence of the choice of the Basquin S-N curve slope),

b: exponent of the Basquin S-N curve slope,

(F_{ai}, F_{mi}, n_i): magnitude, average, number of events triplet at i level,

F'_{ai}: magnitude further correcting the average (as per Goodman or Gerber diagram),

K: ratio (mechanical strength / fatigue limit at N_0 cycles).

There is no geometrical parameter in this calculation. Only two parameters are required, the S-N curve slope coefficient (b) and the ratio K, both representative of a material behaviour.
This method allows the definition of a scalar value per load input point and loading direction, which represents the loading severity in terms of fatigue damage.

F_{eq} may be defined in magnitude at zero average or transformed in corrected magnitude by means of an average value F_{ave}, as per Goodman or Gerber correction.

3. Tractor-plough case

In order to obtain the load between the tractor and some of the tools, a specific measurement framework including three tri-axial force sensors (Figure 2) was carried out. This measurement framework is inserted between the 3-point linkage of the tractor and the tool. The measuring scope of these sensors are as follows in the coordinate system of the sensor: X sensor direction: +/-200 kN, Y sensor direction: +/-150 kN, Z sensor direction: +/-150 kN. The sensors are calibrated over their measuring scope, as well as on two other ranges, one half range (+/-100 kN, +/-75 kN) and one quarter range (+/-50 kN, +/-37.5 kN). The acceptable moment on the sensors is of the order of 1,000 m.daN along each direction.

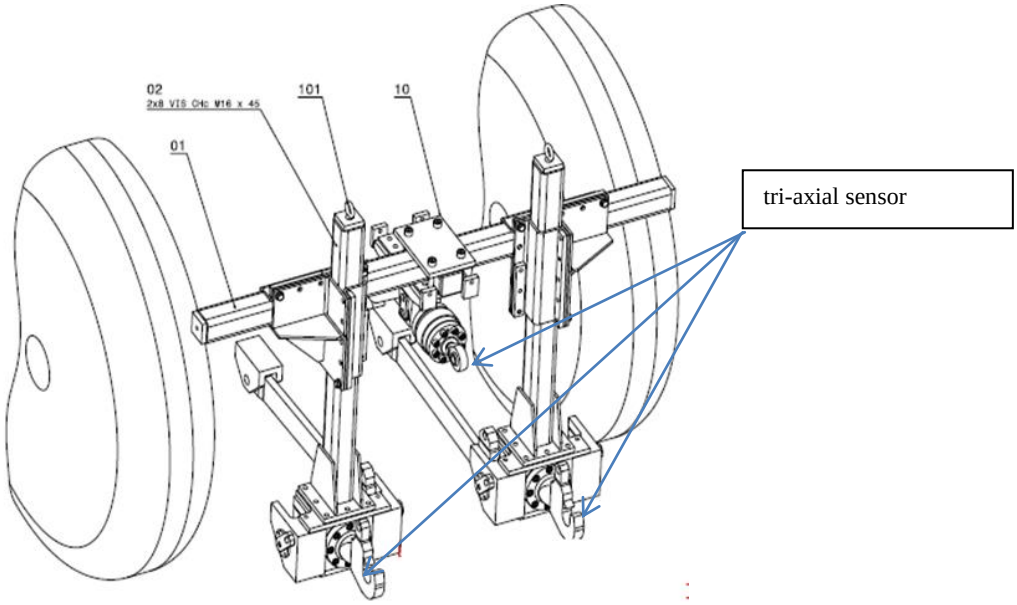

Figure 2 - Measurement framework

The tractor concerned by the study is an AGCO tractor category 3 ref. 6455 (Figure 3). The plough concerned by the tests is a 4-body plough KUHN HUARD Multi-Master 123 type MM1234T75102 No. D5269 (3-body plough + extension for the 4th body) with working wheel (Figure 3).

Figure 3 - Tractor and Plough used for the tests

A specific instrumentation is set up on the tractor, the tractor-plough link and the plough. A total of 38 measurement signals is recorded. During the test campaign, 159 different configurations are recorded. From some of these test configurations (68), 59 different elementary life situations are determined so as to establish a mission profile.

Further to the various exchanges with the industrials, a mission profile in four ranks is defined:

- type of actions (travel, ploughing, etc.),
- type of places: road, path, fields, humps (for the travel),
- type of plough body orientation (RH, LH, up),
- types of speed or depth, etc.

This mission profile allows the distribution of the equivalent loads (Fx, Fy, Fz) to be established with respect to the fatigue strength at the 3 plough linking points. These equivalent loads are determined for an equivalent cycle number of 10^6 cycles. Furthermore, the other values recorded during these tests (pressures, accelerometers, etc.) on the plough or the tractor could be used to correlate calculations with the tests.

4. Application of the "stress/strength" approach to the plough

In order to apply the complete Stress-Strength approach, it is decided to study a mechanically welded area of the plough. The purpose is to check the fatigue strength in service for this area by means of the Stress-Strength method, knowing the loading, further to the measurements performed on the plough, and knowing the Strength of the welded area.

However to ***apply the method***, it is ***necessary to compare similar values***, in this case, stresses.
So the stresses in the concerned area are obtained by means of a finite element- calculation of the plough with the equivalent loads resulting from the measurements.

The data required to implement the approach are as follows:

- CAD of the part: plough,
- Boundary conditions (B.C.),
- Distribution of the loadings in service in Loads,
- Characteristic of the welded assembly in fatigue.

Figure 4 shows the studied area on a simplified FE model of plough where the ploughshares are modelled with masses. The boundary conditions for the calculation to finite elements and the load application points are also presented.

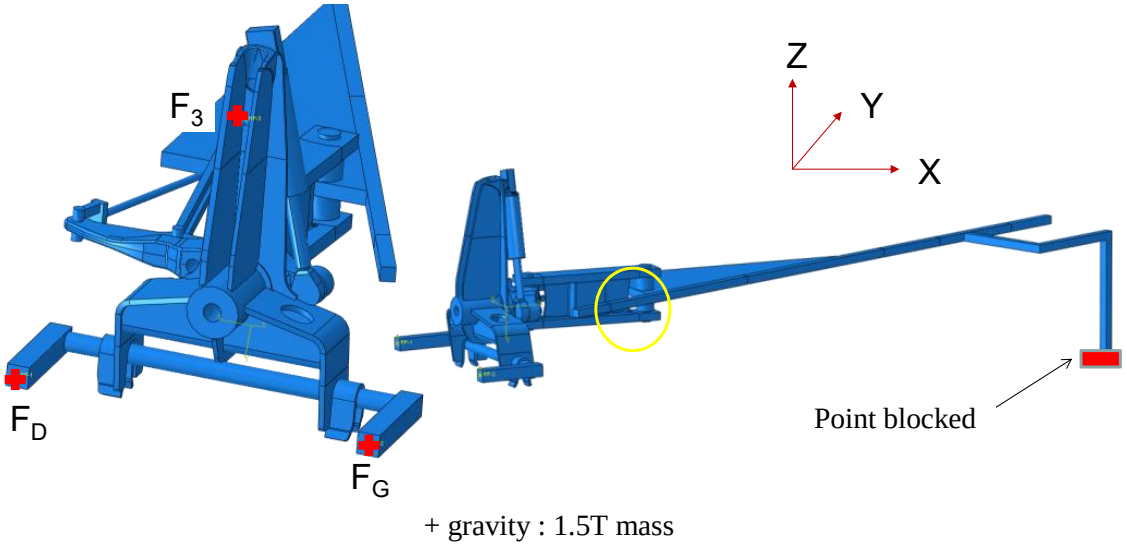

Figure 4 - Boundary conditions, load application points on the plough and studied area on the plough

Two cases are studied (refer to Figure 5): one corresponding to the ploughing position (0° position) and the other one to the transport position (20° position).

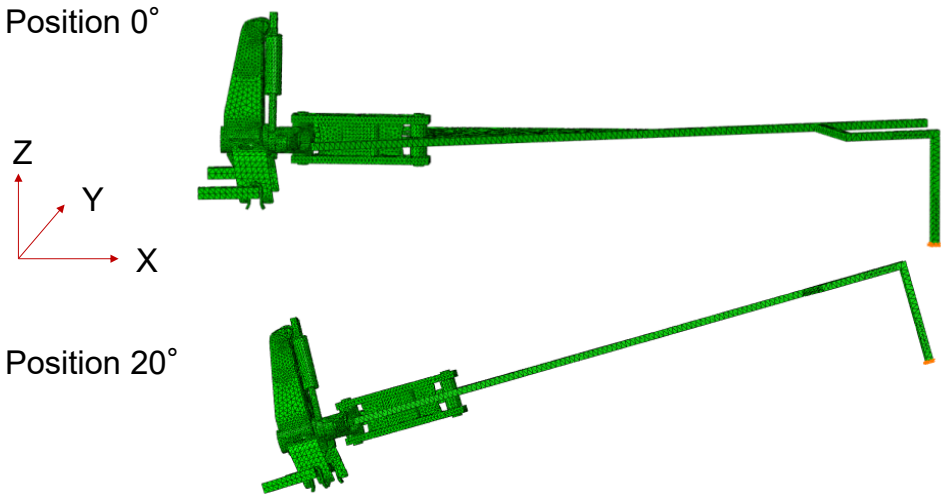

Figure 5 - Studied cases, corresponding position of the plough

The load distributions considered for the calculations are the ones that result from the measurements, these are the distributions of the load magnitudes equivalent to N = 10^6 cycles in the case of a welded assembly (Basquin slope, b = 3). The average load magnitude values considered, for the example, are as follows:

- 1st case: plough at 0° (working position)
  - FXG = FXD = + 17 kN and FX3 = 0 kN
  - FZD = 18 kN, FZG = FZD / 2 = 9 kN and FZ3 = 0 kN
- 2nd case: plough at 20° (transport position)
  - FXG = FXD = -17 kN and FX3 = 21 kN
  - FZG = -14 kN, FZD = -18 kN and FZ3 = + 17 kN

Nota: The values are fictitious; they are only used to develop the example.

Figure 6 shows the finite element meshing of the plough and the studied area. It should be noted that the weld bead is represented and the weld toe is modelled with 1 mm radius so as to apply the "notch stress" method (one of the existing methods to dimension the welded assemblies). The stresses are determined at the weld toe (Figure 7) for each load case and load direction (X and Z) independently.

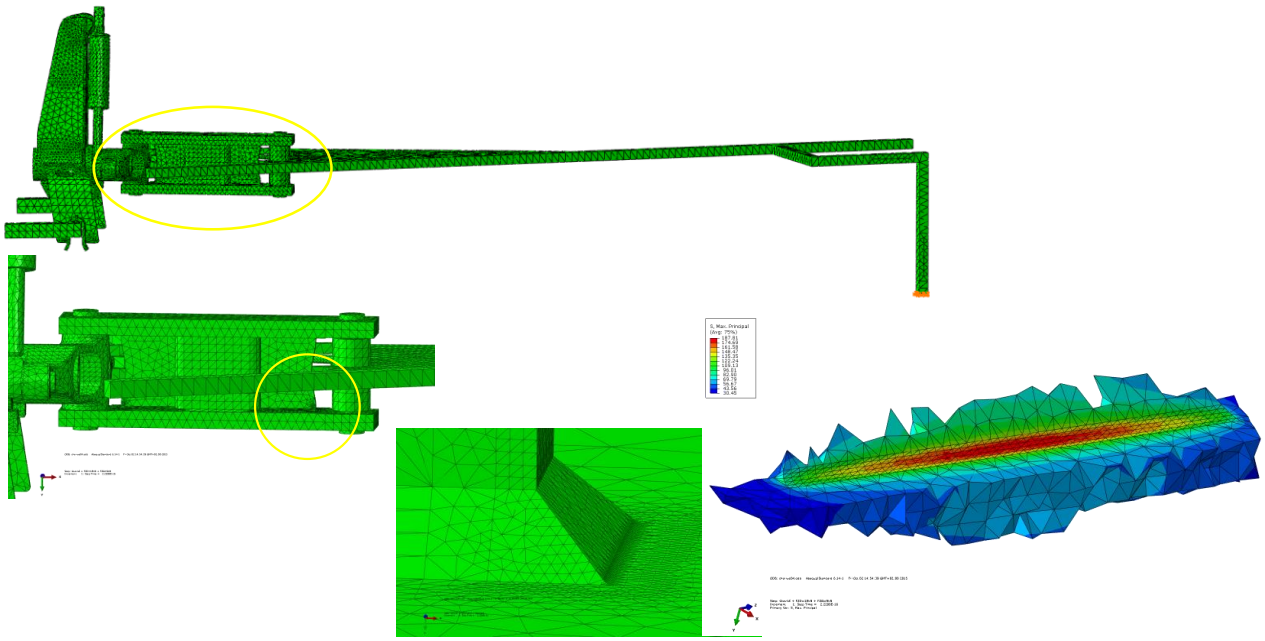

Figure 6 - Finite element meshing with an example of stress cartography at the weld toe

The average stress magnitude values obtained are as follows:

- 1st case: plough at 0° (working position)
  - $F_{XG} = F_{XD}$ = + 17 kN and F_{X3} = 0 kN : σ_a = -70 MPa
  - F_{ZD} = +18 kN, $F_{ZG} = F_{ZD} / 2$ = +9 kN and F_{Z3} = 0 kN : σ_a = +190 MPa
- 2nd case: plough at 20° (transport position)
  - $F_{XG} = F_{XD}$ = -17 kN and F_{X3} = +21 kN : σ_a = +110 MPa
  - F_{ZD} = -18 kN, F_{ZG} = -14 kN and F_{Z3} = +17 kN : σ_a = -240 MPa

The following dispersions are taken on the loads, CV being the variation coefficient (standard deviation / average):

- CV = 0.07 on F_{XG}, F_{XD} and F_{ZD}
- CV = 0.04 on F_{ZG} and F_{X3}, F_{Z3}

In order to determine the most damaging load case, FX and FZ loads are combined in-phase. The load case thus considered corresponds to the one that gives the highest tension stresses, i.e. case No. 1: plough at 0° (working position).

For $N_{eq} = 10^6$ cycles, the stress magnitude is: σ_a = +190 -70 = +120 MPa,

hence an equivalent stress range in service is: $\mathbf{\Delta\sigma_C}$ = 2.σ_a = **240 MPa**

The dispersion considered on the stress is the greatest dispersion on the load, i.e. **CV = 0.07**.

Since the design method considered is the "notch stress" method, the IIW recommendations propose, for a 1 mm radius at the weld toe, a fatigue class FAT 225 (i.e. an acceptable range at 2.10^6 cycles of 225 MPa). This value is given at 95% of non-rupture probability with a confidence interval of 75%.
Since the equivalent stress is calculated for $N_{eq} = 10^6$ cycles, the acceptable stress range must be assessed for the same number of cycles.

For $N_{eq} = 10^6$ cycles, the stress range is **$\mathbf{\Delta\sigma_R}$ = 283 MPa at 95% of non-rupture probability with a confidence interval of 75%.**
The dispersion on the strength is considered as equal to **$\mathbf{CV_R}$ = 0.1**, which corresponds to a correct usual quality.

From the value of $\Delta\sigma_R$ and the value of CV_R, it may be possible to determine the average value: **$\mathbf{\Delta\sigma_{R,m}}$ = 353 MPa**.

First of all, a deterministic design approach is considered.
Knowing the service equivalent stress range of $\Delta\sigma_C$ = 240 MPa and the design strength probabilised at 95% of non-rupture probability with a confidence interval of 75% of $\Delta\sigma_R$ = 283 MPa, the dimensioning criterion is $\Delta\sigma_C < \Delta\sigma_R$ so $\Delta\sigma_C$ = 240 MPa < $\Delta\sigma_R$ = 283 MPa.

The **safety coefficient** γ is therefore assessed by means of the ratio $\Delta\sigma_R$ / $\Delta\sigma_C$, so $\mathbf{\gamma}$ **= 1.18**.
However, this safety coefficient is not associated to a failure probability. This approach remains deterministic.

In order to apply the reliability approach, the Stress (representing the in-service loadings) and the Strength distributions are considered. The DEFFI software is used to assess the failure probability.

Knowing the average service equivalent stress range of $\Delta\sigma C$ = 240 MPa, the associated variation coefficient of CV = 0.07, the average strength of $\Delta\sigma_{R,m}$ = 353 MPa, and the associated variation coefficient of CV_R = 0.1, the **failure probability** is $\mathbf{P_f = 1.923.10^{-3}}$ with a confidence level of 75%.

Figure 7 represents both distributions and the failure probability.

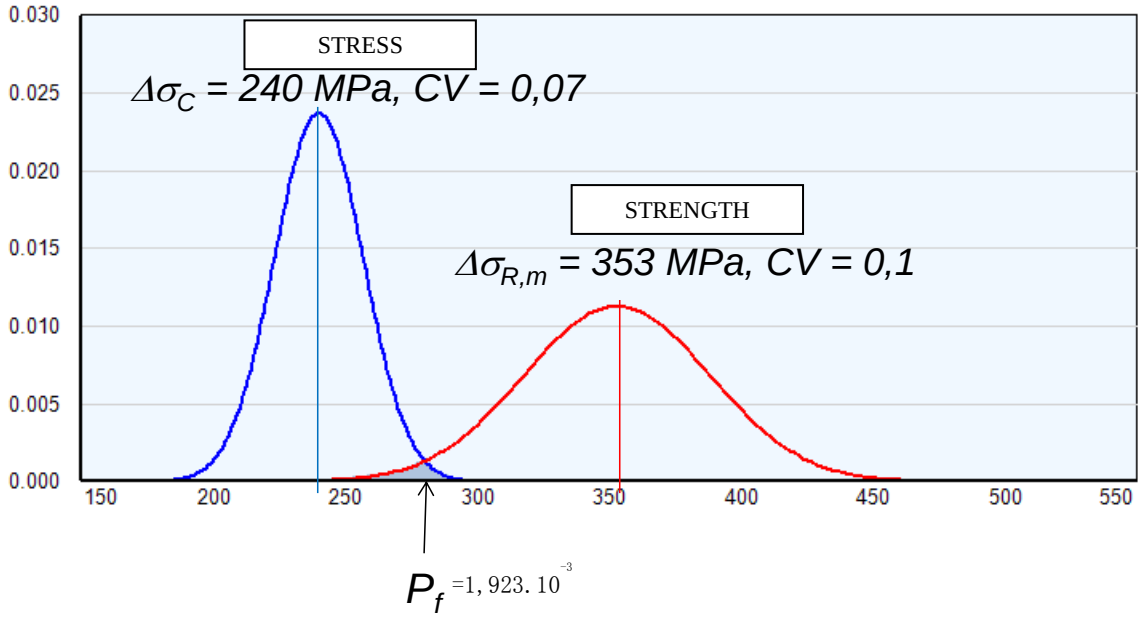

Figure 7 - Assessment of the failure probability thanks to the DEFFI software, knowing the distribution of the Stress and the Strength

Should a more severe loading be considered, that is to say switching from a $\Delta\sigma_C$ = 240 MPa loading to a $\Delta\sigma_C$ = 270 MPa loading with the same variation coefficient (CV = 0.07), the failure probability changes from $P_f = 1.9.10^{-3}$ to $P_f = 1.9.10^{-2}$ with a confidence level of 75%, that is one decade less.

Should one accept a failure probability of 10^{-2} with a confidence level of 75%, while retaining the same loading distribution, the manufacturing quality, that is to say in our case the class of the weld, may be degraded. One can switch from $\Delta\sigma_{R,m} = 353\ MPa$ (with CV = 0.1) to $\Delta\sigma_{R,m} = 325\ MPa$ with the same CV.

5. Conclusions

The loading part of the "Stress-Strength" method was studied on a tractor and plough application case.

The instrumentation approach for the tractor and the associated tool as well as the approach of the mission profile definition (distribution of loadings in service) were transferred.

The "Stress-Strength" method was deployed on a specific case, the plough case, with the purpose of checking the fatigue strength in-service of a mechanically welded area, knowing the loading, further to the measurements performed on the plough, and knowing the Strength of the welded area.

It is important to notice that in order to ***apply the method***, it is ***necessary to compare similar values***, in this case, stresses.

The stresses in the concerned area are obtained by means of a calculation to finite elements of the plough with the equivalent loads resulting from the measurements.

The data required to implement the approach are as follows:

- CAD of the part: plough,
- Boundary conditions (B.C.),
- Distribution of the loadings in-service in Loads,
- Characteristic of the welded assembly in fatigue.

Depending on the result obtained, it is possible to consider degrading the manufacturing quality, assessing the failure probability further to a quality incident, or assessing the failure probability for more severe loading distributions.

The interest of a probabilistic approach for the fatigue design in the agricultural domain has been demonstrated. This non-deterministic approach can help the traditional design approach and deterministic approach and can also provide a better management of uncertainties and risks. This method could be used to realise acceptance files for waivers in production. It could be useful to obtain the necessary changes in the engineering know-how in order to manage industrial projects by mastering their technical risks and at the same time to develop an engineering probabilistic culture in a project team.

Acknowledgements

Authors thank Cetim and Agricultural machinery committee for their financial supports.

References

[1] I. Huther, F. Lefebvre, *Dossier Instruction MAGR : Fiabilité - Chargements* (MAGR Instruction File: Reliability - Loadings) Cetim report No. 029512, June 2010

[2] A. Mahaud, P. Letort, *Fiabilité Chargement - Instrumentation et essais sur ensemble "Tracteur + débroussailleuse"* (Loading Reliability - Instrumentation and tests on "Tractor + brush cutter" assembly), Cetim report No. 048020, June 2012

[3] I. Huther, P. Letort, *Estimation des chargements équivalents en fatigue (cas : débroussailleuse)* (Assessment of equivalent loadings in fatigue (case: brush cutter)), Cetim report No. 050180, December 2013

[4] I. Huther, P. Letort, *Etude MAGR chargement - Instrumentation "chargeur + tracteur"* (Loading MAGR study - "Loader + tractor" instrumentation), Cetim report No. 040180, May 2013

[5] P. Letort; A. Mahaud, G. David, *Instrumentation et essais sur chargeur + tracteur* (Instrumentation and tests on loader + tractor), Cetim report No. 065194, janvier 2014

[6] I. Huther, P. Letort, *Estimation des chargements équivalents en fatigue (cas : chargeur)* (Assessment of equivalent loadings in fatigue (case: loader)), Cetim report No. 071826, June 2014

[7] I. Huther, P. Letort, N. Bedouin, *Etude MAGR chargement - Instrumentation "charrue + tracteur" CDC* (Loading MAGR study - CDC "plough + tractor" instrumentation), Cetim report No. 071827/071830, September 2014

[8] P. Letort, P. Darocha - *MAGR - Fiabilité Chargement - Instrumentation et essais sur ensemble "tracteur + charrue"* (MAGR - Loading reliability - Instrumentation and tests on "tractor + plough" assembly), Cetim report No. 079924, January 2015

[9] F. Lefebvre, I. Huther, *Estimation des chargements équivalents en fatigue (cas : charrue)* (Assessment of equivalent loadings in fatigue (case: plough)) - Cetim report No. 079923, June 2015

[10] JJ. Thomas, A. Bignonnet, 1999 Equivalent fatigue- état de l'art. Journée de printemps SF2M, Paris, Publ. Société Française de Métallurgie et de Matériaux.

[11] A. Bignonnet, H.P. Lieurade, Reliability approach in fatigue design; a mulitpartners project, Fatigue design 2007

[12] A. Bignonnet " Reliability concepts in fatigue Design" in 2nd Int .Conf. on Material and Component Performance under Variable Amplitude. Ed C.M. Sonsino and P.C. McKeighan, Darmstadt, Germany, March 23-26, 2009.

[13] M.A. Miner, « Cumulative damage in fatigue ». Journal of Applied Mechanics, 1945, 67, A 159-A 164.

[14] Fatigue sous sollicitations d'amplitude variable. Méthode Rainflow de comptage des cycles. Principe et utilisation, 1993. Recommandation AFNOR A03-406, 32p

Biolubricants for mobile equipment

J. Dromby, L. Vanden Eckhoudt, M. Lesterlou
Cetim, 52 avenue Félix Louat, 60304, Senlis, France

Keywords : Biolubricants, biodegradable oils, hydraulic components

The constantly changing technical requirements and the new environmental constraints have led to the advent of a wide range of vegetable oil-based lubricants in various applications. Now, it can be expected that the use of these “biodegradable” oils will become more and more strictly required, either in relation to the equipment or to use in “environmental sensitive” areas.

For manufacturers of mobile equipment within Cetim, among which agricultural machines, the question now concerns the performance of these biodegradable oils, in comparison to mineral oils, with regard to the power transmission function (hydraulic motors and pumps).

To answer this question, Cetim designed and realised a test bench for the characterisation of biolubricants likely to be used in hydraulic power transmission systems. The project was broken down into several phases:

- Search for the main existing products and the regulations in force. Among the questions asked by industrial manufacturers, let us mention the miscibility of biodegradable fluids, the friction coefficient and its possible evolution, the endurance of biodegradable fluids, or the acquisition of additional data on “ecolabelled” products.
- Analysis of several oils supplied by industrial manufacturers, in order to compare the physical and chemical properties of biodegradable oils. The results of these analyses were summarised in a report. With regard to the endurance of biodegradable fluids, the trades concerned identified the need to make a test bench so as to get comprehensive results obtained via a neutral bench.
- Designing and manufacturing of the test bench. During this phase, the hydraulic components used for the tests were also defined, and the parameters of the mission profile were adapted to those components.
- Fine tuning of the test bench with the components used for the comparative tests, then first reference test performed with a mineral oil.
- Tests with 2 biodegradable oils. The tests were carried out in the same conditions as those of the reference test. The results obtained were then compared to the results of the reference test.
- Today, a test is carried out on a third biodegradable oil.

The purpose of this presentation is to share with you the problems and difficulties encountered and the results obtained.

1. Context and objectives

The constantly changing technical requirements and the new environmental constraints have led to the advent of a wide range of vegetable oil-based lubricants in various applications. Now, it can be expected that the use of these “biodegradable” oils will become more and more strictly required, either in relation to the equipment or to use in “environmental sensitive” areas. For manufacturers of mobile equipment within Cetim, among which agricultural machines, the question now concerns the performance of these biodegradable oils, in comparison to mineral oils, with regard to the power transmission function (hydraulic motors and pumps). To answer this question, Cetim designed and realised a test bench to characterise biolubricants likely to be used in hydraulic power transmission systems.

Among the questions asked by industrial manufacturers, let us mention the miscibility of biodegradable fluids, the friction coefficient and its possible evolution, the endurance of biodegradable fluids and the acquisition of better knowledge on behaviour "ecolabelled" products. The hydraulic components used for the tests were defined and the parameters of the mission profile were adapted to those components. Then the test bench was fine-tuned with the hydraulic components used for comparative a first "reference" test was carried out with mineral oil. Other tests were carried out with 2 biodegradable oils, in the same testing conditions as those of the reference oil. The results obtained were compared together. Today, a 3rd biodegradable oil is in testing process.

2. Operation of the biofluid test bench

The biofluid test bench is comprised of 2 parts. The first part of the bench, mainly electromechanical, generates the necessary power to drive the "pump" components and the necessary power to load the "motor" components. This part also makes it possible to control the input (drive) or output (load) torque or rotation speed and to measure the input and output conditions (torque / speed), and it also includes the power transmission and regeneration system supplied by the electrical system. The main feature of this loading system is that it allows 4-quadrant torque-speed operation.

The second part of the bench is mainly hydraulic and operates with the tested oil. A complete system, comprised of a reservoir, a pump and a hydraulic motor, allows the oil to be stressed under similar conditions to those occurring in a hydraulic drive system. Hydraulic units measure hydraulic pressures, flow rates and temperatures at the inlet and outlet of the various components and, where applicable, on the external drains. All the electromechanical and hydraulic components, as well as the control station, are installed on a single chassis. For the components, the tests are carried out at room temperature, but the temperature of the oil inside the reservoir is controlled by a kidney loop.

The operator interface for the control of the biofluid test bench is a software program installed on a computer integrated into the control station. Main functions of the software are: indication and control (display of values, manual control of motors and actuators, programing of steps, sequences and cycles, configuration of alarms and shutdown upon fault, etc.) and supply of the process values in a .csv file, in 2 recording frequencies (1 Hz and 100 Hz). The computer communicates with the programmable logic controller via a TCP link for the management of the display of the values and controls, and via a PROFIBUS DP link to provide a fast history (100 Hz) of the process values during the testing characterisation cycles of the bench.

Overall view of the test bench and overall view of the control station.

3. Tests with the biodegradable oil

The mission profile selected for the tests is suitable for the components used and was defined by industrial manufacturers. It is similar to endurance tests performed on a hydraulic excavator and considered to be extremely severe. For the endurance cycles, the maximum pressure is 300 bar, the maximum flow rate is 50 dm^3/min and the input speed of the pump is 1,500 rpm. Eight cycles were carried out, for a total of 2,304 hours.

The test carried out shows that it is extremely important to monitor any changes in the flow rate of the pump, especially during the step at 20%. As a matter of fact, as the flow rate of the pump is adjustable with a set-up adjustment performed at low temperature, it is possible to obtain different hot flow rates, which may lead to operation of the motor outside the recommended range (drop in the efficiency at low rpm in case of excessively low flow rate, or even motor shutdown): it can result different behaviour of the oils over time which will be difficult to compare if the oils have not performed the same work. Therefore, we implemented a protocol to monitor the flow rate cycle by cycle through systematic analysis of all the recorded data, and the flow rate can be adjusted if necessary.

The curve shows that the accumulated "delay" at the beginning of the test, due to the pumps which were not delivering the expected flow rate on the 100% step, was gradually caught up (mainly by adjusting the flow rate in the 20% step). At the end of cycle 2, the difference of volume between the 2 tests exceeded 7%. This difference was reduced to 0.01% at the end of the test (end of cycle 8).

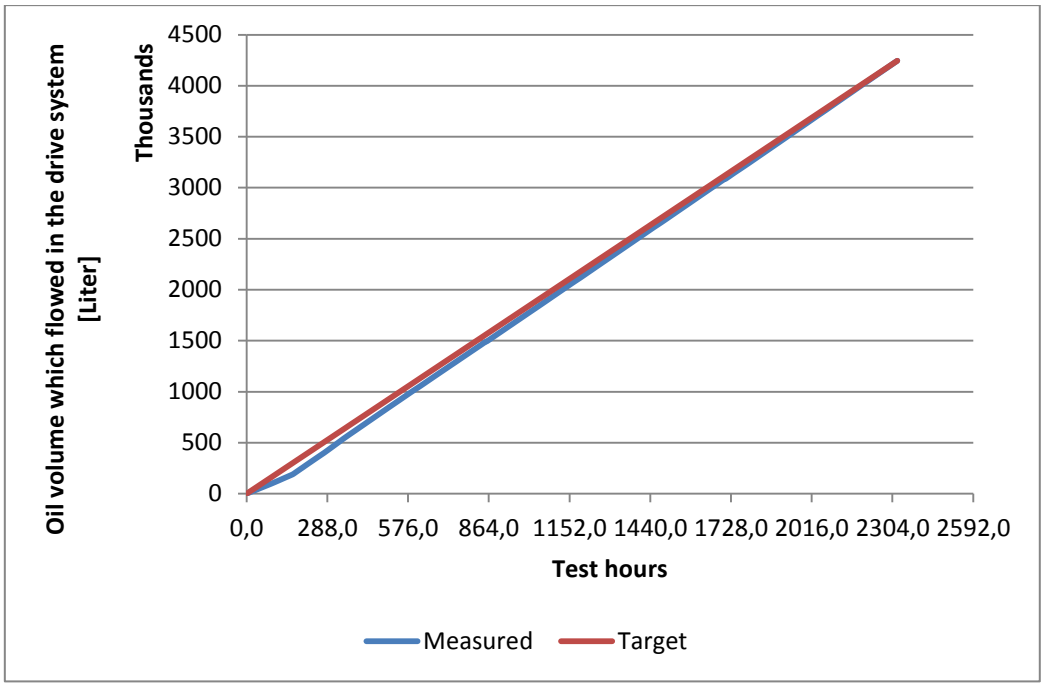

Flow rate monitoring curve during the 5 first cycles.

4. Evolution of the performance of the tested components

The mission profile specifies that the pressure / flow rate characteristics must be recorded at the beginning of each cycle (i.e. at 0 hrs; 288 hrs; 576 hrs; 864 hrs; 1,152 hrs; 1,440 hrs, etc., of operation) at a temperature of approximately 30°C. The efficiencies of the components during steps 1 and 2 were extracted from the recorded data on an ad hoc basis. The graph below gives a view of the evolution of efficiencies during the 100% step, for each oil. The overall efficiency corresponds to the efficiency of the whole hydraulic system. The objective is to compare the mechanical power at pump input and the mechanical power at motor output. The pump efficiency corresponds to the efficiency of the whole pump (main pump + booster pump).

At this stage of the test, the pump efficiency values are extremely similar for the different oils. However, we noticed that the motor efficiency was rather unexpectedly better and more constant with the biodegradable oil after 5 cycles.

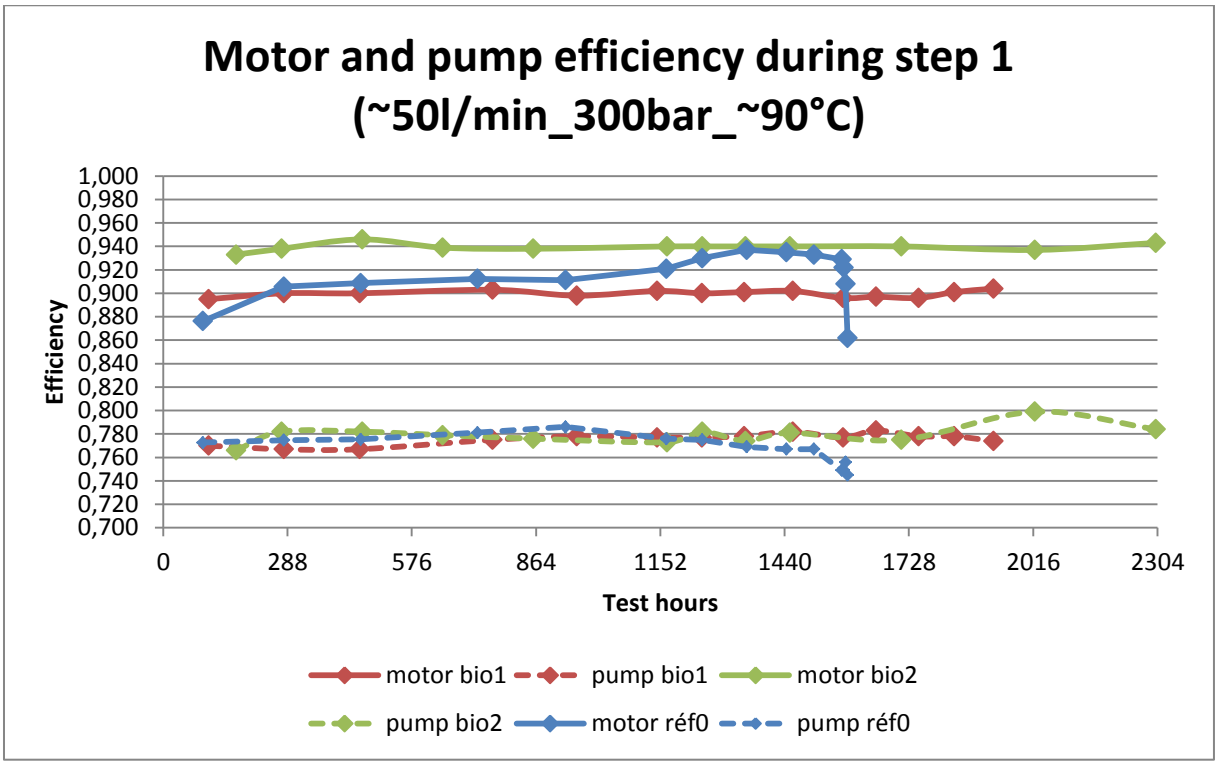

5. Results of the oil analyses

All the oil samples were analysed. The viscosity of the Bio2 oil at 40°C and 100°C increases linearly, and the viscosity at 40°C increases more significantly than the viscosity at 100°C. The water content is rather constant and higher with the Bio2 oil.

The viscosity index characterises the quality of a lubricant. The higher the viscosity index the lower the influence of temperature on the viscosity of the oil. In our case, the viscosity index decreases, this allows us to say that the influence of temperature will increase over time. The difference of viscosity between low temperatures and high temperatures increases gradually. Compared to the previous oils, since the viscosity values at 100°C and 40°C are higher for the Bio2 oil, the viscosity index cannot decrease significantly to reach the same level as the 2 other oils. Until 1,440 hrs, the 2 Bio oils remain equivalent, with a similar decrease of the viscosity index. Beyond that time, comparison is impossible. The evolution of the 2 bio oils over time seems to be related to the losses of additives. The Bio2 oil appears to be the oil which features the lowest temperature sensitivity.

The TAN (Total acid number) value makes it possible to measure the oxydation rate in an oil. The higher the TAN value, the higher the degradation of the oil. The TAN value significantly increases during the tests, this being an indication of a significant degradation of the oil. This degradation should have led to premature wear of the components, however this did not happen. Slight copper and zinc contamination was found. Moreover, a slight drop in the phosphorus content was found, which may indicate a slight drop in the extreme pressure additive.

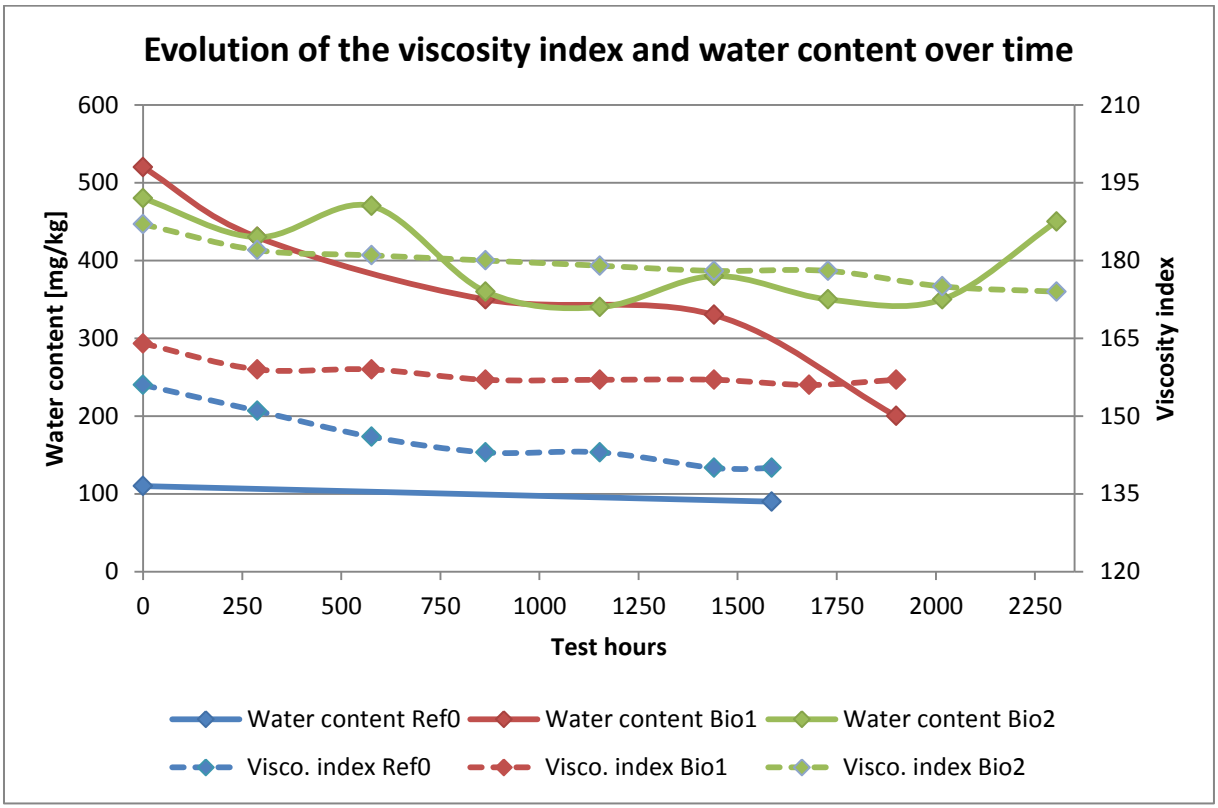

6. Conclusions

The tests carried out with this 2nd biodegradable oil reached the defined maximum objective of 8 cycles. The mission profile applied was the same as at of the reference oil, with regard to the mean hydraulic power (same pressure and same mean flow rate) and the temperature conditions (48-90°C). The 8 cycles carried out correspond to 2,321 hours of operation, for a target of 2,304 hours. As the sequences included rest periods amounting to 12.5% of the time, the tested components operated for 2,031 hours.

The hydraulic motor, which could not complete the 8 cycles without failure during the first 2 tests (reference oil and 1st biodegradable oil), exhibits some incipient degradation (flaked cam) which had no effect on the overall efficiency.

The analyses of the oils samples mainly show a much faster increase in the TAN when compared to the 2 previous oils. The graph below gives, for information, a comparison of the tested oils according to different criteria. The grades (from 0 to 5) for each criterion stem from the results obtained.

N°	Oil type	Average cost [€/L]
0 (réf.)	Mineral	1,9
1	Bio with saturated esters	7,2
2	Bio with unsaturated esters	4

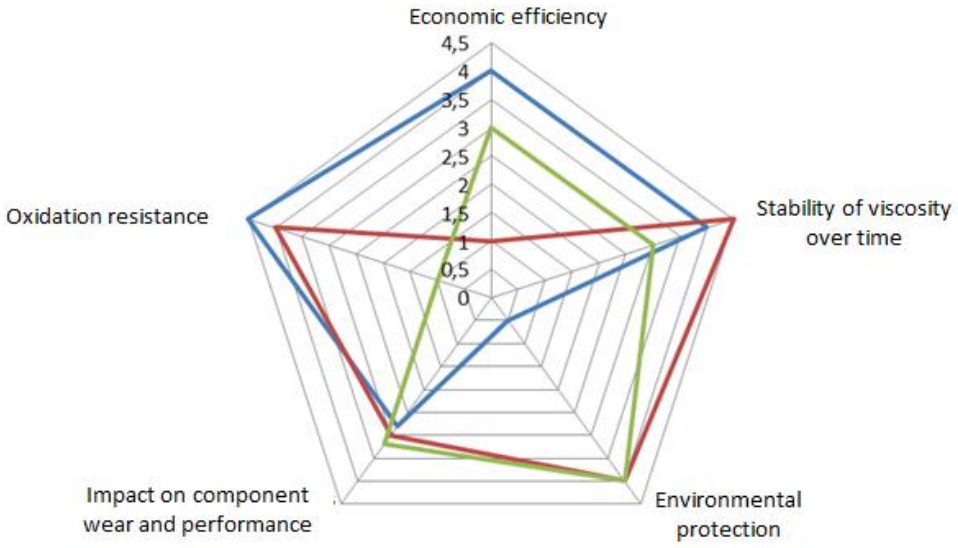

Empirical fuel consumption model of tractor road travels

Debroize Didier [a*], Gauthier Frédéric [a]

[a] Station des Cormiers, Chambre d'Agriculture de Bretagne, La Bourdiniere, 35340 Saint Aubin du Cormier, France

* Corresponding author. Email: didier.debroize@bretagne.chambagri.fr

Abstract

Farms can participate in the fight against global climate warming in particular by reducing their energy consumption. Within direct energy use in agriculture, the mechanization's fuel consumption represent a significant share of energy. For example in 2011, that part was about 53 % in France. Farm fuel consumption is the result of multiple operations each with their own characteristics. To identify where improvements can be made, we decided to model mechanized operations. So, it's possible to simulate different farming practices with the model and estimate potential gains or losses. To develop the model, experimental data is used, collecting in a project named Ecofuel. The aim of the Ecofuel project is to measure tractors operating parameters and context parameters in regards with their use. All this parameters were measured for 30 tractors over a period of 1 year at a frequency of 1Hz. The project database contains more than 18000 hours of work recorded. To achieve this experimental work, an android application was developed, called TractorCANWatch, to record data over tractors CAN bus. In this paper, we present a work focuses on roads travels, which are becoming more frequent due to the increase of the utilised agricultural land of farms. Strong variations in fuel consumption between road displacement situations were observed due to implements weight and load, tractor characteristics, road network and drivers. Taking into account many parameters like traveled distance, altitude variations, tractor power, weight and load, from our experimental data, an empirical model is estimated to evaluate on road fuel consumption.

Keywords: experiment, tractor fuel consumption, road travel, empirical model, slurry transport, spatial database.

1. Introduction

In France, fuel consumption represents a large part (53 % in 2010 – Martin, 2014) of direct energy consumption of farms. In the fight against global climate warming, the reduction of this consumption is a major challenge for farms. However, in mixed farming situations (crop/animal breeding), this consumption is the sum of all the individual consumptions resulting from the large number of operations needed to achieve productive goals. A lot of factors affect the consumption of these individual consumptions as productions, plot dispersion, number and characteristics of field operations, characteristics of tractors and implements, type of soils, shape of fields, road network and weather conditions. To help farmers to master their consumption, it is essential to understand which factors are relevant for their farm. It is also very important to be able to analyze impacts of different levers and quantify them.

The global aim of this work is to model mechanization work of farms and to quantify working time, crop margins and mechanization costs. This should allow to know the strengths and weaknesses of the farm. Then, the possibility to test different evolutions will permit to help farmers to choose the most adapted to their needs.

In recent years, we notice farm acreage increasing. For example, between 2000 and 2010 in Britany, farm acreage increased of 31 %. Consequently, the distance between the headquarters of the farm and the plots has increased too. This evolution causes an increase of road travels and associated fuel consumptions. Most of the time, road travels are considered as lost time and mechanization choices (power of tractors, characteristics of implement, *etc*.) are made to limit their amount. So, it is important to bring a better knowledge about these operations and to understand their effect on farm fuel consumption. There are few references on fuel consumption of tractors during road travels and its importance around global fuel consumption of farms. Juostas (2008) showed that a tractor and a trailer (loaded with gravel – total weight of 18 t.) used from 2 $km.h^{-1}$ to 37 $km.h^{-1}$ had an increase of its hourly fuel consumption from 6 $l.h^{-1}$ up to 25 $l.h^{-1}$. If recalculated in $l.km^{-1}$, the fuel consumption decreased from 3.3 to approximately 0.70 $l.km^{-1}$. This example shows the importance of speed in fuel consumption. Saint Pierre et al (2010), in a paper on eco driving for cars, made a fuel consumption model based on acceleration/deceleration time and gas pedal position. So, the speed has an effect but the variations of speed are also relevant to evaluate fuel consumption. Lacour (2010), in Ecodefi project, used slurry spreading data to define the cumulative fuel consumption for on road transport. The effect of displaced mass, travel speed and tractor efficiency is quantified. It is also nearly obvious that elevation and its variations have an effect on fuel consumption.

This paper present a method to determine an empirical model to calculate fuel consumption for tractors road travel. The specificity of the model presented here is to use macroscopic values related to the displacement as input parameters. The data used to build the model are from the EcoFuel project. So, we first present the Ecofuel project and the dataset used for the model. Next, we present the method to calculate the empirical model. Finally, model validity will be discussed to understand the conditions of its use.

2. Materials and Methods

2.1. The Ecofuel project

The Ecofuel project aim at record the real use of tractors in farms with a global view. Farms are chosen about their main characteristics such as production, size, organization, type of operations, *etc*. There are mainly mixed farming farms: milk production or pigs breeding and crops with sometimes contractor work. For the selected farms, all the tractors are recorded during 12 to 15 months to be sure to get one complete year of data, the global fuel consumption and the different operations explaining this consumption. In order to explain instantaneous fuel consumption, all the data were recorded at a 1 Hz frequency. To achieve this, the acquisition system (image 1) based on a programmable logic controller (OMRON SYSMAC CJ1M-CPU13-ETN) was defined and installed on the tractors. Sensors are also installed on the tractors and linked to the data acquisition system. Data are saved in text files on a CompactFlash card. The start and stop of the engine triggers automatically the start and stop of the data acquisition system.

More precisely, the aim is to record data allowing to measure and explain tractor work and fuel consumption. So we defined the data that were needed and the associated sensors and the way to install them on tractors. Data recorded on tractors are the following: GPS data (latitude, longitude, elevation, speed and horizontal dilution of precision hdop), implement which is used (information given by the driver through a number on a keyboard), engine speed (alternator signal), ground speed (wheel measurement), way of direction, lifting height (rotary potentiometer), rear power take-off on or off, mechanical front drive engaged or not, driver on seat (yes or no) and the date and time. Fuel consumption was measured by 2 fuel consumption chamber 5cc sensor (730 ST series) from Aeroproduct. Calibration measurements made on these sensors showed an increase of the error for lower consumption values. For this reason, we decided not to use road travels where mean consumption were lower than 10 $l.h^{-1}$.

Image 1: Photo of the data acquisition box installed on a tractor

Image 2. The android tablet with TractorCANWatch application and the Bluetooth key plugged in a tractor

Even if we are able to get data from very different tractors (the older one was from 1972), to install our data acquisition system and the sensors on a tractor is a long and expensive task. The CAN bus on new tractors have in its messages a lot of the information we collect in Ecofuel project. So it can be an easier way to collect data for our purposes. So, we developed a new data acquisition system (image 2) based on CAN bus: an android application named TractorCANWatch. This system brings together a Bluetooth key plugged in diagnosis plug and an android tablet with TractorCANWatch. The Bluetooth key reads messages from the Can Bus and transfer them to the tablet. They are synchronize with GPS data and information entered on tablet screen (implement used and task) and stored on the tablet. The start and stop of the acquisition system is made by the driver. He can manage to get statistical values (mean consumption and speed, *etc*.) during the work of the tractor.

With the first data acquisition system, 25 tractors from 8 farms have been recorded giving more than 60 billion lines of data (> 17,000 hours). Some tractors are from contractors. We got data also from a combine, an automotive sprayer and two telehandlers.

2.2. Data validation

All these data are sent to a SqlServer database to be processed. Characteristics of tractors (nominal power and engine speed, maximal ground speed, *etc.*) and implements (type, working width, *etc*) are also recorded. Indeed, sensors may dysfunction and it is essential to validate the quality of data. The aim of this validation is to quantify data quality with a value. If GPS data are missing, they appear as zero, which is not possible, especially for latitude or longitude. GPS data contains horizontal dilution of precision (hdop) which is a qualitative value of the precision. When hdop is lower than 1, the quality of GPS data is the maximum. For engine speed, the minimum and maximum values allowed had been measured and can be checked. During the recording period, tractors were visited to collect the data files approximately every two months. Sensors were tested to check if they were ok or not.

For each farm and tractor, it is essential to separate work phases. For it, spatial location is a very important information. So, the plot map of each farm is recorded as polygons. It should include the headquarters of the farm and all others locations visited by the tractors of the farm (neighbor plots, cooperative, agricultural supplier, *etc*). Spatial procedures allow to link data with corresponding plots through the polygons. Then we consider that the data which are not linked to a plot are to be linked to roads or lanes. If GPS data are missing (problem of reception), we link these data to a specific plot ("No GPS"). If too many "No GPS" data appear in a road travel, it can't be used for modelling.

Beyond measure of fuel consumption, the knowledge of used power by the tractor according to operations is of great interest to be able to characterize the work made. On tractors, it is not possible to get a direct measure of used power. So, we use an indirect measure through a tractor testing platform which measures PTO torque, engine speed and fuel consumption. PTO torque ($N.m^{-1}$) multiply by engine speed ($rad.s^{-1}$) give the net power (kW). The fuel consumption ($g.h^{-1}$) divided by net power gives specific consumption ($g.kWh^{-1}$) which is the energetic indicator. Approximately, one hundred measuring point have been carried on a tractor to get a global view of the power cartography. From these points, we interpolate specific consumption values to get a power cartography (fig. 1).

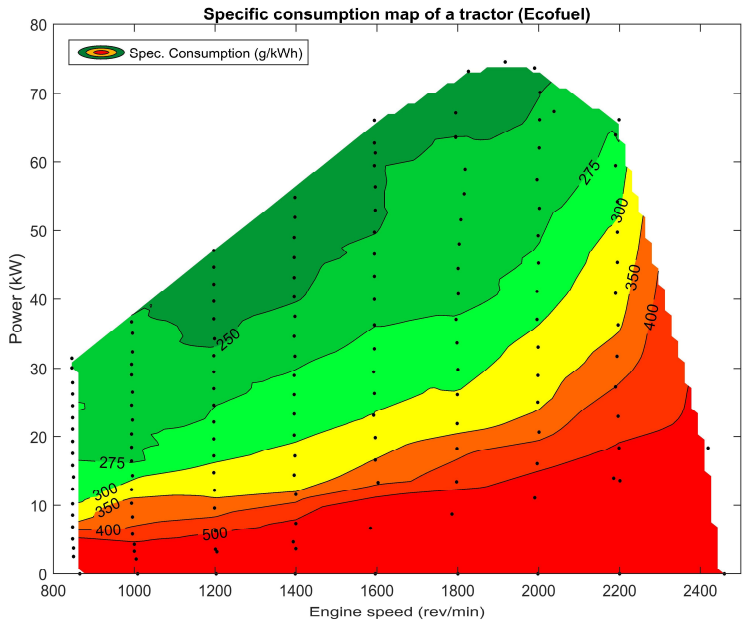

Figure 1: Fuel specific consumption of a tractor coming from measuring points on a tractor test bench

2.3. Data description

2.3.1.Tractor displacements

From the database, we extracted work sequences during which tractors were on roads and lanes. These work sequences have been made with implements that don't have any load, i.e. they don't carry any material (seeds, fertilizer, slurry, manure, grain, silage, *etc*). So, their weight don't vary significantly. They are qualified as tractor displacements. They are mainly tillage implements (plough, rotative harrow, cultivator, roller, *etc*) or harvesting implements (mower, gyrotedder, hay tedder, round baler …). On these road travels, we checked that all GPS data were on roads and lanes and calculated synthetic values that can be used for modelling. These data are tractor power (maximum power from the tractor testing platform test), mean specific consumption (measured with values from tractor testing platform test). The weights of the tractor, of the implement have been estimated.

We extracted 1,268 road travels from the database representing more than 5,800 km and approximately 190 hours spent on road. 10 tractors are represented from 77 to 165 kW (fig 2). 70 different implements (fig 3) have been used between once and 290 times (25 implements have been used more than 10 times and 3 more than 100 times).

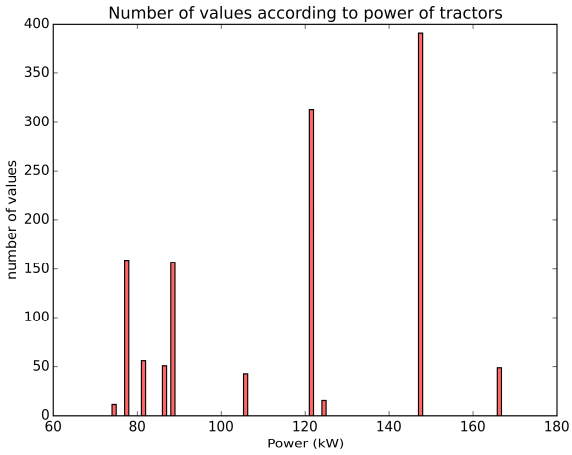

Figure 2: Number of data with power of tractors

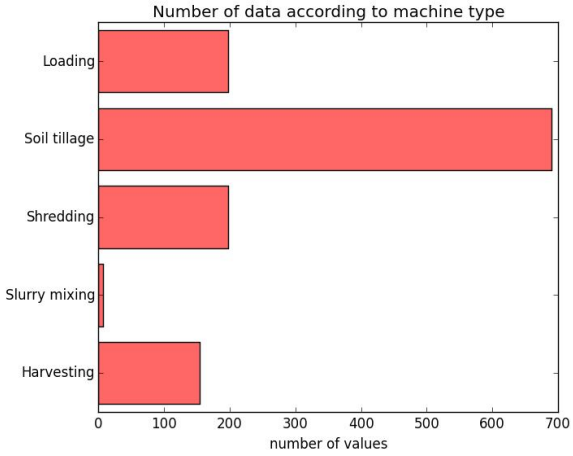

Figure 3: Number of data with type of implements

2.3.2.Slurry transports

The estimation of weight is a problem when the load can vary in a large part. Farm yard manure and yields may vary in quantity and density. With slurry transport, the load weight can be estimated with low uncertainty. Slurry density is close to 1 $kg.l^{-1}$ and filling ratio can be estimated to 90%. When the transport goes from farm sight to a farm plot, the slurry tanker is said to be empty. When the transport goes from a farm plot to farm sight, the slurry tanker is said to be full and 90% of its capacity is added as additional weight. So we collected 764 slurry transport values from 6 tractors-slurry tanker pairs with power varying from 96 to 209 kW (fig 4) and capacity from 14 to 22 m^3.

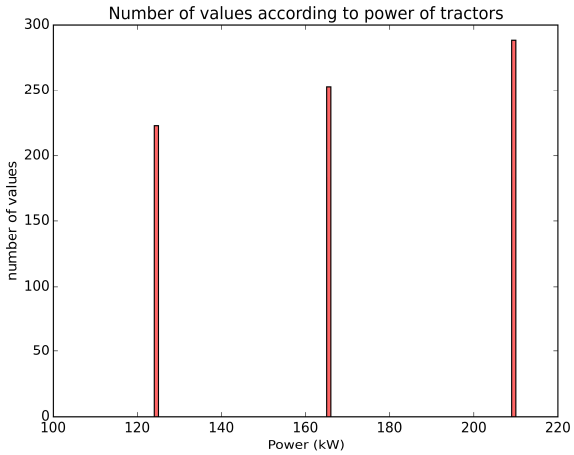

Figure 4: Slurry transports - number of data with power of tractors

3. Results and Discussion

The estimation of the tractor fuel-consumption model for on road travel is based on data of the Ecofuel project presented in this paper. The aim is to build an empirical model to predict fuel consumption with well-known input variables. This input variables can be classified in 3 groups: variables relative to the route (e.g. distance, slope, etc.), variables relative to the vehicle (tractor + working implement) such as the mass or engine's characteristics and variables relative to the driver. Since our dataset does not contain any variables relative to the driver, only variable relative to the route and the vehicle are used. Concerning the route, the distance (D) in kilometers which is calculated from the GPS speed, and the cumulated positive altitude (S) in meters which is the sum of all positive elevation changes over the route are used.

Concerning the vehicle, 3 variables are used. The first one is the mass (M) in tons of the tractor with the working tool. It is not measured but determined either from the identification plates of the material or estimated according to the type of the tractor or the type of the working tool. The second one is the tractor maximum power (P) in kW measured with the engine test bench. The third one is the mean specific fuel consumption (Cs) expressed in $g.kWh^{-1}$. Cs is calculated from the tractor engine cartography. We defined it as the mean specific fuel consumption where the tractor power is greater than 0.2 x P. Table 1 presents summary statistics of the variables.

Table 1 : Statistical value of the variables for the displacement dataset

	Mean	Minimum	Maximum
C (l)	2.3	0.3	30.6
M (t)	9.2	5.4	13.9
D (km)	4.6	0.8	77.4
S (m)	54.2	0.0	780.8
Cs (g/kWh)	319.8	242.5	382.2
P (kW)	117.4	74.0	165.8

The simplest linear empirical model which can be built:

$$C = K + a_1 D + a_2 M + a_3 S + a_4 Cs + a_5 P, \quad (1)$$

with K a constant and a_i the model's coefficients. The masse-distance interaction was also introduced into the model, modeling the fact that the mass effect depends on the distance or *vice versa*. Indeed, the greater the distance of the displacement is, the smaller the frequency of obstacles encountered on the route would be. Therefore the proportion of stopping and starting phases, during which the mass has a greater influence, would be smaller in long distance displacement. The model becomes:

$$C = K + a_1 D + a_2 M + a_3 S + a_4 Cs + a_5 P + a_6 D \times M, \quad (2)$$

R software version 3.3.1 (2016-06-21) was used to estimate the linear model. First, model variables were selected with a stepwise algorithm based on the Akaike Information Criterion (AIC) in the R MASS package (version 7.3-45). AIC coefficient is minimized when all variables and the mass-distance interaction are kept. In a second step, Cook's distance were calculated from all points in the sample to remove points that have a strong negative influence on linear regression. Out of the 1,268 measurement points in the sample, 77 points were removed for which the Cook's distance was greater than 4/1,268 (Bollen et al. 1990). The new linear model was calculated with this new data sample. Estimated coefficient values are presented in the Table 2.

Table 2 : Results of the multiple linear regression with the equation 2

	Coefficients	Std. Error	P value
K (l)	-1.5162	0.1379	< 2e-16
A2 (l/t)	-0.0056	0.0069	0.421
A1 (l/km)	0.2420	0.0099	< 2e-16
A3 (l/m)	0.0103	0.0003	< 2e-16
A4 (l*kWh/g)	0.0033	0.0003	< 2e-16
A5 (l/kW)	0.0055	0.0007	2.9e-14
A6 (l.t-1.km-1)	0.0107	0.0009	< 2e-16

According to the p value the mass coefficient is not significantly different from 0. Therefore, this variable can be removed from the model. So, the equation 2 becomes:

$$C = K + a_1 D + a_3 S + a_4 Cs + a_5 P + a_6 D \times M. \quad (3)$$

The new results for the multiple linear regression with equation 3 is presented in Table 3. For all the coefficients the p value are significant and the adjusted R-squared is equal to 0.967. The most influencing variables are the distance, the mass-distance interaction and the cumulated positive altitude. To validate the model, the K-fold cross validation method from the DAAG R package (version 1.22) are used. Data are randomly assigned into 5 subsets. Each subset is removed, in turn, while the remaining data is used to calibrate the regression model which is then used to predict the deleted observations. Figure 5 presents the residuals of the regression (difference between observed and predicted values) as a function of predicted values for each fold. We can see that the error is bigger for small consumption values but exceeds 1 liter only for a few points. This suggests that the model predicts better large consumptions. Overall the root mean square error (RMSE) is quite low: 0.29 liter. The RMSE is calculated as follows:

$$RMSE = \sqrt{\frac{\sum_{i=1}^{N}(C_i - \hat{C}_i)^2}{N}}, \quad (4)$$

with $\hat{C}_i$ the predicted value, C_i the measure value and N the sample length.

Table 3 : Results of the multiple linear regression with the equation 3 for displacement data

	Coefficients	Std. Error	P value
K (l)	-1.5049	0.1379	< 2e-16
A1 (l/km)	0.2448	0.0085	< 2e-16
A3 (l/m)	0.0104	0.0003	< 2e-16
A4 (l*kWh/g)	0.0034	0.0003	< 2e-16
A5 (l/kW)	0.0051	0.0005	< 2e-16
A6 (l.t-1.km-1)	0.0102	0.0007	< 2e-16

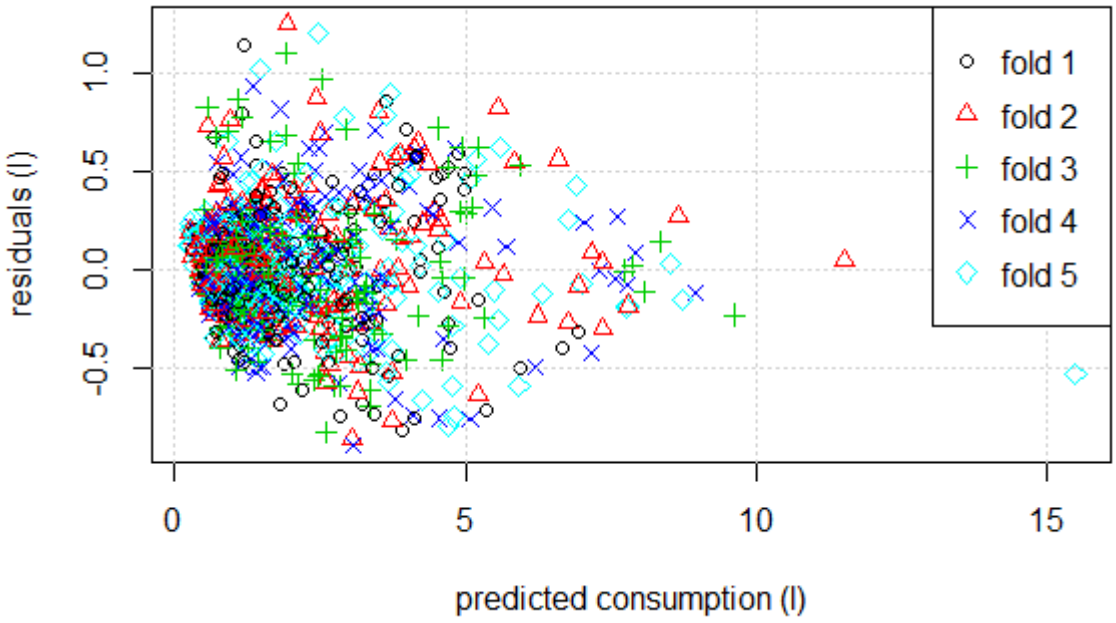

Figure 5 : Measured consumption versus predicted consumption for each cross-validation fold.

The same method of data processing was used on manure transport data. In this case, the involved masses are greater important. Table 4 presents statistical data on the sample. The lowest mass for transport data is 17.4 t whereas the highest one is 13.9 t for travel data. So, there is no overlapping values for this variable between the 2 sets of data. As for the other variables, the ranges of variation are generally lower for transport data but are included in the range of variations of the displacements data. It should also be noted that the measurements were carried out on the same farms and with the same tractors for the two datasets. The sample consists of 764 trips, or about 382 return trips. The slurry tanker is full to go and empty on return.

Table 4 : Statistical value of the variables for the transport dataset

	Mean	Minimum	Maximum
C (l)	4.7	0.4	25.6
M (t)	27.7	17.4	37.7
D (km)	5.6	0.9	30.1
S (m)	56.0	1.1	394.4
Cs (g/kWh)	272.3	242.5	312.7
P (kW)	169.9	124.0	209.0

53 points for which Cook's distance is greater than 4/764 are removed. With this second dataset the linear model are estimated with equation 2. The adjusted R-squared is equal to 0.99 and the RMSE is equal to 0.31 liter. Coefficients are presented in the Table 5 and the Figure 6 presents the cross-validation results. Similarly for the displacement data, the most influencing variables are the distance, the mass-distance interaction and the cumulated positive altitude. We also notice that the residuals do not exceed 1 liter.

Table 5 : Results of the multiple linear regression with the equation 2 for transport data

	Coefficients	Std. Error	P value
K (l)	-5.4261	0.2130	< 2e-16
A2 (l/t)	0.0183	0.0025	5.9e-13
A1 (l/km)	0.3267	0.0129	< 2e-16
A3 (l/m)	0.0251	0.0007	< 2e-16
A4 (l*kWh/g)	0.0126	0.0006	< 2e-16
A5 (l/kW)	0.0092	0.0005	< 2e-16
A6 (l.t-1.km-1)	0.0095	0.0003	< 2e-16

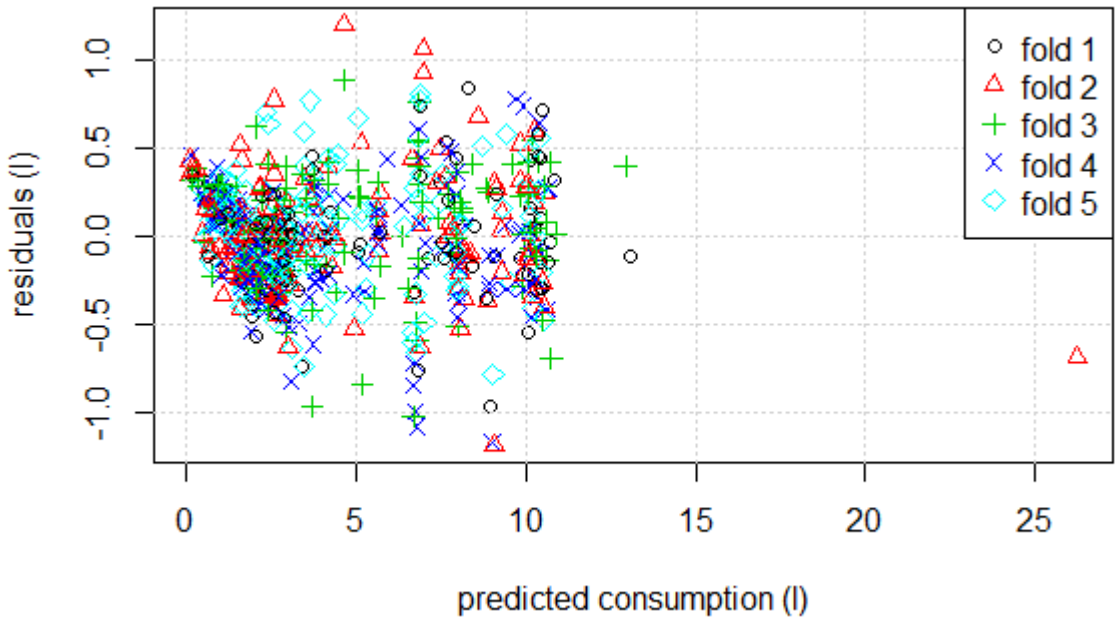

Figure 6 : Measured consumption versus predicted consumption for each cross-validation fold.

Models coefficients for displacement and transport are of the same order of magnitude. The validity domains of the 2 models are given by the minimum and maximum values of Table 1 and Table 4. It is also necessary to pay attention to the variation of the cumulated positive altitude with respect to the traveled distance (Figure 7). Indeed, for mountainous areas, where there can be strong altitude differences over a short traveled distance, the empirical models may no longer be valid.

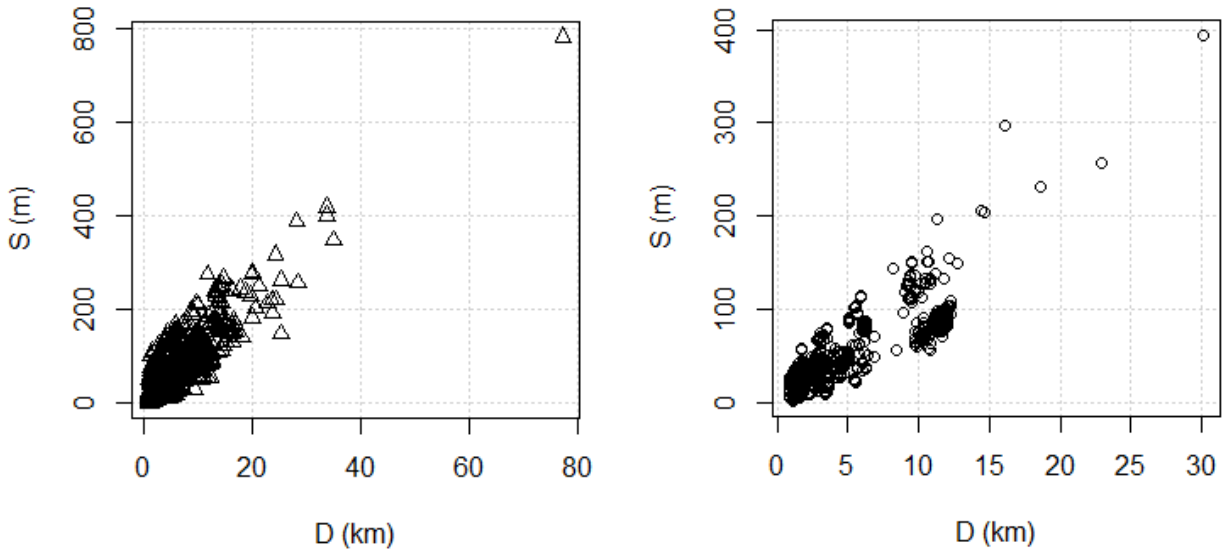

Figure 7 : Cumulated positive altitude for the displacement data (left) and for the transport data (right)

4. Conclusions

In Ecofuel project, data on the operation of tractors and implements were recorded on 7 farms. Some of this data has been used in this paper to estimate an empirical linear model on the fuel consumption of tractors on the road. Given the difference in load for the travel and transport data, two different models were estimated. The model was based on distance, total weights of tractor and implements, cumulated positive altitude, specific consumption and tractor power. These variables can be known easily in most of crop/animal breeding farms. For both models, the root mean square error is equivalent and is about 0.3 liter. It can be noticed that models better predict large consumptions. As the most important gains to be made are on farms for which headquarter to plots distances are important, the consumption estimates with the models will be more accurate.

The next validation step of this work is to calculate the total fuel consumption for transport and displacement over the 7 farms of the Ecofuel project and compare them to the measure one. It will then be possible to quantify an overall error in estimating the fuel consumption of tractors on the road for the 7 farms.

The final objective is to estimate the total fuel consumption of tractors on farms. To do this, the same work must be carried out for the consumption of fuels in the fields. This work is much more complicated because there are a lot more parameters to take into account.

References

Saint Pierre, G., & Andrieu, C. (2010, May). Caractérisation de l'écoconduite et construction d'un indicateur dynamique pour véhicules thermiques. In Conférence Sécurité Routière. Prévention des Risques et Aides à la Conduite.

Juostas, A., & Janulevičius, A. (2008). Investigation of tractor engine power and economical working conditions utilization during transport operation. Transport, 23(1), 37-43.

Lacour, S., Galiègue, Y., Vaitilingom, G., Pradel, M., Gallet, P., & Guiscafré, P. (2010). The contribution of field experiments to Life Cycle Assessment of agricultural works: application to spreading works. In International Conference on Agricultural Engineering–AgEng2010 Towards Environmental Technologies (pp. 6-8).

Bollen, Kenneth A.; Jackman, Robert W. (1990). Fox, John; Long, J. Scott, eds. Regression Diagnostics: An Expository Treatment of Outliers and Influential Cases. Modern Methods of Data Analysis. Newbury Park, CA: Sage. pp. 257-91. ISBN 0-8039-3366-5.

Martin JP – Ministère de l'énergie et du développement durable. http://www.statistiques.developpement-durable.gouv.fr/fileadmin/documents/Produits_editoriaux/Publications/Chiffres_et_statistiques/2014/chiffres-stats517-conso-energie-agriculture-mai2014.pdf Accessed February 13, 2017

Hydrostatic Transmission designed for energy efficiency and productivity

Jean Heren*, Mathilde Demoulin
Poclain Hydraulics
* Corresponding author. Email: jean.heren@poclain.com

See Following Pages

The High Performance system based on Poclain Hydraulics' innovation is notable for achieving performance well above current standards.

When combined within the same transmission, the components of the High Performance range reveal their full potential. The unique design of the High Performance system enables it to function under extreme pressure and speed conditions, and achieve outstanding energy efficiency that minimizes the machines' fuel consumption.

The design studies and validation tests put in place by our teams mean that our High Performance system is perfectly in line with your machines' architecture and performance. Time to market will be accelerated in order to reduce your development costs.

MHP Motor

PW Pump

PWe Pump

SDCT Controller

A High Performance transmission dedicated to sprayer

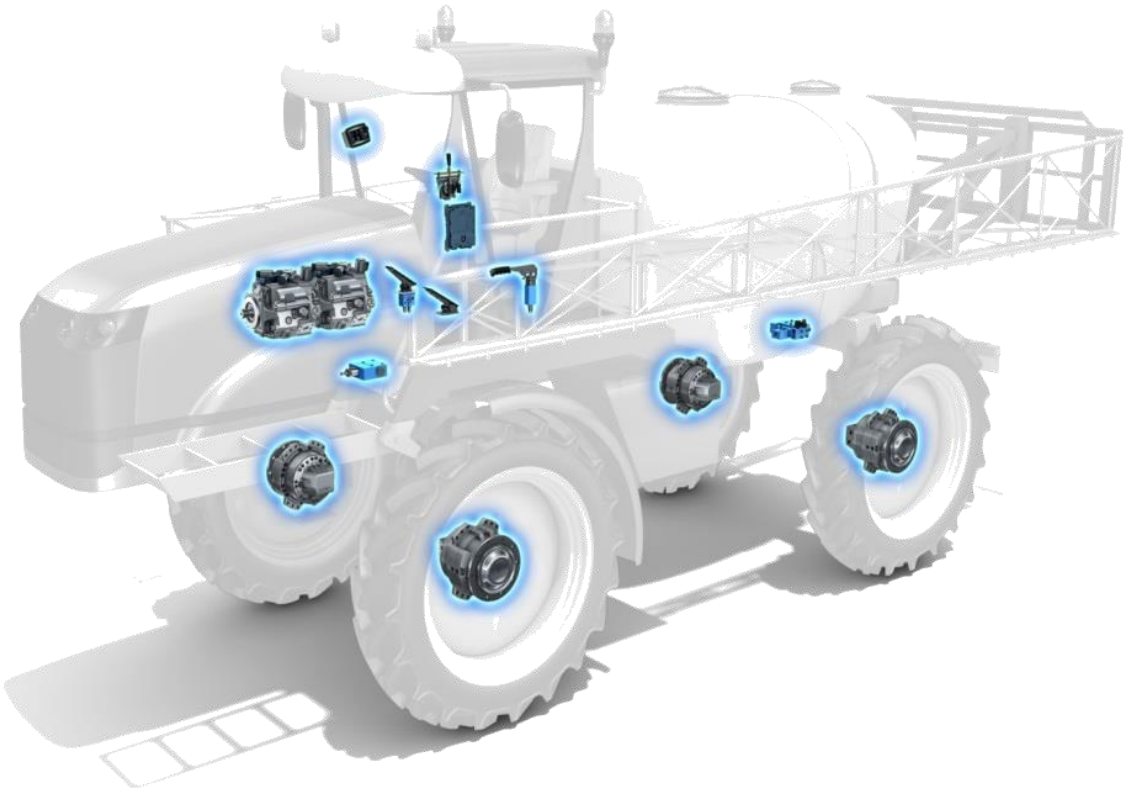

Reduce fuel consumption

Reduced diesel engine speed to match actual power requirement thanks to EcoDrive™ software.

Reduce fuel consumption thanks to the hydrostatic transmission efficiency components.

Pushing forward the borders of productivity:

Increase the speed up to 60 kph on the road. Up to 40 kph on the fields.

Wet discs friction brake with boosted hydrostatic braking leads to low wear components.

Extreme gradability thanks to 500 bar max pressure and TwinDrive™ to overcome any traction problem.

What is TwinDrive™ solution?

By using two pumps assembled in tandem, TwinDrive™ solution provides an instantaneous and automatic traction control solution, without compromising the overall transmission efficiency.

Improvement of the driving comfort

Smoothness is guaranteed by the Automatic or sequential seamless speed Shifting

Innovative Design for suspension: A patented solution to combine wheel drive and suspension sliding rods with license agreements with OEM.

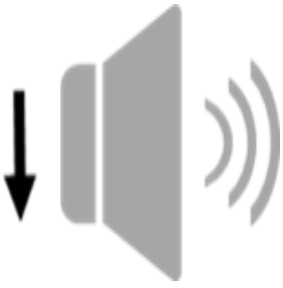

Quietness: Direct drive gearless wheel motors. Lower Engine RPM thanks to EcoDrive ™ software.

Easy to integrate

Direct drive solution with few rotating parts and robust mechanical sub components

Easy & Efficient diagnostic using Phases configuration software.

Positive and fail safe “SAHR” brake combined in one package to perform consistent service, parking & secondary brake.

A single fluid solution w/o frequent maintenance

Wet discs friction brake with boosted hydrostatic braking lead to low wear device.

High Performance at the wheels : MHP 20/27

The heart of the HIGH PERFORMANCE Transmission is the MHP motor. It has been designed with Agriculture Machinery market in mind. It fully addresses the main requirements of this market which are higher productivity (higher speed at high power), low fuel consumption and reduced down time.

Power and Speed

This motor creates a real breakthrough in the cam-lobe/ radial piston technology: the maximum rotation speed can reach up to 370 rpm and the maximum power level 280 kW.

Efficiency

The MHP motor new distribution designs allows to greatly reduce the internal pressure drops, even at high speeds. This feature combined with the fact that it works without planetary gear box results in very high efficiency levels all over the operating map. Our lab bench tests have shown that compared to a conventional bent axis axial piston motor with a planetary gear box, the average gain in efficiency of the motor can reach 36% over a compounded duty cycle presented below:

	Moto reducer	***MHP27***
Efficiency Field 1*	0,79	0,93
Efficiency Field 2*	0,66	0,93
Efficiency Road*	0,53	0,86
**** @150 bar***	**0,67**	**0,91**

+36% Efficiency

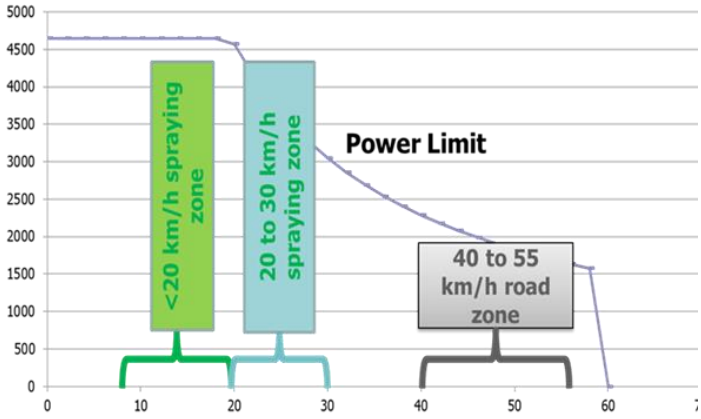

	kW	l/kWh	Hours /year	Annual Budget Liters
Power need with competition	98,47	0,35	500	17 232
Power need with PH	71,28	0,35	500	12 474
Power loss difference	**27,19**	**0,35**	**500**	**4 725 (saved)**

Transmission ratio

The new design built around 8 cam-lobes permits the use of full displacement as well as of multiple combinations of partial displacements. The axially located main displacement shifting spool can be activated by two external pilot signals, allowing the use of the MHP motor with three different displacements. This results in a transmission ratio of 4.

Noise

The MHP motor is intended at working as a direct drive, with no gear box. Its rotating group operates at the same speed as the driven wheels. When wheel angular speeds reach levels of 120 rpm or more, the low sound level of the Poclain motor become really obvious and is a big benefit when compared with competing technologies that use two stages of gears: both for the operator's comfort and for the farming community quietness.

Powerful Brake

The MHP motor includes a wet disk self-contained service brake: the brake relies on a stack of multiple disks that when compressed by the dynamic brake piston create a maximum braking torque of 33 000 Nm. The brake also works as a SAHR (spring applied hydraulically released) parking brake : when no brake release pressure is applied, a second piston compresses the same set of multiple disks to reach a parking brake torque of 18 000 Nm. The brake is very strong, its discs are permanently flushed and they can dissipate up to 1 million Joules of energy. Its disk splines mesh directly on the main drive shaft, which is the best design in terms of safety: the brake directly stops the wheel shaft; there are no sets of planetary gears between the wheel rotating drive and the actual brake.

On top of this combined brake design, the wheel motors can also produce a very high hydrostatic braking torque. Even when motors are used in small displacement (as is often the case at high speeds), the integral boosted brake design allows to "switch on" the non-active cam-lobes to reach a torque equivalent to the full motor displacement.

Reliability

Major efforts has been dedicated to ensure that the MHP motor undergoes all necessary endurance tests. The MHP is capable of working in very demanding environments, with high radical loads (it has been designed to work with 4WD 26T sprayer), high axial loads : large 54" wheels used by crop sprayers with tire diameter up to 2100mm and lots of dirt & debris threatening to damage the seals. Its reinforced oil sealing as well as protection against environmental dirt and its close cover design have been designed to make this motor very robust against leakage risks. In anticipation of future trends in the Agriculture market, the MHP motor has been qualified for max pressure of 500 bars

Range

The new MHP range is the cornerstone of the new range of HIGH PERFORMANCE Motors that will enhance the current line of Poclain Hydraulics cam lobe motors.

The main pieces of this transmission, beside the MHP motors, are the new PW pump, the new CT ECU controller and a new software called EcoDrive™.

The PW Pump is the new heavy duty closed loop pump from Poclain Hydraulics. Displacements available today are 85cc & 96cc. Displacements of 115cc & 130cc are planned for production release in 2016. The pumps are capable of reaching 500 bars and speed of 3850 rpm. They stand out through their compact length (the shortest on the market) and their exclusive electronic displacement control that provides precise and dynamic stroke control, a key feature to allow smooth motor displacements shifts. Their design with short piston strokes and robust sliding plate guarantees outstanding efficiency and good resistance against cavitation.

The PW Pump can be piloted with its own "integrated" control unit : this is the PWe pump. Several standard software can be loaded into this "on-board" controller. The most simple is the CAN Bus control which allows the PWe pump to be controlled via CAN by most external ECU controllers on the market. Other software can provide more functions so that the PWe with its inboard software become "self-sufficient" and can be used without any external additional controller.

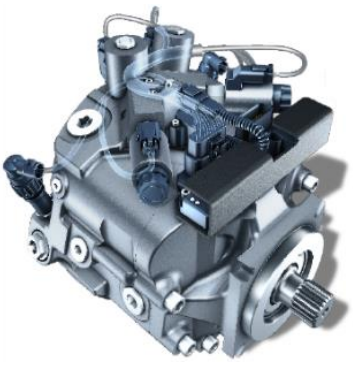

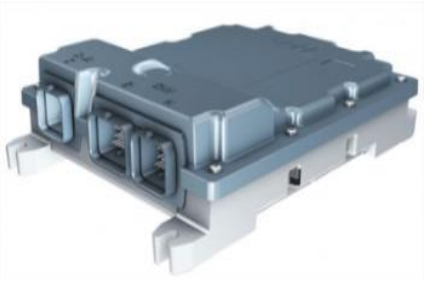

To match the PW pump, Poclain Hydraulics has developed a new range of ECU controllers, called Smart Drive CT range. The CT 200 & CT 300 controllers feature enhanced calculation capability, an increased number of inputs and outputs. They can be uploaded with software that support all functions assigned to hydrostatic transmissions such as pump management, engine control, driving ramp management, automotive drive mode, antistall, combined friction and hydrostatic braking, smooth motor displacement shifts, protection against excessive power, pressure and temperature, diagnosis and errors management. They are certified IP67 and compliant with safety standards as required by Machinery Directive 2006/42/EC and compatible with performance level d (Pl-d according to ISO 13894-1).

With the CT-Design software, Poclain Hydraulics is making access to electronically controlled hydrostatic transmissions easier by allowing OEM's to create their own management software. Thanks to a library of fully tested software functions, each customer using CT-DESIGN can, without any further help, combine the necessary functions to generate their software in just a few clicks, and reduce development time and costs.
In order to use the CT-DESIGN software, customers will first need to acquire a user license from Poclain Hydraulics.

A specific software layer is required for the above components' excellent performance to be fully revealed. Having gained a better knowledge of each component's best efficiency points, the R&D office of Poclain Hydraulics has developed software capable of exploiting them in the most effective manner possible, and only when necessary. This is the logic behind EcoDrive™ system management, a key part of the HIGH PERFORMANCE transmission by Poclain Hydraulics.

The principle is as follows: the EcoDrive software automatically adjusts (with no particular action required from the operator) the diesel engine speed, while guaranteeing the machine's travel speed by adapting the displacement of the pump and of the wheel motors. The MHP motors' high displacement ratio of 4 enables high road speeds while maintaining diesel engine speed at a low level, its optimum fuel consumption point. At the slightest increase in demand for power, the diesel automatically revs up again.

The test on a complete machine

Two Sprayers – Two Transmission Systems

Poclain hydraulics has operated for years extensive test benches allowing components validations and benchmarks of most technologies available on the market. In the heart of the Picardie farm-land, Poclain Hydraulics also invested in outdoor test tracks for mobile machinery. Poclain Hydraulics' facilities include a 660m long track, 20% and 30% slopes and have access to agricultural fields located immediately next to its R&D department.

The test tracks in Verberie (France)

Late 2013, our radial piston engineering team benchmarked several drive units, based on bent axis hydraulics motor and planetary gearboxes versus the preliminary concept of the HIGH PERFORMANCE transmission and control which could be converted with our HIGH PERFORMANCE system.

The test to be performed were not only carried out on the test track in house, but also on open road roundtrip and on field.

Within an interval of 3 months, successive tests were performed. First with the original transmission (bent axis motor and planetary gear-box) and then repeated with Poclain Hydraulics transmission. All physical parameters were recorded during those tests in order to measure the performances: flow, speed, pressure, temperature, noise, vibration, fuel consumption, GPS positioning… Series of tests were performed with the sprayer having either empty tank or full tank (approximate total weight of 20 tons), recording several sequences to get accurate results.

The circuit in the field : 1km in 2 directions

The road circuit : 14km

The sprayer equipped with the Poclain Hydraulics transmission over performed by far the original transmission. Overall behavior and driving feelings were excellent (more reactive, easier to control and quieter during high speed driving sequences). Even if those performances are not easy to convert in numbers, for sure, the low level of noise added to better steering capabilities are positively influencing the overall driving comfort level. When it comes to fuel economy, results were impressive: on the global cycle (on road + on field), Poclain Hydraulics measured 14% overall improvement directly related to the hydraulic transmission efficiency and 30% improvement when EcoDrive™ mode was activated. During the loop of 14 km on road, the EcoDrive™ saved 3 liters of fuel in 20 minutes at 42 kph average. Temperature stabilization was the other evidence of the efficiency improvement, with fluid being stabilized at 12°C below the level of the original high speed motor and gearbox combination.

Those results confirm that Poclain Hydraulics technology can greatly improve vehicle performances!

Instantaneous fuel consumption

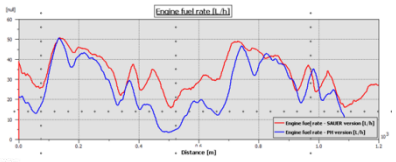

Cumulated fuel consumption

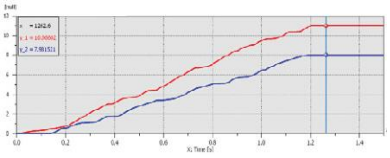

Temperature stabilization

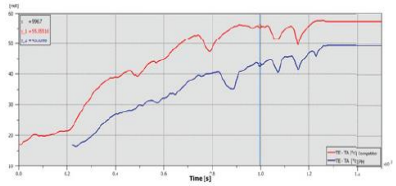

The Gain with EcoDrive™

The most demonstrative figures of this test show how important fuel consumption reductions can be. Let's take a closer look on the EcoDrive™ software influence.

Thanks to the EcoDrive™ software, the diesel engine speed is continuously adjusted to the actual power requirements.

At 15 kph and 65 kph the test machine equipped with EcoDrive™ software and the HIGH PERFOMANCE components demonstrate gains in term of instantaneous fuel consumption compared to the same machine with a standard software.

The gain with Boosted Brake ™

Why a Boosted Brake™ ?

Boosted Brake™ provides increased hydrostatic braking capabilities. It enables regulation requirements to be met in terms of braking distances, whilst reducing the use of the friction brakes. Boosted Brake™ complements the diesel engine's retardation capacity. It also avoids engine. Over-speed when braking. Using the principles of hydrostatic braking through the hydraulic motor's entire displacement capacity and not just the partial displacement that is active when braking occurs, it converts the machine's kinetic energy into heat in the oil in the hydrostatic transmission system. This heat is then evacuated in the cooler. Boosted Brake™ is especially interesting for all machines subject to high and/or repeated deceleration, both on the road and in the field. It is recommended for machines with diesel engines with a low retardation capacity.

The Braking is more efficient and engine is preserved: that is an essential point to ensure the lifetime of the machine

Environmental impact assessment of field mechanisation for a sustainable agriculture

Jacopo Bacenetti, Daniela Lovarelli, Marco Fiala

Department of Agricultural and Environmental Sciences. Production, Landscape, Agroenergy. Università degli Studi di Milano, via G. Celoria 2, 20133 - Milano, Italy.

* Corresponding author. Email: jacopo.bacenetti@unimi.it

Abstract

For the assessment of the environmental impact of agricultural machinery operations the collection of primary data is very useful because it permits to consider the local pedo-climatic and operative variables. However, only with recent technologies installed on modern tractors this can be more easily carried out.

In this study, the aim is to present a methodology that permits to improve the reliability of inventories for environmental sustainability studies carried out with the Life Cycle Assessment (LCA) approach. The tool ENVIAM is presented; it is characterised by the construction of an agricultural machinery operation made of single working times. In each of them, fuel consumption and engine exhaust gases are calculated and finally summed in a total value for the operation. To improve the capabilities of this tool, measurements have been carried out on field using a tractor equipped with CAN-bus, a data-collection software, GPS and engine exhaust gas analyser in order to measure fuel consumption and engine exhaust emissions data and to develop a prediction model for these variables.

The combination of CAN-bus, GPS and engine exhaust gas analyser is very effective and results having a widespread and promising role on several points of view, among which the environmental one. In particular, monitoring the field operation permits to identify the conditions in which improvements and inputs reductions can be reached.

Keywords: Agricultural machinery, big data processing, efficiency improvement, environmental sustainability, Life Cycle Assessment

1. Introduction

During recent decades, there has been a growing interest in quantifying and reducing the environmental impact of agricultural productions, mainly for freshwater pollution and emissions of greenhouse gases (Notarnicola et al., 2015). Among the agricultural activities, mechanisation is related to a substantial share of these negative effects (Niero et al., 2015).

Although lately standardised and extensively accepted methods for environmental impact assessment were developed (ISO 14040 series, 2006), their application to mechanical field operations is still limited (Lovarelli et al., 2017). This is due, on one side, to the difficulties in inventory data collection since they are site and time dependent and, on the other side, to the carefulness of machinery manufacturers that are developing concerns about the consumer (farmer) perceptions. With regard to inventory data collection, data can be obtained from both a primary source (i.e. directly collected or measured) and a secondary source (i.e. databases, scientific literature). Certainly, primary data are the most reliable but also the most difficult and time consuming to get. Especially for agricultural productions, the geographical, temporal and managerial specificities are much relevant on the inventory fulfilment and on the subsequent environmental impacts quantification. This is mainly because the local variables (soil texture, field shape, climate and seasonality, machinery adopted and management choices) can affect most of the environmental loads (Bacenetti et al., 2015).

Considering mechanisation of field operations, the availability on the market of modern tractors and implements and of new techniques or management strategies determines the importance of collecting primary data for appropriate assessments. In particular, thanks to modern technologies installed on modern tractors such as CAN-bus (Controller Area Network), a huge amount of data is accessible and is measurable constantly and simultaneously to the work on field (Fellmeth, 2003; Pitla et al., 2016). These data describe how the engine works as well as instant working features and interactions in the tractor, which encompasses the possibility of deeply increasing the analyses reliability on modern machinery and of optimising inputs use and management (Bietresato et al., 2015).

Primary data are needed. In fact, although secondary data are more easily available, they may include simplifications and average values that do not describe correctly the studied system. Specifically, the most important side effect of secondary data is that it results unfeasible to quantify the reduction in environmental load achievable with new machines and innovations in technologies, with machines already available on the market (e.g., minimum and strip tillage, sod-seeding) but not included in databases or, merely, by selecting more suitable machines or performing a proper coupling between implement and tractor. In fact, in the most used database applied in Life Cycle Assessment (LCA) studies (i.e. ECOINVENT®), the impact of the most common field operations is included; however, it is assessed considering average pedo-climatic (e.g., soil texture and moisture), operative (field shape, slope and transfer distance) and mechanical conditions (engine features during transfers, turns and working phases) and, consequently, is not always reliable.

In this context, the tool ENVIAM (ENVironmental Inventory of Agricultural Machinery operations) was developed to support the environmental impact evaluation by fulfilling inventories for field machinery operations used in defined

local working conditions (Lovarelli et al., 2016). Its application already showed that site and time specific data are very important and can show considerably different results from the average ones (Lovarelli et al., 2017). Therefore, improving the capabilities of a tool such as ENVIAM is essential. The high-level modelling can be reached by monitoring field operations through the modern technology and instrumentation, which is a very useful step forward to agricultural sustainability assessment, efficiency increase and inputs use.

The aim of this study is to describe the main methodological steps to follow to have a reliable quantification model and tool appropriate for inventories that can be obtained thanks to the technological capabilities of recent machinery. In fact, by monitoring a tractor working in several different conditions, it is possible to model the behaviour of the engine also along other field operations with high accuracy. Moreover, this determines the possibility of understanding how the inventory reliability affects the environmental impact results of agricultural machinery operations got through the Life Cycle Assessment (LCA) method.

2. Materials and Methods

The study is inserted in the context of:

(i) the Life Cycle Assessment (LCA) approach, with focus on the inventory fulfilment and on its reliability, and on the consequent environmental impact assessment;

(ii) the mechanisation efficiency improvement, monitoring of work conditions, optimisation of inputs use and technological innovations.

2.1. Life Cycle Assessment

The Life Cycle Assessment (LCA) (ISO 14040, 2006) is a standardised method adopted worldwide for quantifying the potential environmental impacts of processes for products or services during their whole life cycle using a holistic approach. In more details, there are four steps in LCA:

(i) goal of the study, selection of the functional unit, description of the system and of the system boundary;

(ii) Life Cycle Inventory (LCI) data collection, in which the flow of materials and energy from the studied systems and the environment are identified and quantified;

(iii) Life Cycle Impact Assessment; during which, thanks to specific characterisation factors, the inventory data are converted in few numeric indicators of environmental impact;

(iv) interpretation of the results and identification of the process hotspots.

The Life Cycle Inventory is the most complex phase, due to the inputs and outputs data collection that must be trustworthy, in order to obtain correct environmental results. In particular, often, inventory data are obtained from databases (e.g., ECOINVENT®), which may represent a simplification and/or an inappropriate inventory of data for the specific studied system. This occurs because, as explained previously for field operations, the collection of data concerning working times, fuel and lubricant consumption and pollutants emitted into air with the engine exhaust gas emissions is not easy.

2.2. ENVironmental Inventory of Agricultural Machinery operations (ENVIAM)

ENVIAM was developed at the Department of Agricultural and Environmental Sciences, Production, Landscape, Agroenergy at the University of Milan to fulfil the Life Cycle Inventory phase of a LCA study for the most common field operations for crop production (Figure 1).

The strength is that the inventory is completed thanks to the accurate quantification of mechanical parameters (e.g., tractor and machinery characteristics and coupling), of fuel, lubricant and materials consumption, and of engine exhaust gases emissions. In more details, this tool permits to couple tractors and implements having a wide selection of alternative machinery in two databases and permits to fulfil the inventory following a more detailed method: the operation is split in several working times and variables such as absorbed power, fuel consumption and related exhausts emissions are calculated in each of these single working times. The identified working times have been selected from Reboul (1964) and are most significantly distinguished in the effective work on field, turns at the headlands, transfers, refilling/emptying, maintenance, etc. The mechanical and operative variables (e.g., engine load, engine speed, brake specific fuel consumption, working time) affecting power, fuel and engine exhausts are selected for each of the working times and are used to calculate the related fuel consumption and exhaust gases emission; finally, they are summed to obtain the total value of the whole operation.

A user-friendly system characterised by tests is also available to highlight possible inconsistencies on the mechanisation point of view. Further details can be found in Lovarelli et al. (2016, 2017).

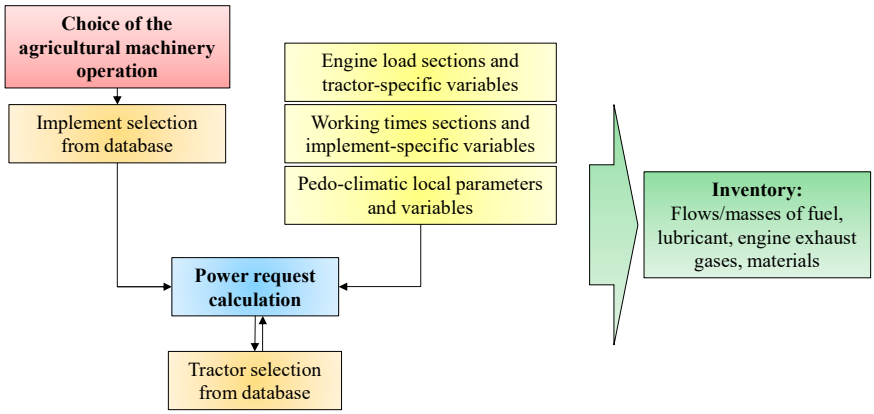

Figure 1. Schematic flow of ENVIAM steps.

One of the major benefits of ENVIAM is that the mechanical calculations permit to couple tractor and implement at the user discretion; therefore, the data about coupling can be referred either to already existing contexts (e.g., from interviews with farmers/workers) or to hypothesised conditions of which studying the inventory results. Another benefit is related to the possibility of building the operation (and therefore the inventory) as sum of working times that compose the operation, which permits to recognise directly what are the most affecting portions on the inventory. Moreover, the alternative implements available on the market also affect the environmental impact, due to different material composition and mass; therefore, the availability in the databases of different implements among which to choose is essential for inventory reliability.

Adopting ENVIAM, the substantial differences in environmental impacts of analyses carried out with local data instead of average data have already been proved through case studies. The deepening of knowledge and the improvement of the quantification tool capabilities has resulted being a much interesting step in view of more accurate assessments related to the machinery innovations.

2.3. Researched improvement

As a first concern, in ENVIAM are available calculation methods and models that require a quite small amount of input information and therefore, although giving very interesting results, may represent a simplification of the complex engine-tractor-implement system. Among these, fuel consumption is one of the major variables that also affects engine emissions.

In particular, it is well known that fuel consumption is affected by several engine characteristics, as well as by operative ones. As regard to the operative characteristics, they involve the pedo-climatic working conditions, the operation in progress, the driver abilities and the sudden variations in engine characteristics (e.g., torque and engine speed). Similarly, and even much more sharply, are again the operative variables that mostly affect (together with the Emissive Stage of belonging) the exhaust gases emissions. Although both fuel and exhaust gases' quantification is already performed in the actual version of ENVIAM, a progress has been foreseen as an essential step in the improvement of inventory data collection. This has been carried out by involving the monitoring, measurement and model development of fuel consumption and exhaust gases emissions following the steps shown in Figure 2.

Figure 2. Steps completed from the experimental trials to the model conclusion.

2.3.1.CAN-bus application

Among the techniques developed to map, understand and study the activity of the tractor engine and of the related devices while working on field, the most widespread system is CAN-bus (Controller Area Network). CAN-bus is a frequently available serial high-speed wired data network connection present on modern tractors that permits to electronic devices to communicate with each other and that, coupled with storing instrumentation, permits to collect a huge amount of data directly deriving from the tractor while working on field and with a very detailed time scale (Speckmann and Jahns, 1999). CAN-bus was introduced by Robert Bosch GmbH in 1986, firstly for an automotive

application. Applied to agricultural tractors, it is normed with SAE J1939 that defines the connections of electronic devices installed on machinery and then also following the standard protocol ISO 11898 (ISO, 2003).

CAN-bus has permitted to use and take advantage of electronics on agricultural machinery, which results in substantial improvements in the monitoring and big data collection. Mostly, the use of big data is very helpful in the sustainability evaluations because it permits to study each operation, improve the efficiency and control (and potentially reduce) inputs introduction. However, the electronic communication can be applied to other several scopes, such as diagnostics on board, maintenance scheduling, precision agriculture, etc.

Considering the application to data collection for both mechanisation and sustainability assessments, the application of CAN-bus and other instrumentation has two main advantages: first, the continuous monitoring of the operation on field and second, the model prevision that can reach a very high precision thanks to the data collected in a very detailed temporal scale. Implementing such big data of the tractor engine features (e.g., engine speed, engine torque, power) as well as of the working time and speed and of the pedo-climatic features (e.g., soil texture, field shape), permits to build a detailed map of the work of the tractor and, when applied to ENVIAM, to calculate its outputs with additional precision on the operation under study.

The most interesting progress completed with big data referred to tractor engines is that, once the data are collected for the tractor on different working conditions, a robust prevision model can be created. Furthermore, the model itself can be used to predict the behaviour of the tractor working with other implements and during other operations. This means that the monitored tractor is mapped and its behaviour can be reconstructed, although without having further primary data. Therefore, once enough data are available for a robust model development, the prevision becomes essential to further analyses.

2.4. Methods

In order to have the primary data for the improvement of the reliability and applicability of inventories about agricultural machinery, field experiments were carried out at the Swedish Machinery Testing Institute (Umeå, Sweden) and at the Department of Energy and Technology at the Swedish University of Agricultural Sciences in Uppsala. Field experiments were made using: (i) CAN-bus for registering engine data and tractor-related data and a software for data collection and storage; (ii) GPS (Global Positioning System) to have the tractor position and to link this position to the collected data; (iii) a portable emission analyser for exhaust gases emissions measurement and storage (CO_2, CO, NO_X).

Figure 3 shows the tractor and the on-board mounted gas analyser system. The software for storing CAN-bus data is shown in Figure 4.

Figure 3. Valtra N101 tractor with the implemented system to collect exhaust gases for the gases analyser.

Figure 4. On-board software for the collection and storage of CAN-bus data.

The modelled variables were:

(i) fuel consumption (FC; dm^3/h) and

(ii) exhaust gases emissions (EM; g CO_2/h, g CO/h, g NO_X/h).

For all of them, the modelling was carried out introducing the equation reported below (Eq. 1) dependent on torque (M; Nm), engine speed (s; rpm) and engine-specific coefficients (Jahns et al., 1990; Lindgren, 2008). Torque and engine speed were gathered from the measurements, while the 9 coefficients adopted were calculated referred to the equation modelling the semi-static condition and were identified using the minimisation of the error related to variance. FC and EM were quantified per second, following the sensibility of CAN-bus, and afterwards were quantified for all working times. The equation was validated through data obtained during measurements completed with the same tractor.

$$FC = c_1 \cdot s + c_2 \cdot s^2 + c_3 \cdot s^3 + M \cdot (c_4 \cdot s + c_5 \cdot s^2 + c_6 \cdot s^3) + M^2 \cdot (c_7 \cdot s + c_8 \cdot s^2 + c_9 \cdot s^3) \quad (1)$$

where *FC* is fuel consumption, volume time $^{-1}$; $c_1..c_9$ are engine-specific coefficients, dimensionless; *s* is engine speed, routes time^{-1}; *M* is torque, force length.

FC and EM were also expressed as specific values (brake specific fuel consumption, bsfc, g/kWh; specific emissions, EM_{spec}, g/kWh) in order to be widely comparable.

3. Results and Discussion

Data processing involved a first geographical and spatial analysis of the fields and then the model application for fuel consumption and exhaust gases emissions.

Consequently, the worked fields were analysed in their shape. The available GPS coordinates were used to identify the tractor spatial position and to distinguish the field shape and working states that describe the tractor working activity. This distinction permits to have data and results related to at least three working states, as also shown in Figure 5:

(i) effective work on field (moving forward while working, with a straight direction);

(ii) turns at the headlands (turning position);

(iii) stationary (no change in position, mainly with idling conditions).

In each state, characterised therefore by similar but not equal working features, the measured fuel consumption and exhaust gases were identified to have a series of values referred to the same grouping of states. According to the plan definition of each field and each operation, working features such as working speed, engine speed, torque, engine load, differed.

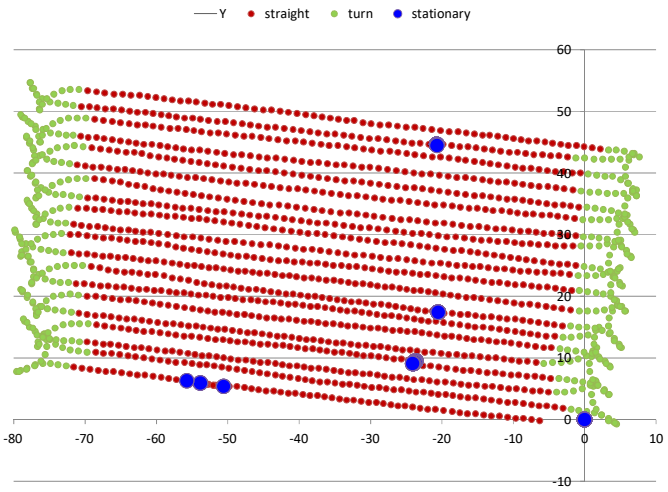

Figure 5. Working states on a field obtained thanks to the processing of the tractor GPS coordinates. Red represents the effective work, green is the turn on headlands and blue is stationary position with no-work ongoing.

Offsetting the positions, both CAN-bus and engine exhaust gases emissions from the analyser could be related to the same temporal position. All results from the measurement, monitoring and from the consequent modelling were also linked to the spatial position of the GPS and, therefore, were attributed to each working state.

With a complete data collection from a tractor in which the combinations concerning power (i.e. product of torque and engine speed) are established, other field operations - even with much different absorbed engine power - can be retraced because the engine features that describe the operation are already mapped. In more details, once the tractor-specific combinations are available, assessments related to fuel consumption and exhaust gases emissions can be obtained thanks to the modelling. Therefore, FC and EM from any operation carried out with the same tractor can be calculated.

A very interesting possibility concerns also the monitoring of exhaust gases emissions that, being measured on field during the operation, represent a step forward in defining the normative emissive limits. Attributing emissions to working states showed that, commonly, considerable and consistent differences emerge along the operation. Especially, with stationary-idling conditions and transient conditions, exhaust emissions of NO_X, CO and CO_2 increased a lot, and they represented up to 15% of the total working time. Measuring data on field it might result more difficult to respect the emissive limits, mainly because they are defined in steady-state conditions and not on field; therefore, although in the steady-state measurements engine exhaust emissions comply with the law, on field there exist more variability. For example, also during turns at headlands the measured engine emissions resulted higher than during the effective work.

From the results, it emerges the huge potential of this technology (CAN-bus + GPS + gas analyser) for environmental sustainability and for the reduction of inputs use. The possibility of linking any collected data and of performing big data processing permits to understand the behaviour of agricultural machinery along any operation. According to the goal, an optimisation of fuel consumption can be reached, mainly by understanding what are the engine conditions that determine the best fuel use and by adopting them. Moreover, any engine feature such as engine speed, engine load, torque, power, etc. can be monitored on a time interval that depends on the sensitivity of the adopted instrumentation and can be used for specific research requirements.

4. Conclusions

In this study was shown that the reliability of inventories carried out with local variables is very important, since the inventory data can deeply affect the downstream results of the study. Primary data are always more reliable than secondary data but their most important side effect is that they can be difficult, time consuming and expensive to get. However, with the spreading of modern technologies on agricultural tractors and modern machinery in general, the collection of primary data regarding mechanisation of field operations is getting easier. First, because the technological improvements are available on any modern tractor and secondly because data can be collected without any specific manpower utilisation, since an assembled software can store them while the tractor is working on field; then those primary data must be processed. Due the ease in measurements with CAN-bus, GPS, emissions analysers and analysis software, inventories for environmental impact assessments can be fulfilled with high reliability. In particular, engine-specific equations able to describe fuel consumption and exhaust gases emissions depending on torque and engine speed and any relevant available information can be developed for the studied tractor.

With such a big amount of available data, a huge potential for tractors analysis can be hypothesised. As shown in the study it is possible, among others, to measure data on field with specific equipment and to assume that the engine's

behaviour is the same for other operations, although the operations themselves can differ. In fact, the implement coupled with the tractor – within the same engine features - does not affect the variables concerning the engine behaviour. Accordingly, after having measured tractor data on field and after having analysed and developed specific coefficients for fuel and emissions quantification, different operations can be built, and detailed and reliable inventories can be realised, distinguishing engine by engine.

References

Bacenetti, J., Fusi, A., Negri, M., Fiala, M., 2015. Impact of cropping system and soil tillage on environmental performance of cereal silage productions. Journal of Cleaner Production. 86, 49-59.

Bacenetti, J., Lovarelli, D., Fiala, M., 2016. Mechanisation of organic fertiliser spreading, choice of fertiliser and crop residue management as solutions for maize environmental impact mitigation. European Journal of Agronomy. 79, 107-118.

Bietresato, M., Calcante, A., Mazzetto, F., 2015. A neural network approach for indirectly estimating farm tractors engine performances. Fuel, 143, 144–154.

Fellmeth, P., 2003. ISO11783 a Standardized Tractor – Implement Interface. iCC 2003 CAN in Automation, 8–13.

ISO 11898, 2003. Organization for Standardization. Standards catalogue – ISO/TC 22/SC 3 – electrical and electronic equipment.

ISO 14040 series, 2006. Environmental management – Life Cycle Assessment – Requirements and guidelines. International Organization for Standardization.

Jahns, G., Forster, K-J., Hellickson, M., 1990. Computer simulation of diesel engine performance. Transactions of the ASAE. 764-770.

Lindgren, M., 2004. Engine Exhaust Gas Emissions from Non-road Mobile Machinery. Ph.D Thesis, Department of Biometry and Engineering, Swedish University of Agricultural Sciences, Uppsala, Sweden.

Lovarelli, D., Bacenetti, J., Fiala, M., 2016. Life cycle inventories of agricultural machinery operations: a new tool. Journal of Agricultural Engineering. XLVII, 40-53.

Lovarelli, D., Bacenetti, J., Fiala, M., 2017. Effect of local conditions and machinery characteristics on the environmental impacts of primary soil tillage. Journal of Cleaner Production. 140, 479-491.

Niero, M., Ingvordsen, C. H., Peltonen-Sainio, P., Jalli, M., Lyngkjær, M. F., Hauschild, M. Z., Jørgensen, R. B., 2015. Eco-efficient production of spring barley in a changed climate: A Life Cycle Assessment including primary data from future climate scenarios. Agricultural Systems, 136, 46–60.

Notarnicola, B., Salomone, R., Petti, L., Renzulli, P.A., Roma, R., Cerutti, A.K. (Eds.), 2015. Life Cycle Assessment in the Agri-food Sector. Case Studies, Methodological Issues and Best Practices. Springer. pp. 415.

Pitla, S. K., Luck, J. D., Werner, J., Lin, N., Shearer, S. A., 2016. In-field fuel use and load states of agricultural field machinery. Computers and Electronics in Agriculture, 121, 290–300.

Reboul C., 1964. Temps des travaux et jours disponibles en agriculture. Official document of CIOSTA Institute. Economie rurale. 61 pp. 50-80. 1964.

Speckmann, H., Jahns, G., 1999. Development and application of an agricultural BUS for data transfer. Computers and Electronics in Agriculture, 23, 219-237.

Disseminating and Promoting Smart Farming Technologies – The Smart AKIS Network.

David Tinker [a,*], Maria Kernecker [b], Andrea Knierim[b], Angelika Wurbs[b], Sandra Wolters[c], Frits van Evert [c], Natalia Bellostas[d], Samy Aït-Amar[e], Thanos Balafoutis[f], Spyros Fountas[f]

[a] DTA Ltd / EurAgEng, 17 Chandos Rd., Ampthill, MK45 2LD, UK.

[b] Leibniz Centre for Agricultural Landscape Research (ZALF), Eberswalder Straße 84, 15374 Müncheberg, Germany

[c] Wageningen University & Research, Dept of Agrosystems Research, PO Box 16, 6700 AA Wageningen, The Netherlands

[d] Iniciativas Innovadoras, Zabalgaina St., Zizur Mayor, 31180. Navarre. Spain.

[e] ACTA, 149, rue de Bercy, 75595 Paris cedex 12, France

[f] Agricultural University of Athens, Laboratory of Agricultural Engineering, Iera Odos 75, Athens 11855, Greece

* Corresponding author. Email: secgen@eurageng.eu

Abstract

This paper summarises the early stages of the Smart AKIS project which aims to collect and disseminate Smart Farming Technologies (SFT) in line with farmers' needs. The methodology of collecting information and opinions from over 270 farmers from seven countries about SFTs is given. The methodology of collecting and analyzing the results of 718 scientific articles and 201 research projects to determine what the research topics and results are also outlined. Further information about the 164 SFT products that had been submitted by mid-January 2017 and entered into the inventory database are also summarized. There is outline information on how to submit research and product information to the inventory database on an on-going basis so that it can be promoted to end users (farmers, farming-advisors and contractors) and also seen by potential funders and collaborators for further product development and research collaboration which is also an objective of the Innovation Workshops which are starting in February 2017 around the seven countries.

1. Background and Introduction

The rapidly evolving Information and Communication Technologies have caused such a fast development in Smart Farming Technologies that researchers, equipment suppliers and certainly farmers and their advisers are struggling to keep up with the technologies available, whether commercially offered or completing the final stages of applied research projects. The self-sustaining Smart-AKIS network (www.smart-akis.com) has been designed for an effective exchange between industry, applied research, agricultural advisors and the farming community. The aim is that directly applicable solutions are widely disseminated and the grassroots needs and innovative ideas are comprehensively acquired. This will contribute to closing the divide between applied research and commercial innovation and will benefit the agricultural engineering and technology industry and the farming industry.

"Smart Farming Technologies" (SFT) covers the marketable, affordable, reliable and time-saving technologies developing from:

- farm management information systems,
- precision farming and
- agricultural automation and robotics.

The benefits are related to more efficient application of inputs, increased work speeds, comfort, improved decisions and enhanced flexibility.

The Smart AKIS project is the European Network on Smart Farming and will integrate aspects of the innovation processes and will lead to interactive, innovation-based, collaborations among researchers, developers and suppliers, advisors and farmers through multi-actor workshops.

AKIS is the acronym for Agricultural Knowledge and Information Systems, or Innovation Systems; both meanings are applicable in this project.

This paper outlines an early stage of the project with the following aspects:

- Collection and analysis of farmer SFT use and opinions,
- Collection and analysis of the existing, and impending, knowledge related to SFT a) from research and projects and also b) available from suppliers of SFT. Both sets of information are combined into an "inventory"
- Production of easily accessible end-user material for use by farmers and their advisors and
- Innovation support workshops to enable farmers and advisors, researchers and SFT suppliers and research funders to meet and discuss current useful developments, potential projects and supply and marketing networks.

This paper highlights particularly the farmer survey, industry solutions and research project results, and the on-going collection process for the Smart-AKIS inventory and provide background for applied researchers and suppliers of SFT.

The project goal is to enable the European farming community to regularly use treat Smart Farming Technologies and so bridge the gap between practice and research by identifying and delivering new Smart Farming solutions to fit farmers' needs.

The project of 13 partners from seven countries is supported by the EC Horizon 2020 program and the European Innovation Partnership Agricultural Productivity and Sustainability (EIP-AGRI). The project has a focused approach, concentrating on Smart Farming Technology for crop production. CEMA is a partner and with its national member Associations (including AXEMA) it ensures that there is a strong involvement of the machinery industry and the EurAgEng society, with 18 national societies (including SitmAfgr), brings in over 2000 European professional agricultural engineers.

Smart AKIS is aware that many Smart Farming solutions are available in the market now, but that many social and economic obstacles remain for the wider adoption of such technologies by farmers who increasingly demand that new solutions fit their requirements. As a Thematic Network, Smart AKIS adopts a multi-actor approach, targeting all stakeholders involved in agricultural innovation processes, such as farmers, farmer-associations, research organisations, advisory and extension services, agronomists and agricultural consultants, agricultural equipment suppliers and providers of smart farming solutions.

2. Methodologies

2.1 Farmer survey. The partners of Smart AKIS, led by the team at ZALF, prepared a comprehensive questionnaire[1] and surveyed more than 270 farmers and experts from all over Europe to understand and respond to the:

- Needs and interests of Smart Farming by farmers from France, Germany, Greece, Netherlands, Serbia, Spain and UK and
- Factors hindering the adoption of Smart Farming in Europe.

2.2 Published research survey. Teams at the universities in Wageningen and Athens undertook a systematic review of literature collection methods before retrieving over 11000 articles[2]. These articles were then manually assessed, over two rounds of filtering, to select only those relevant to SFT, using first the abstract, and then using the full article. The final selection was based upon those of practical relevance and in practical development. This led to about 718 articles being in the database with data from a further 201 EU research projects. An ongoing on-line survey is included for researchers to add to the database details of SFT research which is at an imminent stage for publication. This survey follows the EIP-Agri Common format for interactive innovation projects [3].

2.3 Industry solutions survey. Following the format and analysis of "Published research survey" this survey was also promoted for industry solutions[4]. The survey was made available online to suppliers of SFT and promoted by various networks including FIWARE, FRACTALS and Smart Agrifood II as well as the project members, especially CEMA and EurAgEng. Contacts were also made with suppliers at precision farming events, agricultural machinery shows and similar events to encourage SFT suppliers to complete the survey and be added to the database. These personal contacts invariably needed an email to give further details of the project and its expected outcomes to highlight the advantages for SFT suppliers to be involved. As for the "Published research survey" the survey entries were added to a database for analysis.

2.4 Innovation support. Smart AKIS is holding Innovation Workshops, including to generate innovations and to assist the marketing and uptake of products and projects on Smart Farming in France, Germany, Greece, Netherlands, Serbia, Spain and UK. Targeted at farmers and advisors, suppliers and researchers these dissemination, innovation and networking events will also encourage research funders and other investors to attend and help promote further R&D projects as well as marketing of commercially available Smart Farming Technologies for the end-users. The 21 Workshops will start from late February. A set of guidelines have been produced by Smart AKIS to help ensure that the workshops cover the project needs, build on best practice and produce analyzable outcomes.

Although a snap-shot of research and industry surveys has been taken for the current reports, submissions to both the research and industry (products) surveys for entry to the inventory database can be completed up to September 2018 by researchers and industry suppliers. The survey is given in the appendix of the reports [2, 4] and can be completed on-line via the Smart AKIS website.

3. Results and Discussion

By its nature this paper is a collection of the results from project reports and documents and much of the information below is taken directly from these, which should be referred to for greater detail and analysis.

3.1 Farmer survey.

The full results are available in a project report[1] and further analysis will be included in scientific papers. Much of this summary is also taken from a project summary briefing[5].

Project partners interviewed more than 270 farmers from France, Germany, Greece, Netherlands, Serbia, Spain and UK.

3.1.1 Current situation perceived by farmers.

- Crop disease reduction and soil conservation are farmers' main challenges but farmers are unsure whether smart farming can overcome them.
- Reducing harvest losses was considered most important in Greece (89%) and Serbia (90%). Reducing water use was also ranked as highly important in Greece (61%) and Serbia (74%) but surprisingly less important in Spain (50%).
- Farmers perceive the benefits of smart farming in terms of productivity and managing inputs rather than the environmental benefits.
- Private independent advisors, other farmers, and agri-tech providers are the three most important sources of information and support. Public extension and banks are least important.
- The most useful SFT are considered as 1) Robots for monotonous work processes (e.g. weeding, hoeing, harvesting), 2) Real-time diagnostics via drones, satellite imagery, or smart phone sensors, 3) Integration of various Smart Farming Technologies, and 4) Data for information and decision support.
- High cost and poor compatibility between devices and systems remain the main barriers for adoption.

3.1.2 Farmers views looking ahead

- Alliances with agro consultants might help a better penetration and adoption and Smart Farming as a service may fit farmers' needs. This is shown in the later research and industry surveys by contractors being a main user.
- Suppliers, consultants and advisors could usefully focus further on dissemination of existing technologies and the development of new ones on the farmers' main areas of interest: including Robots and Smart Equipment, remote diagnosis and monitoring and big data for farm management.
- Further adoption may be facilitated by lower cost, suitable equipment size, compatibility between equipment ("plug and play") and ease of use.

3.1.3 The main project ideas and needs captured from the survey include:

- GPS and similar devices (e.g. auto-steering) are mainly used in arable crops.
- Agricultural apps were selected more by vineyard and orchard farmers.
- Weather stations and soil moisture sensors with automatic data upload are more valuable for orchards and vineyards that rely on irrigation.
- Drones, mapping, and aerial imagery are potentially of more interest for arable growers.

Three-quarters of the farmers said they experiment on their farms. For example:

1. most frequently with equipment: building, adapting, and adjusting machinery to improve work processes;
2. testing new technologies and cropping patterns: including trying new varieties and rotations;
3. cultivation: including seeding, drilling, tillage, soil management and other management methods.

Over half of the farmers provided suggestions for existing SFT to make them more acceptable or useful. For example: improving access to SFT, the overall technological system, device level, data level, costs and compatibility.

3.2 Published research.

These findings and conclusions are shown by Wolters *et al* [2] and the main points are given here.

The total number of research related entries is 919 (as at January 2017); formed of 718 scientific articles and 201 research projects. The number of articles are growing quickly and the Technology Readiness Level most commonly

given (41%) is 5 (*Technology validated in relevant environment*) and fewer (29%) are in TRLs 7-9 (*System prototype demonstration in operational environment* to *Actual system proven in operational environment*).

The clear majority of research projects are investigating recording or mapping technologies to get more information on agronomic variables in the field. Research articles are more about farm management information systems or apps.

There are many field operations involving SFTs in projects and articles but scouting of crops or soil was the largest topic for articles (39% of those with a topic given) with irrigation and fertilizer application also very important.

Considering the keywords used as a way of classifying SFTs used in the research articles and in projects then machinery related or focusing on farming practices and / or production systems are most common. Plant production, fertilizer application and water- and soil management are also considered very important.

The applications for SFTs are similar for research articles and research projects. Many entries, 40% of scientific articles and 60% of research projects, focus on replacing an already existing technology but mostly this does not require a major change to an existing system. Significant learning is often required for the correct application of SFTs. In many situations, there is more than one purpose or application to a SFT and the effects of the SFTs can be observed directly by the farmer.

Regarding the application of SFTs, contractors were most often identified as the most likely users of SFTs.

Using SFTs often brings an increase in revenue, a reduction in stress and labour for the farmer and a reduction in energy use. A reduction in costs was often expected by implementing SFTs. There were also some improvements expected regarding environmental aspects.

SFT is in continuous development, it was seen that there is a tendency toward the scouting of crops and soils with information technology solutions. Regarding the application of SFT, research SFTs are often building on existing technology. Although significant learning is required this does not often lead to large time investments for farmers. The results of SFT are easy to observe. Both revenue and environmental aspects are of great importance in SFT development in the research sector.

3.3 Industry Solutions.

This information is from the second report by Wolters *et al* [4] and shows a submission of 164 survey entries related to products (January 2017) and these can be classified mostly as recording or mapping tools. The development of farm management information systems and Apps is also an important group and is like the research entries [2]. There are also many developments for variable rate technology. Slightly fewer entries were involved in guidance or controlled traffic farming technology or robotic systems. Overall, there is a consistent spread between the different classifications from 43 to 77 of the 164 in the five classifications.

Many products submitted can be used for fertilisation, disease control and pesticide application related operations. However very few SFTs involve post-harvest storage which is again like that found in the research entries[2].

Often the SFT product replaces a tool or technology that is currently being used and can then be used readily without making major changes to the existing system.

In contrast to research SFTs, the SFT products are mostly presented as very easy to use and in most cases, do not require significant learning.

Sometimes, the SFT can be beneficial in ways other than originally developed by the supplier. SFTs are estimated to have effects that can be directly observed by the farmer and they do not require large time investments. Results from SFTs can often be interpreted directly.

Like the research SFTs entries, the stakeholders that are most likely to use product SFTs are contractors.

The main keywords involved with products are: farming equipment and machinery, farming practice and agriculture

production but these are often combined with other options, particularly: production, fertilisation and soil and water management. In contrast keywords related to environmental aspects such as farming-forestry competitiveness, biodiversity and nature management, waste byproduct and residues management, energy management and climate and climate change were less frequently associated with marketed SFTs.

The results from the product entries show quite strong similarities with the list of research entries. Most positive links are in revenue, (soil) biodiversity and variable and input costs. On the other hand, emission reductions are often expected as well as a reduction of stress or fatigue for farmers.

An example of the on-line inventory database for the Dashboard, Overview and Details of a product are given here.

Figure 1 Screen shot of the Inventory Dashboard

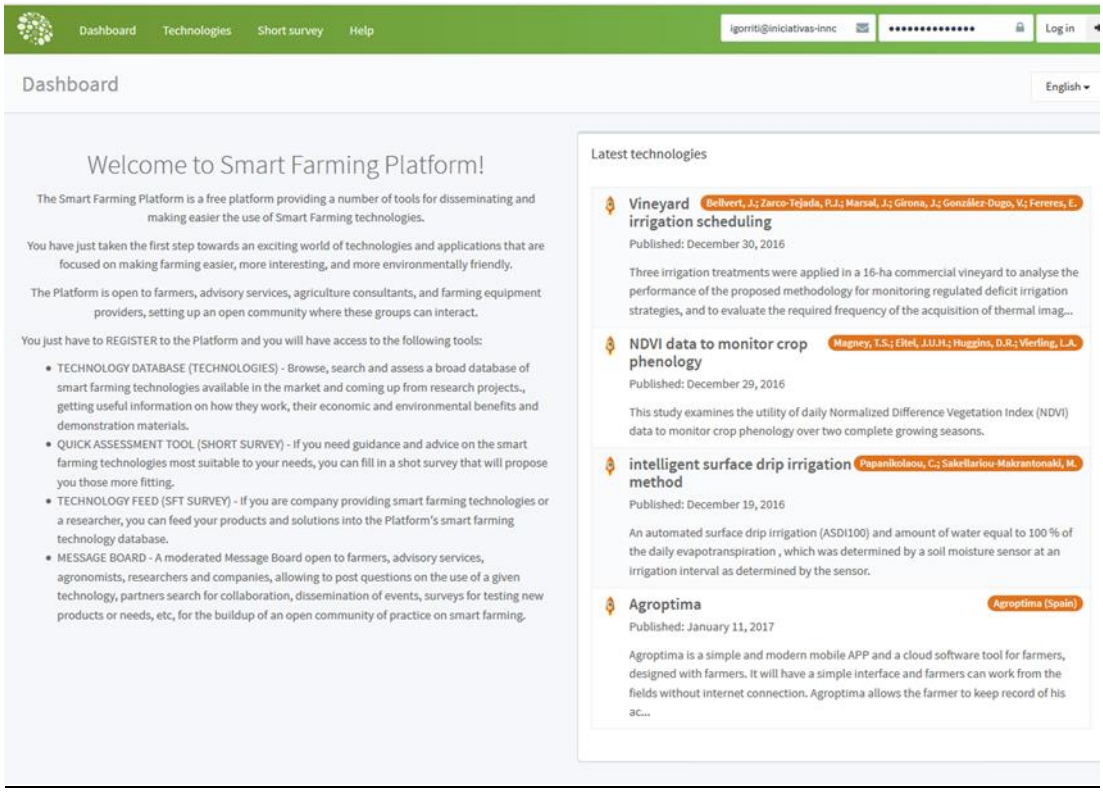

Figure 2 Screen shot of the Overview of Technologies

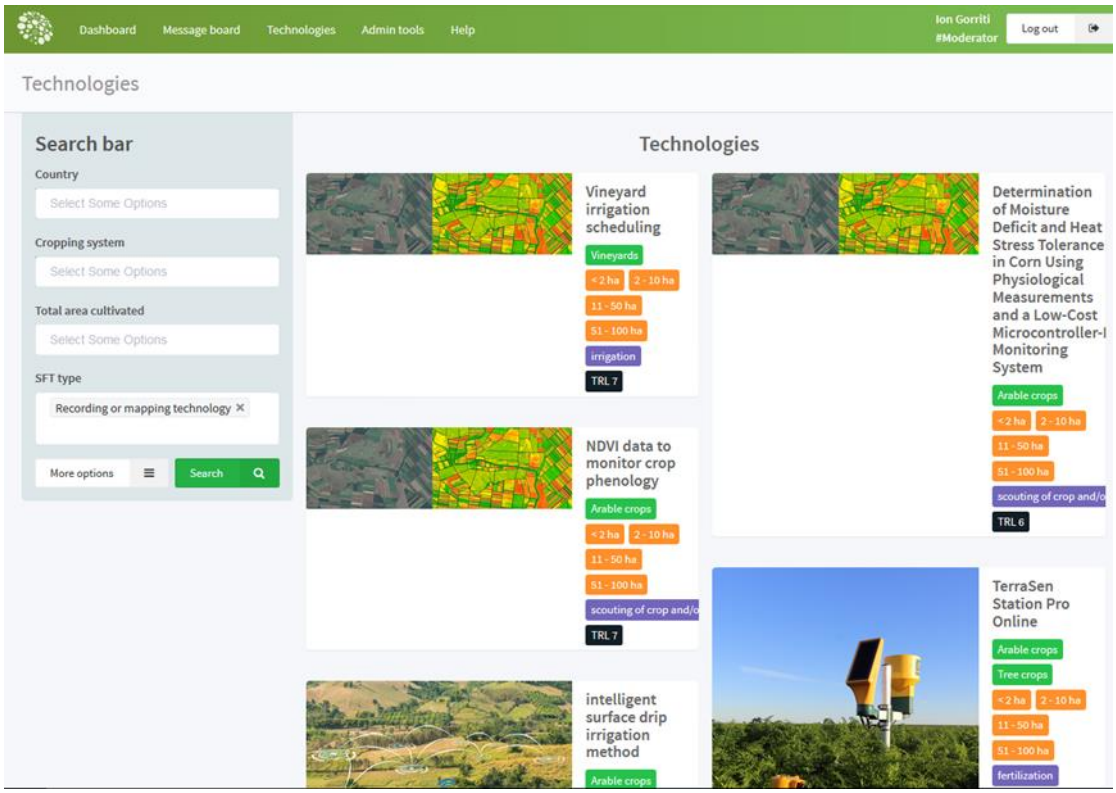

Figure 3 Technologies filtered during search of inventory database.

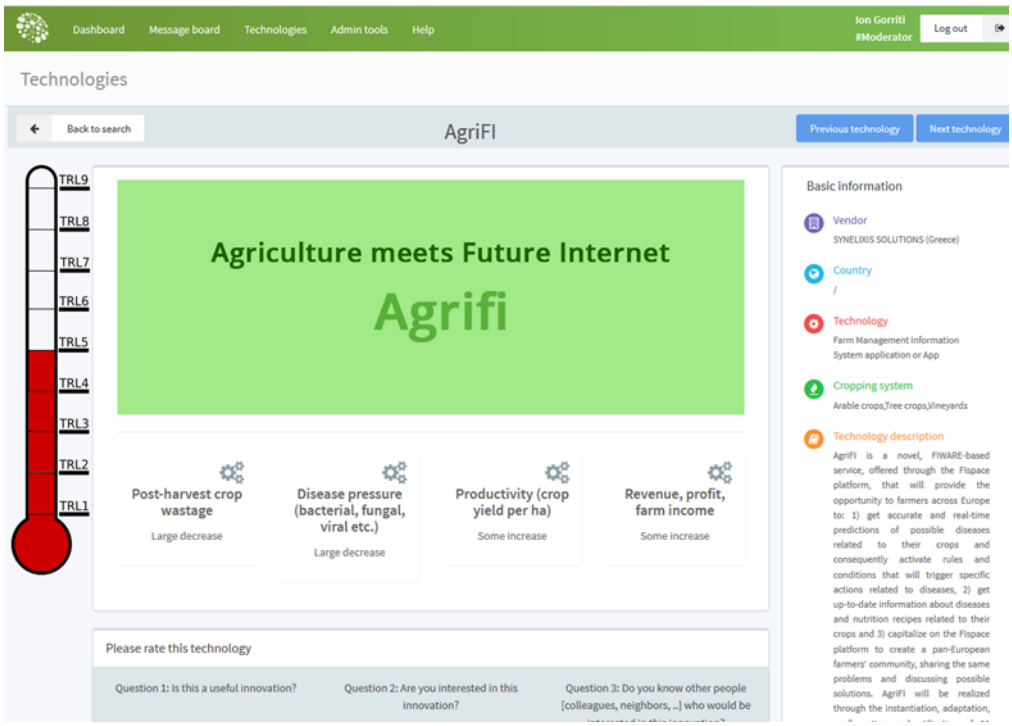

3.4 Innovation Support.

A program of Workshops in the seven partner countries will start from late February 2017. If, as a researcher, product supplier, potential funder or distributor, you are interested in taking part in Smart AKIS Innovation Workshops, please

contact your Smart AKIS Contact Point.

France: Pauline Bodin, ACTA. pauline.bodin@acta.asso.fr
Germany: Klaus Erdle, DLO. k.erdle@dlg.org
Greece: Matina Voulgaraki, Agricultural University of Athens (AUA). stavou@aua.gr
Serbia: Milica Trajkovic, BioSense. trajkovic.milica.ns@gmail.com
Spain: Alberto Lafarga, INTIASA. alafarga@intiasa.es
The Netherlands: Harm Brinks, Delphy. h.brinks@delphy.nl
UK: David Tinker, DTA Ltd / EurAgEng. d.tinker@ntlworld.com

Results from these workshops will be available later although attendees will have the opportunity to benefit immediately.

Acknowledgements

This project has received funding from the European Union's Horizon 2020 research and innovation program me under grant agreement no. 696294.

References

1 Kernecker M, Knierim A, Wurbs A. 2017. Deliverable 2.2: Report on farmers' needs, innovative ideas and interests. Available from https://www.smart-akis.com/index.php/network/results/

2 Wolters S,Balafoutis T, Fountas S, van Evert F. 2017. Deliverable 1.2 Research project results on Smart Farming Technology. Available from https://www.smart-akis.com/index.php/network/results/

3 European Commission DG AGRI – Directorate H.5. Research and Innovation. EIP-AGRI Common format for interactive innovation projects. Accessed January 2017 via https://ec.europa.eu/eip/agriculture/en/content/eip-agri-common-format

4 Wolters S,Balafoutis T, Fountas S, van Evert F. 2017. Deliverable 1.3 Industry solutions on Smart Farming Technology. Available from https://www.smart-akis.com/index.php/network/results/

5 Anon 2017. Triggering Smart Farming adoption in Europe – Project Briefing Note. Presented to EC February 2017. Currently not published.

A typology of the uses of precision farming in an arable crops oriented region in Northern France

Alicia Ayerdi Gotor[a], Elisa Marraccini [b], Christine Leclercq [b], Olivier Scheurer [c,*]

[a] UP 2012-10-102 AGHYLE, UniLaSalle, Beauvais, France

[b] UP 2012-10-103 INTERACT, UniLaSalle, Beauvais, France

[b] UP 2012-10-103 INTERACT, UniLaSalle, Beauvais, France

* Corresponding author. Email: Olivier.scheurer@unilasalle.fr

Abstract

The objectives of our study were to fill the knowledge gap on the use of Precision Farming (PF) at the farm level and to understand the reasons of the adoption of these techniques. Among the PF techniques, GPS guidance (assisted or manual), section control, and variable rate application were considered. Our purpose was to support local extension services to evaluate the potential of these techniques at the territorial level.

We conducted 23 semi-structured interviews in farms already using PF techniques and located in the Oise NUTS 3 (Northern France). In each farm, the use of every PF technique has been described. We defined "use of a PF technique" as a set of descriptors, i.e. the technical characteristics of the equipment, the field operation(s) concerned, the targeted crop(s), the aim of the use, the drivers of the adoption of the technique, the perceived impacts by the farmers along with the drivers of those impacts.

Most of the farms (70%) make a combined use of GPS guidance (mainly assisted) and section control, whereas variable rate application is less common (15%). Less than 20 % of the surveyed farmers used assisted guidance for all the technical operations. The section control was used for both liquid nitrogen and phytochemicals spraying by 55% of the farmers. A typology of the uses of PF techniques in these farms has been built adapting a method for farm typologies (step by step comparison of the uses). Three to five types of use have been generally defined for each PF technique (vs one type of variable rate application). These types differ for the drivers of the adoption of the technique that are of very different kind, e.g. the need of reducing on-farm work, an adaptation to irregular field morphology or improvement of the sowing efficiency in conservation agriculture.

Even those literature accounts mainly for economic and environmental advantages of PF techniques, the social impacts (work time reduction and well-being at work) seem to be more important for the surveyed farmers. These social impacts are hence becoming the main motivation for PF techniques far ahead from the economic impacts.

The perspectives of this explorative study are to extrapolate some indicators to identify and quantify the possible users of PF techniques at the regional level. Further research should also be implemented to assess the PF evolution and adoption trajectories along with the medium-term impacts on cropping systems at the farm level.

Keywords: Precision farming, Impacts, Adoption, Farm-level, Use

1. Introduction

The evolutions in automation and communications have made that farm machineries constructors are offering products allowing farmers to have a panel of new management, diagnosis and optimization practices (Gavaland & Goutiers, 2013). Precision Farming (PF), considered as the group of techniques and tools that led to accurate agricultural operations, help to automate some of them and to reason inputs (P. J. Zarco-Tejada, N. Hubbard, & P. Loudjani, 2014). Besides, PF can manage the field spatial and temporal variability, and may reduce the environmental impact of farm operations by optimising the use of inputs (Reichardt & Jürgens, 2009). The expected impacts of the PF can hence be grouped in three main areas: economic, environmental and social (Batte & Arnholt, 2003; EPRS, 2016; Reichardt & Jürgens, 2009). Meanwhile few and partial data are available concerning the economic and environmental benefits of PF (EPRS, 2016; P. Zarco-Tejada, N. Hubbard, & P. Loudjani, 2014). Few studies have been conducted in France to evaluate PF benefits on French farms, neither to evaluate the adoption of these techniques nor the trends of adoption (Arvalis, 2015). Field trials on machine guidance impact or fertiliser overlapping have shown reduction of overlapping but the quantity saved depends mainly on the parcel shape (Bousquet, 2016) or on the heterogeneity of the field characteristics, e.g. soil quality (Deutscher Bundestag, 2006 quoted by Pölling et al., (2010)). Regarding the expected benefits of PF, they are often theoretical or based on experimental data only targeting a technique (EPRS, 2016). These experiments did not provide enough data about the conditions they were obtained and so the possibilities of extrapolation are limited, because they are only based on reduction of overlapping or treated surface, based on geometrical theoretical surface but not on real measures (Diacono, Rubino, & Montemurro, 2013; EPRS, 2016).

The adoption and use of these PF techniques by farmers depend on many factors, nevertheless profitability remains the key one (Swinton & Lowenberg-DeBoer, 1998; P. Zarco-Tejada et al., 2014). Some studies highlighted that also farm and individual farmer characteristics have to be taken into account, even though individual farmer characteristics do not seem to be statistically significant (Castle, Lubben, & Luck, 2016; Fountas et al., 2005; Paustian & Theuvsen, 2016). For example in Germany, Paustian & Theuvsen (2016) have highlighted that a big farm size (more than 500 ha of arable

land) and the involvement in contract works as another branch of activity are among the adoption factors, whereas a lower arable surface and presence of cereals are negatively correlated to the adoption. A recent study at the European level, stated that the potential of PF adoption in Europe is related to a high rate of cropland, a high rate of cereals, a high number of hectares per working unit, along with the economic power of the region (EPRS, 2016). According to this, a part of Northern Western European countries would have the higher potential for PF techniques adoption, particularly Danemark, Germany, France and the UK. However, using yield mapping systems sales as an indicator of PF adoption, these authors concluded that the adoption was slow in France until 2010.

The objectives of this study were to understand how PF adoption is made by farmers, which are the on farm PF uses and the perceived benefices by farmers having already adopted PF. We particularly investigated PF techniques applied in arable farms. We particularly focused on three main groups of techniques: guidance, section control and variable rate application. The study region is Oise, an arable crops oriented region in Northern France. PF uses are defined according to Cockburn (1997), who defined a use case as the series of related events of interactions between the treated system and its external actors for a particular goal. In our case, a use case is defined as the combination of aimed for objectives, the utilization modalities (technical operation x crop) and the context (adoption factors) (Figure 1)

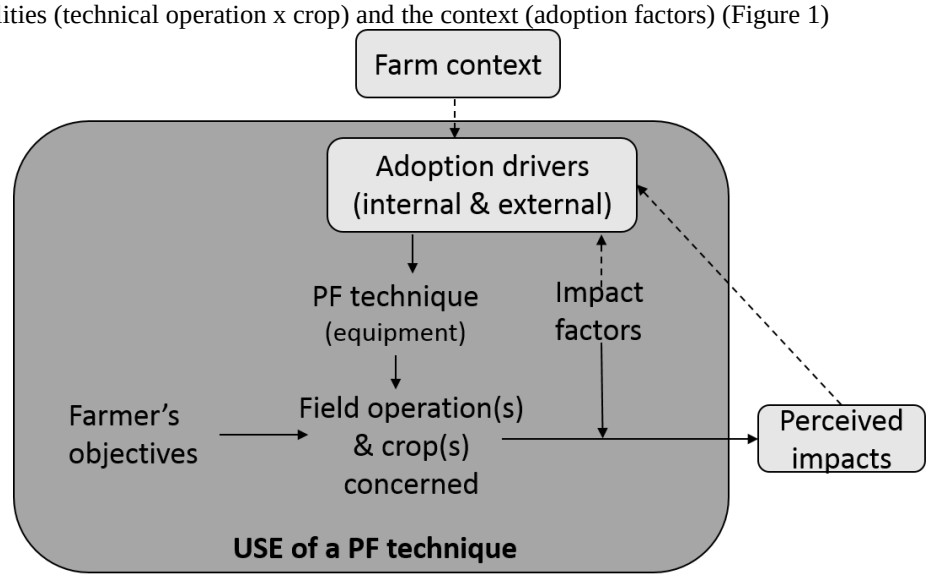

Figure 1 : Analytical framework of the study

2. Materials and Methods

We investigated the uses of PF techniques in the Oise region (NUTS 3), Northern France. According to Pölling et al. (2010), Oise region is located within a high potential area for PF farming adoption. We investigated 23 farmers PF practitioners in the Oise region. Those farmers were randomly selected from a database of the local Agricultural Chamber of 40 PF practitioners of the region. Interviews were semi-structured in order to acquire information about the use of PF. Detail of the main information collected is given in Table 1.

The farm typology of the Picardy region (CRAP, 2010) has been used to validate the consistence of the interviewed farms with regional farm diversity.

Table 1 : Description of the structured interviews made to practitioners farmers

General question	MAIN COLLECTED DATA	OBJECTIVE
General Farm Features - Context	- Age, legal status, employees - Farm size, Parcels (size, shape, soil types, slope) - Crop rotation(s)/Sequences - Crop operation(s) - Regulatory framework - Agricultural equipment	- Characterization of the farm and get knowledge about the user constrains and assets which can influence the PF impacts or to be a brake or a motivation to be used - Detect internal factors of PF adoption or impact factors - Give information about the crop rotation of the farm that can allow classing the farm in regional typology.
PF techniques & Agricultural Equipment & characteristics	- PF used, why, description and precision of the PF	- Objectives, assets and constraints in three main domains : economic, social,

	- Historic of the introduction and adoption - Advantages/disadvantages - Objectives to use it - Projects, why?	environmental per PF - Determine the adoption pattern/PF and the factors that induced the change
Terms of uses	- Which crops, which parcels, why? - Nature of the technical operation - Origin of the information: advice, follow-up	- How many hectares concerned - Impact factors - Reasons of use - Effect(s)/hectare
Impacts	Which observed impacts: inputs, fuel, yields, life quality, spent time on crops, precision & quality of the technical operation	Determinate the linking from the perceived impacts (primary or secondary impacts) to the final impacts (interpretation for classification)
Source of information	Do you look for new technology? How? Why?	

The adoption drivers have been considered of two origins: internal, which take into account the characteristics of the farm such as parcels (shape, heterogeneity...) or a specific crop operation (i.e. night working) and the farmer wishes; and external as external influencing the farmer's use, e.g. having contract works or a neighbour using a PF technique. The internal adoption drivers will have an identified expected objective for the use of the chosen PF technique, whereas external adoption drivers have not directly associated to an objective for the PF use.

A typology of PF uses has been developed based on the objectives, the adoption drivers, and the PF technique use. The method was adapted from Landais (1998), who was working on the implementation of farm typologies to illustrate the diversity of farms on a regional scale. In our case, the typology was based on the PF technique uses instead of the farms. This implies that each farm using several PF techniques can be classed in several types. Once classed by PF technique, farms are grouped according to crops and technical operations concerned by the technique, targeted objectives, adoption drivers (internal and external) and impact factors, obtained also from the global analysis of each farm. In this case each farm belongs to a type of use. The attribution of several types of use to the interviewed farm allowed finding combinations of PF techniques. According to these results, a farm typology has been built based on the observed PF techniques combinations.

The impacts of each PF technique use perceived by each farmer, have been grouped by use type in order to obtain the primary impacts occurrence in the farmers' discourses. The benefices of the primary impacts were then identified. For example, for reducing overlapping perceived benefits where work time saving and input reduction. Final impacts classified the benefits in three impact categories: economic, social and environmental. In the previous example time saving was classified as social and economic final impacts, whereas input reduction was environmental and economic.

3. Results and Discussion

3.1 Farms characterization

The 23 farms analysed, represented seven of the fifteen types described in the Picardy farms typology, with a majority of "diversified-cereal" and "sugar beet" types (Figure 2); their mean UAA is 254 ha (Figure 3). In NUTS3 Oise region 20% of farms are within the "diversified cereal >100ha" type, polyculture-mixed farms represented 12%. Each Picardy type it is not equally represented in the region (CRAP, 2010). Within these interviewed farms, 6 major precision farming techniques have been observed (Figure 4a): Section control of the sprayer and of the fertilizer spreader; Guidance manual and assisted (Figure 4b)); Variable rate application; hoeing guidance. This last technique was only found in two cases combined with another PF technique. Each major precision farming technique has two or more PF use types. The guidance was the most adopted PF technique, whereas variable rate application was the less adopted. The tendency is identical to the one found by the Ohio farmers (Batte & Arnholt, 2003). Despite the different socio-economical and agricultural contexts of these areas Fountas et al., (2005) retrieved that PF users are quite similar in USA and Europe.

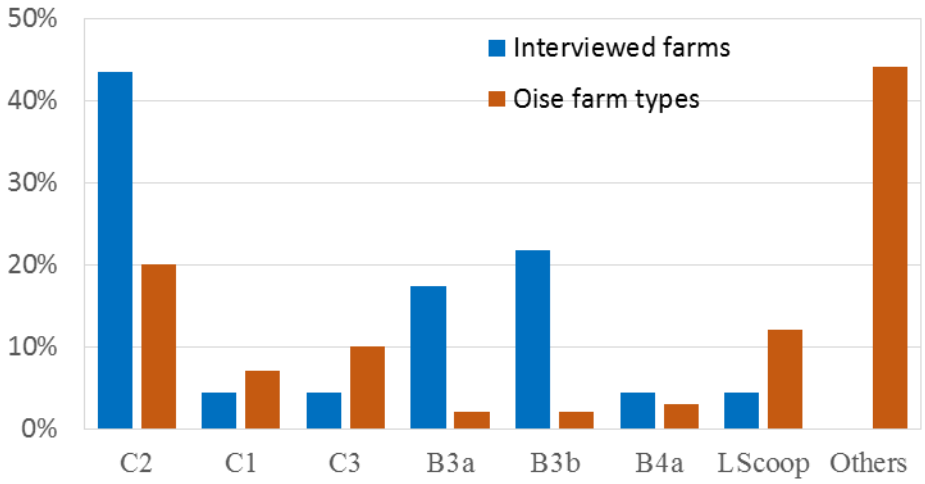

Figure 2 : Occurrences of the farm types of the Picardy typology in the 23 interviewed farms compared to the occurrence of the types in entire NUTS3 Oise Region. C2: Diversified cereal farm >100ha; C1: Specialised cereal farm <100ha; C3: Specialised cereal farm >100ha; B3a: Diversified sugar beet farm 120-200ha; B3b: Diversified sugar beet farm > 200ha; B4a: Specialised sugar beet farm 110-300ha; LScoop: mixed farm

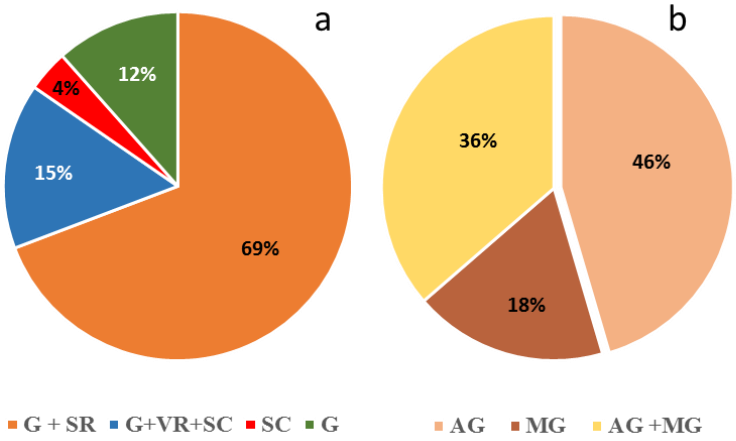

Figure 3 : Distribution of the PF techniques in the 23 studied farms (a). SC: Section Control; G: Guidance; VR: Variable rate application. Types of guidance found in 23 studied farms within those who use Guidance (b): AG: Assisted Guidance; MG: Manual Guidance

3.2 Adoption drivers

Table 3 presents the PF adoption drivers of the 23 interviewed farms. Internal drivers seemed to be more diversified than external ones. The external drivers are not related to a specific technique, whereas internal ones may be more specific at the beginning of adoption. Among the internal adoption drivers, except for farmers having an individual interest for new technologies, the targeted impacts were mainly the increasing of technical efficiency and the wellbeing at work.

Table 2 : PF adoption drivers related to different techniques and targeted impacts. SC: Section Control; G: Guidance; VR: Variable rate application.

	Drivers	PF Technique(s)	Main targeted impacts
INTERNAL	High size of cultivated land by one farmer	G & SC	Wellbeing at work Work time saving
	Constraining field properties (shape, slopes) or environmental (watercourse)		
	One (or more) element of crop management practices requiring higher precision (1)	G and/or SC	Wellbeing at work Technical efficiency
	High soil heterogeneity	VR	Technical efficiency
	Farmer interest for new technologies	G &/or SC &/or VR	
	Need to renew a piece of machinery	G &/or SC &/or VR	Technical efficiency
	Need of free time increasing	G &/or SC &/or VR	Technical efficiency
EXTERNAL	Shared ownership	G &/or SC &/or VR	
	Belonging to a CUMA(2)	G &/or SC &/or VR	
	Environmental constraints	G &/or SC &/or VR	
	Investment aid(s)	G &/or SC &/or VR	

(1) Spraying at night, need of field marking, crop and cover crop seeding in conservation agriculture, mechanical weeding on sugar beet

(2) CUMA: Coopérative d'Usage de Matériel Agricole: Agricultural Equipment Use Cooperative

Probably, once a farmer has adopted a PF technique and has observed one or several benefits, he will be more susceptible to adopt another PF technique, either by adding a new material or following the machinery renewal (Reichardt & Jürgens, 2009).

3.3 Typology

The analyses of the PF uses in the interviewed farms have led to a typology of uses (Table 3). They also have shown several degrees of implementation with different combinations of techniques and uses. The more types of use are present in the population, the more diversity of use combinations is found. Almost all the farms used two or more PF techniques except one. 19 farms of the 23 combined guidance with section control, but according to literature there is not a direct interest to combine these two PF techniques. Some trials have shown that section control alone reduces overlapping by 4% , whereas the section control and guidance combination reduces the overlapping by 2 % (Arvalis, 2015).

Table 3 : Use types of each PF technique in the interviewed farms. C2: Diversified cereal farm >100ha; C1: Specialised cereal farm <100ha; C3: Specialised cereal farm >100ha; B3a: Sugar beet diversified farm 120-200ha; B3b: Sugar beet diversified farm > 200ha; B4a: Specialised sugar beet farm 110-300ha; LScoop: mixed farm

PF technique	Use Type (number of farms)	Farm types on the Picardy typology (CRAP, 2010)	Field operations	Farmer objectives by using the PF technique
ASSISTED GUIDANCE	A (8)	C1, C2, C3, B3a, B3b, B4a, LScoop	- Soil preparation - Crops seeding - Fertilizers spreading	- Well-being at work - Worktime saving
	B (3)	B3a, B3b, C2	- Crops and cover-crop seeding	- Worktime saving - Well-being at work
	C (2)	C2, B3a, B3b	- Crops seeding	- Well-being at work - Technical efficiency
	D (4)	C1, C2, C3	- All operations	- Well-being at work
MANUAL GUIDANCE	E (4)	C2, B3a, B3b	- Cereals harvest	- Well-being at work - Work precision - Technical efficiency
	F (9)	C2, B3a, B3b, C1, C3	- Spraying phytosanitary products - Spraying liquid fertilisers	- Well-being at work - Inputs saving
SECTION CONTROL	G (13)	C2, B3a, B3b	- Spraying phytosanitary products - Fertilizers spraying	- Well-being at work - Worktime saving - Inputs saving
	H (6)	C2, B3a, B3b, C1, C3, B4a	- Spraying phytosanitary products	- Well-being at work - Inputs saving

				- Technical efficiency
	I (4)	C2, B3a, B3b, C1, C3, LScoop	- Solid fertilizer spreading	- Well-being at work - Inputs saving
VARIABLE RATE APPLICATION	J (4)	C2, B3a, B3b	- Spreader and sprayer adapted for last nitrogen input	- Input saving - Technical efficiency
HOEING	K (2)	B3a, B3b	- Hoeing guidance of sugar beets	- Work precision

Guidance is present in all the farms except two; in those farms (Figure 4b) 9 used assisted guidance, 4 manual guidance and 8 owned both. The most frequent used combination was the guidance combined to sprayer section control. The second more used combination was guidance with section control of the sprayer and assisted guidance of the seeder. The third combination was assisted guidance for all the operation except sprayers, with sometimes section control of the sprayer (without guidance). The most complex combination found was assisted guidance of most of the operations, with section control of the sprayer or solid fertilizer spreader, often with variable rate application of nitrogen or harvest guidance. The two farms, where this combination is found practice, both no-till and ploughing, have an UAA around 200ha, and the parcels present in the farm are heterogeneous; for these reasons, the variable rate application is used in combination with the two other PF techniques to be more precise and efficient.

The generalisation of this typology of farm PF uses is not possible because of two main reasons: first, it is only based on 23 farms so multicriteria statistics cannot be applied; secondly, the combinations of uses are not homogeneously and equally distributed within the interviewed farms.

3.4 Impacts

Primary impacts identified for each type of PF technique use where mainly social. Even though the use of the technique is different or the PF technique is different. In the type E (Manual guidance for cereal harvest) and K (Hoeing guidance of sugar beets) only one primary and unanimous impact were identified. This related to the fact that they are crop and technical operation specific techniques. In most of the cases induced impacts, once identified, are shared among most of the farmers practitioners except the case of better application conditions which also requires a particular willing of the farmer to implement it for example in the case of night spraying. Finally, the most recurrent impact category was the economic one.

Table 4 : Perceived impacts related to each use type, light green indicates that less than 75% of the population concerned by this use identified this impact, dark green indicates that over 75% of the population identified this impact for this type of use. The types of PF technique uses are described in Table 3,

Type of PF technique use	**Primary impact**	**Induced impact(s)**						**Impact category**		
		Work time saving	Wellbeing at work	Input reduction	Increase in yield	Less manpower	Better application conditions	**Economic**	**Social**	**Environment**
A	Field marking avoiding							x	x	
	Less concentration required								x	
	Overlapping reduction							x		x
	Work precision							x		
B	Work precision							x		
	Less concentration required								x	
C	Less concentration required								x	
	Overlapping reduction							x		x

	Work precision							x		
D	Less concentration required								x	
	Overlapping reduction							x		x
E	“Run and round” harvesting							x	x	
F	Field marking avoiding							x	x	
	Night work possible							x		x
G	Reduction herbicide							x		x
	Less concentration required								x	
	Faster workflow							x	x	
H	Less concentration required								x	
	Overlapping reduction							x		x
	Night work possible							x		x
I	Overlapping reduction							x		x
	Night work possible							x		x
J	Less concentration required								x	
	Avoiding overlapping in corners							x		x
	Faster work flow							x	x	
K	Work precision							x		

4. Conclusions

Social impacts (wellbeing at work and decreased work time) are commonly perceived (except for variable rate application); they seem to be strong drivers of the adoption of PF techniques, ahead from the economic impacts. Agronomic, economic and environmental impacts are also perceived but almost never quantified. Guidance and section control of spraying are the most adopted techniques, probably because of their multiple impacts and their multiple adoption drivers. In addition, the use of these equipment do not need additional information (application map). For these reasons, they will probably be adopted in the near future by most of the crop producers of the region following the machinery renewal in farms. The lower diffusion of the variable rate application technique could be explained by different reasons: less multifonctionnality, impacts not easily quantified vs higher adoption cost, only one main adoption driver (soil heterogeneity).

Acknowledgements

We warmly acknowledge the students in agricultural engineering of the promo 155 “Agronomie et Territoire” at UniLaSalle for their hard work on an initial phase of the research: Hélène Callewaert, Jean Manuel Clabaut, Juliette Descotes, Lucie Deterpigny, Marie Thérèse Gässler, Estelle Harant, Pierre Lauwerier, François Mathellié, Axel Moilleron, Damien Prévost and Hélène Vanbesalaere and the useful discussions with Sophie Wieruszeski and Florian Vigneron from the Oise agricultural Chamber. 23 farmers accepted to answer to our questions, many thanks to all of them.

References

Arvalis (Ed.). 2015. Agriculture de précision. Paris: Editions Arvalis

Batte, M. T., & Arnholt, M. W. 2003. Precision farming adoption and use in Ohio: case studies of six leading-edge adopters. Computers and Electronics in Agriculture, 38(2), 125-139. doi: http://dx.doi.org/10.1016/S0168-1699(02)00143-6

Bousquet, N. 2016. Limiter les recouvrements grâce aux coupures de tronçons assistées par GPS. 1. Retrieved from www.arvalis-info.fr website.

Castle, M. H., Lubben, B. D., & Luck, J. D. 2016. Factors Influencing the Adoption of Precision Agriculture Technologies by Nebraska Producers.

Cockburn, A. 1997. Structuring use cases with goals, humans and technology. Journal of object-oriented programming, 10(5), 56-62.

CRAP. 2010. Présentation des systèmes d'exploitation agricole de Picardie (pp. 20). http://www.hautsdefrance.chambres-agriculture.fr/fileadmin/user_upload/Hauts-de-France/029_Inst-Hauts-de-France/Exploitation-agricole/Rubrique_%C3%A9conomique/presentation_systemes_EA_dePicardie.pdf.: Chambre Régionale d'Agriculture de Picardie.

Diacono, M., Rubino, P., & Montemurro, F. 2013. Precision nitrogen management of wheat. A review. Agronomy for Sustainable Development, 33(1), 219-241.

EPRS. 2016. Precision agriculture and the future of farming in Europe Scientific Foresight Study (pp. 42+274). Brussels: European Parliament Research Service.

Fountas, S., Blackmore, S., Ess, D., Hawkins, S., Blumhoff, G., Lowenberg-Deboer, J., & Sorensen, C. G. 2005. Farmer Experience with Precision Agriculture in Denmark and the US Eastern Corn Belt. [journal article]. Precision Agriculture, 6(2), 121-141. doi: 10.1007/s11119-004-1030-z

Gavaland, A., & Goutiers, V. 2013. L'agriculture de précision : applications et perspectives en grandes cultures et prairies [Vidéo] http://prodinra.inra.fr/record/211868

Landais, E. 1998. Modelling farm diversity: new approaches to typology building in France. Agricultural systems, 58(4), 505-527.

Paustian, M., & Theuvsen, L. 2016. Adoption of precision agriculture technologies by German crop farmers. Precision Agriculture, 1-16.

Polling, B., Herold, L., & Volgmann, A. 2010. Typology of farms and regions in EU states assessing the impacts of Precision Farming-Technologies in EU-farms (pp. 53): FutureFarm Project.

Reichardt, M., & Jürgens, C. 2009. Adoption and future perspective of precision farming in Germany: results of several surveys among different agricultural target groups. [journal article]. Precision Agriculture, 10(1), 73-94. doi: 10.1007/s11119-008-9101-1

Swinton, S., & Lowenberg-DeBoer, J. 1998. Evaluating the profitability of site-specific farming. Journal of production agriculture, 11(4), 439-446.

Zarco-Tejada, P., Hubbard, N., & Loudjani, P. 2014. Precision Agriculture: An Opportunity for EU Farmers—Potential Support with the CAP 2014-2020. Joint Research Centre (JRC) of the European Commission.

Zarco-Tejada, P. J., Hubbard, N., & Loudjani, P. 2014. Precision Agriculture: An Opportunity for EU Farmers—Potential Support with the CAP 2014-2020. Joint Research Centre (JRC) of the European Commission. doi: 10.2861/58758

Spray deposition in a wind tunnel: perspectives of spray drift simulation based on a kinetic approach of wind speed effects.

MAJID ALHEIDARY[a], JEAN-PAUL DOUZALS[a,*], HERVE FOUBERT[b]

[a]*UMR ITAP, IRSTEA 361 Rue JF Breton BP 5095 F-34196 Montpellier, France*
[b]*SOLCERA Advanced Materials, 1 rue de l'Industrie F-27000 Evreux*
* Corresponding author. Email: jean-paul.douzals@irstea.fr

ABSTRACT

Wind tunnel is a convenient way to study spray drift (Alheidary et al., 2014). Spray drift was studied in control conditions in IRSTEA wind tunnel fitted with a 9m distribution test bench. Based on a spray boom of four nozzles placed frontally, different nozzle types (flat fan, air injection, air injection twin jets), size 02, injection pressure of 2.5 bar were tested at 2, 4 and 7.5 $m.s^{-1}$ and at 40, 60 and 80 cm boom height (Al Heidary et al., 2014). Altogether 54 modalities were tested. Deposition curves including 180 points were analyzed and converted to drift ratio curves as a function of the distance downwind (Douzals et al., 2014). In this work, a sedimentation time (Ts) was calculated based on the horizontal travel speed of droplets due to the wind speed in the wind tunnel. Sedimentation deposition curves are then expressed as a function of sedimentation time allowing some comparison with different wind velocities (ex. at Ts of 1 second corresponds to 2m downwind when wind speed is $2m.s^{-1}$ or 4m at $4m.s^{-1}$ or 7.5m at 7.5 $m.s^{-1}$. As a result, it appeared that both deposition values and drift ratio values showed a quite good correspondence for a given boom height suggesting a strong dependence of the drift deposition to Ts value. In other terms, such kinetic approach allows to simulate the effect of wind speed on spray deposition. One assumption was that dropsize might be similar at a given Ts so *in situ* droplet size measurements were achieved in the wind tunnel by using a Malvern Spraytec device. Wind speeds from 0 to 8 $m.s^{-1}$ were tested at different distances from the boom (0 – 4 m) allowing the scan of Ts range of (0.2 – 2 s) only with flat fan nozzles. A lot of position/wind velocity combinations did not allow any measurement as the droplet density crossing the laser beam was too low. However the results based on about 20 measurements showed a quite good correlation ($r^2 = 0.98$) suggesting that the hypothesis of equivalent droplet sizes for a given Ts is correct. Two main ideas may be drawn in conclusion. First the determination of a sedimentation time allowed the simulation of wind velocity effects with a subsequent decrease in the number of necessary tests. Second, droplet sizes were in accordance with the sedimentation time that would benefit for the development of new low drift nozzles.

Keywords: Spray Drift, Wind tunnel

1. Introduction

Introduction

Spray drift is of great concern because of the impact on human health and the environment as it corresponds to the off-target fraction of the sprayed volume (ISO 22866, 2005). Two main routes can be defined with the sedimentation spray drift that is mostly responsible of the ground contamination of the environment (water, sensitive crops and arthropods), whereas airborne drift mostly impacts the air, bystanders and residents close to the sprayed area. The European Water Framework Directive (WFD, 2000) and the European Directive on the Sustainable Use of Pesticides (EC/128, 2009) were the starting point of the implementation of drift mitigation measures among European Member States with the combination of buffer zones and drift mitigation techniques such as air induction nozzles for field crop sprayers. Although the in-field evaluation of spray drift is a laborious and costly task because of terrain constrains and wind conditions required by the above standard, main spray models are derived from field tests (Holterman et al., 1997; Miller and Hadfield, 1989). Spray drift of field crop sprayers are mostly due to the nozzle type, operating conditions such as nozzle height, operating pressure and forward speed of the sprayer and the atmospheric conditions (Alheidary et al, 2014). In parallel, an extensive amount of studies were also conducted in wind tunnels whereas artificial wind conditions allow routine and more repeatable results (Miller et al., 1993; ISO 22856, 2008; Nuyttens et al., 2009; Miller et al., 2011; Douzals, 2012). However, wind tunnel measurements do not necessarily avoid the variability of the results as shown in Table 1.

Table 1: Variability of drift measurement from wind tunnel or field measurements

Reference	Context - distance	Protocole	Number of replicates	CV
Nuyttens et al, 2009	Wind tunnel - 2m	Vertical array of nylon strings - 2 m/s	18a	180 %
Nuyttens et al, 2009	Wind tunnel - 2 m	Vertical array of nylon strings - 2 m/s	18a	128 %
De Schampheleiere et al, 2009	Wind tunnel - 2 m	Filter papers 25 x 25 cm - 4 m/s	5	74 %
Rautmann et al, 2001	Field test - 5m	Petri dishes - ISO 22866	250b	72 %c
Balsari et al, 2007	Field test – 2 m	Petri dishes - ISO 22401 (no wind)	8	24 %

a: total number of replicates for the reference spray setting; b: total number of replicates for the reference spray setting; c : extrapolated from median and different percentile values from drift tables.

This paper introduces the original results of different setting conditions (nozzle type, wind speed, wind direction and boom height) in a low speed wind tunnel equipped with a distribution test bench. The main objective is to define the dependence of the spray deposition values to the experimental conditions such as wind speed and boom height.

Materials and methods

Modalities

Series of measurements were conducted in IRSTEA-Montpellier wind tunnel from October 2013 to January 2015. The complete description of the wind tunnel measurements is presented (Douzals and Alheidary, 2014) and is summarized in Table 2.

Table 2: Modalities and settings

Nozzle type/angle/size	Commercial name	Pressure (bar)	Boom Positions	Wind velocity m s^{-1}	Boom height (mm)
FF 110 02 FF AI 110 02 AI twin 110 02	Albuz AXI Albuz CVI Albuz CVI Twin	2.5	Frontal	2 4 7.5	400 600 800
			Lateral		

Temperature: 20°C ± 0.1, relative humidity: Min. 95%

Each setting corresponds to a 4 nozzle boom spaced 500 mm. In the frontal mode, the boom is perpendicular to the wind direction and the 4 sprays are equally affected by the wind. In the lateral mode, the boom is parallel to the wind direction. CVI Twin nozzle encompasses 2 jets oriented 60° one from the other.

Drift curve processing

Raw data consist of deposition quantities collected through 5cm grooves and collection tubes along the test bench up to 9 m. First, collected quantities are normalized considering the input flowrate feeding the boom so drift curves are expressed in % of the applied flowrate (Fig. 1).

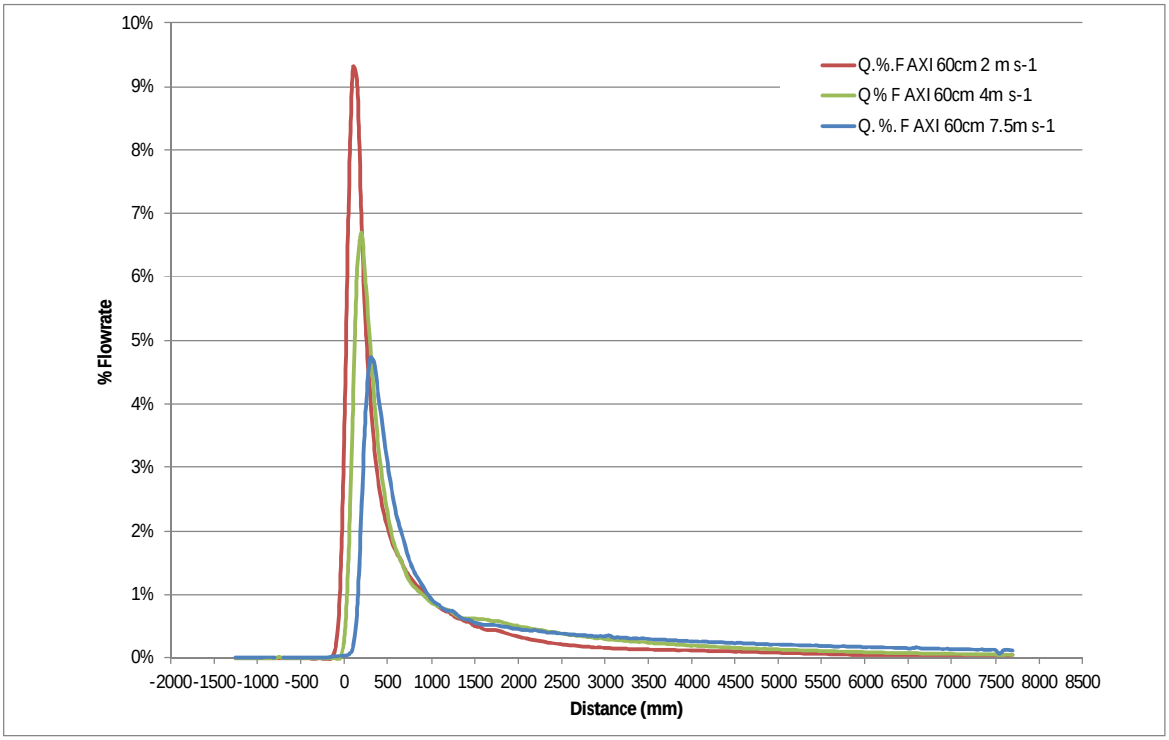

Fig.1: Raw drift curves for different wind velocities – frontal position, AXI nozzle, height 60cm. X=0 corresponds to the position of the boom.

As shown in Fig.1, the most visible effect of an increasing wind velocity is the decrease in the peak value of each curve located in the direct deposition area and only a slight shift of the data in the drift area.
A second normalization is operated through the conversion of the drift curve into a drift ratio curve considering the accumulation of the drift values along the distance and the calculation of the opposite as given by Equation 1(Douzals and Alheidary, 2014):

$$Dr = 1 - \sum_i q \quad [\%] \qquad (1)$$

Where Dr is the drift ratio %, q is the normalized flowrate measured at the position i in %.
The drift ratio values in correspond to the volume fraction still remaining in the air (non deposed) for a given distance.

Results

Effect of the wind velocity

The Fig 2 shows the effect of the wind velocity on the drift ratio values for the flat fan nozzle in frontal position.

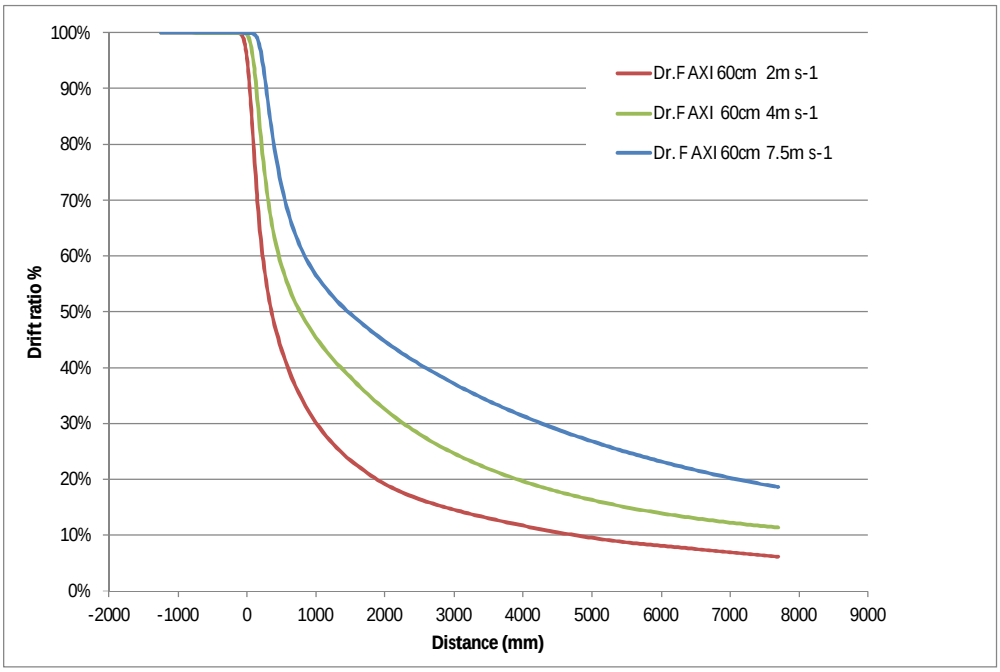

Fig. 2: Sedimentation drift ratio as a function of distance for different wind velocities – AXI nozzle, Frontal position, height 60cm. X=0 corresponds to the position of the boom.

According to fig 2, a drift ratio value of about 20% is observed at 2000 mm (2 m s^{-1}), 4000 mm (4 m s^{-1}) and 7500 mm (7.5 m s^{-1}) suggesting that the drift ratio could be dependent on both the deposition time and wind velocity. Assuming a constant wind velocity in the wind tunnel, a characteristic time can then be calculated taking into account the distance and the wind velocity. This characteristic time was called Time-of-Flight (ToF) and corresponds to the ratio between the drift ratio distance (*d in m*) and the wind velocity (*Vel in m* s^{-1}) given in Equation 2:

$$ToF = \frac{d}{Vel} \quad \text{[Sec]} \quad (2)$$

The curves introduced in fig. 3 are then computed according to the ToF in Fig 3.

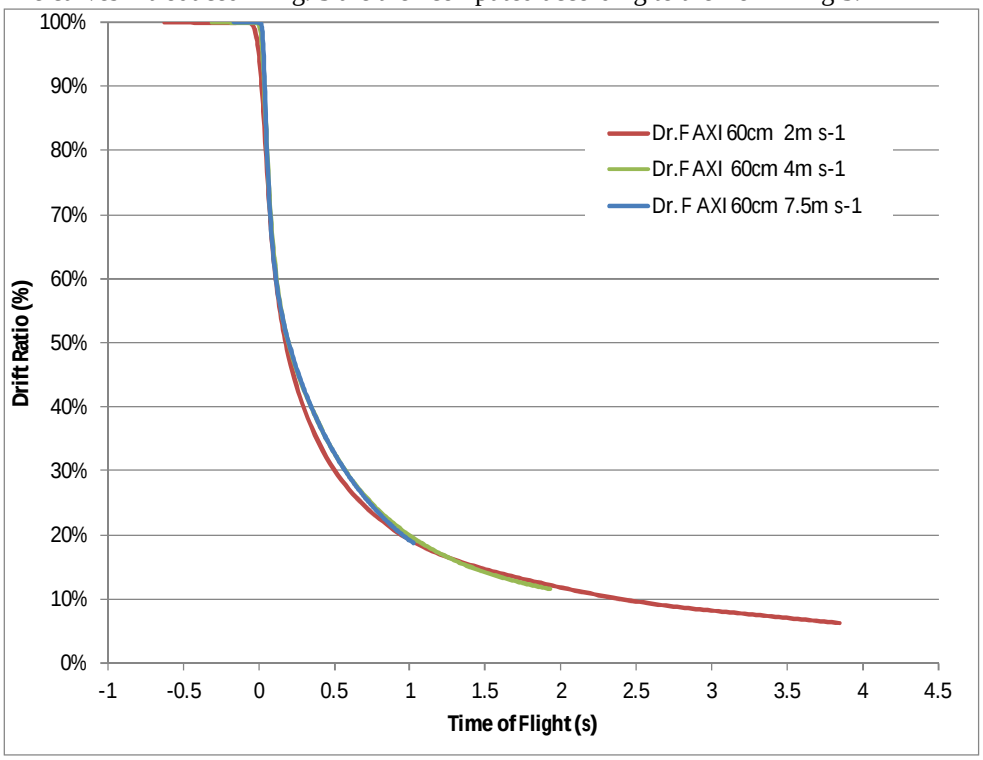

Fig. 3: Drift ratio in function of Time-of-flight at different wind velocities AXI nozzle, frontal position height 60cm. X=0 corresponds to the position of the boom.

The results in Fig. 3 show that the drift ratio curves corresponding to 3 different wind velocities are superimposed when expressed as a function of time-of-flight. For example AXI nozzle with different wind velocities from 2 to 7.5ms^{-1}, at the time-of-flight 1s, the results of this model showed all wind velocities at the same drift ratio (19.18%, 20.04%, and 19.21%) for 2, 4, and 7.5ms^{-1} respectively.
The previous results showed that the conversion of drift ratio curves expressed as a function of distance into a time-of-flight expression is possible with a potential interest for the simulation of the effect of the wind velocity. Data showed that this simulation is more accurate in the case of the frontal position. One possible hypothesis behind these results would be that the droplet size might be linked to the ToF.

Effect of boom height

The effect of boom height on drift ratio values (wind velocity of 4 m s^{-1}) is given in the following Fig. 7.

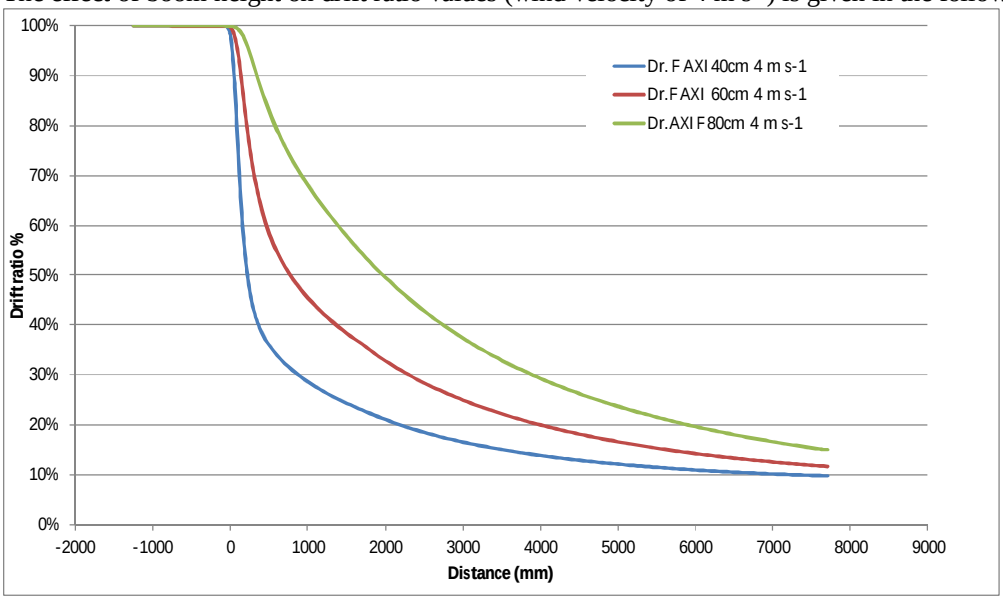

Figure 7: Drift ratio values as a function of the distance for several boom heights. AXI nozzle, frontal position and wind velocity 4 m s^{-1}. The point X=0 corresponds to the position of the boom.

The previous Fig. 7 is converted according to the time-of-flight in order to compare several wind velocities in Fig. 8.

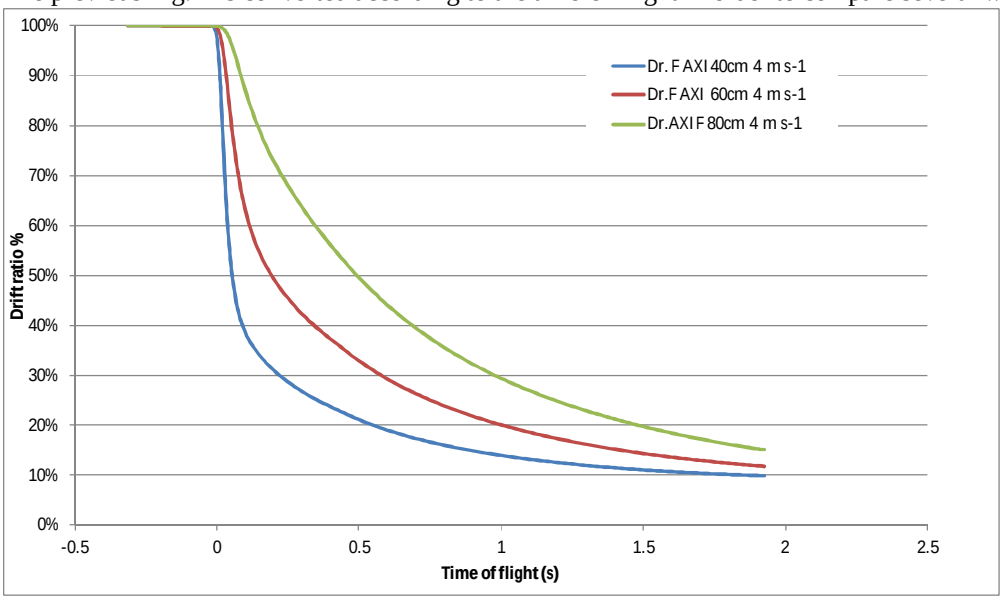

Fig 8: Effect of the boom height on the drift ratio values expressed as a function of ToF, AXI nozzle, frontal position and wind velocity of 4 m s^{-1}.

Proportional conversion

The hypothesis concerning the effect of the boom height was based on a proportional conversion considering 60 cm as a reference height. Then the drift ratio values were converted with the application of a correction factor of 60/40 for the data obtained at 40 cm and a correction factor of 60/80 for the data obtained at 80 cm.

The results of this conversion applied to Fig. 8 data is shown in Fig. 9.

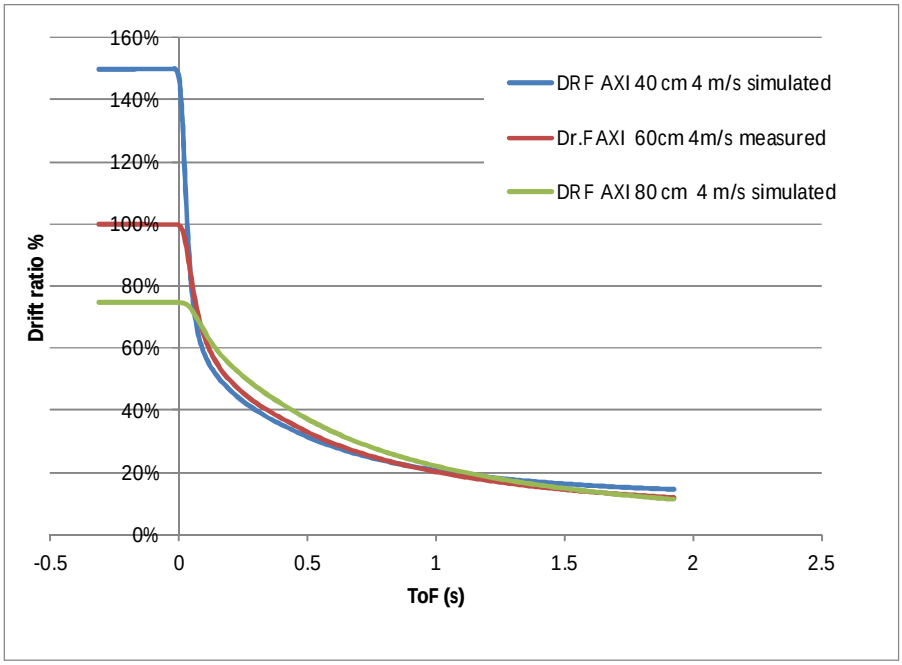

Fig.9: simulation of the boom height according to a proportional conversion, AXI nozzle, reference height 60cm, wind velocity 4m s^{-1}

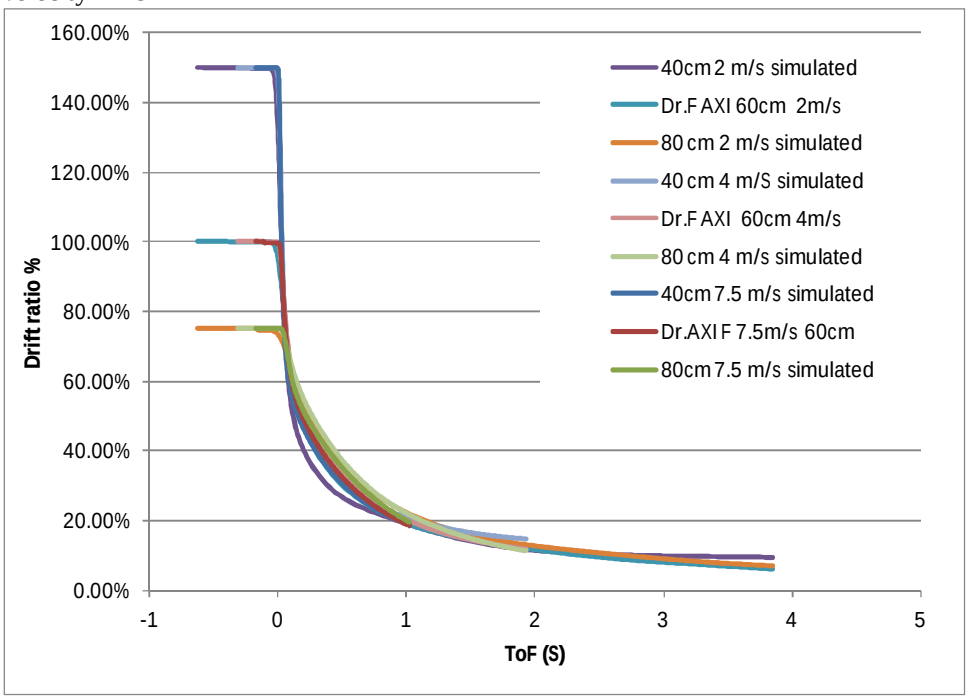

Fig 10: Evolution of the drift ratio of AXI nozzle resulting from the simulation of the boom height for wind velocities of 2, 4 and 7.5 m s^{-1}.

The Fig. 10 shows the result of the simulation of all conditions of wind speeds and boom heights for the AXI nozzle.

The following Fig 11 shows the result of the simulation of the drift ratio values considering only one reference point for each nozzle corresponding to a boom height of 0.6m and a wind velocity of 4 m s^{-1}.

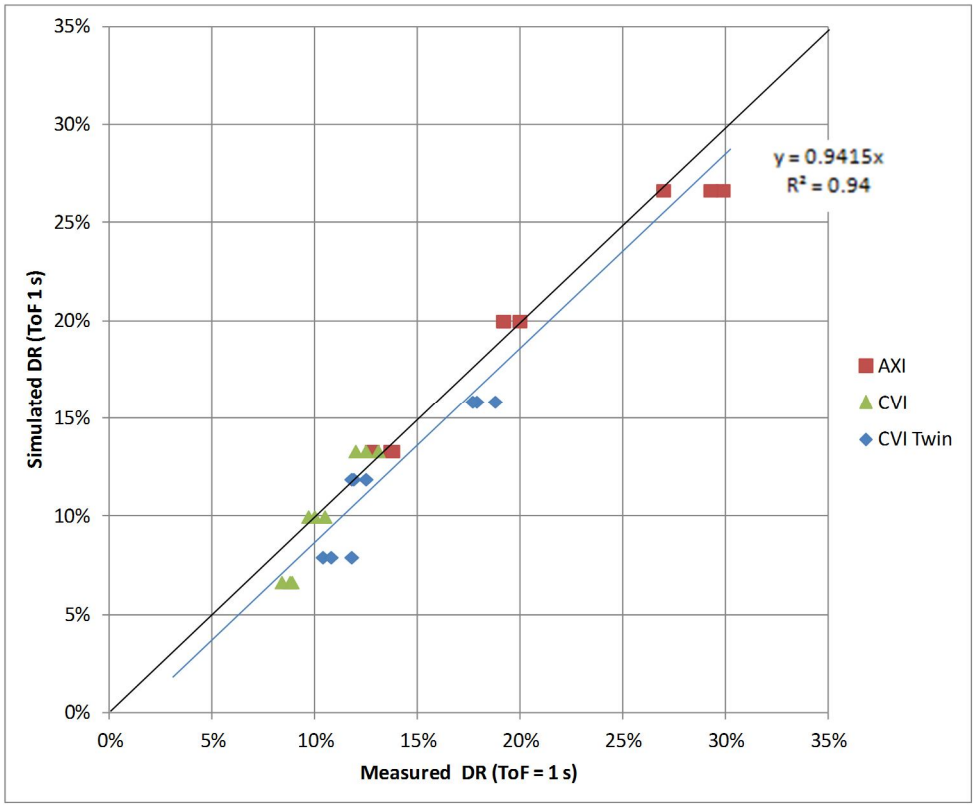

Fig 11: Simulation of drift ration values at 40 and 80 cm and different wind speeds from the data measured at 60 cm, frontal position of the boom.

The linear regressions showed in fig 11 confirmed the performance of the boom height and wind speed simulation.

Conclusions

54 modalities carried out in IRSTEA-Montpellier wind tunnel were used to build predictive spray drift simple models based first on the sedimentation kinematics (time-of-flight) and second on a homothetic model (simulation of the boom height). Although the effect of wind speed and boom height is known for a long time, the results shown in this paper give quantitative correspondence between the different factors through the Time of Flight and/or the homothetic conversion. However the performance of both simulations was mostly dependent on the boom position whereas frontal position gave generally better qualitative results compared to the lateral position. The simulation of several settings is then possible from at least one initial condition (ex. 4 m s^{-1}; 60 cm) with an acceptable accuracy. The perspectives of this work rely first in the definition of stable and repeatable wind tunnel protocols. Second the time of flight approach would practically allow the implementation of an inboard drift model to manage hazardous situations due to the wind speed and direction.

References

Alheidary M, Douzals JP, Sinfort C, Vallet A. 2014. Influence of spray characteristics on potential spray drift of field crop sprayers: a literature review. Crop Prot, 63, 120-130.

Balsari P, Marucco P, Tamagnone M. 2007. A test bench for the classification of boom sprayers according to drift risk. Crop Prot 26, 1482-1489.

De Schampheleire M, Nuyttens D, Dekeyser D, Verboven P, Spanoghe P, Cornelis W, Gabriels D, Steurbaut W. 2009. Deposition of spray drift behind border structures. Crop Prot 28 (12) 1061-1075.

Douzals JP, 2012. Asymmetric classification of drift reducing nozzles considering frontal or lateral wind conditions. Proceedings of AgEng meeting 2012 Valencia, Spain. DOI: 10.13140/RG.2.1.3343.2804

Douzals JP and Alheidary M, 2014. How spray characteristics may influence spray drift in a wind tunnel Asp. Appl. Biol. 122, 271-278.

Holterman HJ, van de Zande JC, Porskamp HAJ., Huijsmans JFM, 1997. Modelling spray drift from boom sprayers. Computers and Electronics in Agriculture 19, 1–22.

ISO 22866, 2005. Equipment for crop protection - Methods for field measurement of spray drift. 17p.

ISO 22856, 2008. Equipment for crop protection – Methods for the laboratory measurement of spray drift - wind tunnel, 14p.

Miller PCH & Hadfield DJ, 1989. A simulation model of the spray drift from hydraulic nozzles. Journal of Agricultural Engineering Research 42, 135–147.

Miller, PCH, 1993. Spray drift and its measurement. In: Matthews, G.A., Hislop, E.C. (Eds.), Application Technology for Crop Protection. CAB International, Wallingford, pp. 101-122.

Miller PCH, Ellis MCB, Lane AG, Tuck CR, 2011. Methods for minimising drift and off-target exposure from boom sprayer applications. Asp. Appl. Biol. 106, 281-288.

Nuyttens, D. ; Taylor, W.A.; De Schampheleire, M.; Verboven, P.; Dekeyser, D., 2009. Influence of nozzle type and size on drift potential by means of different wind tunnel evaluation methods. Biosyst Eng 103 (3), 271–280.

Rautmann D, Streloke M, Winkler R, 2001. New basic drift values in the authorization procedure for plant protection products. Mitt. Biol. Bundesanst. Land Forstwirtsch. 383, 133-141.

Reichard DL, Zhu H, Fox RD, Brazee RD, 1992. Wind tunnel evaluation of a computer program to model spray drift. Trans. ASAE, vol. 35(3): 755–758.